CRANFIELD UNIVERSITY

LASZLO HETEY

IDEALISATION ERROR CONTROL FOR AEROSPACE VIRTUAL STRUCTURAL TESTING

SCHOOL OF ENGINEERING

PhD THESIS

CRANFIELD UNIVERSITY

SCHOOL OF ENGINEERING

PHD THESIS

Academic Year 2008 - 2009

LASZLO HETEY

IDEALISATION ERROR CONTROL FOR AEROSPACE VIRTUAL STRUCTURAL TESTING

Supervisor: Dr. James Campbell

March 2009

ABSTRACT

This thesis addresses idealisation error control for the nonlinear finite element method. The focus is on accurate failure prediction of mid-size aerospace structures. The objective is the development of technologies that shorten the certification process of new airplanes, by replacing expensive and time consuming testing with reliable calculation methods. The SAFESA (Safe Structural Analysis) approach was applied to the collapse analyses of stiffened metal panels. ABAQUS/Standard was thereby the utilised nonlinear solver. Because the original SAFESA procedure is tailored for linear analyses, the methodology needed an update.

The first analysis case is a stiffened panel compression test which was arranged as a lecture demonstration at Cranfield University. The analysis behaviour is highly nonlinear due to the thin-walled properties of the panel. The second analysis investigates an Airbus compression panel. Until failure, the panel behaves geometrically less complicated because the major load bearing parts are thick-walled and bend smoothly. The main research work is the critical analysis of important modelling assumptions concerning the used material model, boundary conditions and geometrical imperfections. In both cases, the method helped to identify idealisation errors and to build a reliable FEM model. In order to deal with the nonlinear error sources, minor extensions to the original method had to be made.

The major achievement is the development of the first expert system which applies the idealisation error control methodology. CAD data import, geometry visualization, a knowledge-based decision making advisor and audit trail functionality were implemented. The expert system leads the user through a step-by-step idealisation process. Each decision is documented and a confidence level must be supplied. This way, every uncertainty is flagged out as potential error source. An interactive interface was created, which provides the user with expert advice on how to treat the idealisation errors. The software has been validated and shown to meet the program objectives.

ACKNOWLEDGEMENTS

I would like to thank my supervisor Dr. James Campbell for his guidance and assistance throughout this PhD program. Thanks to Prof. Rade Vignjevic for his advice during the research. Your comments helped me to progress and to focus on the important aspects of the project.

I am grateful to the MUSCA project for the sponsoring and to Cranfield University for providing the working environment. Many thanks to Airbus UK for supplying the panel test data and Morten Ostergaard, John Smyth and Nigel Pready of Airbus UK for their help.

I had the pleasure of being part of Cranfield University and cooperating with great researchers and helpful staff. My infinite thanks goes to Jason Brown for our late-night “special purpose” chats. He shared many secrets about mechanical engineering and how to take it easy in general. Thanks to Dr. Kevin Hughes for various kinds of support, Dr. Les Oswald for the grid computing support, Dr. Helen Lockett for explaining some ideas of her PhD thesis to me, Berry Walker for help with the panel tests, scanning and the test machine calibration and Marion Bastable for being the best secretary around.

During this research I discussed results and problems with some brilliant researchers. Thank you, Prof. Alan Morris, Prof. Alan Rothwell, Prof. Jens Lang, Dr. Adrian Murphy, Dr. Matthias Heitmann, Dirk Schumann, Philipp Römelt, Christian Sandor and the QtOpenCascade team. In the last weeks of completing this thesis, several reviewers helped me with their comments on parts of the thesis. Thank you, Henrik Rudolf, Antoine Godbille, Ryszard Maciol, Andrea Calonghi and Caroline Bacle. Special thanks to Katrin Milde for proof reading this thesis. I had the pleasure of sharing an office with other PhD students of the Crashworthiness group. Thank you, Juan Reveles, Ravindran Sundararajah and Seimon Powell for helpful discussions and collective breaks. Finally, thanks to all open-source programmers for sharing their knowledge.

Most importantly, I thank my girlfriend Barbara for her support and love. I would also like to thank my parents and family for providing moral support and simply letting me have a good time whenever I took a break at home. Thanks to all the people I met and enjoyed time during my three years on campus. Thank you Toni, Florian, Jenny, Philipp, Javier, Lucia, Andrea, Holger, Zhengjie, Chichi, Slavisa, Aurelie, Francesco, Oleg, Christian, Edmon, Beck, Daxon, Liyun, Stratos, Shuguang, Susan, Leonardo, Bonolo, Zsombor, Zsofia, Richard, Barnabas, Beata, Ryszard, Nicolai and my friends from the badminton club.

CONTENTS

LIST OF FIGURES

LIST OF TABLES

NOTATION AND ABBREVIATIONS

u	=	Displacement
σ	=	Stress
ε	=	Strain
E	=	Young's (elastic) Modulus
υ	=	Poisson's Ratio
l	=	Length
A	=	Area
$\{f\}$	=	Force Vector
$[K]$	=	Stiffness Matrix

PDE	=	Partial Differential Equation
FEM	=	Finite Element Method
FEA	=	Finite Element Analysis
CAD	=	Computer Aided Design
CAE	=	Computer Aided Engineering
SAFESA	=	SAFE Structural Analysis
NAFEMS	=	National Agency for Finite Element Methods and Standards
ESDU	=	Advisory Origination (Engineering Sciences Data Unit)
ABAQUS	=	Software package for FEM
NASTRAN	=	Software package for FEM (NASa STRuctural Analysis)
PCL	=	Patran Command Language
MATLAB	=	Numerical computing environment (MATrix LABoratory)
ASCII	=	American Standard Code for Information Interchange
IGES	=	Initial Graphics Exchange Specification
STEP	=	STandard for the Exchange of Product data
GUI	=	Graphical User Interface
CLIPS	=	Expert Shell (C Language Integrated Production System)
KBS	=	Knowledge Based System
API	=	Application Programming Interface
C/C++	=	Programming languages
Qt	=	Cross-platform graphical library

1. INTRODUCTION

Today's engineering tasks are complex and demands for minimising weight and maximising performance are standard requests. This work focuses on idealisation error control for the virtual testing of aerospace structures. The idea is to replace complex and expensive tests with reliable simulations.

1.1 Motivation for this Research

For the certification of new airplanes, the manufacturer has to demonstrate different aspects of safety. The structural stability of the wings is a critical factor. The limit load is defined as the highest load expected in the lifetime of a wing; the ultimate load is 1.5 times the limit load. Safety authorities require proof that wings can withstand the ultimate load, thereby including a safety margin of 50%. This demonstration is performed during complex tests, as shown in Figure 1.1.

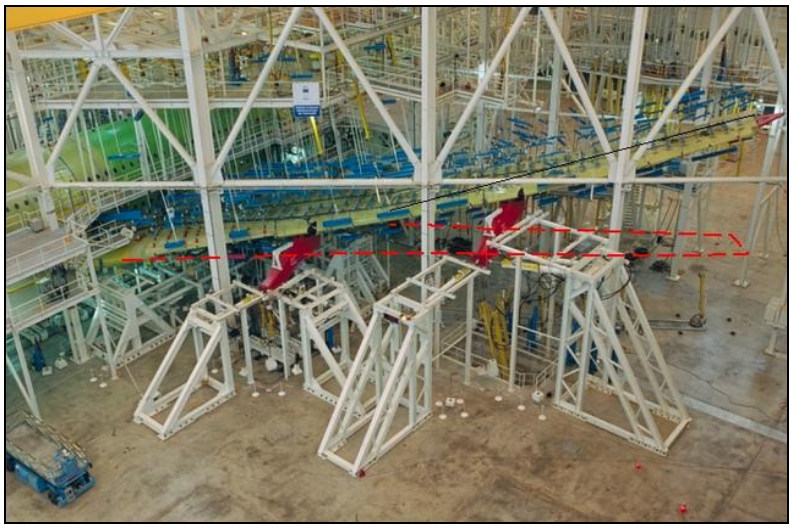

Figure 1.1: Airbus A380 wing load test [46]

The accurate calculation of the ultimate load is important, as the carried payload is the crucial factor for the economical success of an airplane. The currently developed Airbus A380 is an excellent example, as it couples an incredible size with a moderate weight. The finite element method (FEM) is the most suitable analysis method today. By dividing the whole structure into many small elements, a very good problem idealisation can be achieved. Each finite element is mathematically described with basic equations and contributes to the global solution by interacting with neighbouring elements.

However, because different sources of nonlinearity exist, the precise numerical failure prediction is a difficult task. The material will be stretched outside the linear elastic range, which leads to a change in the load paths and boundary conditions. Usually, the model building is based on experience and no general idealisation procedure is followed. The development of technologies for reliable FEM modelling was the motivation for the conducted research.

1.2 MUSCA Project

MUSCA (nonlinear static multiscale analysis of large aerostructures) is a research project addressing the aforementioned issues. This project is funded under the Sixth European Commission Framework Programme and lead by EADS. It unites major aircraft producer and research institutions such as EADS, Airbus, Dassault Aviation, Saab, Alenia, DLR, NLR, FOI, Cranfield University and others. Design and certification involves a number of structural tests ranging in complexity from simple coupon tests to the final full-scale test, as shown in Figure 1.2. MUSCA concentrates on static failure testing in the mid-range, from structural details to large components.

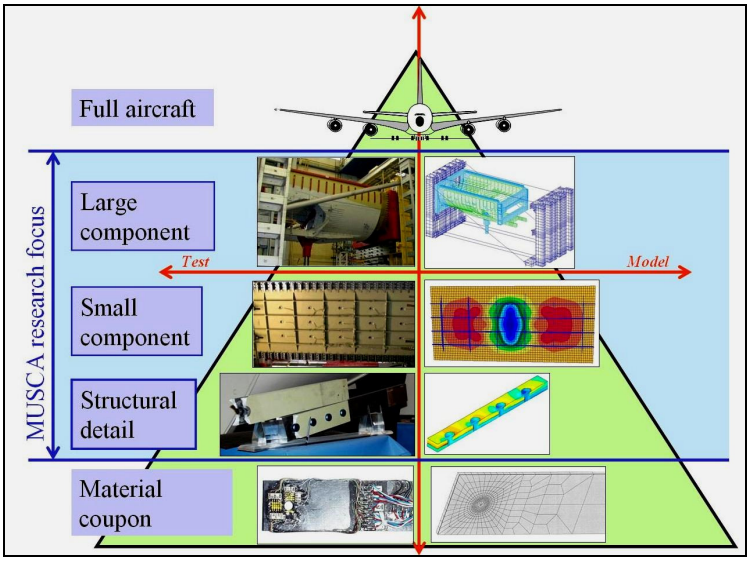

Figure 1.2: Test and analysis pyramid [91]

This research is funded in part by MUSCA. It is located in the work package Model Quality Assessment. The contribution of the PhD project is specified in [90] as: "… one partner will use the SAFESA Idealisation Error Control Procedure which is based on test results, hierarchical modelling, sensitivity analysis etc." The SAFESA procedure was developed about a decade ago at Cranfield University in order to create a method for reliable

FEM. In this work the procedure is applied to the highly nonlinear case of stiffened panel failure tests. Stiffened panels are very efficient load-carrying members and are the basic components for the construction of airplanes, satellites and ships. The Airbus panel model and high-quality test data were supplied by the project partner Airbus UK.

1.3 Statement of Objectives

In the context of FEM validation and verification [113] reliable error control techniques are required. A definition of V&V is given in [130]:

- Verification is the process of determining that a model implementation accurately represents the developer's conceptual description of the model.
- Validation is the process of determining the degree to which a model is an accurate representation of the real world from the perspective of the intended uses of the model.

Figure 1.3 is a derivative of a diagram presented in [130] and shows the different phases of modelling and simulation. It provides an insight into the interaction of reality/experiment, computer and conceptual model. The real-world structure is analysed to obtain the conceptual model (mathematical equations). The extracted equations are used to build a computer model. At this point SAFESA can be applied to validate the model.

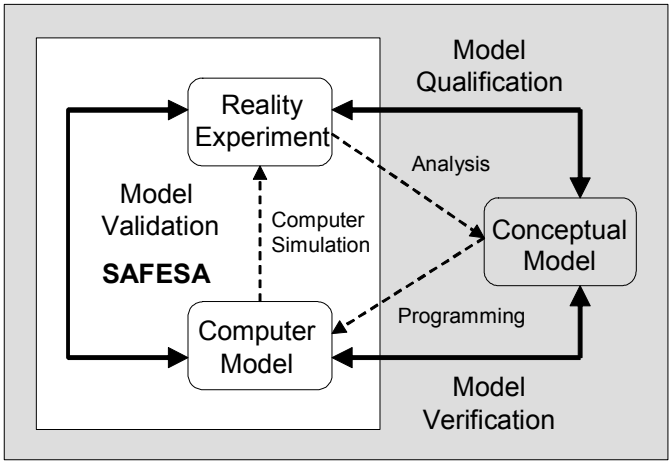

Figure 1.3: SAFESA in the validation and verification process

The original SAFESA procedure is tailored for linear static structural analyses. Applying this method to nonlinear cases was not yet investigated and carries the risk of neglecting some specific nonlinear error sources. A critical revision of the procedure is therefore important.

Structural testing of aircraft components adds significantly to the overall cost of designing and certifying a new aircraft. If testing can be reduced based on validated and safe numerical analysis methods, then this provides a significant technological advantage. This motivates research and the development of support tools. Expert systems seem hereby appropriate, because these programs help making decisions based on previous experience. Until now no software for idealisation error control exists.

The objectives of this project can be stated as:

1. **Updating the SAFESA methodology for nonlinear analyses,**
2. **Nonlinear idealisation error control demonstration,**
3. **Expert system development for FEM idealisation.**

In addition, this research is motivated by the fact that the reality of the engineering world is changing. Improvements in computing power enable the analyst of today to calculate larger geometries with higher complexity. Engineers are therefore much better trained in using analysis software than doing hand calculations. This leads to a mentality of blind belief in computer, and wrong analysis results are the consequence. The development of supporting tools will help making FEM modelling more reliable.

1.4 Methodology

In order to reach the project goals, the first phase is devoted to knowledge acquisition. A literature review will summarise current knowledge. Then modern FEM software is examined. This includes pre-processors, solver and result visualisation tools.

In a second phase the idealisation error control method is applied on stiffened panel compression tests. For familiarisation with SAFESA and the nonlinear FEM solver, a smaller test panel will be analysed first. This panel is used as a lecture demonstration at Cranfield University. The second analysis is the Airbus compression panel, which is similar to those used in aircrafts. Both studies will test the application range of the SAFESA method for nonlinear cases.

In the third phase the idealisation error control expert system is developed. Knowledge gained during the previous steps will determine the

program design. The objective is to implement a tool which practically helps making reliable FEM models.

1.5 Literature Review

This section gives an overview over the available literature on the relevant topics. The Finite Element Method is one of the most powerful approaches to analyse the failure behaviour of structures. The textbooks Zienkiewicz et al [144], Hughes [58], Cook et al [29], Schwarz [119] and Bathe [10] provide a general introduction into the FEM. Nonlinear aspects and the modelling of stiffened panels are reviewed in the following. After that, literature on idealisation error control and expert system development will be presented.

Post-buckling analysis of stiffened panels with nonlinear FEM

Nonlinear FEM is an advanced engineering topic, which involves many risks of errors. Reference books are Crisfield [31, 32] and Belytschko [13]. They are detailed and require a mathematical background. Chapter 17 of Cook et al [Cook01] and Chapter 6 of Bathe [10] give a good practical introduction without being too theoretical. Ramberg and Osgood [110] wrote the reference article for the elastic-plastic material model, which is used to model metals. ESDU [43] and the US department of defence [82] published metal data handbooks with tabulated properties. Dieter [35] together with Avallone and Baumeister [6] cover the entire scope of mechanical behaviour of metals.

Stiffened Panels are widely used in the construction of ships and airplanes. Classical theory books are Timoshenko and Gere [132], Bleich [18] and Burge [20]. Interesting textbooks on structures for aircraft engineering are Bruhn [19], Niu [96, 97] and Megson [80]. All these references helped to understand the theory of stiffened panel failure prediction. ESDU data sheets [38-42] give guidelines for the practical calculation of the different panel failure modes and were applied in this research. Recent theoretical articles by Paik et al [102] and Hughes et al [57] discuss modelling and computational aspects. The basic approach in panel buckling research is still performing experiments. The monographs of Singer [121] and [122] give a complete overview of performed experiments, available test data and references.

How to perform buckling and post-buckling analyses with FEM software is described in the ABAQUS documentation [1]. The provided examples are very helpful and have been a major source of knowledge in this project.

Current research focuses on weight reduction, nonlinear modelling assumptions, local-global simulation and validation methods: Bathe et al [11], Hu and Jiang [56], Kling and Degenhardt [65], Palacios [105], Young et al [142, 143], Heitmann et al [52, 53], Lynch et al [78], Murphy et al [93, 94], Hughes et al [57] and Paik and Seo [103, 104]. Each of these publications provided practical details for the modelling of stiffened metal panels. Idealisation aspects like contact modelling, boundary conditions and geometrical imperfections were found to have a strong influence on the correct failure prediction [52, 53, 56, 57, 78, 103, 104]. However, no publication described the use of idealisation error control techniques. Several nonlinear solvers were applied, the most commonly cited being ABAQUS.

The study of the PhD theses of Murphy [92], Lynch [77] and Heitmann [54] was very relevant for this work. They all investigated post-buckling of metallic panels used in airplanes. The focus was on efficient failure simulation for the design of lighter structures. They used ABAQUS and studied idealisation aspects like geometrical imperfection, material variance, joint and contact modelling. Some of their identified error sources were studied in more detail in this research.

Valuable information was also obtained from research on stiffened composite panels and cylindrical shells. Compared to metal panels, composite panels offer weight savings, but they experience sudden failure as no plastic deformation occurs. The modelling of composite panels, as described in Caputo et al [23], Degenhardt et al [33, 34], Orifici et al [100, 101], Rolfes et al [114] and Zimmermann et al [145], is demanding as materials are still under development. FEM meshes require more elements because several material layers need to be modelled. The buckling of cylindrical shells is analysed in Schneider et al [118] and Hühne et al [59]. They compare compression test results with numerical simulations and analyse idealisation aspects. In [118] geometrical imperfections are measured and included in the FEM model, and [59] studies the impact of geometrical and loading imperfections. Both studies conclude that geometrical imperfections of cylinders have a large impact and need to be included in the model.

Joint modelling for structural assemblies is a very active research topic because realistic FEM modelling is difficult. Joints can rarely be idealised with their actual three-dimensional shape because the model size would become too large. Usually, one-dimensional beam or spring elements are used in FEM models, which is a considerable simplification. Rutman and Bales-Kogan [115], Langrand et al [71] and Carroll et al [24] investigate modelling strategies for nonlinear solvers. Gundbrig [49] systematically

compares the theory with numerical simulations and test data. He studied the impact of pre-tension, nonlinear properties and failure. Some of the described modelling aspects will be investigated in this research.

Idealisation error control and SAFESA

Almost every book on FEM covers error control in some way. The most common topics are discretisation and meshing errors, rounding errors and problems solving the resulting system equations. Another category of literature explains how to use FEM software and highlights common application mistakes. However, literature on idealisation error control is rare, for instance nothing can be found in standard FEM books like Zienkiewicz et al [144] and Hughes [58].

In the first chapter of Bathe [10] a good example for choosing the appropriate mathematical model for a simple bracket structure is given. Szabó et al [127] introduce mathematical modelling for engineering computations in chapter 1, and give instructive examples in chapter 17. Chapter 10 of Cook et al [29] is the best text on this subject. Different sources of idealisation errors are described, such as element selection, material properties, boundary conditions, loading and connections in structures. Error treatment procedures like sub-modelling and model checking are explained. Felippa [45] chapter 8 outlines practical guidelines for modelling of loading and boundary conditions. Kurowski and Szabó [68, 69] explain techniques for finding and correcting modelling errors using recent FEM programs. Procedures for error control and model verification specifically for MSC.Nastran describes Stockwell [124].

Verification and validation (V&V) comprises the whole process of solving an engineering problem and includes idealisation error control. Babuška and Oden [7], Oberkampf et al [98] and Thacker [130] introduce V&V and its application scope. Roache [113] is the most detailed text on V&V and focuses on Computational Fluid Dynamics specific problems. Knight et al [66, 67] assess strategies and existing tools for performing V&V for safety-critical spacecraft applications. Special emphasis is placed on reliable FEM and knowledge-based support software. Due to design errors made in the past, they express the need for improved expert systems in mechanical engineering.

The SAFESA procedure will be described in chapter 2. Previous related work was published in Shephard et al [120] and Bathe [9]. In [120] a framework for controlling structural idealisation is explained and [9] describes hierarchical modelling for performing reliable analysis. Knight [Kigh04] proposes independently a similar error control terminology. The

official SAFESA documentation [116] is a NAFEMS report. Research publications are Morris et al [84, 85] and Vignjevic et al [137]. Both [84] and [137] outline the procedure and demonstrate its use on examples. Vignjevic [138] provides additional information, which is utilised as lecture notes at Cranfield University. The recent textbook from Morris [86] summarises the experience that has been gained and proposes an extension of the methodology. The following Cranfield theses provide further application examples. Hadi [50] applies idealisation error control on static loading of an airplane wing. Attwal [4] analyses natural frequencies of a rocket sled. Attwal [5] also describes the investigation of free vibrations of an aircraft floor structure, and static loading of a wing panel. These studies provide reference examples for linear SAFESA, which were the basis of research in this work.

FEM input parameter as Young's modulus, Poisson's ratio, yield stress, boundary conditions and geometrical imperfections have an amount of variance which influences simulation results, see Roache [113], Oberkampf et al [98] and Thacker [130]. Haugen [51] provides a detailed introduction of material uncertainty. This book publishes tabulated results for numerous metals and was the main source of information on material variance. The following publications provide practical guidelines on how to analyse structures with uncertainty. Schenk and Schuëller [117] describe buckling analyses of cylindrical shells with random geometric imperfections. Pradlwarter et al [107] present reliability estimation for a satellite with material and geometrical uncertainties. Mateus and Witz [79] studied the influence of side aspect ratios, geometric imperfections, boundary conditions and material variance on plates. Thacker et al [129, 131] and Pepin et al [106] studied the collapse of spherical shells (marine floats) with input variation. Tests and numerical simulation were repeated until statistically relevant data were compiled. The key result was that variation in yield stress has the largest impact on structural failure. A similar technique was developed in this research to simulate the impact of variance on geometry and material input.

Expert systems for FEM

FEM modelling is an excellent application area for expert systems. Many complex decisions have to be made and experience is crucial. Dym [37] gives a general introduction to different application areas. The aim of expert systems is helping to make design decisions. For this purpose expert knowledge must be formulated in rules, see Knight et al [66] and references therein. The present "state of the art" textbooks are Jackson [62] and Giarratano and Riley [47], which comprehensively describe theory and applications.

Early publications on expert systems for aircraft structural design, such as Bennett et al [14], Gregory and Shephard [48], Taig [128] and Cagan et al [21], date back from the 1980s. Those programs used much less powerful computers but their basic functionality is still used today. Recent developments, like Li and Qiao [73], Yañes et al [140] and Vandenbrande et al [136], focus on CAD data import and automatic FEM solver input generation. Expert systems which are directly integrated into FEM software are particulary useful. The development of tools for the pre-processor MSC.Patran is described in [27, 44, 141]. Other computer aided engineering programs with integrated expert systems are CATIA [72, 74], I-DEAS [95] and AMRaven [89, 123]. A general mechanical expert system is ICAD [8, 15]. Chapter 5 introduces expert systems and will describe these publications in more detail.

1.6 Thesis Structure

This first chapter described the project background, research goals and related literature. Chapter 2 explains the concepts of nonlinear FEM and the SAFESA method. Relevant FEM solvers are compared in order to find the most suitable one for this study. After that, the post-buckling analysis of stiffened panels is introduced. Chapter 3 describes the SAFESA analysis of the Cranfield panel test. Starting with design calculations, all potential error sources are examined. Chapter 4 presents the idealisation error analysis of the Airbus panel test. As this structure is more complex the modelling procedure took more effort. Industry supplied test data allowed a reliable result validation. Chapter 5 describes the development of the expert system. After reviewing existing tools the software design will be explained. Finally, the program that was implemented is demonstrated with an application example. Chapter 6 discusses results and draws conclusions. The Appendix provides stiffened panel documents, ABAQUS input, the updated SAFESA method and the expert system user guide.

2. NONLINEAR FEM AND SAFESA

During the last decades the finite element method (FEM) became the dominant analysis method in structural mechanics [10, 29]. A variety of engineering disciplines (such as aeronautical, biomechanical and automotive industries) commonly use integrated FEM in design and development of their products. The success of the method has led to the idea of replacing structural tests by computational analysis. This raises the question of how to qualify a structure by analysis alone, particularly in safety critical situations. The aim of the SAFESA procedure is to enable structural qualification to be carried out reliably and accurately using FEM. After explaining the theory, this chapter will then introduce error control techniques and finally outline nonlinear FEM software.

2.1 Finite Element Method

The FEM is a numerical method for solving problems which are described by partial differential equations. A domain of interest is represented as an assembly of finite elements with approximating functions. A continuous physical problem is transformed into a discretised finite element problem with unknown nodal values. For a linear problem a system of linear algebraic equations has to be solved.

2.1.1 Elliptic partial differential equations

A partial differential equation (PDE) is an equation involving a function of several variables and its partial derivatives. Mechanical field problems can be described with elliptical PDE's [119]. All independent variables have the meaning of spatial coordinates and the function usually describes a stationary or equilibrium situation. The three-dimensional LAPLACE equation:

$$\left(\frac{\partial^2}{\partial x^2} + \frac{\partial^2}{\partial y^2} + \frac{\partial^2}{\partial z^2} \right) \; u(x,y,z) = 0 \tag{2.1}$$

describes the shape of a stretched membrane or problems in electro-statics. It is a special case of the POISSON equation:

$$\left(\frac{\partial^2}{\partial x^2} + \frac{\partial^2}{\partial y^2} + \frac{\partial^2}{\partial z^2} \right) \; u(x,y,z) = f(x,y,z) \tag{2.2}$$

which appears in almost every field of physics. The analysis space Ω is bound by several boundary curves, and the union of all curves is denoted Γ. Boundary conditions need to be specified in order to define the problem correctly:

$$u(x,y,z) = \alpha \text{ at } \Gamma_1 \text{ (DIRICHLET condition)} \tag{2.3}$$

$$\frac{\partial u(x,y,z)}{\partial n} = \beta \text{ at } \Gamma_2 \text{ (NEUMANN condition)} \tag{2.4}$$

$$\alpha + \beta = \gamma \text{ at } \Gamma_3 \text{ (CAUCHY, ROBIN or mixed condition)} \tag{2.5}$$

α, β and γ are therefore functions at the boundary. Although methods for solving PDE exist, in most practical situations the equations cannot be solved analytically. After introducing some mechanical relations the numerical solution of PDEs will be explained in the following.

2.1.2 Displacement-stress-strain relations

A three-dimensional elastic body subjected to surface and body forces is examined. For the given geometry, applied load, displacement boundary condition and material property the displacement field for the body is sought. Corresponding strains and stresses are also of interest. The displacements along coordinate axis x, y and z are defined by the displacement vector $\{u\}$:

$$\{u\} = \{x\ y\ z\}^T \tag{2.6}$$

Strain-displacement relations extract the strain contained in a displacement field. Normal strain ε is the change in length divided by the original length. Shear strain γ is the amount of change in the angle between two material lines initially perpendicular to each other. Six different strain components can be placed in the strain vector $\{\varepsilon\}$:

$$\{\varepsilon\} = \{\varepsilon_x\ \varepsilon_y\ \varepsilon_z\ \gamma_{xy}\ \gamma_{yz}\ \gamma_{zx}\}^T \tag{2.7}$$

For small strains the relationship between strains and displacements is:

$$\{\varepsilon\} = [B]\{u\} \tag{2.8}$$

where $[B]$ is the matrix differentiation operator:

$$[B] = \begin{bmatrix} \partial/\partial x & 0 & 0 \\ 0 & \partial/\partial y & 0 \\ 0 & 0 & \partial/\partial z \\ \partial/\partial y & \partial/\partial x & 0 \\ 0 & \partial/\partial z & \partial/\partial y \\ \partial/\partial z & 0 & \partial/\partial x \end{bmatrix} \tag{2.9}$$

Normal stress σ and shear stress τ components form the stress vector $\{\sigma\}$:

$$\{\sigma\} = \{\sigma_x \ \sigma_y \ \sigma_z \ \tau_{xy} \ \tau_{yz} \ \tau_{zx}\}^T \tag{2.10}$$

which is related to strains for the elastic body by Hook's law:

$$\{\sigma\} = [E]\{\varepsilon\} \tag{2.11}$$

The elasticity matrix $[E]$ for isotropic materials (as metals, but not composites) has the following appearance:

$$[E] = \begin{bmatrix} \lambda+2\mu & \lambda & \lambda & 0 & 0 & 0 \\ \lambda & \lambda+2\mu & \lambda & 0 & 0 & 0 \\ \lambda & \lambda & \lambda+2\mu & 0 & 0 & 0 \\ 0 & 0 & 0 & \mu & 0 & 0 \\ 0 & 0 & 0 & 0 & \mu & 0 \\ 0 & 0 & 0 & 0 & 0 & \mu \end{bmatrix} \tag{2.12}$$

where λ and μ are elastic constants expressed through the Young's (elasticity) modulus E and Poisson's ratio υ:

$$\begin{aligned} \lambda &= \frac{\upsilon E}{(1+\upsilon)(1-2\upsilon)} \\ \mu &= \frac{E}{2(1+\upsilon)} \end{aligned} \tag{2.13}$$

2.1.3 Principle of virtual displacement

There are several possibilities to generally derive the finite element method [29, 10]. As the FE-analyses in this work are focused on structural problems the principle of virtual displacement (or virtual work) is used to introduce the FEM

[29, 54]. A very small virtual displacement δu is applied on a structure in equilibrium state. This small displacement must not violate compatibility or displacement boundary conditions. The necessary external work for this displacement and the saved inner deformation energy of the structure will equal.

$$\delta U = \delta W \tag{2.14}$$

The virtual deformation energy δU describes the amount of work, which is performed inside the structure by stress σ and strain ε.

$$\delta U = \int_{\Omega} \{\delta\varepsilon\}^T \{\sigma\} d\Omega \tag{2.15}$$

The virtual external work δW is done by body forces F in space Ω and surface tractions T on surface Γ.

$$\delta W = \int_{\Omega} \{\delta u\}^T \{F\} d\Omega + \int_{\Gamma} \{\delta u\}^T \{T\} d\Gamma \tag{2.16}$$

Inserting of 2.8 and 2.11 into the equilibrium 2.14 and exploiting $([B]\{\delta u\})^T = \{\delta u\}^T [B]^T$ gives:

$$\int_{\Omega} \{\delta u\}^T [B]^T [E][B]\{u\} d\Omega - \int_{\Omega} \{\delta u\}^T \{F\} d\Omega - \int_{\Gamma} \{\delta u\}^T \{T\} d\Gamma = 0 \tag{2.17}$$

With the FEM, the structure is divided into elementary shapes where the nodal displacements can be calculated. The deformation in every element results from the shape functions $[N_i^{(e)}]$ which are derived from the node locations. Global displacements $\{u^{(e)}\}$ follow from the assembly of all local displacements $u_i^{(e)}$ at the n-elements.

$$\{u^{(e)}\} = \sum_{i=1}^{n} [N_i^{(e)}] \{u_i^{(e)}\} \tag{2.18}$$

In 2.17 the problem is still solved exactly. The equation is replaced by 2.18 and can be solved with a system of linear equations. Insertion into 2.17 leads to an expression for every element:

$$\int_{\Omega} \{\delta u^{(e)}\}^T [N]^T [B]^T [E][B]\{u^{(e)}\} d\Omega$$
$$- \int_{\Omega} \{\delta u^{(e)}\}^T [N]^T \{F\} d\Omega - \int_{\Gamma} \{\delta u^{(e)}\}^T [N]^T \{T\} d\Gamma = 0 \tag{2.19}$$

This equation is fulfilled independently of the virtual displacements. The deformations are constant for the integration over the element. It follows:

$$\underbrace{\int_{\Omega} [N]^T [B]^T [E][B] d\Omega}_{[K^{(e)}]} \{u^{(e)}\} \underbrace{- \int_{\Omega} [N]^T \{F\} d\Omega - \int_{\Gamma} [N]^T \{T\} d\Gamma}_{\{f^{(e)}\}} = 0 \tag{2.20}$$

Here $[K^{(e)}]$ is the element stiffness matrix and $\{f^{(e)}\}$ the load vector of the i-th element. The assembly of all element stiffness matrices and all load vectors leads to a system of equations for the whole structure:

$$[K]\{u\} = \{f\} \tag{2.21}$$

$[K]$ is known as the global stiffness matrix, and $\{f\}$ is the vector of the applied loads. The solution $\{u\}$ consists of the nodal displacements.

2.1.4 Solution procedure

In order to give a general overview how the finite element method works, the main steps of the solution are listed below.

Discretising the continuum. The first step is to divide a solution region into finite elements. The element mesh is typically generated by a pre-processor program. Element shapes are triangles, rectangles, tetrahedrons, etc, but curved shapes are allowed also. The elements need to cover the whole space and must not overlap, see Figure 2.1. The mesh description consists of nodal coordinates and element connectivity.

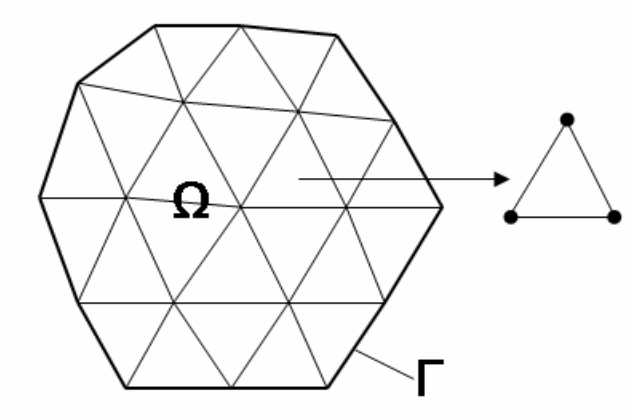

Figure 2.1: Finite element meshing

Selecting interpolation functions. The shape functions $[N_i^{(e)}]$ in (2.18) are used to interpolate the field variables over the element. Continuity conditions need to be fulfilled and polynomials are selected as interpolation functions. The degree of the polynomial depends on the number of nodes assigned to the element. Figure 2.2 illustrates linear shape functions for one- and two-dimensional elements using Lagrange interpolation.

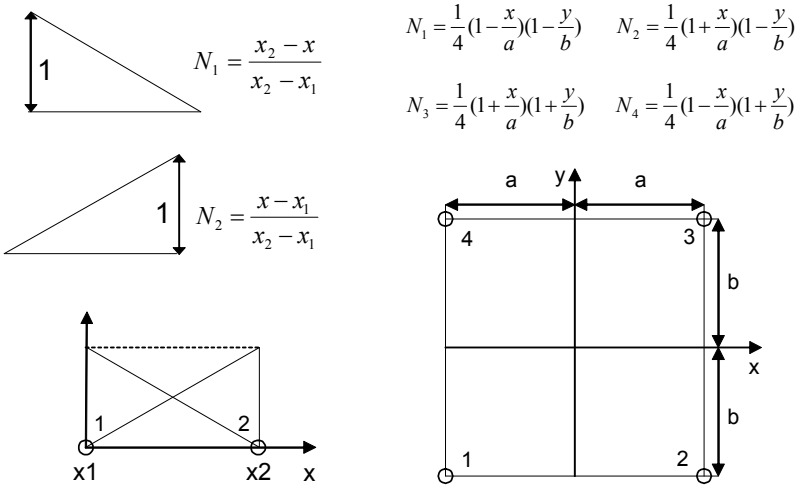

Figure 2.2: Linear shape functions for bar and rectangle element

Assembly of the element equations. The global equation system is assembled using all element equations. Element connectivities are used to create a system matrix with a narrow bandwidth. That means only few entries outside the matrix diagonal become populated. Then boundary conditions are applied. Hereby it is important to constrain the model correctly.

Solving the global equation system. The equation system is typically sparse, symmetric and positive definite. Symmetry and sparsity are used to economise

storage and computations. Direct or iterative methods can be applied for the solution.

Strains and stresses in the structure are calculated from the resulting nodal displacements. For this purpose, local strain-displacement and stress-strain relations analogous to (2.8) and (2.11) are used:

$$\{\varepsilon^{(e)}\} = [B][N]\{u^{(e)}\} \tag{2.22}$$

$$\{\sigma^{(e)}\} = [E][B][N]\{u^{(e)}\} \tag{2.23}$$

An important FEM result is von Mises stress, which is used to predict the yielding of materials under any loading conditions.

$$\sigma_{Mises} = \sqrt{\frac{(\sigma_x - \sigma_y)^2 + (\sigma_y - \sigma_z)^2 + (\sigma_z - \sigma_x)^2 + 6(\tau_{xy}^2 + \tau_{yz}^2 + \tau_{zx}^2)}{2}} \tag{2.24}$$

Von Mises stress has the same numerical value regardless of the coordinate system in which it is computed. This qualifies it as a general indicator for material nonlinearity.

2.2 Nonlinear FEM

A nonlinear structural problem is one in which the structure's stiffness change as it deforms. All physical problems are nonlinear. Linear analysis is a convenient approximation for modelling purposes, but it is inadequate for structural simulations where substantial departure from linearity is common.

2.2.1 Sources of nonlinearity

Sources of nonlinearity in structural mechanics are shown in Figure 2.3.

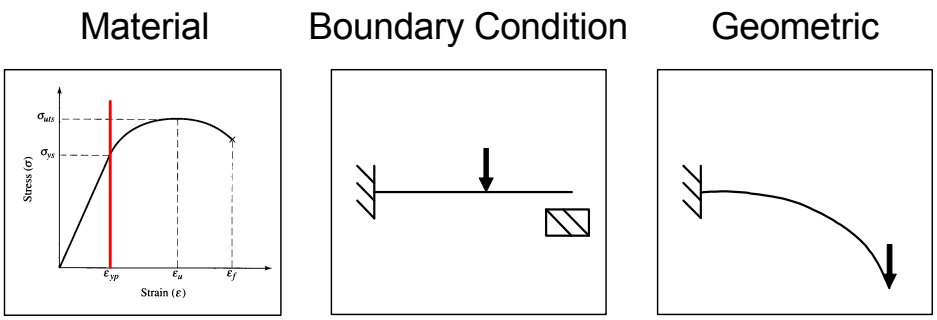

Figure 2.3: Sources of nonlinearity

Material nonlinearity appears when the material is stretched outside the linear elastic range. Most metals have a fairly linear stress-strain relationship at low strain values. At higher strains the material yields and is permanently deformed. With hardening, metals gain stiffness up to the point where the material fails. Rubber and composite materials behave differently [1] but were not used in this research. **Boundary nonlinearity** occurs if the boundary conditions change during the analysis. The boundary is the outer structural surface or an interface in an assembly and is usually defined using contact. A gap between adjacent parts may open or close and contacting surfaces can have sliding contact with friction. **Geometric nonlinearity** is present when geometrical changes during the analysis affect the response of the structure. This can be caused by large deflections, rotations or snap-through. Due to this deformation internal load paths change and the structure behaves differently.

In the loading process of stiffened panels all three forms of nonlinear behaviour occur. Buckling is a natural, geometric nonlinear phenomenon, which will induce contact behaviour between panel sub-components. Typical aircraft panels will pass into the material plastic range before structural collapse. The following sections describe methods for solving nonlinear problems.

2.2.2 Newton-Raphson method

When the FEM is used for solving nonlinear elastic-plastic problems, the load or displacement is applied in increments. Equilibrium is sought in each increment by minimising the force residual, i.e. the difference between the external and internal forces. A popular method for establishing equilibrium is the Newton-Raphson scheme [29]. The algorithm for finding zero values of a real-valued differentiable function $g : \Re \to \Re$ is explained as follows:

$$g(x) = 0 \tag{2.25}$$

The process is started with an initial guess x_n, which is reasonably close to the zero value, as shown in Figure 2.4. Then the function is approximated by its tangent line, and the x-intercept of this tangent line will be computed. The new value x_{n+1} is typically a better approximation than the original guess.

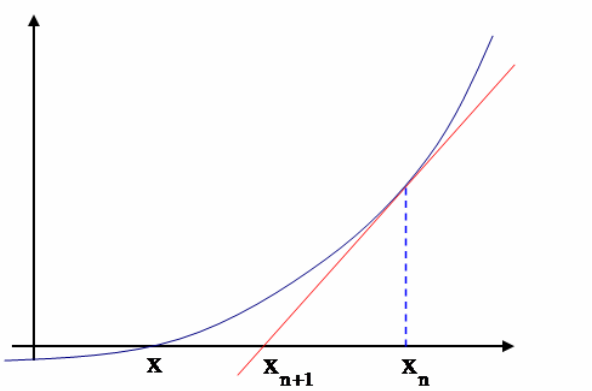

Figure 2.4: Functionality of the Newton-Raphson method

The algorithm is formulated as:

$$x_{n+1} = x_n - \frac{g(x)}{g'(x)} \tag{2.26}$$

In numerical calculations the derivative $g'(x)$ can be approximated by using the **regula falsi**:

$$g'(x_n) = \frac{x_n - x_{n-1}}{g(x_n) - g(x_{n-1})} \tag{2.27}$$

The concept can be applied to solve systems of k equations, which means finding the zeros of continuously differentiable functions $g : \Re^k \to \Re^k$. The derivative becomes the Jacobian matrix $J(x)$:

$$[J(x)] = \frac{\partial g}{\partial x}(x) = \begin{bmatrix} \frac{\partial g_1}{\partial x_1} & \frac{\partial g_1}{\partial x_2} & \cdots & \frac{\partial g_1}{\partial x_k} \\ \frac{\partial g_2}{\partial x_1} & \frac{\partial g_2}{\partial x_2} & \cdots & \frac{\partial g_2}{\partial x_k} \\ \vdots & \vdots & \ddots & \vdots \\ \frac{\partial g_k}{\partial x_1} & \frac{\partial g_k}{\partial x_2} & \cdots & \frac{\partial g_k}{\partial x_k} \end{bmatrix} \tag{2.28}$$

The iteration formula for a system of k equations is:

$$x_{n+1} = x_n - [J(x_n)]^{-1} g(x_n) \tag{2.29}$$

The classic Newton-Raphson method is usually avoided because the Jacobian must be formed and solved at each iteration, which is very expensive.

2.2.3 Modified Newton-Raphson method

The modified Newton-Raphson method uses the same algorithm as the Newton-Raphson iterative procedure, but tries to economise computations. The Jacobian is calculated only at the first iteration and kept constant during the remaining iterations of the increment [1]. System equation (2.21) can now be formulated as:

$$([K_{Lin}]+[K_{NonLin}])\{u\}=\{f\} \tag{2.30}$$

The linear part $[K_{Lin}]$ of the stiffness matrix is constant, but the nonlinear part is dependent on the values of u and σ. In order to get a force-displacement relation for the increment, the actual tangent stiffness $[K_n]$ and the changing load components are calculated.

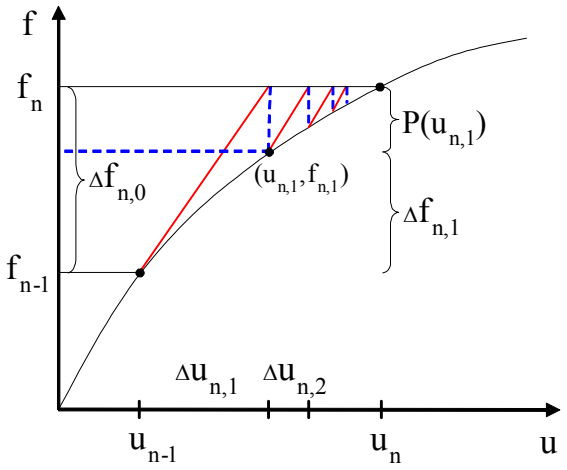

Figure 2.5: Modified Newton-Raphson method

Starting from the displacement $\{u_{n-1}\}$ and the load $\{f_{n-1}\}$, the tangent stiffness $[K_n]$ is calculated, as shown in Figure 2.5.

$$[K_n(\{u_{n-1}\})]=[K_{Lin}]+[K_{NonLin}(\{u_{n-1}\})] \tag{2.31}$$

With help of $[K_n]$ and the initial load increment $\{\Delta f_{n,0}\}$ the displacement change $\{\Delta u_{n,1}\}$ is obtained.

$$\{\Delta u_{n,1}\} = [K_n^{-1}(\{u_{n-1}\})]\{\Delta f_{n,0}\} \tag{2.32}$$

This results in the new load balance:

$$\{\Delta f_{n,1}\} = \{\Delta f_{n,0}\} - \{P(u_{n,1})\} \tag{2.33}$$

with $\{f_{n,1}\} = \{f_{n-1}\} + \{\Delta f_{n,1}\}$, $\{u_{n,1}\} = \{u_{n-1}\} + \{\Delta u_{n,1}\}$ and $\{P\}$ as the inner load vector. In a second iteration the displacement increase is:

$$\{\Delta u_{n,2}\} = [K_n^{-1}(\{u_{n-1}\})]\{\Delta f_{n,1}\} \tag{2.34}$$

and a new load balance follows:

$$\{\Delta f_{n,2}\} = \{f_{n,2}\} - \{P(u_{n,2})\} \tag{2.35}$$

with $\{f_{n,2}\} = \{f_{n,1}\} + \{\Delta f_{n,2}\}$ and $\{u_{n,2}\} = \{u_{n,1}\} + \{\Delta u_{n,2}\}$

The iteration continues until a defined convergence criterion is met. This can be a value for the norm of the residual or the magnitude of the load increment.

2.2.4 Modified Newton-Raphson method with damping

The modified Newton-Raphson procedure is a robust algorithm and is utilised in all major commercial nonlinear solver software. However, the solution procedure will run into convergence difficulties if the analysed structure exhibits instabilities as skin-buckling, stringer failure or global collapse.

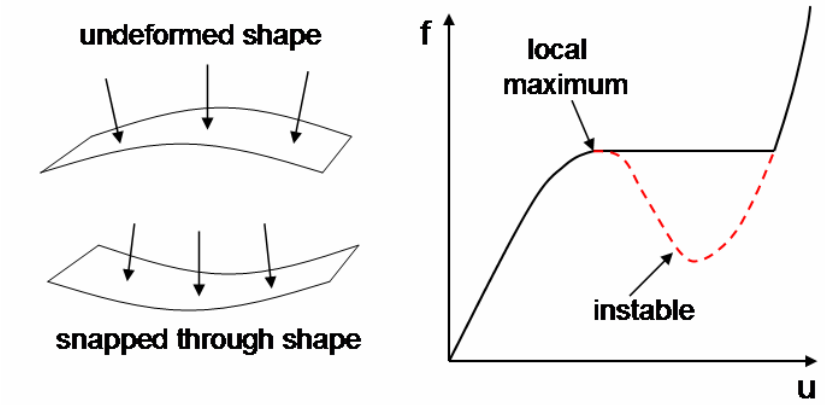

Figure 2.6: Snap-through stability problem

In so called snap-through problems the geometry changes spontaneously as shown in Figure 2.6. The algorithm remains at the local maxima when the load-displacement response shows a negative slope. The damped Newton-Raphson method provides a mechanism for stabilising problems through automatic addition of volume-proportional damping $[D]$ to the model. With the help of artificial damping the system loses energy and the load-displacement path stabilises.

$$\{f\} = [K]\{u\} + [D]\{u\} \tag{2.36}$$

It follows a redistribution of the forces:

$$\{f\} = \{f^{outer}\} + \{f^{inner}\} + \{f^{damp}\} \tag{2.37}$$

The added term makes the algorithm proceed to an equilibrium state and the damping then vanishes. The following definition of the damping term is specific to the solver ABAQUS [1].

$$\{f^{damp}\} = c\{v\}[M] \tag{2.38}$$

The vector of the damping forces is composed of the damping constant c, the vector of nodal velocities $\{v\}$ and the mass matrix $[M]$.

$$\{v\} = \frac{\{\Delta u\}}{\{\Delta t\}} \approx \frac{\{\Delta u_n\} - \{\Delta u_{n+1}\}}{df} \tag{2.39}$$

Nodal velocities and the time increment $\{\Delta t\}$ have no physical meaning for quasi-static problems and are approximated with a displacement-force ratio. The damping parameter can also be defined manually and showed to influence the solution behaviour in some cases [54, 77]. (Sensitivity analyses for models used in this research indicated that the default parameter is appropriate.) The modified Newton-Raphson method with damping has proved to be the most stable and economic solution method for stiffened panel failure simulations [54, 77, 92].

2.3 SAFESA

SAFESA (SAFE Structural Analysis) [116] is a procedure for formally controlling idealisation errors in linear static FEM, and was originally developed at Cranfield University, see Morris et al [84, 85] and Vignjevic et al [137]. The aim of the method is to provide a systematic procedure whereby an engineer is able to perform an analysis of a structure in such a way that any error which may occur as a result of the idealisation process is controlled. This means that certain error bounds will be obtained, and will reduce variation in results when a structure is analysed using different codes or by different analysts.

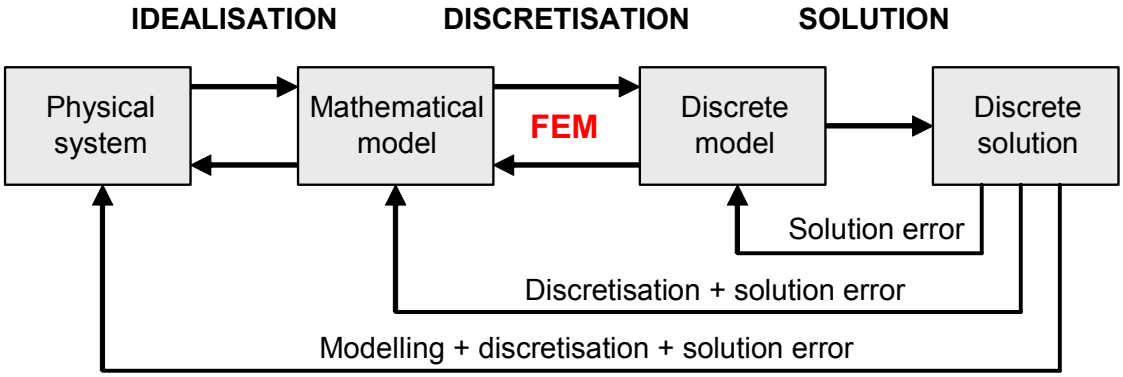

Figure 2.7: The FEM analysis process [45]

The idealisation process represents the step of converting the real-world structure into an idealised structure that can be modelled in practice using the finite element method (FEM), see Figure 2.7. Within this process the analyst is required to make a series of assumptions, generally simplifications, which contribute to the error in the final analysis. The aim is to provide a rigorous process for identifying these assumptions and controlling the resultant error.

2.3.1 Location in the FEM procedure

In order to develop an idealisation error control it is helpful to classify the whole analysis process and identify clearly which error sources need to be addressed, see [85] and [116]. The location of SAFESA within the FEM analysis process is displayed in Figure 2.8.

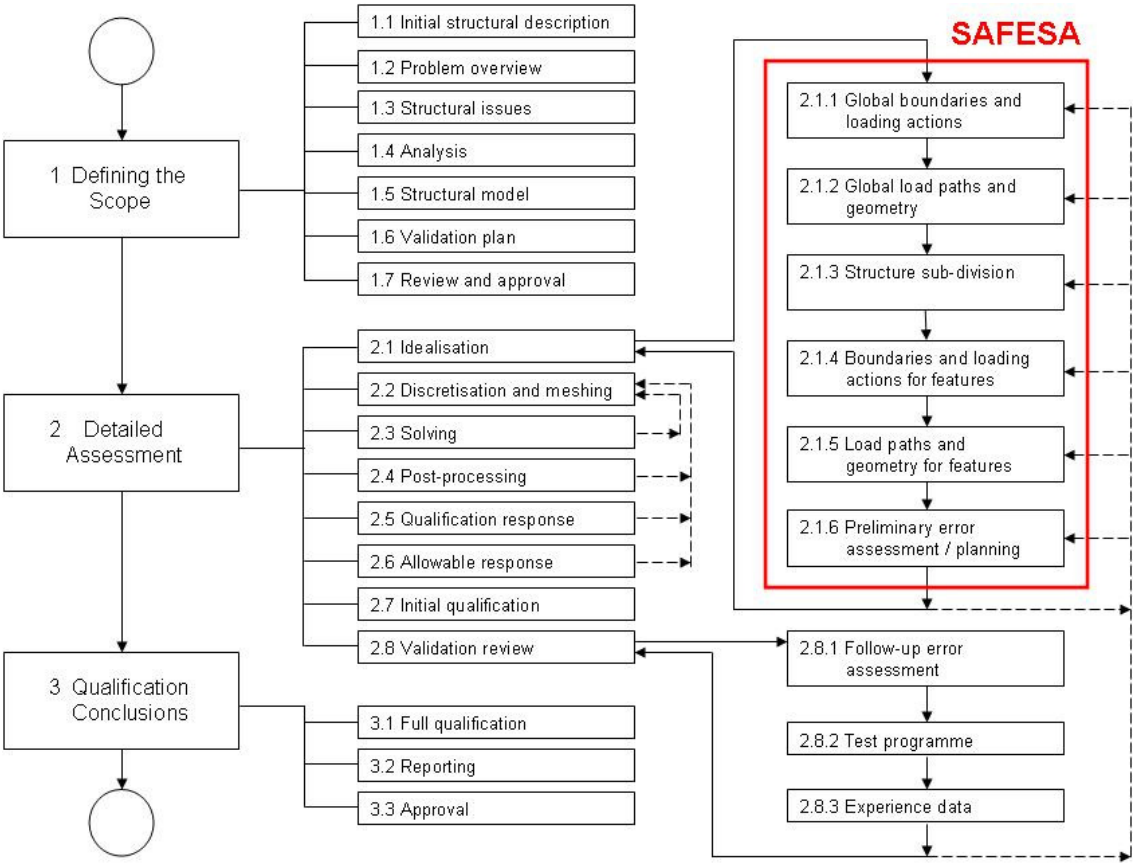

Figure 2.8: SAFESA within the FEM procedure

Three global stages can be identified:

- **Defining the scope**
  This initial stage involves defining the qualification criteria, bounding the structure, analysis and validation planning.
- **Detailed assessment**
  Detailed analysis and preliminary qualification is performed. This involves identification, qualification and treatment of errors.

  In stage 2.1 the idealisation process transforms the high level description of the real structure into a computer model.

  Stages 2.2 to 2.8 yield a numerical solution of the computer model and involve discretisation, meshing, solving, post processing and validation of the model.
- **Conclusions**
  Finally, calculated results are compared with the acceptance criteria and conclusions for the structural capability are drawn.

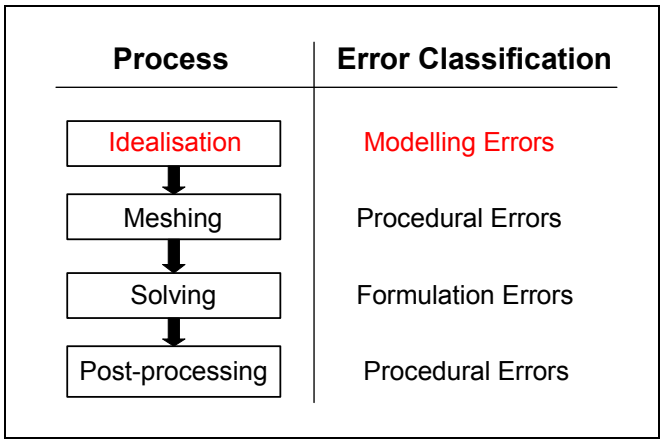

Figure 2.9: Location of FEM errors

Errors are categorised depending on where they are generated within the analysis, see Figure 2.9. Modelling errors are generated in the idealisation process, procedural ones during meshing and post-processing, and formulation errors in the process of solving the finite element model. It is clear that modelling errors will propagate right from the beginning, and that all following steps depend on a sensible idealisation.

2.3.2 SAFESA analysis steps

Controlling and treating errors in the idealisation process requires that a step-by-step procedure is adhered to. Each step within this process may itself be considered as a process with input data, an action and output data, as shown in Figure 2.10. During the procedure, information is fed from one step to the next in a linear sequential manner and includes possible feed back loops, i.e. the process can be iterative. Therefore, it is unlikely that a simple sequential pass through the process will be sufficient.

It is important to notice that only experience and simple calculations can be used in the first iteration. A flagging technique is used to determine that errors at a specific step in the method have not been adequately treated and must be analysed at a later stage or during one of the feedback loops. The method has a stopping criteria which requires that no error flags remain set when the final step is completed.

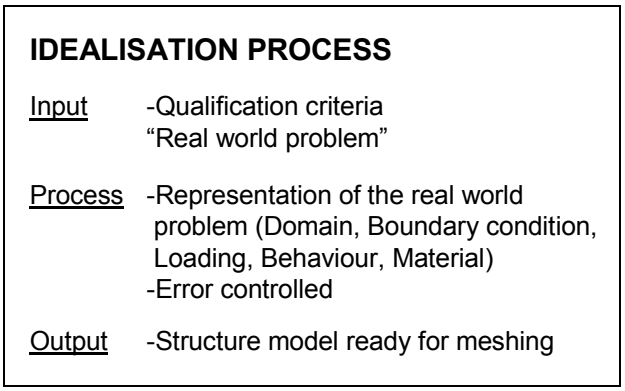

Figure 2.10: Schematic idealisation process

The error control procedure applies at the idealisation stage 2.1. Analysis input is a description of the real world problem (drawings, CAD model …) and the output is a description of the structure ready for meshing. The procedure follows a systematic process (a detailed outline can be found in the appendix):

- **Step 1 & 2: Global idealisation, such as boundaries, boundary conditions, loading and load paths for the structure as a whole.** Geometrical simplifications such as omitting unnecessary structural details like bolt holes or curved corners can be made. Boundary conditions and loading actions have to be chosen in a way that they conform with FEM modelling capabilities. Error bounds are estimated and all ambiguity is flagged out for later investigation.

- **Step 3: Decomposition of the structure in features and primitives.** The feature represents a recognisable entity to the analyst, which exhibits coherent, structural properties. This step is carried out after the global idealisation, but may be repeated for individual features if necessary. The main ideas behind this step are the study of feature interconnections, and the decomposition of a big problem in smaller ones.

- **Step 4 & 5: Repeating the first two steps on the local level.** New boundary conditions and loading actions have to be derived from feature contact surfaces. This process may follow directly from the definitions at a higher level, but in general will require more detailed description here.

- **Step 6: Assessment of the performed analyses so far.** Either error bounds can be given or additional testing (**Step 7**) will be necessary. This step also requires the planning of all sensitivity studies, hierarchical modelling and test programmes which have been flagged in steps 1 to 5.

- **Step 7: Run the test programme.** Execution of corroborative tests. The results will be compared with the assumed behavior. If the assumptions were inappropriate, they get adapted to the test result.

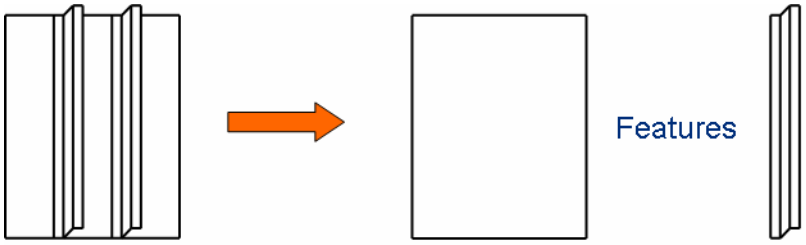

Figure 2.11: Assembly decomposed into features

Figure 2.11 shows the idea of structural decomposition in step 3. A stiffened panel is disassembled into its features: plate and stiffener. Substructures can be defined as:

- **Feature** – A component of a structure exhibiting a specific characteristic. It is desireable that the feature boundary conditions can be described in reasonably simple terms, as this will aid in the analysis of the load paths and any further subdivision of the feature that may be required.
- **Primitive** – Is a part of a feature. Its description will depend on the accuracy required for the analysis and may need reconsideration when errors arising from sources within the primitive are considered.

2.3.3 Error sources and treatment

The following error sources can be identified during the idealisation process:

Mathematical model – The derivation of a mathematical model employs physical laws, mathematical manipulation and sensible approximations. These approximations are required to yield a useful set of expressions from the underlying physical laws. Each approximation introduces simplifications and associated errors. Therefore, the errors introduced by each assumption must be considered.

It is possible to introduce specific assumptions over portions of the domain, which allow simplification of the mathematical model by reducing the physical dimensionality. This is the case when using shell theory for modelling a three-dimensional structure.

Domain – Very often errors are generated by eliminating geometric details. An understanding of the factors that influence the analysis is critical to the successful application of domain simplification. In most cases, domain simplifications are carried out on the basis of previous experience in the solution of similar problems.

Material properties – Material parameters are probabilistic in nature and have to be specified. Any deviation from the correct values introduces error into the solution.

Boundary conditions, loading – In addition, these model input parameters are difficult to abstract from the physical situation because reasonable simplifications need to be made. Very often structures are modelled with a built-in support by removing all degrees of freedom at the involved nodes. This simplification does not exist in reality.

The idea of the error control approach is using the various error estimations as a base from which the idealisation is refined until the error estimate is acceptably small. Table 1 summarises error sources and treatment techniques:

	Control techniques				
Error source	Experience rules	Simple calculations	Experimental test Results	Hierarchical modelling	Sensitivity analysis
Mathematical model	X	X	X	X	X
Domain	X	X		X	X
Material properties	X	X	X		X
Boundary conditions and loading	X	X	X	X	X

Table 2.1 Idealisation error sources and control techniques

The most convenient technique for improving reliability is to employ experience related to successfully applied idealisations of a particular structure type. By gaining experience, analysts develop and document specific sets of idealisation rules that are appropriate to their specific class of problems.

Hierarchical modelling means changing the level of idealisation. The whole structure is decomposed into features and primitives, and the resultant smaller problems will be solved. **Sensitivity analyses** study the effect of small changes in the value of input parameters on the resultant output parameters. Input parameters comprise material properties, the domain and boundary conditions.

By following this error control approach, the position and role of testing changes. Normally, testing is performed as the main validation, that a structure

will perform as required. Here, its role is to validate that the finite element modelling process is appropriate and the errors are controlled and bounded. Testing is now part of the error analysis and it is the responsibility of the analyst to define the test parameters in order to obtain appropriate error information.

The objective of this research is to apply the error control methodology to nonlinear analyses and to identify its weaknesses. Material modelling and boundary condition errors have been studied with the original SAFESA, but they are much more complex in the new context. Geometrical nonlinearity does not occur in linear analysis, as materials only deform elastically. New error potential also results from the fact that the structures of interest can break or partly fail.

2.4 Nonlinear FEM Software

Nonlinear FEM software is utilised by all manufacturing industries, and there is a choice of several programs. ABAQUS [2] is used by most MUSCA partners and was often cited in the literature. After a comparison with NASTRAN, the main nonlinear modelling details will be presented at a later stage.

2.4.1 Pre-processors

Pre-processors are utilised for FEM model building and result visualisation. Pre-processor functionality is sometimes incorporated in computer aided design (CAD) and finite element analysis (FEA) packages. Prominent examples are I-DEAS [61] or CATIA [25], which offer CAD, pre-processor, FEM and result visualisation in one program. For this project the pre-processors MSC.Patran [88], ABAQUS/CAE [2], Hypermesh [60], Truegrid and I-DEAS [61] were tested. Finally, the first two were selected.

MSC.Patran (version 15) is tightly linked to MSC.Nastran, which offers seamless job submission and result visualisation. The interface to other FEM solvers is more elaborate, as the input files need to be adapted. CAD data import is one of the strong sides of Patran, but the usability could be improved. ABAQUS/CAE (version 6.7-1) is part of the ABAQUS package. Building small models and result visualisation works perfectly. However, it is difficult to work with more complex geometries and especially CAD data import. Therefore, this tool was mainly used for mesh refinement and the visualisation of models generated with Patran.

2.4.2 Nonlinear solvers

Panel post-buckling publications describe the use of ABAQUS [23, 33, 52-54, 57, 65, 77, 78, 79, 92-94, 100, 101, 114, 145], NASTRAN [55, 100, 101, 118],

ANSYS [23], STAGS [117, 142, 143], ADINA [56], LS-Dyna [100] and SAMCEF [33] as well as company in-house programs [56, 66]. Solver comparison studies [33, 100, 101] do not express recommendations, but the solver most commonly cited is ABAQUS. For this project the implicit solvers ABAQUS/Standard (version 6.6-1) [1], MSC.Nastran (version 2005) [87] and NX Nastran (version 2006) [135] were compared.

The studied model is a stiffened panel compression test, similar to the one described in the next chapter. The model was discretised with NASTRAN Quad4 and ABAQUS S4R shell elements. NASTRAN's nonlinear solver 106 with the convergence tolerance level "Very high" was applied, all other parameters remained at the default setting. (The improved nonlinear solver 600 [105] was during that period not available at Cranfield.) ABAQUS modelling aspects will be explained in the rest of this chapter. Figure 2.12 shows the load-shortening graphs using models with a sufficient number of elements and identical meshes.

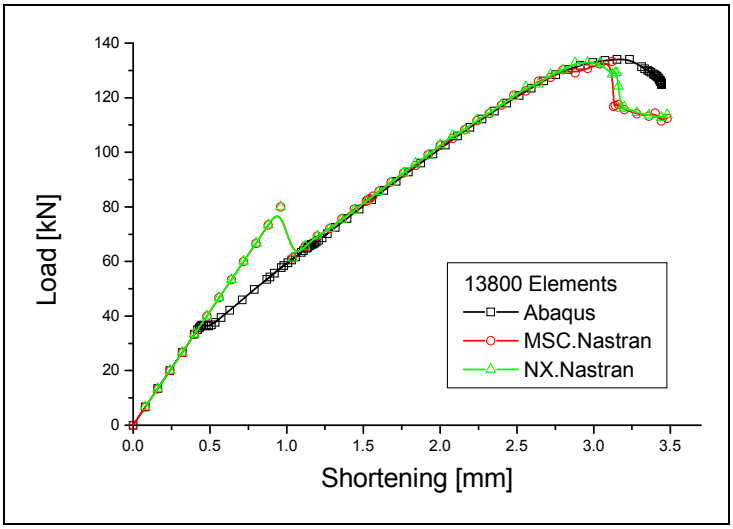

Figure 2.12: Nonlinear solver comparison

All solvers predicted a collapse load of about 130 kN but differed in simulating the onset of global buckling. The ABAQUS solution shows only a light drop of stiffness at around 0.6mm displacement. NASTRAN's solutions displays a much bigger drop at around 0.9mm displacement, which seems incorrect. MSC and NX Nastran give almost identical solutions. The final collapse is similar in both models, with the ABAQUS curve looking smoother. ABAQUS showed a better solution performance in respect of solution robustness, calculation speed and memory requirement. NASTRAN suffered from numerical difficulties, which lead to simulation crashes. Therefore, ABAQUS was selected as the appropriate solver.

2.4.3 ABAQUS solution procedure

ABAQUS/Standard is a general purpose nonlinear solver. For quasi-static analyses the Lagrangian FEM formulation is used, what means that the mesh is embedded in the material and moves and deforms with the material. The simulated process in quasi-static analyses is slow and time dependency of the solver is not necessary. Units are not prescribed by default and have to be chosen consistently. SI-units are used in this work. Displacement is given in mm, force in N and stress in $\mathrm{N/mm^2}$.

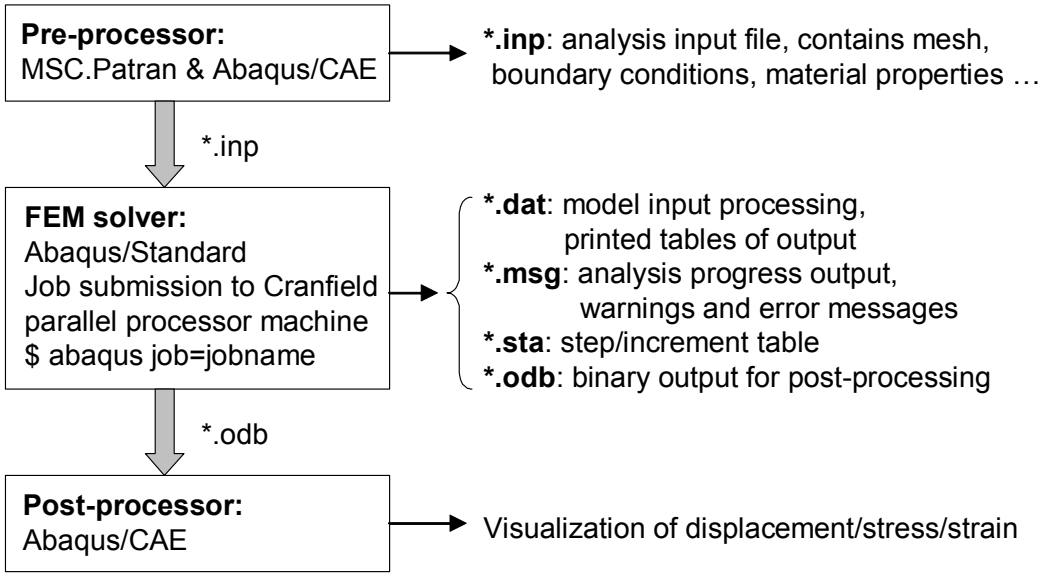

Figure 2.13: ABAQUS solution process

Figure 2.13 shows the ABAQUS solution process. The FEM model is saved in the input files *.inp using a pre-processor. Pre- and post-processing is performed at a local PC. The actual simulations were run on Cranfield's Astral multi-processor machine. Results were written as ASCII tables in *.dat files, or were saved in binary *.odb format. Output needed to be limited to important parameters; otherwise the file size became too large.

2.4.4 Shell elements

Shells are the most commonly employed finite elements in this kind of analysis. Three-dimensional panel structures are sufficiently thin to be modelled with two-dimensional elements [29]. The element description in sections 2.1.3 and 2.1.4 explain basic ideas. After finding interpolation functions, elements need to be transformed into general coordinates and adopted to the used plate theory.

The ABAQUS shell element library [1] is divided into three categories consisting of general-purpose, thin and thick formulations, as shown in Table 2.2. Thin elements provide solutions for problems that are adequately described by Kirchhoff's shell theory and thick elements yield solutions for structures that are best modelled by shear flexible Midlin shell theory [29]. General-purpose elements provide solutions to both thin and thick problems. These elements adapt their properties depending on the thickness of the plate [16]. For most applications general-purpose elements are suitable.

ABAQUS element	Element order	Strain	Thin / thick	Hourglass control	Integration	DOF/ node
S4	First	Finite	General purpose	No	Full	6
S4R	First	Finite	General purpose	Yes	Reduced	6
S4R5	First	Small	Thin	Yes	Reduced	5
S8R	Second	Small	Thick	No	Reduced	6
S8R5	Second	Small	Thin	No	Reduced	5

Table 2.2 Conventional ABAQUS shell elements [1]

Thick shell problems assume that the effects of transverse shear deformation are important to the solution. Thin shell problems, on the other hand, assume that transverse shear is small enough to be neglected. A shell with a thickness-length ratio greater than 1/15 can be considered "thick". Shells with a smaller ratio are considered as "thin".

First order elements S4, S4R and S4R5 use 4 nodes, and second order elements S8R and S8R5 use 8 nodes. Second order elements should be more accurate, because they use quadratic interpolation. But results of first order elements can be more accurate because shear locking is avoided. In general, a finer mesh with first order elements is preferable then using second order elements. Elements whose names end with the number "5" use only 5 degrees of freedom at each node: three translations and two in-plane rotations (no rotations about the shell normal). Only S4 and S4R are general purpose elements, capable of handling finite element strain properly.

Shell elements with the letter "R" use reduced integration, which significantly reduces running time. A 4-noded element with reduced integration uses only one Gauss point to form the element stiffness. Linear reduced integration elements tend to be too flexible, because they suffer from their numerical

problem called hourglassing [1]. This problem can be successfully treated with mesh sensitivity studies.

All elements use numerical integration to calculate the stresses and strains independently at each section point (integration point) through the thickness of the shell, thus allowing nonlinear material behaviour. By default, ABAQUS uses five section points through the thickness of a shell.

2.4.5 Material modelling

The panels analysed in this research consist of metals, mainly aluminium alloys. The elastic-plastic material model is suitable to model the linear and nonlinear behaviour. There are two possibilities to derive the material stress-strain curve, either directly by transforming test data, or by applying the Ramberg-Osgood [110] formula.

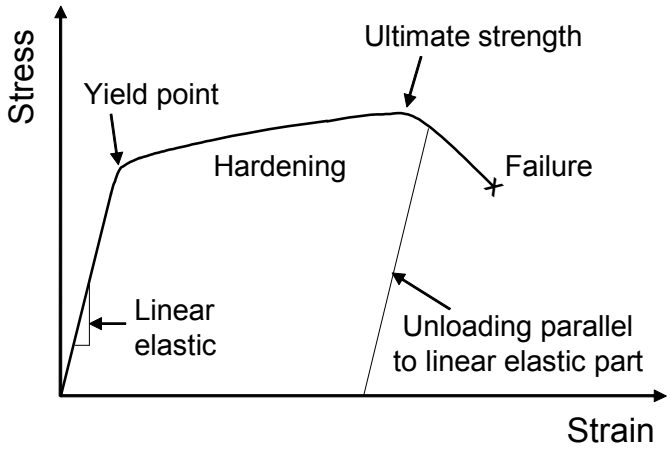

Figure 2.14: Stress-strain curve of an elastic-plastic material

Figure 2.14 illustrates different stages in the loading of metallic materials. Most metals show an approximately linear elastic behaviour at low stress magnitudes, and the material stiffness (Young's or elastic modulus) is constant. At higher stress levels nonlinear behaviour begins, which is called plasticity. The plastic behaviour starts at the yield point and permanent (plastic) deformation occurs. In most metals the initial yield stress is at 0.5 to 1% of the elastic modulus. Another aspect is the practical determination of the yield stress. Usually a plastic strain of 0.2% is used to define the (offset) yield point. The highest stress which the material can withstand is the ultimate strength, afterwards materials will fail.

A ductile metal has approximately the same stress-strain behaviour in tension and compression if true stress and strain rates are used. For that reason

ABAQUS requires the definition of true stress and strain [1]. True strain is defined as the change in length divided by the length:

$$d\varepsilon_{true} = \frac{dl}{l} \tag{2.40}$$

Here l is the current length, l_0 the original length and ε_{true} the true (or logarithmic) strain:

$$\varepsilon_{true} = \int_{l_0}^{l} \frac{dl}{l} = \ln(\frac{l}{l_0}) \tag{2.41}$$

Properties of metals are often determined in engineering tension tests, in which the material's change in diameter is neglected. In such situations the value needs to be transformed into true stress and strain [35]. Engineering (nominal) strain is the length change per unit undeformed length:

$$\varepsilon_{eng} = \frac{l - l_0}{l_0} = \frac{l}{l_0} - \frac{l_0}{l_0} = \frac{l}{l_0} - 1 \tag{2.42}$$

Adding a one and taking the natural logarithm on both sides, it follows:

$$\varepsilon_{true} = \ln(1 + \varepsilon_{eng}) \tag{2.43}$$

Engineering (nominal) stress is defined as force per unit undeformed area. The relation between true and engineering stress considers the incompressible nature of the materials.

$$l_0 A_0 = lA \tag{2.44}$$

The current area is related to the original one by:

$$A = A_0 \frac{l_0}{l} \tag{2.45}$$

Inserting this relation in the definition of true stress gives:

$$\sigma_{true} = \frac{F}{A} = \frac{F}{A_0} \frac{l}{l_0} = \sigma_{eng} \frac{l}{l_0} \tag{2.46}$$

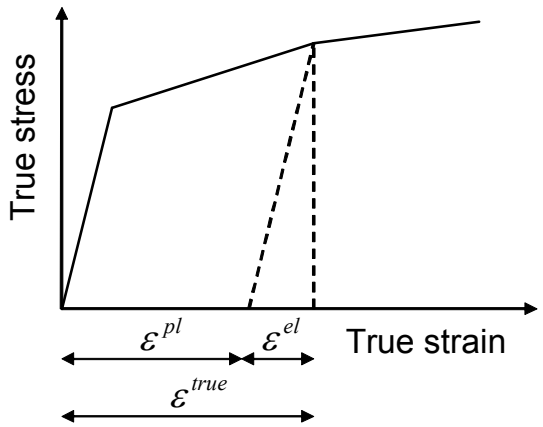

Figure 2.15: Decomposition of strain into elastic and plastic components

The true plastic strain is obtained by subtracting the true elastic strain from the value of total true strain, see Figure 2.15.

$$\varepsilon^{pl} = \varepsilon^{true} - \varepsilon^{el} = \varepsilon^{true} - \sigma^{true} / E \tag{2.47}$$

Applying equations 2.43, 2.46 and 2.47, tension test data can be transformed into the required format. The ABAQUS material definition has the following structure:

```
*Material, Name=Aluminium
*Elastic, Type=ISO
68000.,0.33
*Plastic
330,0.
340,0.0036
350,0.0077
```

Here, an aluminium alloy is defined with a Young's modulus of 68000 $\mathrm{N/mm^2}$ and Poisson's ratio of 0.33. Yielding starts at 330 $\mathrm{N/mm^2}$ true stress. The plastic strain increases with the given values for the stress increase.

The second possibility to derive the true stress-strain curve is using the Ramberg-Osgood formula [110].

$$\varepsilon = \frac{\sigma}{E} + K\left[\frac{\sigma}{E}\right]^n \tag{2.48}$$

K and n are material constants. Another form of the formula is presented in the ESDU data sheet [40].

$$\varepsilon = \frac{\sigma}{E} + \frac{f_n}{Em}\left[\frac{\sigma}{f_n}\right]^m \tag{2.49}$$

Using this formulation is convenient, as the material constants f_n and m for many alloys are published [40, 43, 82]. Plastic strain is then calculated from the derived curve using equation 2.47. The ABAQUS elastic-plastic material model works well until the ultimate stress is reached. Material failure cannot be predicted.

2.4.6 Joint modelling

Joint modelling is closely related to material and contact modelling. Joints usually cast different structural parts together, which involves contact. But the joints (as rivets and bolts) are objects which need to be modelled themselves. In a large scale model, it is generally not possible to model the real shape of the joints because the necessary mesh size would become too large. Another aspect is that in stiffened panels hundreds of joints exist. Therefore, joints are usually modelled with one-dimensional elements. Common joint models use springs, beams, connectors and multi point constraints (MPC). ABAQUS [1] recommends the Cartesian connector element, which will be described in this section. In section 3.6 different joint models will be compared.

The simplest joint element in ABAQUS is a spring, which is called SPRING2. It is defined between the two nodes i and j.

$$\Delta u = u_i - u_j \tag{2.50}$$

The displacement change Δu is a line between the nodes and is determined by the applied force F and the stiffness k:

$$\Delta u = \frac{F}{k} \tag{2.51}$$

Springs can have elastic and plastic behaviour, as shown in Figure 2.16.

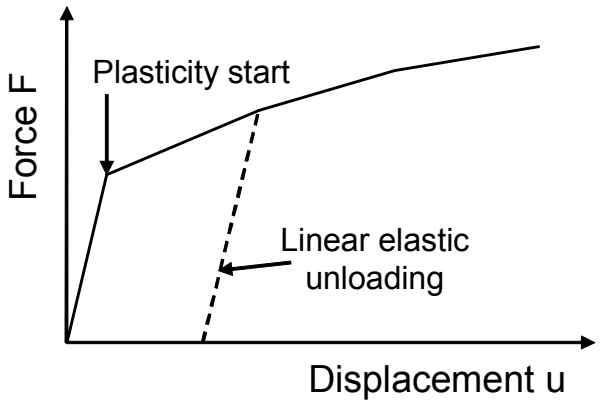

Figure 2.16: Elastic-plastic connector properties

Connector elements provide flexible joint modelling. They can integrate springs in each three-dimensional direction, and define nonlinearity, plasticity and failure. Following code defines connector elements in element set “Bolts_right” with the behaviour “Bolt1”.

```
*Connector Section, Elset=Bolts_right, Behavior=Bolt1
Cartesian
*Connector Behavior, Name=Bolt1
*Connector Elasticity, Component=1
30000.
*Connector Plasticity, Component=1
*Connector Hardening, Definition=Tabular
5000, 0.0
6263, 0.8195
7314, 1.2760
```

Linear stiffness of 30000N/mm is defined for the first component, which can be the x, y, or z-direction depending on the location of the two nodes. The connector starts to deform plastically when a force of 5000N is reached. Connector stiffness and hardening need to be derived from the real joint properties as length, cross sectional area and Young’s modulus.

The plasticity formulation in connectors is similar to metal plasticity, as described in section 2.4.5. For connectors the stress σ corresponds to the force F, the strain ε corresponds to the relative motion u, and the plastic strain ε^{pl} corresponds to the plastic relative motion u^{pl}. The connector relative motion u remains elastic until the yield force has been reached. Joint failure can be defined depending on a stress level or a maximum deformation with *Failure or *Damage.

One-dimensional elements are usually defined between two nodes. A convenient feature is the definition of mesh-independent connector elements with *Fastener. This makes the mesh design independent of the joint positions. The contacting surfaces and the coordinates of the joints need to be specified for this.

2.4.7 Contact definition

Contact modelling is either surface or contact element based. Figure 2.17 illustrates both modelling options for contacting surfaces A and B.

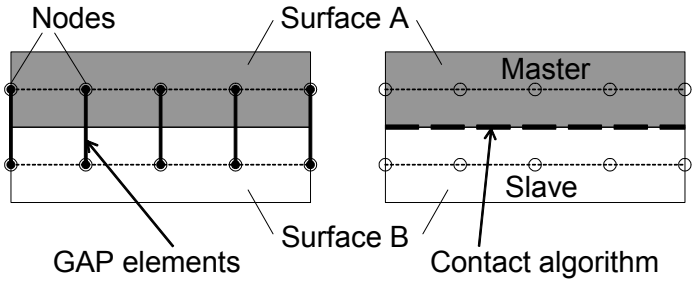

Figure 2.17: Element and surface contact

Gap elements define contact between two nodes. The gap can be open or closed, and the distance d between the nodes is called clearance. An initial clearance has to be specified. If d is positive the gap is open and if $d = 0$ the gap is closed. When d is specified negative, the gap is considered over-closed, which is physically not reasonable. Surfaces connected with gap elements may open but cannot penetrate each other. GAPUNI is the suitable unidirectional gap element between two nodes.

```
*Element, Type=GAPUNI, Elset=Gap_Elements
  10,    208,   6385
  11,    205,   6382
*Gap, Elset=Gaps
0.
```

In this example gap elements 10 and 11 have been defined for the element set “Gap_Elements”. The clearance is 0., which means the gap is initially closed.

Surface based contact is the more appropriate but more complex approach. The distance separating two surfaces is also called clearance. Contact constraints are applied if the clearance becomes zero and a contact pressure is generated. Surfaces separate when the pressure between them becomes zero or negative, and the constraint is removed. ABAQUS provides a pure master-slave contact algorithm. Nodes on the slave surface cannot penetrate the

master surface, but master nodes can penetrate the slave surface. The selection of slave and master surfaces is therefore important. The rules are:

- Slave surfaces should be more finely meshed.
- If mesh densities are similar, the surface with harder material should be designated the master surface.
- A node (not element) based surface can only be a slave.

ABAQUS offers “node-to-surface” and “surface-to-surface” discretisation. In the case of node-to-surface contact, the slave surface is defined as a group of nodes. Each slave node interacts with a point projection on the master surface. The contact condition involves a single slave node and a group of nearby master nodes. In surface-to-surface contact, the constraints are enforced over the slave surface, rather than at discrete slave nodes. This provides more accurate results because the surface penetrations are applied in an average sense over the slave surface.

Two tracking approaches which account for the relative motion of contacting surfaces are provided. The “Finite-sliding” formulation requires constantly determination which part of the master surface is in contact with each slave node. This is a complex calculation as both surfaces may deform. “Small-sliding” establishes a relationship between slave nodes and the master surface at the beginning of the simulation. These relationships are maintained throughout the analysis, which makes computation for small-sliding less expensive. A general guideline is that problems in which a point that’s in contact with a surface does not slide more than a fraction of an element dimension can use small-sliding.

Characteristic	**Contact formulation**			
	Node-to-surface		Surface-to-surface	
	Finite-sliding	Small-sliding	Finite-sliding	Small-sliding
Account for shell thickness	No	Yes	Yes	Yes
Allow self-contact	Yes	No	Yes	No
Default constraint enforcement	Direct method	Direct method	Penalty method	Direct method

Table 2.3 Comparison of ABAQUS contact characteristics [1]

Table 2.3 summarises contact properties. The node-to-surface, finite-sliding formulation does not account for shell thickness. Self-contact is the result of large deformation in a model and cannot use the small-sliding tracking

approach. Enforcement of contact constraint can lead to convergence difficulties. The direct method strictly enforces the specified pressure-overclosure. In the penalty method, this behaviour is approximated by choosing contact forces proportional to the penetration distance, which leads to numerical softening.

The first step in a contact definition is to create surfaces with *Surface using previously defined node or element sets. For shell elements, the side which is involved in contact needs to be specified. The side facing the element normal is called “spos”, the opposite side “sneg”. Contacting surfaces must face in the direction of the opposite surface. Then, pairs of surfaces which may contact are specified with the *Contact Pair command.

```
*Elset, Elset=Stiffener_Top, Generate
120,  229,  1
*Elset, Elset=Plate_Bottom, Generate
230,  339,  1
*Surface, Name=Surface_top
Stiffener_Top_1, sneg
*Surface, Name=Surface_bottom
Plate_Bottom_1, spos
*Contact Pair, Interaction=Int_1, Type=Surface To Surface
Surface_top, Surface_bottom
*Surface Interaction, Name=Int_1
*Friction
0.15
```

The first surface (Surface_top) is the slave and the second (Surface_bottom) the master. It is necessary to specify whether the magnitude of relative sliding will be small or finite. Finite-sliding is the default and does not need to be specified. With *Surface Interaction additional properties, such as *Friction, can be specified. Friction should only be included if it has a significant influence on the model, because it adds unsymmetrical terms to the stiffness matrix.

2.4.8 Geometrical nonlinearity

Geometrical nonlinearity is treated by using the Newton-Raphson method. The analysis *Step definition requires the inclusion of the parameter Nlgeom. The modified version of the Newton-Raphson method with damping, as described in section 2.2, is selected with *Static, Stabilize.

```
*Step, Inc=500, Nlgeom
*Static, Stabilize
0.05,1,,0.10
```

Nonlinear analyses apply displacements or force increments in steps. In this code example, a maximum of 500 increments is allowed to complete the step. The initial increment is 5%, and the maximum increment is 10% of the complete analysis.

This chapter introduced linear and nonlinear FEM, the SAFESA method and the solver ABAQUS. The idea was to provide all necessary information for doing a nonlinear idealisation error analysis. In the next two chapters this knowledge will be applied.

3. CRANFIELD PANEL ANALYSIS

3.1 Introduction

This chapter describes the idealisation error control analysis of a stiffened panel compression test. The aim is to find out if the SAFESA method can easily be applied to a nonlinear case. It is part of the learning process for the development of an expert system at a later stage. The panel studied here is used in the Structural Stability lecture module given by Dr. Campbell and was tested in the School of Engineering at Cranfield University.

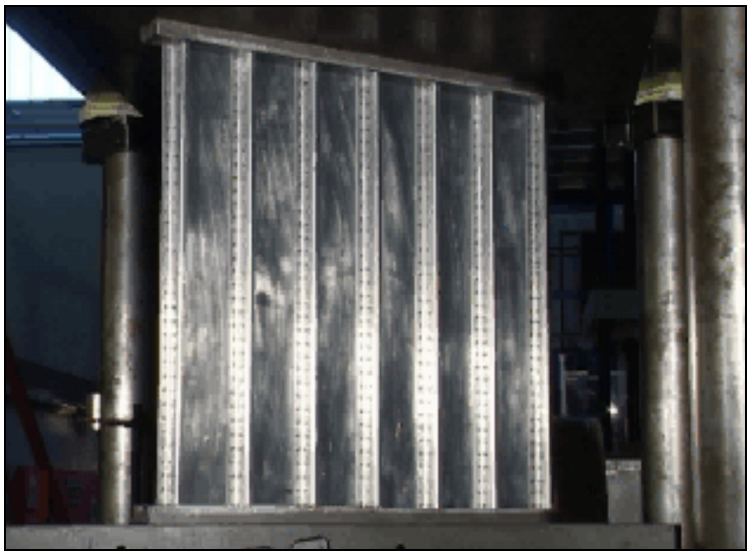

Figure 3.1: Panel testing at Cranfield University

The panel consists of seven Z-section stiffeners riveted to the skin, see Figure 3.1. The panel design is used at Cranfield for a class exercise in the post-buckled design of stiffened panels. The test machine does not allow a precise recording of the loading process. (Other available machines were too small for the panel or could not apply a compressive load large enough to cause failure.) Incomplete experimental data is a common situation in structural engineering and underlines the importance of reliable FEM.

3.2 Design Calculations

The classical approach to predict panel failure is based on design calculations, typical of those used by the aircraft industry [22]. The outcome of this calculation will help to understand the structural behaviour and is an important step towards a realistic model. Theory and examples are published in ESDU data sheets and textbooks [20, 30, 38-42]. When loading stiffened panels axially

different failure modes occur. The results from design calculations for the example panel [22] are summarised in Table 3.1:

Failure Mode	Applied load [kN]
Skin local buckling between stiffeners	19.78
Torsional buckling of outer skin-stiffener	100.83
Flexural (Euler) buckling of skin-stiffener	110.04
Inter-rivet buckling	142.66
Stringer crippling	144.18

Table 3.1: Design calculation for the used panel

The skin local buckling is not a global failure mode, instead it represents a change in stiffness of the panel. The skin buckles and if the panel is unloaded it will return to its initial shape. All other failure modes lead to collapse of the structure. Torsional buckling at approximately 100 kN is the critical failure mode.

These calculations assume a perfect geometry and a uniformly applied load. Real test conditions will deviate from this idealisation, especially when local buckling starts. The other reservation is the design of the panel with stringers at the free edges. In real aerospace structures the sides have a more rigid constraint, and the failure mode is flexural buckling.

3.3 SAFESA Procedure

This section follows the SAFESA method for assessing the idealisation process from an error treatment viewpoint.

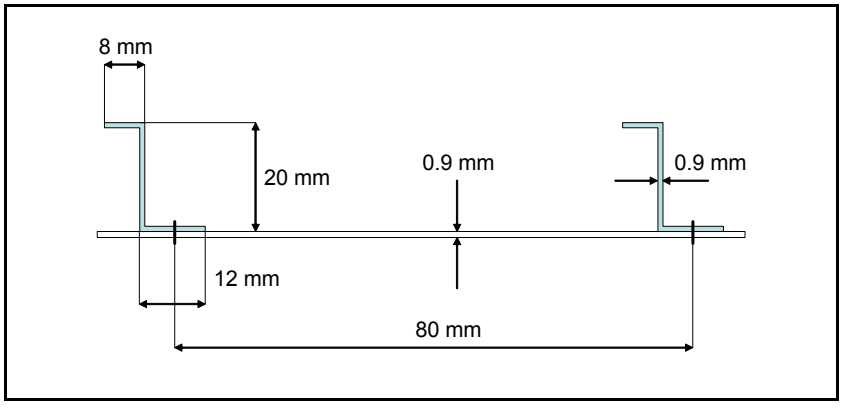

Figure 3.2: Side view of the panel idealisation

STEP 1: Definition of boundary, boundary conditions and loading actions

Input:

1. Real World Problem

Geometry: As shown in Figure 3.1, the structural components are:

Rectangular plate, length: 500mm x width: 492mm and 0.9 mm thickness. Due to clamping the free out-of-plane deformable length is reduced to 467mm.

Z-shaped stiffeners, length: 500 mm x thickness: 0.9 mm; height: 20mm, top-section: 8mm, bottom-section: 12mm, see Figure 3.2 for details.

Rivets; The stiffener is riveted on the plate with a rivet pitch of 14mm.

Material: Plate and stiffeners are made of aluminium L165 (2014A-T6). Rivets (snap head SP80) are made of aluminium L69 and have a diameter of 2.38mm (3/32”).

Loading: The applied load is axially compressing the panel until collapse.

Boundary conditions: As can be seen in Figure 3.1, both ends of the panel are held in position by the test machine. The ends are cast into a prismatic Cerrobend (alloy of bismuth, lead, tin and cadmium) fitting.

2. Qualification Criteria

The aim is to determine the maximum load. The FEM result must not differ more than 10% from the test load.

Process:

1. Domain definition and error treatment

1.1 Define domain:

The stiffened panel represents the domain of interest for the analysis. Usually a stiffened panel is part of a bigger assembly. Here we look only at one single unit.

1.2 Define boundary conditions:

The panel with the attached Cerrobend cast is elastically placed into the test rig. While the test machine compresses the panel, rigid contact between the rig and the panel is assumed. The top end of the panel will be modelled rigid and the bottom end clamped.

Flag 1 Check sensitivity to the boundary condition type. How much does the rotational constraint at the ends influence the solution?

The other two sides have no constraints, as in the real test.

2. Loading:

External pressure is compressing the panel axially until collapse. No shear forces. In the model this is realised via a displacement in the axial direction.

Flag 2 Investigate the influence of applying load or a displacement.

Output:

1. Structure geometry and boundary conditions as above.
2. Loading as above.
3. Errors: boundary conditions and loading actions.

STEP 2: Definition and error treatment of load paths, geometry idealisation

Input:

1. Coarse idealisation of boundary conditions
2. Coarse idealisation of loading
3. Real structure geometry
4. Qualification criteria

Process:

1. Overall behaviour:

There are five stages in the loading process until failure:

- Linear elastic material deformation at lower stress levels.
- Local buckling of the plate between the stiffeners.
- Global out-of-plane bending of the whole structure. At this point the stringers start buckling and most of the load is sustained by the stiffeners.
- Failure of a joint. This failure is unlikely, as no rivet failed in ten observed tests.
- Collapse of the structure which is caused by one of the failure modes described in the previous section.

Flag 3 Check the predicted modes as described in section 3.2. Stiffened Panel Design Calculation:

- Local buckling at 19.78kN
- Torsional buckling at 100.83kN

2. Load paths:

The load is applied to one end of the panel. As the other end is clamped all pressure will be absorbed by the structure.

3. Geometry idealisation

3.1 Domain reduction:

The structure has one plane of symmetry but the whole structure is modelled.

3.2 Mathematical model:

As panel and stiffeners are thin-walled, the structure is modelled with shell elements. Shell theory is applicable, i.e. the length-thickness ratio is large:

- Plate (l/t = 492/0.9 = 546.67)

- Stiffener (l/t = 8/0.9 = 8.9)

Flag 4 The model assumes a perfectly shaped geometry. How much does geometrical imperfection influence the solution? These imperfections result from the production process and are always present.

3.3 Dimensional reduction:

The shape of the stiffeners will be simplified, because finite elements have basic shapes. Corners will have sharp edges although the real panel has rounded edges.

Flag 5 Investigate the influence of different stiffener shapes, e.g. rounding the edges.

The shape of the rivets is neglected, i.e. the plate and the stiffeners are plane. The resulting error is assumed to be negligible.

3.4 Revision of essential and natural boundary conditions:

As no simplification due to symmetry is applied, and the idealisation of the geometry does not affect the boundary conditions, nothing changes.

4. Analysis type:

Nonlinear quasi-static.

Flag 6 The panel is loaded until failure, and exceeding of 0.2% strain will occur. Therefore, an adequate nonlinear material model (e.g. elastic-plastic) has to be applied.

5. Material idealisation:

Modulus of elasticity $\mathrm{E} = 68000\ \mathrm{N/mm^2}$
Poisson's ratio $\upsilon = 0.33$
Yield stress $\sigma_{\mathrm{y}} = 340\ \mathrm{N/mm^2}$

Flag 7 How much scattering is in the parameters E, υ and σ_{y}?

Output:

1. Overall idealisation of geometry and material properties.
2. Type of analysis: nonlinear quasi-static.
3. Structural behaviour: shell elements for panel and stiffener.
4. Errors flagged out, otherwise not significant.

STEP 3: Breakdown of the structure

Input:

1. Idealised geometry, boundary conditions and loading action for the structure or feature.
2. Load paths within the structure or feature.
3. Structural behaviour within the structure or feature.

Process:

1. Breakdown of the structure into lower level features:

The structure is divided into two parts:

Feature 1: Stiffener

Feature 2: Panel

Output:

1. The structure is divided into stiffener and panel.

STEP 4: Definition of boundary conditions and loading action for features

Input:

1. Features from step 3
2. Outputs from steps 1 and 2

Process:

1. Boundary conditions for features 1-2: panel and stiffener

Both ends of the panel are held on, as described previously.

The panel-stiffener interconnection is of interest. Rivets will be modelled with one-dimensional elements. The panel has tight contact with the stiffeners.

Flag 8 Study the influence of the different possibilities to model the contact. Following cases should be considered:

- Current model: rigid shell connection (plate and stiffener share same nodes)
- Rigid shell connection & increasing the width (of the plate) at the bottom of the Z-stringer
- Contact using GAP elements or alternatives
- Modelling the rivets with springs, beams, constraints

2. Loading actions for features 1-2: panel and stiffener

Loading actions specified earlier remain unchanged.

Output:

1. Idealised boundary condition.
2. Idealised loading known.
3. Errors: panel-stiffener interconnection.

STEP 5: Definition and error treatment of load paths and idealisation of geometry for features

Input:

1. Idealised boundary conditions for the feature
2. Idealised loading for the feature
3. Real geometry of the feature
4. Qualification criteria

Process:

1. Behaviour of the feature:	As before
2. Load paths:	As before
3. Geometry idealisation	As before
3.1 Domain reduction:	As before
3.2 Mathematical model:	As before
3.3 Dimensional reduction:	As before
3.4 Revision of essential and natural boundary conditions:	As before
4. Analysis type:	As before
5. Material idealisation:	As before

Output:

1. Idealised geometry and material: as before.
2. Type of analysis: as before.
3. Structural behaviour: as before.
4. Errors: as before.

STEP 6: Assessment

Input:

1. Real world problem
2. Idealised structure
3. Error estimates

Process:

1. Assessment at feature level:

The error source at the feature level is the panel-stiffener contact modelling (Flag 8).

2. Assessment at the global level:

The following error sources will be studied in the sensitivity analyses and tests:

Flag 1. Sensitivity to boundary conditions

Flag 2. Applying load / displacement

Flag 3. Accordance with predicted failure modes

Flag 4. Geometrical imperfection

Flag 5. Shape of the stiffeners

Flag 6. Material model

Flag 7. Scattering in material parameters

Output:

1. A geometry scan is necessary to study the magnitude of geometrical imperfection (Flag 4).

   In order to analyse material parameters, coupon tests can determine the stress-strain curve for the used material (Flag 7).

2. Second iteration required.

STEP 7: Test program

Input:

1. Real world problem
2. Idealised structure
3. Error estimates

Process:

1. Geometry scan to study geometrical imperfections.

2. Material test to get elastic-plastic material parameter.

Output:

1. Geometry scan from the backside of the panel.
2. (Elastic-plastic material parameter.)

Step 6 concludes that tests are necessary. The test outcome is described in the next section. At this point the first idealisation cycle is finished, i.e. the model of the stiffened panel is completed and ready for meshing, solving and post-processing.

3.4 Supporting Test Data

Panel tests are repeated twice a year, which allowed the observation of different aspects. The panels were fabricated by hand at Cranfield University, with a new one produced for each test. Riveting and the Cerrobend casting introduced geometrical imperfection. Another element of uncertainty is the test equipment.

3.4.1 Geometry scan

A Cyclone Series 2 digitising system from Renishaw [111] was used to scan the panel surface, see Figure 3.3. This optical laser machine has a resolution of 5µm. The output is an ASCII file with a data matrix of scanned points.

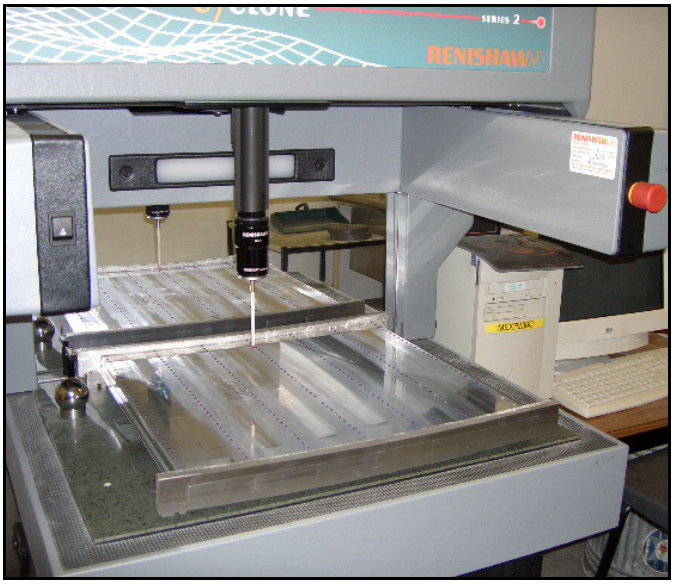

Figure 3.3: Scanning machine with the stiffened panel

The surface was scanned with a distance of 2mm between each point in x- and y-direction. The coordinates and respective z-values were recorded. Figure 3.4 shows lines of axially recorded out-of-plane deflections.

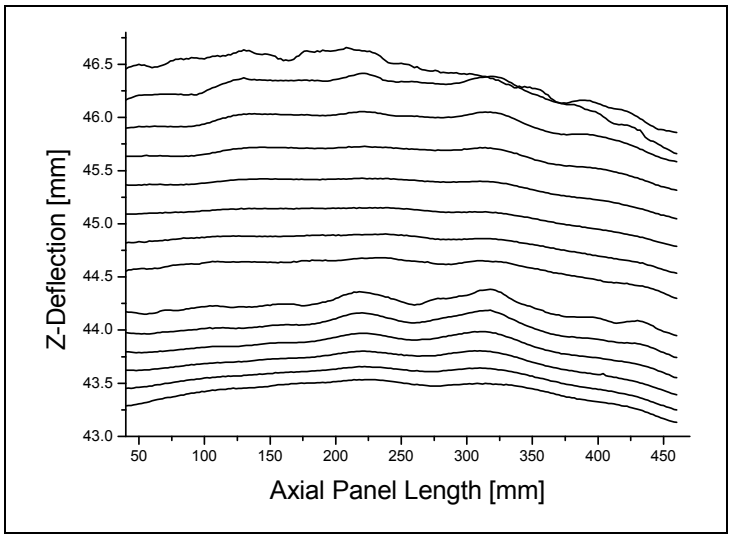

Figure 3.4: Scanned surface lines of the panel

Through casting, the scanned panel length of 500mm is reduced at both ends by 40mm. The different start values (43.3 to 46.4mm) are caused by the curved shape of the panel. This curvature is the result of adding the Cerrobend cast. The graph shows that there are local distortions and a global curvature. The data are analysed in section 3.6.6 and will be used to model geometrical imperfections.

3.4.2 Material properties

Material coupon tests were not carried out within this project. The initial idea was to extract test specimens from the boundary of tested panels, which would have added another source of error. Upon enquiry, a test protocol from Kaiser Aluminium was obtained. The (civil aviation approved) certificate states that the metal conforms to aluminium L165, see Appendix A.2. Therefore, published material parameter will be used in this analysis.

3.4.3 Joint deformation

In several panel tests the used rivets did not fail but deform. In order to model the amount of plastic deformation, the rivet length was measured before and after the test. The used digital calliper has an accuracy of 0.01mm. The rivets (snap head SP80) with a head diameter of 2.38mm (3/32” inch) had a measured length between 4.41 and 4.80mm.

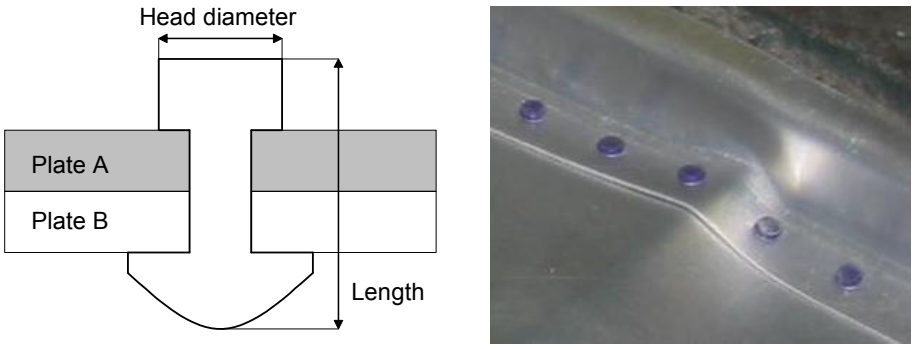

Figure 3.5a, b: Rivet model and deformed panel with rivets

Figure 3.5a illustrates a rivet which connects two plates. Rivets in the middle of the panel sides are of special interest as the panels show the largest deformations in this area, see Figure 3.5b.

Rivet number	**1**	**2**	**3**	**4**	**5**
Pre-test length [mm]	4.43	4.49	4.70	4.46	4.51
Post-test length [mm]	4.43	4.51	4.74	4.48	4.51

Table 3.2: Rivet length before and after the panel test

Table 3.2 shows the lengths of the five middle rivets before and after testing. A correct measurement was difficult as the rivets mainly deform sideways. The central rivet had a peak length increase of 0.04mm, which is about 1% of its length. The study suggests the addition of a plastic term in the joint definition.

3.4.4 Test machine calibration

The used compression machine was built in the middle of last century. There were doubts about how precise the panel failure load could be determined. Therefore, a test machine calibration was arranged.

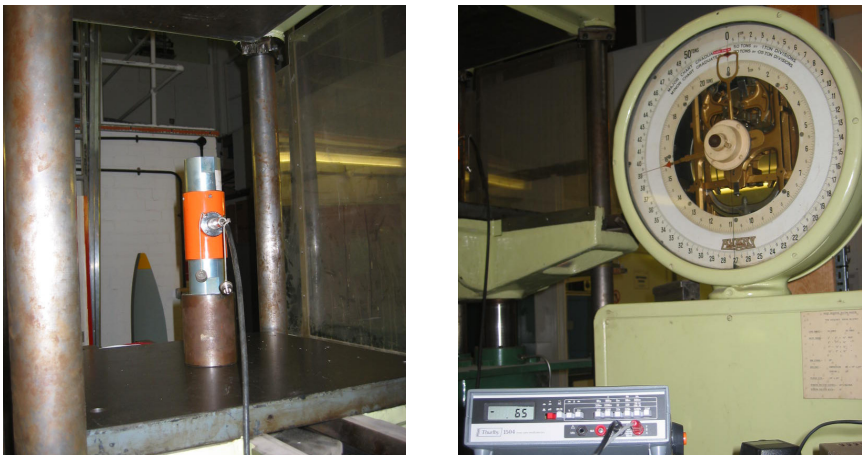

Figure 3.6a, b: Calibration test equipment

Figure 3.6 shows the test equipment. The picture on the left shows the load cell, which allowed an accurate load history measurement. The right picture shows the compression machine with its arrow based display. The digital display of the load cell can be seen in the bottom left corner. Recording both values simultaneously using a camera allowed a correct calibration.

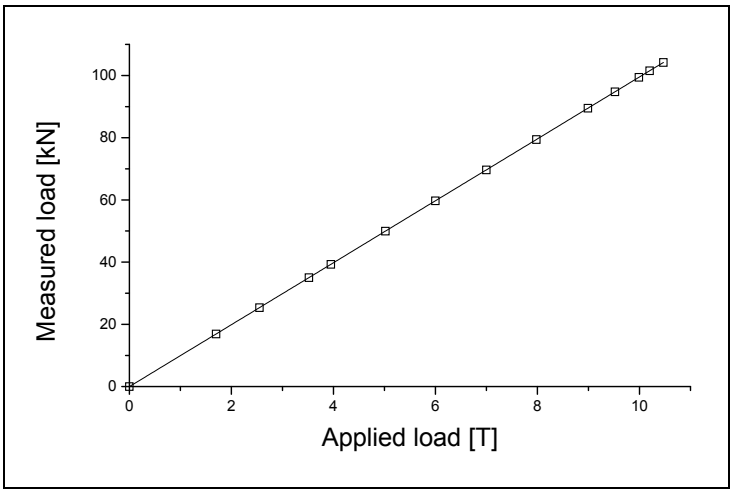

Figure 3.7: Applied versus measured load

Figure 3.7 plots the applied against the measured load. The straight graph implies a direct proportionality. The test rig measures load in tons [T] with 1ton corresponding to 10kN. The load cell delivered values in kN. The crucial range is around the panel failure load. At 10T applied load, the measured load was 99.53kN, which means an error of less than 0.5%.

3.5 Reference Model Building

The three-dimensional panel assembly is modelled with two-dimensional shell elements. Both ends of the panel are cast into a prismatic Cerrobend fitting. The panel is placed elastically in the test machine. The lower part of the test rig is fixed and the upper part is moving downwards in order to compress the panel. In the FEM model this is realised via boundary conditions, as shown in Figure 3.8. Side C is clamped, as all degrees of freedom are fixed. Side A is moving axially towards side C. This is realised via multipoint constraints (MPC). As in the real test, sides B and D are not constrained.

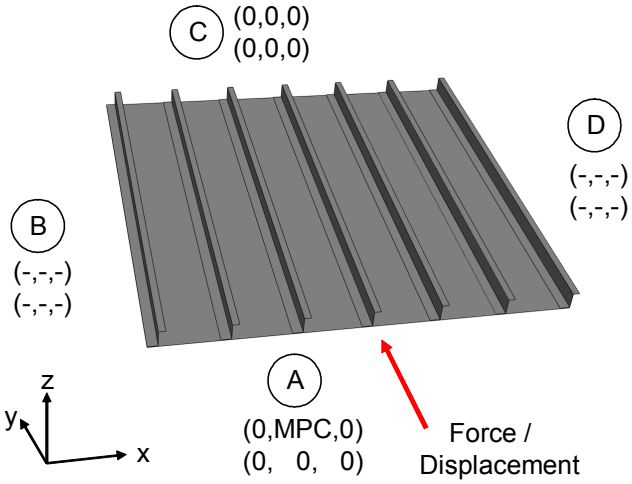

Figure 3.8: FEM geometry with boundary conditions

The nonlinear analysis is performed using the damped Newton-Raphson method. Panel failure is defined as a drop in the load-shortening curve. The panel-stiffener bonding is realised by using the same nodes at the contact interface. The solution behaviour shows local buckling, and the panel fails due to global buckling.

3.5.1 Mesh sensitivity study

In order to find out how many elements are necessary, the model was meshed with different numbers of elements.

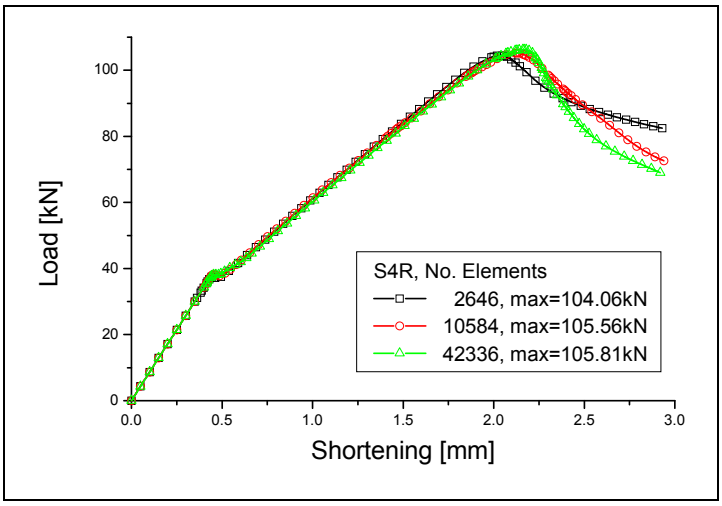

Figure 3.9: Mesh sensitivity using S4R elements

Figure 3.9 shows results from the mesh sensitivity study using S4R elements. The predicted failure with the coarse mesh size is too small. The load-

shortening curves using the middle and fine meshes differ after the panel has already failed. It follows that the middle size with 10584 elements is sufficient for the model.

3.5.2 ABAQUS shell element selection

The element choice influences the solution behaviour. First and second order shell elements were compared using different mesh sizes. The models showed similar load-shortening curves and differed in the collapse load, see Table 3.3.

Model	El. Type	No. El.	Dof's	Anal. [%]	Incr.	Ult. load [MN]
Coarse	S4R5	2646	16512	100	120	103.19
	S4R	..	..	100	116	104.06
	S4	..	..	100	118	108.83
	S8R5	..	64770	100	125	105.19
	S8R	..	48894	100	115	104.92
Middle	S4R5	10584	64770	100	140	104.58
	S4R	..	..	100	140	105.56
	S4	..	..	100	137	106.17
	S8R5	..	256542	79.7	119	104.25
	S8R	..	193038	100	138	104.27
Fine	S4R5	42336	256542	100	127	104.62
	S4R	..	..	100	134	105.81
	S4	..	..	100	131	105.28
	S8R5	..	1021110	58.2	104	104.18
	S8R	..	767094	95.5	141	104.34

Table 3.3: Summary of the mesh sensitivity study

The degrees of freedom "Dof's" were extracted from the ABAQUS *.dat file and indicate the real model size. "Anal. [%]" displays what percentage of the analysis was completed. 100 percent completion mean that the maximum displacement of 4mm, which is far beyond panel failure, was successfully applied. The number of solution "Increments" indicates the computing work. An analysis required at least 100 increments because the maximum step size was set to 1%. The coarse mesh leads to great ultimate load differences between the element types. Middle and fine meshes show more consistent results. The

use of S4 and S4R elements results in a slightly higher failure load. These elements are based on a finite strain formulation, which is necessary for this analysis type, see section 2.4.4. S4R was chosen as the appropriate element type because it is more economic than S4.

3.6 Analysis of all Flagged Error Sources

Application of SAFESA flagged out the following error sources:

- Material model
- Applying load / displacement
- Contact between panel and stiffener
- Sensitivity to boundary conditions
- Shape of the stiffeners
- Geometrical imperfection
- Scattering in material parameters
- Accordance with predicted failure modes

The analysis of the error sources is described in the following text. The model was improved iteratively, and a comparison between solutions is made on the basis of the results within each error source. The resulting error is the relative change in failure load of the reference model when applying an alternative idealisation. The obtained error values were finally rounded to half-percent values. Smaller variations can be neglected because they also occur when changing FEM solution parameter, such as the maximum step size or the stabilisation factor.

3.6.1 Material model

The material used was aluminium L165 (2014A-T6) with:

- Modulus of elasticity $\mathrm{E} = 68000\ \mathrm{N/mm^2}$
- Poisson's ratio $\upsilon = 0.33$
- Yield stress $\sigma_{\mathrm{y}} = 340\ \mathrm{N/mm^2}$

The nonlinear behaviour of metals is modelled using the Ramberg-Osgood formula [110]. The stress-strain relation was calculated using equation 2.49 and tabulated material data [30] with $f_n = 296\ \mathrm{N/mm^2}$ and $m = 17$.

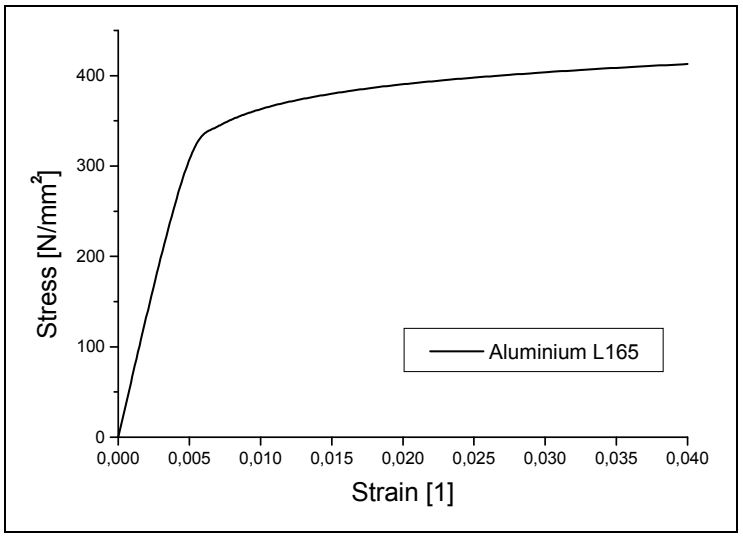

Figure 3.10: Ramberg-Osgood model of aluminium L165

Figure 3.10 shows the obtained true stress-strain curve. Plasticity starts at around 0.5% strain. Using equation 2.47 the data were transformed into the ABAQUS material definition format.

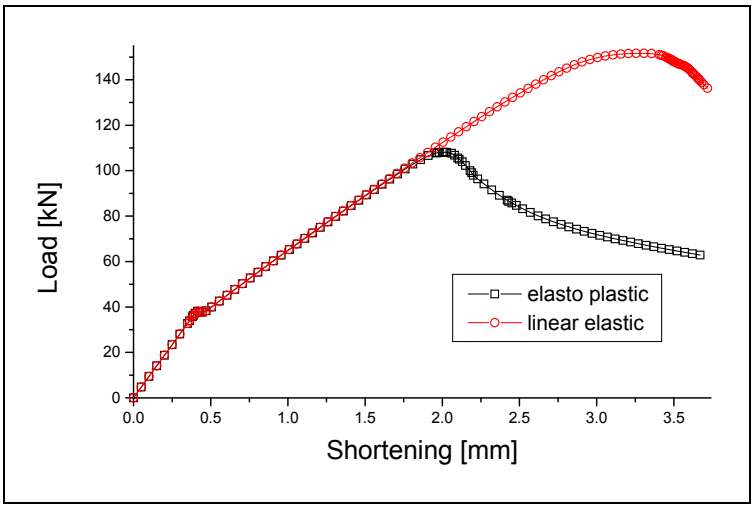

Figure 3.11: Linear vs. nonlinear material model

Using a correct material model is crucial, as is visible in Figure 3.11. The solution graph changes dramatically. However, the material model is output of an idealisation and not from the real test data. An idealisation error of 1% is assumed.

3.6.2 Applying load versus displacement

This error source arises from a modelling simplification. The hydraulic test rig is actually load controlled. This means load is applied and the displacement is

measured. The problem with a load controlled FE analysis is that the applied load is always increasing. After failure, the capability of the panel to sustain load decreases.

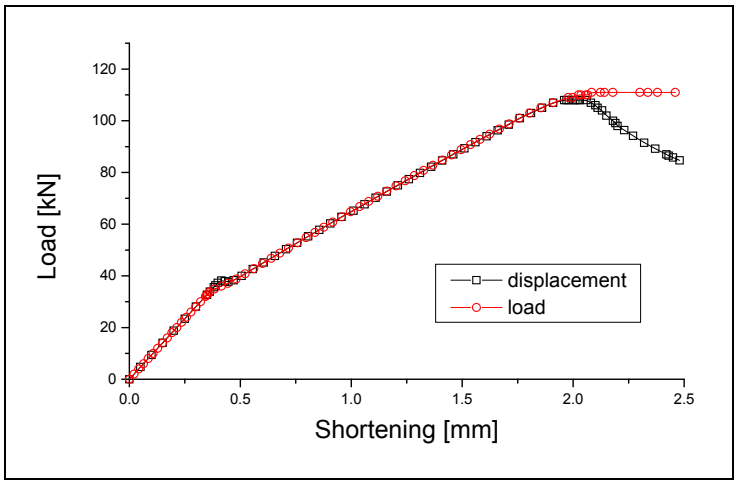

Figure 3.12: Displacement vs. load controlled analysis

Figure 3.12 compares the effect of doing a load or a displacement controlled analysis. Both models predict roughly the same collapse load. Therefore, the displacement controlled analyses will be used further without including a modelling error.

3.6.3 Contact between panel and stiffener

The panel-stiffener contact, as shown in Figure 3.2, can be modelled in different ways. An appropriate contact modelling for the stiffener and panel surfaces, and a model for the rivet have to be found. The actual shape of the rivets and the rivet holes in the plates are neglected, as there are too many (7x36=252) rivets.

In ten compression tests of the panel design, none of the rivets failed. The assumption to neglect the rivet failure modelling is therefore justified. However, the ductile behaviour of the rivets must be taken into account.

3.6.3.1 Simple contact models

The simplest model node_equ_edge uses a rigid shell connection. The stiffener top is directly connected to the plate elements, using the same nodes, as shown in Figure 3.13. The strength of this structure will be lower than what occurs in reality, because the stiffener bottom is neglected.

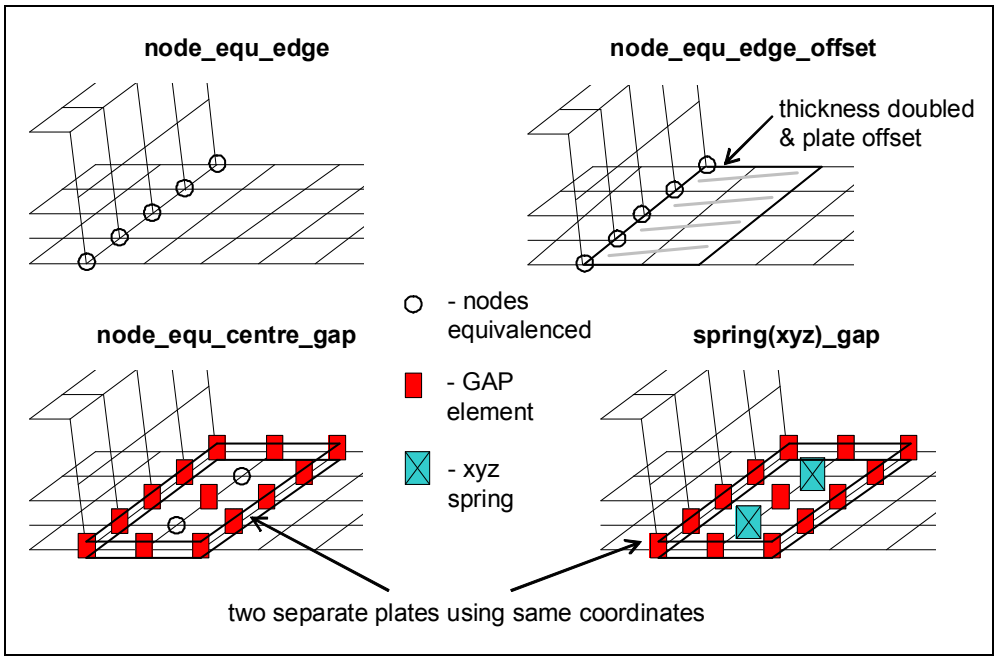

Figure 3.13: Simple contact models

Table 3.4 lists the results using the first model node_equ_edge, and modifications of it. In node_equ_edge_offset the plate thickness along the contact area was doubled and given a shell offset upwards. This idealisation leads to a solution that is too stiff. Two contacting plates have less residual strength than one with the thickness of the two plates combined.

Model	Collapse load [kN]
Node_equ_edge	108.12
Node_equ_edge_offset	140.41
Node_equ_centre_gap	121.20
spring(xyz)_gap	118.86

Table 3.4: Simple contact models

The other simulations model the base of the z-stringer explicitly, where the rivets are represented using a combination of GAP **elements**, springs and equivalencing nodes at the corresponding locations, as shown in Figure 3.13. In nod_equ_centre_gap and spring(xyz)_gap, every second node along the midline of the stiffener-plate interface was equivalenced or connected with xyz-springs. All the remaining nodes were connected via GAP elements. The springs were oriented in x-, y- and z-directions. The stiffness was estimated to represent the material used for the rivets. The collapse load of these models lies between that of the previous two. The model spring(xyz)_gap is the most realistic, but need to be investigated further.

3.6.3.2 Rivet and contact modelling

Rivets connect stiffeners to the panel. As the rivets slightly deform but do not fail, this allows different modelling approaches to be used. ABAQUS [1] offers the following joint models:

Multi-point **constraints** (MPC's) allow constraints to be imposed between different nodes of the model. This is an efficient way, as it reduces the size of the problem. Out of the ABAQUS library of MPC's, the following constraints are of interest here:

- **mpc_beam** constrains the displacement and rotation at the first node to the displacement and rotation at the second node.
- **mpc_link** keeps the distance between the two nodes constant.
- **mpc_pin** makes the displacements of the two nodes equal.
- **mpc_tie** makes all active degrees of freedom at the two nodes equal.

Connector elements perform functions similar to multi-point constraints. In contrast, connector elements do not eliminate degrees of freedom; the constraints are enforced with Lagrange multipliers. The following connectors will be tested:

- **conn_beam** has the functionality of mpc_beam.
- **conn_link** has the functionality of mpc_link.
- **conn_weld** has the functionality of conn_beam (mpc_beam); in addition the node locations will be joined.
- **conn_cartesian** provides a connection between two nodes that allow independent behaviour in three local Cartesian directions. This behaviour can be elasticity, plasticity, damage, failure or friction. The elastic-plastic parameters used in this analysis were calculated from rivet dimension, measured plastic deformation and published material properties.

Using **beams** can be considered the most realistic approach, because rivets are small beams. This is problematic as these beams are very short, and can generate numerical instabilities.

Contact can be modelled in two ways: either using contact elements (GAP's) or with a surface based approach. Furthermore, one needs to decide if the contacting surfaces use the same geometry coordinates (coordinates, not nodes!) or have a real distance. There are four contact variations as shown in Figure 3.14:

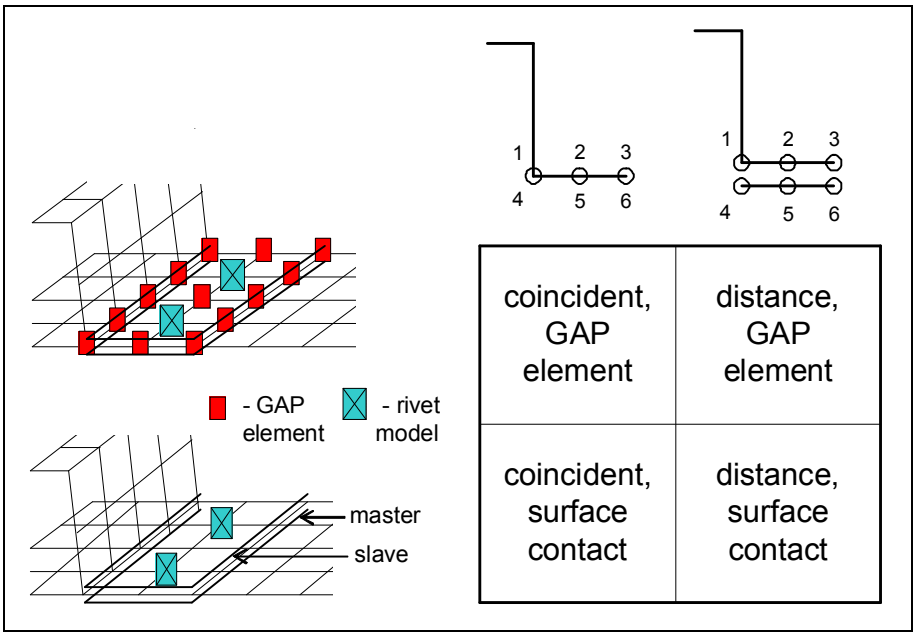

Figure 3.14: Contact variations

Gap elements define contact between nodes. It allows nodes to be in contact (gap closed) or separated (gap open) with respect to particular directions.

Surface contact is more practical [1], as the gap elements do not need to be created. Two surfaces where the contact algorithm will be applied need to be defined. ABAQUS offers diverse contact formulations, which were described in section 2.4.7. All analyses in this investigation use the surface-to-surface together with finite-sliding contact formulation, as it demonstrated to be the most stable.

Table 3.5 compares failure loads of all possibilities to model contact and the rivets. For the coincident-node geometries fewer rivet models are available; beams, conn_beam, mpc_beam and mpc_link need a real length for their definition. All models converged, except for the beam models. This is due to stability problems arising from use of such short beams to connect two contact surfaces. The collapse load varies between 114.43 and 122.55kN, a difference of around 7%.

Gap element and surface based contact showed very similar solution behaviour. The difference between coincident and distance models is that conn_beam, conn_cart and conn_weld behaved stiffer in the distance models. The most realistic contact idealisation involves the use of a distance, which is more in line with the physical setup. The surface based contact can cope better with complex geometry nonlinearity than contact using gap elements.

	Coincident		Distance	
	Model	Collapse load [kN]	Model	Collapse load [kN]
GAPUNI contact Element	conn_beam_gap	119.20	conn_beam_gap	122.55
	conn_cart_gap	118.86	conn_cart_gap	120.54
			conn_link_gap	114.44
	conn_weld_gap	119.20	conn_weld_gap	122.55
			mpc_beam_gap	122.55
			mpc_link_gap	114.43
	mpc_pin_gap	119.31	mpc_pin_gap	118.45
	mpc_tie_gap	119.20	mpc_tie_gap	119.20
			beam_gap	(124.87)*
				*not converged
Surface based contact	conn_beam	119.88	conn_beam	122.22
	conn_cart	117.85	conn_cart	119.67
			conn_link	114.93
	conn_weld	119.88	conn_weld	122.22
			mpc_beam	122.22
			mpc_link	115.13
	mpc_pin	118.22	mpc_pin	117.16
	mpc_tie	119.97	mpc_tie	120.08
			beam	(120.09)*

Table 3.5: Comparison of all contact and rivet models

The correct joint model is bounded between two extremes. conn_beam and mpc_beam model a rigid connection, which is too stiff. conn_link and mpc_link on the other hand will model a joint that is too loose. The conn_cart connector is able to model best the rivet deformation. This element allows the definition of the specific stiffness and can be extended to more complicated rivet models, e.g. failure.

All presented rivet models use a connection between two nodes. This was done in order to compare the different possibilities. A more convenient way to define the connectors is using the mesh independent approach with ABAQUS *Fastener elements. Hereby, joint coordinates and the contacting surfaces need to be specified. This makes it much easier to change the mesh size.

The surface based contact with distance and Cartesian connector elements that were finally selected make the FE model more realistic compared to the first model node_equ_edge. The collapse load increased from 108.12 to 119.67kN, which is around 10%. A small idealisation uncertainty of about 1% will remain, as the rivet properties were calculated using engineering assumptions.

3.6.4 Sensitivity to boundary conditions

This error investigation is motivated by the fact that the panel is not rigidly connected to the test machine. Top and bottom are cast into Cerrobend and the panel remains in direct contact with the test rig, see Figure 3.1. The Cerrobend cast adds additional stiffness to both ends and prevents movement and rotation of the panel during the test. However, it is not a rigid cast and minor rotation around the end axes can occur. Figure 3.15 shows the Cerrobend cast. Some hollows close to the stiffeners are visible, which indicate geometrical imperfections and reduced stiffness.

Figure 3.15: Cerrobend cast with imperfections

Figure 3.16 illustrates two boundary condition idealisations. “End cast + constraint band” casts the ends nodes and allows only an axial displacement of the nodes in the constraint band. The figure highlights the nodes of the constraint band. “Cerrobend modelled” models the Cerrobend explicitly with solid elements; the elastic stiffness was estimated to be 10% of the aluminium used.

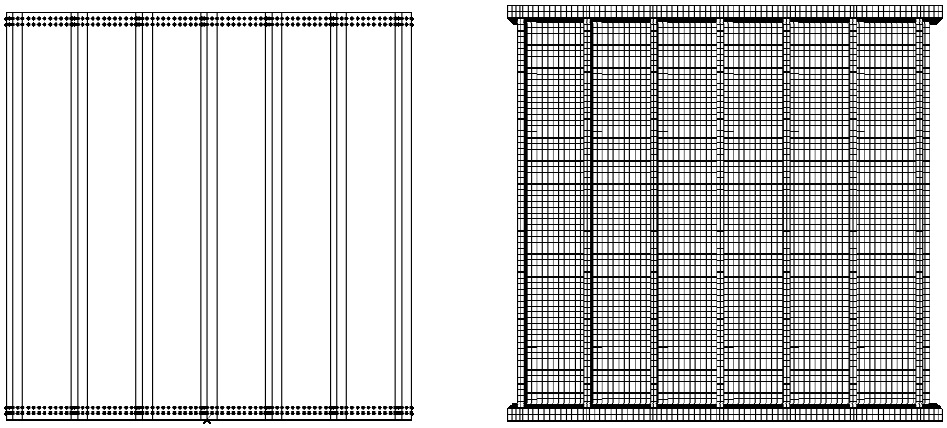

Figure 3.16: “Ends cast + constraint band” and “Cerrobend modelled”

Table 3.6 shows results of boundary condition variations. The true model will lie between “Free rotation around ends” and “Ends cast”. “Free rotation around ends” uses a reduced constraint. In FEM language this means constraint (0,0,0,0,0,0) versus (0,0,0,-,0,0), see Figure 3.8.

Model	Collapse load [kN]
Free rotation around ends	71.92
Ends cast (reference)	118.30
Ends cast + constraint band	116.60
Cerrobend modelled	114.65

Table 3.6: Boundary condition impact

Allowing the panel to rotate around the axes of the ends has a big impact on the collapse load, but is an exaggeration of the actual panel end flexibility. “Ends cast + constraint band” seems to be the most realistic variant and will therefore be used in an improved model. The effect of including the constraint band is that the local buckling shape changes from 4 to 3.5 wavelengths (see section 3.6.8) along the panel length. As the flexibility of the end platen is not adequately modelled, an idealisation error is estimated as up to 3%.

3.6.5 Shape of the stiffeners

Stiffeners were modelled rectangular, which is a simplification of the structure. Figure 3.17 illustrates the arched shape of a real stiffener.

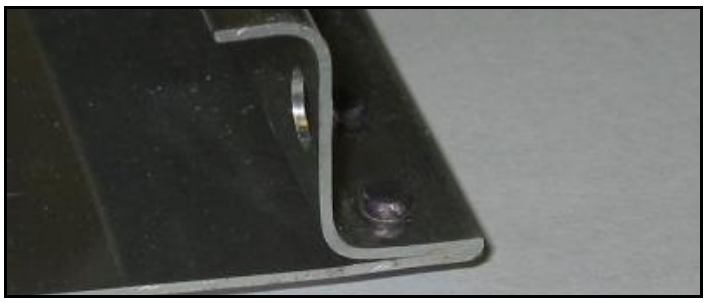

Figure 3.17: Curved shape of a stiffener

Modelling a curved shape with the FEM is a complex task, as elements have triangular or rectangular shape. The analysis approach is to refine the mesh size.

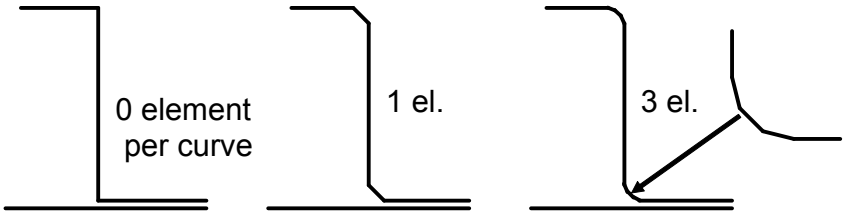

Figure 3.18: Idealisation of curved panel corners

Figure 3.18 shows different idealisations of the curved stiffener shape. “0 element per curve” is the reference model. The middle model uses one, and the right one uses three additional shell elements for one curve. A drop in ultimate strength for the more curved models is the result, see Table 3.7.

Model	**Collapse load [kN]**
Reference	119.37
1 element per curve	117.86
3 elements per curve	118.49

Table 3.7: Impact of edge curvature

Omitting the curved shape introduces an idealisation error. The author believes that the decrease in collapse load is caused by shortening the contact area. The stiffener contacts an area of length times 12mm in the reference model, as can be seen in Figure 3.2. In the one and three “element per curve” models it shortens to length times 10mm. Due to distortions, the real contact area can become even smaller, which can be seen in Figure 3.17.

The stiffener-plate contact area is the most stabilising part of the whole panel, as it has the biggest thickness. Disturbances in this area affect the whole panel. An improved model must take this into account. Because meshing curved shapes introduces other inaccuracy, an idealisation error of 1% will remain.

3.6.6 Geometrical imperfections

Geometrical imperfections are deviations from the perfect structure, which are always present. They occur during production and transport. The analysis of the scan data revealed that the panel differs systematically from a flat surface. The panel becomes slightly curved through the Cerrobend casting.

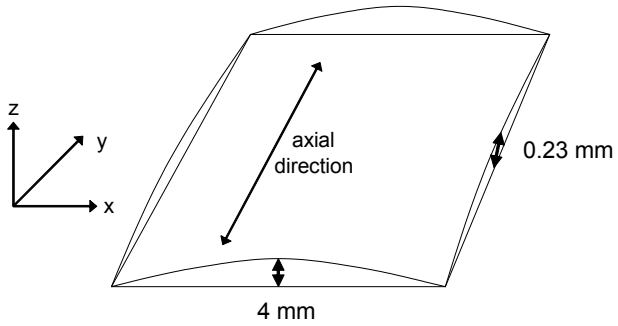

Figure 3.19: Systematic geometrical imperfection

Figure 3.19 illustrates systematic imperfection of the panel. The panel is arched 4mm along its top and bottom sides and 0.23mm axially. This curved shape is the new “perfect” geometry. To obtain magnitudes of local imperfections, the difference of the scanned surface and the curved shape was analysed.

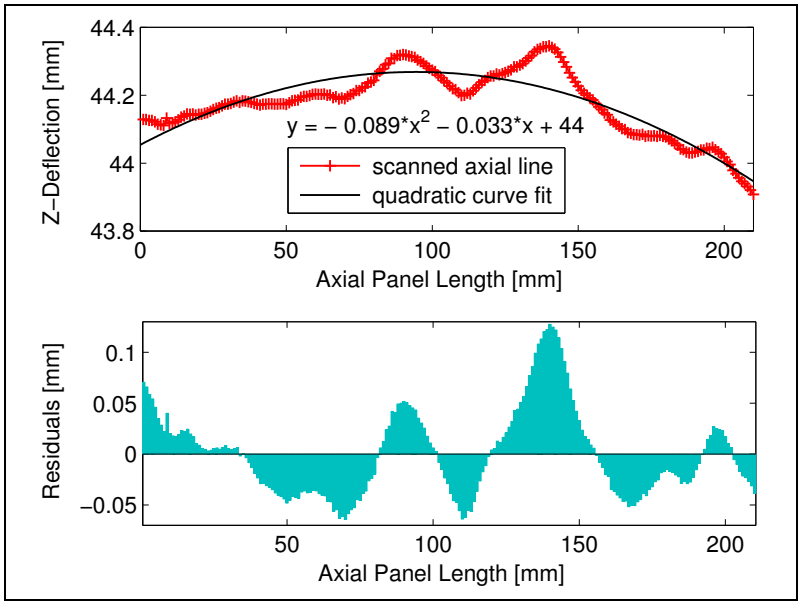

Figure 3.20: Quadratic curve fit and residuals along panel axis

Figure 3.20 shows the analysis of one representative “scanned axial line” using MATLAB. A “quadratic curve fit” using the Eulerian least square method was calculated, which maps the axial curvature of 0.23mm. The difference between both lines is plotted as residuals in the bottom graph. These residuals determine the imperfection per scan line.

Because the imperfection per scan line will be smoothed through the quadratic fit within each line, the global imperfection was calculated as well. This is done by averaging all scanned lines and calculating a curve fit of this average. The residuals of the global curve fit and each scanned line determine the global imperfection.

Imperfections	Average [mm]	Maximum [mm]
Per axial scan line	0.02	0.18
Global	0.05	0.57

Table 3.8: Local and global imperfection

Table 3.8 shows the imperfection magnitudes. The maximum imperfection per scan line is 0.18mm and the maximum global imperfection 0.57mm. This corresponds to about 20% and 60% of the panel thickness respectively.

There are three possibilities of adding imperfection to a FEM model:

1. generating a new mesh, which includes the imperfection,
2. adding the shape of a buckling mode,
3. changing node coordinates directly.

The first option is the most elaborate because an entirely new model has to be created. The other two options can be performed easily with the ABAQUS command *Imperfection.

3.6.6.1 Systematic imperfection

A new mesh was generated to map the panel shape of Figure 3.19. The collapse load decreased only slightly, see Table 3.9. It appears that there is a trade-off for the two curvatures. The axial bending weakens the structure, but the side bending stiffens the structure. The panel was slightly transformed into a stiffer cylindrical structure.

Model	Collapse load [kN]	Solution increments
Reference	119.34	161
Systematic imperfection	118.99	482

Table 3.9: Impact of systematic imperfection

Using the curved shape introduced numerical difficulties. The analysis converged only after experimenting with different solver parameters. The convergence problems were caused by using initially curved surfaces together with the selected contact algorithm.

3.6.6.2 Eigenmode imperfection

A standard procedure to incorporate geometrical imperfections is adding the shape of an eigenmode to the structure [53, 78, 93]. The first eigenmode represents the theoretical buckling shape, i.e. the shape the panel will most likely deform into. The shapes of the first and third eigenmode are visible in Figure 3.21.

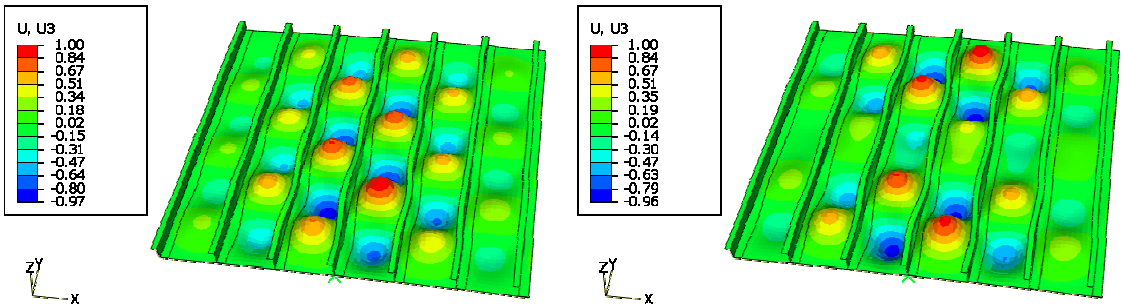

Figure 3.21: Out-of-plane deformation of first and third eigenmode

Table 3.10 shows the impact of adding different magnitudes of the first eigenmode. Depending on the magnitude, the collapse load decreases. Also the effect of applying different eigenmodes was studied. The first, second and third eigenmode were added with a magnitude of 100% panel thickness. The highest decrease of collapse load was observed with the first, and the lowest with the third mode.

Model	**Collapse load [kN]**
Reference	119.34
1st eigenmode, 1% panel thickness	118.89
1st eigenmode, 10% panel thickness	117.27
1st eigenmode, 100% panel thickness	114.93
2nd eigenmode, 100% panel thickness	115.05
3rd eigenmode, 100% panel thickness	118.73

Table 3.10: Impact of eigenmodes

Applying eigenmode imperfections decreases the panel stiffness for certain modes. But the analysis of the scan data did not show that the imperfections have an eigenmode shape.

3.6.6.3 Local imperfection

Table 3.11 display the impact of applying local imperfections. These imperfections were added to the mesh with the magnitude of the measured values (about 50% panel thickness), and also approximately with their geometrical distribution.

Model	Collapse load [kN]
Reference	119.34
Local imperfection, 5% panel thickness	120.13
Local imperfection, 50% panel thickness	119.36
Local imperfection, 500% panel thickness	118.79

Table 3.11: Different magnitudes of local imperfections

These results indicate that the panel collapse behaviour is insensitive to small local imperfection. Therefore, it depends where the imperfection is applied. Even big dents in the plate between two stiffeners do not significantly affect the panel failure behaviour. Imperfections around sensible areas, such as the middle of the outer stiffeners, have a much larger influence. Local imperfection of the measured magnitude will be included into the improved model.

3.6.7 Scattering in material parameter

This error source is strongly linked to the material model. Material properties can vary greatly and depend on temperature, thickness, production process and alloy composition. Alloy specifications are not too definite, e.g. the proportion of copper in aluminium L165 may vary by 1.1% (3.9-5.0%) [43]. In order to obtain reliable information, specimen tests with the panel material would be necessary. It was not possible to assemble statistically significant data within the scope of this research. Therefore, published data were consulted. ESDU [43] and MIL-HDBK-5H [82] both specify mean values for elasticity and yield stress for the used alloy, but do not specify variability. Haugen [51] lists specific values of alloys similar to the used L165 (2014A-T6), see Table 3.12.

Material	Tensile yield strength			
	Mean [N/mm^2]	Mean [ksi]	Standard deviation	Sample size
2014 (AMS 4135)	(517.13)	63.0	1.75	20
2014-T651	(496.44)	72.0	2.07	19
2024-T4	(248.91)	36.1	1.91	61

Table 3.12: Variation in static strength of aluminium alloys [51]

Published yield strength was given in ksi units and was transformed in the table to $\mathrm{N/mm^2}$ using the factor 6.895 [82]. Standard deviations of about 2 imply a variable quality of the used materials. The model will use the producer supplied mean values as described in a previous section. An idealisation error of 1% results when modelling the material with a standard deviation of 2 for Young's modulus and yield strength.

3.6.8 Accordance with predicted failure modes

Section 3.2 described design calculations for the used stiffened panel. Local skin buckling should start at 19.78kN and the collapse load was determined as 100.83kN. Torsional buckling was predicted as the collapse mode of the panel.

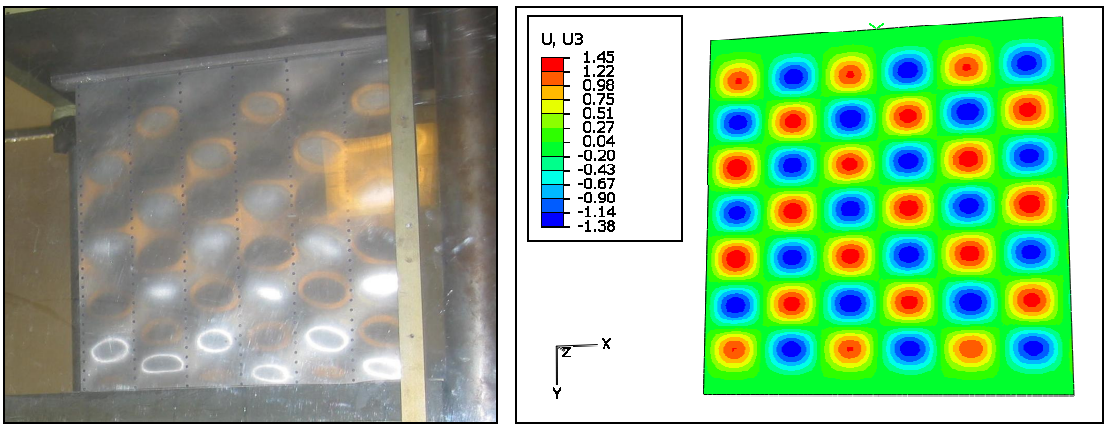

Figure 3.22: Local buckling of test panel and simulation, Magnitude of out-of-plane deformation shown in the FEM model

Figure 3.22 compares the out-of-plane displacement of the test with the FEM solution during local buckling. Clearly visible local buckling starts at about 23kN in the simulation. This is reasonably close to the value from the design calculation. Test and simulation shape display 3.5 wavelengths axially and look very similar.

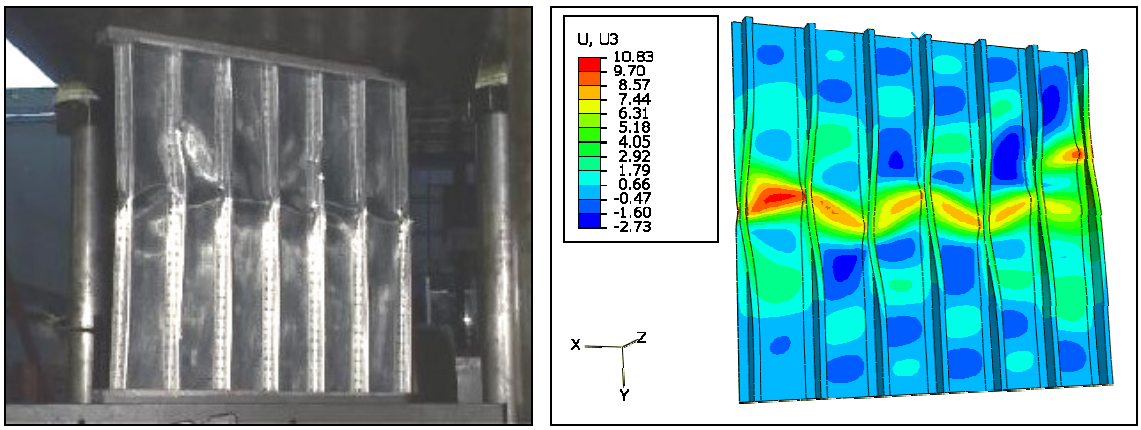

Figure 3.23: Collapse deformation of test panel and simulation

Figure 3.23 compares the real and the calculated failure shape. The predicted torsional buckling is visible at the outer stiffeners, followed by flexural buckling.

3.6.9 Overall error assessment

Error source	Analysis outcome	[%]
Material model	The model uses an appropriate elastic-plastic material model, but leaves an idealisation error.	1.0
Applying load / displacement	Application of displacement instead of load does not change the solution process.	-
Contact between panel and stiffener	A suitable contact model was found. Rivets are modelled with an estimated stiffness, what leaves some uncertainty.	1.0
Sensitivity to boundary conditions	The Cerrobend modelling was improved. Panel end rotations cause an idealisation error.	3.0
Shape of the stiffeners	The final model includes curved shapes but leaves an idealisation error.	1.0
Geometrical imperfection	Local imperfections are incorporated into the model.	-
Scattering in material parameters	This error source was analysed using published material variances.	1.0
Accordance with predicted failure modes	The solution shows correct behaviour and fails in accordance with the predicted mode (torsional buckling).	-

Table 3.13: Overall error assessment

Table 3.13 summarises the idealisation error analysis. “[%]” lists the estimated error which will be left in the final model. In practice, the error sources are not independent. However, from this analysis it is not possible to calculate a maximum idealisation error for the final model. In a worst case scenario the error is additive, giving a maximum idealisation error of 7%.

3.7 Final Model

The final model incorporated all improvements, as listed in Table 3.13. Important parts of the ABAQUS input are provided in Appendix B.1. The model includes the curved stiffener shape and contains local imperfections. The analysis is displacement controlled and uses 379000 S4R shell elements. The increase in the number of elements is the consequence of a more complex model. It is important to place sufficient shell elements between two connector elements to model inter-rivet deformations.

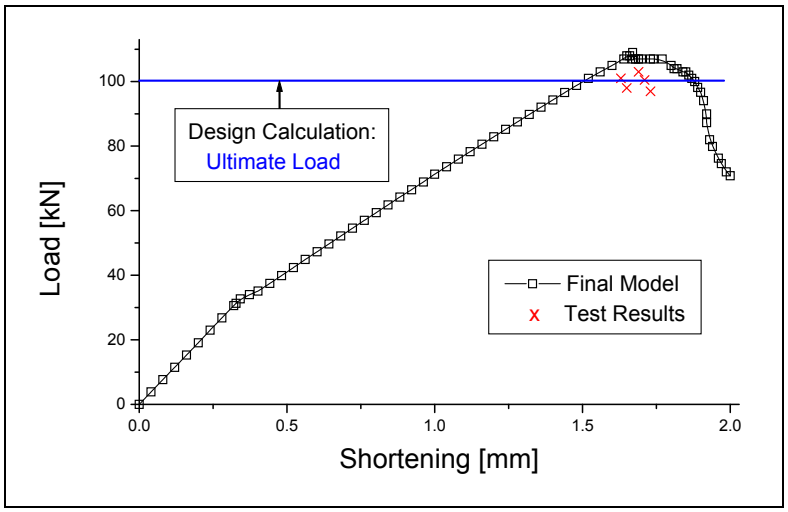

Figure 3.24: Final model, design calculation and test data

Model	Collapse load [kN]
Final model	108.60
Design calculation	100.83
Tests	97.00 .. 103.00

Table 3.14: Collapse load of the final model, design calculation and tests

Figure 3.24 and Table 3.14 summarise the results. The final model predicts a failure load of 108.60kN. In tests, ultimate strengths between 97 and 103kN were measured. The design calculation is in accordance with the test results, but the FEM model overestimates the average test collapse load by 8%.

Figure 3.25: Panel testing and load display (short before collapse)

The investigated panel is thin-walled (skin and stringer thickness are both 0.9mm), which leads to strong geometrical nonlinearity. The study revealed that the main idealisation error sources are the stiffener shape, boundary conditions, material model and contact modelling. Geometrical imperfections did not show a significant impact. The final FE model overestimates the mean test failure load by 8%. This is slightly more than the accumulated idealisation error of 7%.

3.8 Discussion

It was an interesting challenge to study the idealisation error control methodology and to apply it to a nonlinear case. The outcome is important for the planned expert system development. The SAFESA methodology helped to understand the idealisation process and yielded concrete error estimates. The paper-based analysis was not difficult to apply. Nonlinear error sources were obvious or were identified during the discussion of the results with experienced staff. Initially, the main motivation for the decomposition in SAFESA step-3 was not understood very well. The aim is to correctly model the interfaces of the structural assembly. This aspect should be highlighted in the idealisation support software.

The interpretation and validation of the test results was more difficult. Initially, the inaccuracy of the test machine was estimated to be up to 20%. The machine calibration revealed that the error is only 0.5%. In any case, the complete recording of the load-shortening process is not possible. A project to design a new test panel which fits into better test equipment is ongoing. Another aspect is the building of an appropriate material model. Published material parameters differ considerably and material coupon tests could not be realised in the course of this project. The material model that was used can be further refined by performing coupon tests.

Another important consideration is the sensible interpretation of the analysis results. The overall error assessment is difficult because the idealisation error sources cannot be regarded independently. Changing boundary conditions can easily change the simulation behaviour and lead to a larger impact of joint modelling etc. A summation or a probabilistic treatment of the error sources both have their own drawbacks. Further research is required to study the amount of the error source dependency.

The Cranfield panel test was designed as a lecture demonstration. Unrestrained side boundary conditions are problematic because they are not in line with the conditions of real aerospace panels. The Cerrobend casting technology could also be improved. Panel end rotations that occurred could be measured for more realistic modelling. Some open questions remained after the analysis of

geometrical imperfections. In certain cases, an increase of the panel failure load after adding imperfections was observed. Another result of the analysis is that increasing the number of elements is necessary to correctly model the inter-rivet deformations. Coarser meshes with only two or three shell elements between joints do not allow the material to deform adequately during the simulation.

FEM model generation with pre-processors, the use of ABAQUS and job submission to the Cranfield multi-processor machine were demanding tasks in the beginning. Little details can have a very detrimental impact. A profound understanding of solver minimum and maximum step size, the used contact model and the choice of a stabilisation factor for the Newton-Raphson method are crucial. Analysis output must be restricted to the required parameters, because the output file *.odb can easily become too large. The knowledge gained during this study enabled the analysis of more complex problems.

4. AIRBUS PANEL ANALYSIS

4.1 Introduction

In this chapter the idealisation error control procedure is applied on the Airbus compression panel test. It is representative of the structural test that could in practice be replaced with virtual testing. The structure is more complex than the Cranfield panel, which makes the idealisation process demanding. CAD drawings, a previous FEM model and test data were provided as an application case within MUSCA project. This section gives a brief overview of the test case. A detailed description of the panel is part of the error control procedure and will be covered in the following section.

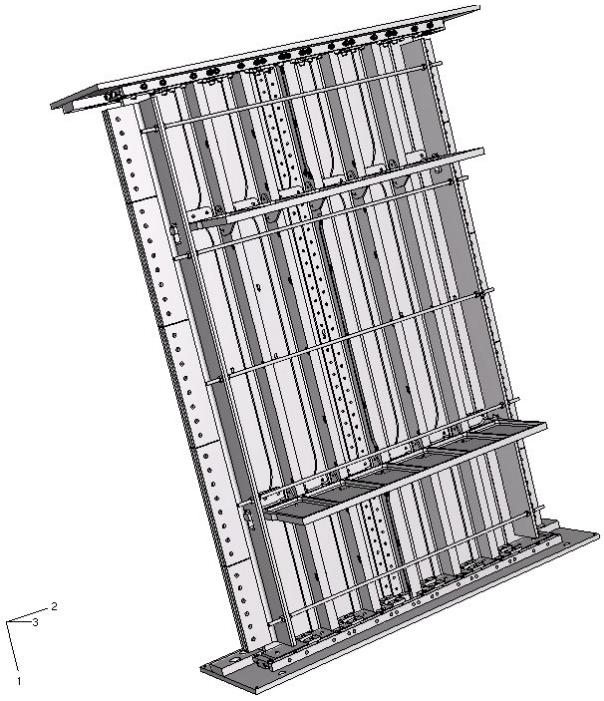

Figure 4.1: Airbus stiffened panel [91]

The structure shown in Figure 4.1 is a stiffened panel similar to those used in aircrafts. It consists of two stiffened panels connected with a butt joint to form a single unit. The panel length is 1.72 m, and the width is 1.03 m. It is manufactured from different alloys of aluminium and has a mass of 440 kg. The unloaded edges of the structure are supported by a steel side frame to provide appropriate boundary conditions.

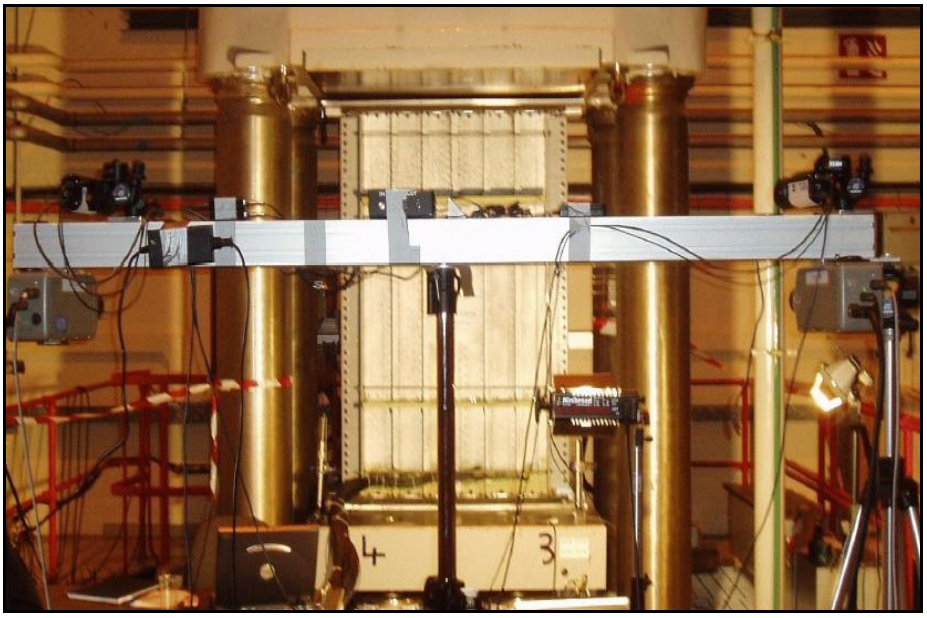

Figure 4.2: Panel testing at Airbus UK [91]

Figure 4.2 illustrates the experimental environment. The panel was tested at Airbus UK and data were recorded using cameras, strain gauges and displacement transducers. While experimental data are not required for the error control procedure, the data do allow a verification of the model.

4.2 SAFESA Procedure

This section describes the application of the error control procedure for the collapse analysis of the compression panel.

STEP 1: Definition of boundary, boundary conditions and loading actions

Input:

1. Real World Problem

Geometry: Figures 4.1-4.8 show the components of the structure:

Two rectangular plates (which are connected via a connecting plate, called buttstrap) with length: 1721mm x width: 513.5mm x thickness: 8.8mm. At the sides where the panel contacts the side frame, the plates have a thickness of 15.9 mm, as shown in the upper part of Figure 4.4.

The **buttstrap** has length: 1721mm x width: 150mm x thickness: 6.5mm. The assembly of the two plates and the buttstrap is 1030mm wide.

Five stiffeners with cross sections shown in Figure 4.4. The cross section of the middle stiffener differs from the others. The length of all stiffeners is 1721mm. Stiffeners are riveted onto the plates, and the central stiffener is bolted on the buttstrap and plates.

Two Ribs, which are depicted in CAD drawings in Figures 4.5 and 4.6. The ribs have a plane surface on one side and six convex shapes on the other side. At the rib bottom there are six struts, which are located in between the stiffeners.

Ribs are connected to stiffeners with help cleats, as shown in Figure 4.5. Altogether there are **ten cleats** in the model. The cleat geometry is shown in Figure 4.8.

Top and bottom of the panel are rigidly attached to **end platen**, which is visible in Figure 4.1. This end platen aim to provide appropriate boundary conditions.

The **Side frame** restrains the panel in out-of-plane deflection. It has a length of 1630.1mm and contacts 53.5mm of the panel in plane direction, see Figure 4.3 and 4.4. The frame sides consist of two L-shaped stiffeners, which are bolted to a solid plate. Both frame sides are interconnected using beams, see Figure 4.7.

All parts are joined together by a number of **rivets and bolts**.

At this point of the analysis the **assembly** as a whole is of interest. Details are given to illustrate this rather complicated structure.

Material: Plates, buttstrap, stiffeners, ribs, cleats and rivets are made of different aluminium (7000 series) alloys.

The side frame is made of steel.

Loading: The test rig lifts the lower part, as shown in Figure 4.2. The applied load is compressing the panel axially until collapse.

Boundary conditions: As it can be seen in Figure 4.1 and 4.2, top and bottom ends of the panel are cast into end platen.

The sides of the panel are connected to the side frame, which prevents out of plane deflection.

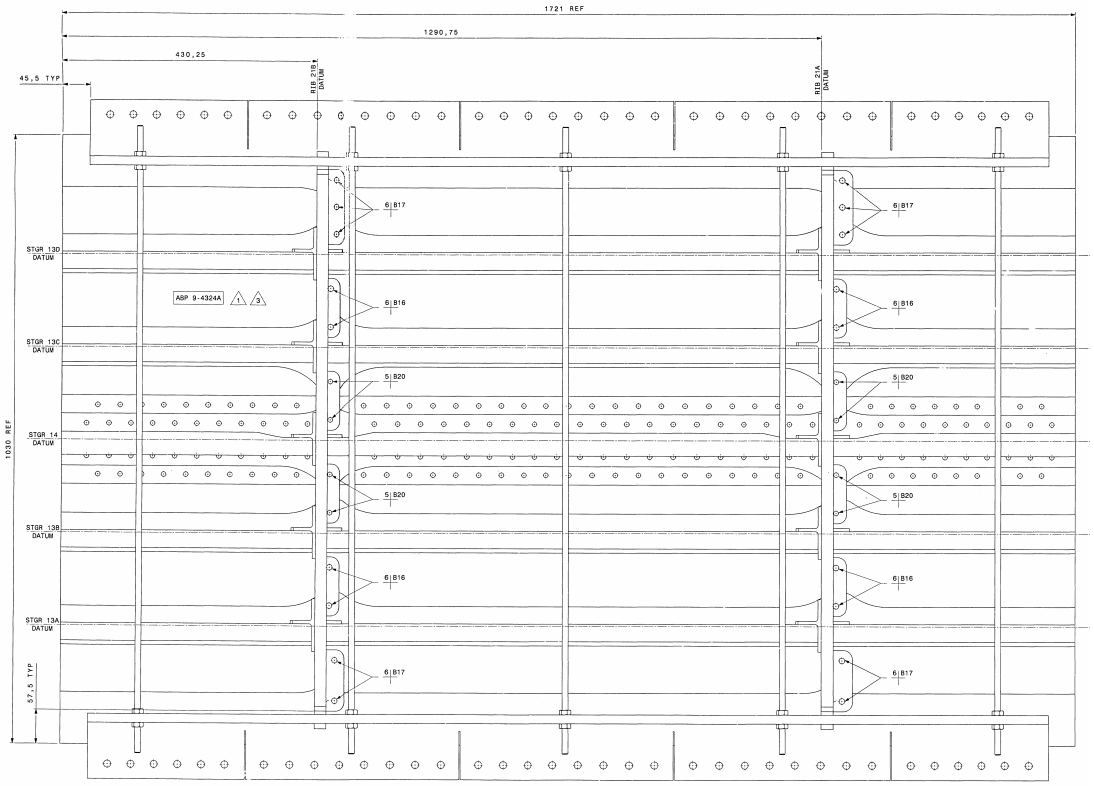

Figure 4.3: CATIA drawings of the panel assembly [91]

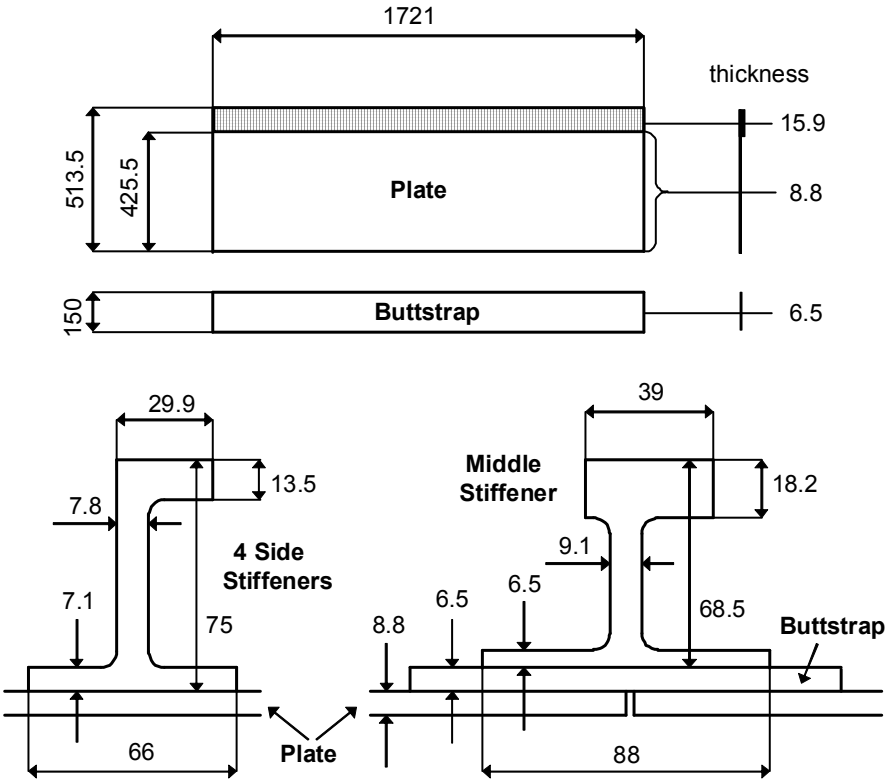

Figure 4.4: Geometry details of plate, buttstrap and stiffeners

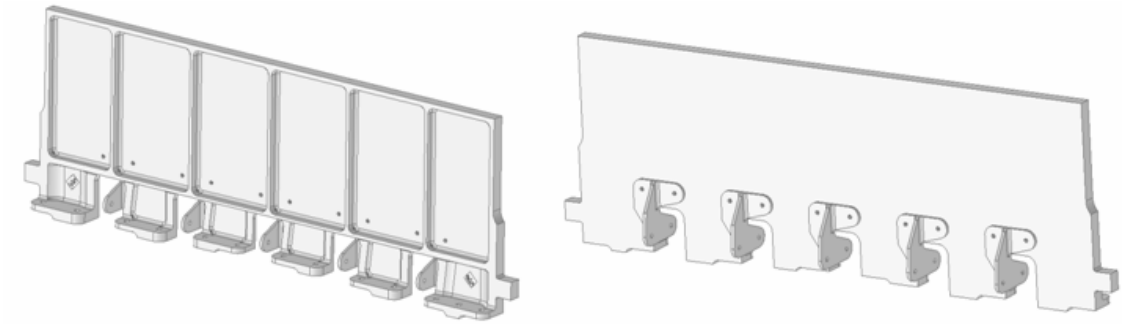

Figure 4.5: Front and back view of the rib with cleats

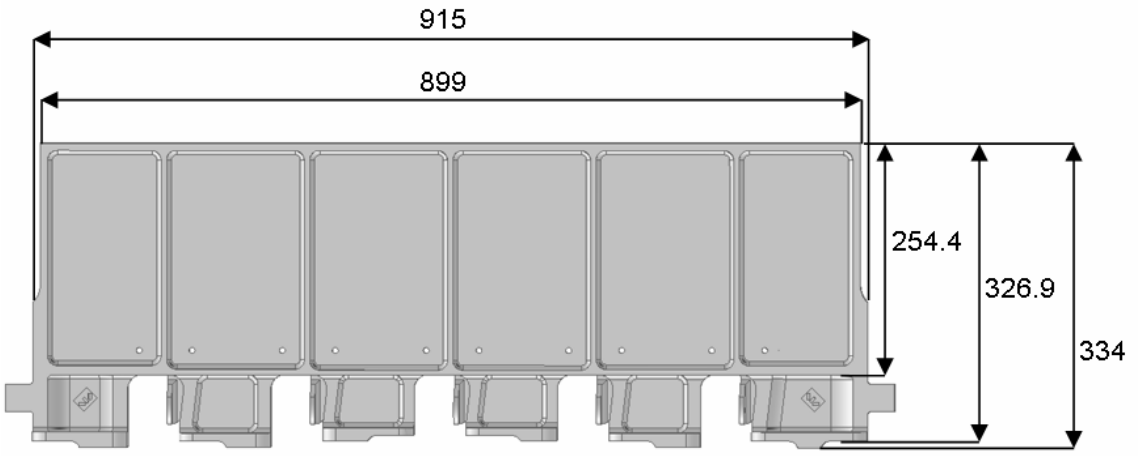

Figure 4.6: Dimensions of the rib

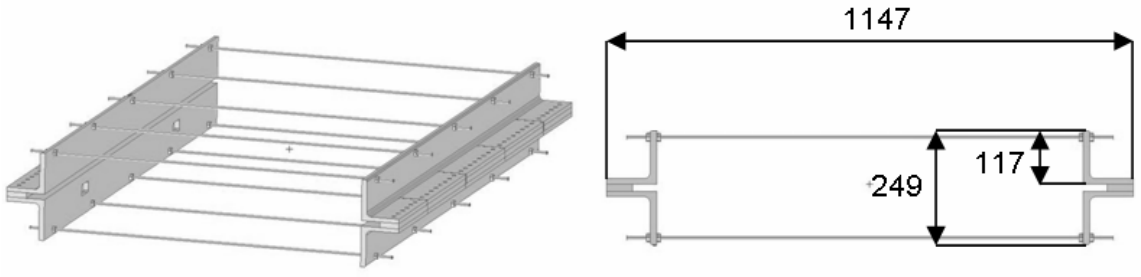

Figure 4.7: The side frame prevents out-of-plane deformation

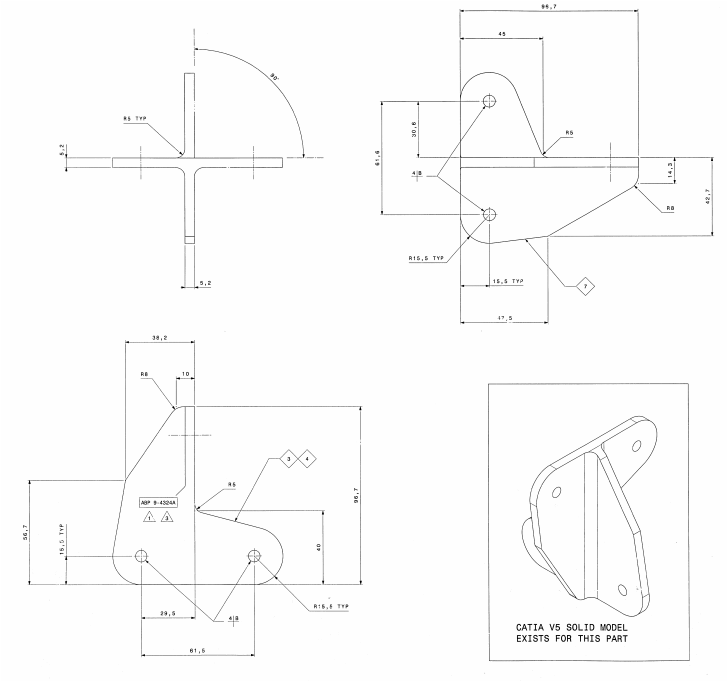

Figure 4.8: Geometry of a cleat [91]

2. Qualification criteria

The aim is to determine the maximum load at failure with an uncertainty error of less than 10%.

Process:

1. Domain definition and error treatment

1.1 Define domain:

The stiffened panel composed of plates, buttstrap, stiffeners, ribs and cleats represents the domain of interest for the analysis.

The top and bottom are attached to end platen, which will be modelled with appropriate boundary conditions. Therefore, the end platens are excluded from the domain.

The panel has sliding contact with the side frame, which is included in the model.

1.2 Define boundary conditions:

The panel with attached end platens is elastically placed into the test rig. While the test machine compresses the panel, rigid contact between the rig and the panel is assumed. In order to axially apply a uniform pressure, the top side of the panel will be modelled rigid and the bottom side clamped.

Flag 1 Check the sensitivity to the boundary condition type. How much does the rotational constraint at the ends influence the solution?

The side frame is attached to both sides of the panel and will be modelled in one piece. There is no connection of the frame to the test rig. Therefore, no additional boundary conditions apply for the sides.

2. Loading:

External load is compressing the panel axially until collapse. No shear forces. In the model this will be realised via a displacement in axial direction.

Output:

1. Structure geometry and boundary conditions as above.
2. Loading as above.
3. Errors: boundary conditions, see Flag 1.

STEP 2: Definition and error treatment of load paths, geometry idealisation

Input:

1. Idealisation of boundary conditions and loading
2. Real structure geometry
3. Qualification criteria

Process:

1. Overall behaviour:

There are five stages in the loading process until failure:

- Linear elastic material deformation at lower stress levels.
- Local buckling of the plate between the stiffeners. As the plate is a relatively thick one, this will probably not happen with this panel.
- Global bending of the whole structure. At this point the stringers start buckling and the load path will change.

- Failure of a rivet or bolt connection. This local failure will most likely be followed by a global collapse of the panel.
- Collapse of the structure. The structure deforms plastically and the capability to carry load is decreased.

2. Load paths:

The external load is applied axially to one end of the panel. As the other end is clamped all pressure is absorbed uniformly by the structure. When nonlinear behaviour starts the load path will change.

Flag 2 Do load paths really change during the FE simulation? Check the stress output.

3. Geometry idealisation

3.1 Domain reduction:

The structure has no plane of symmetry and is modelled as a whole.

3.2 Mathematical model:

Plates, buttstrap and stiffeners are plane, and will be modelled using shell elements. Classical shell theory is applicable, i.e. the length-thickness ratio is large:

- Plates are thin shells (l/t = 513.5/8.8 = 58.35)

- Buttstrap (l/t = 150/8.8 = 17.05)

The critical cross sections of the stiffeners' tops are shown in Figure 4.4.

- Stiffeners 1,2 & 4,5 (l/t = 29.9/13.5 = 2.21)

- Middle stiffener (l/t = 39/18.2 = 2.14)

Flag 3 Is it realistic to model the stiffeners with shell elements? The aspect ratio of the top surfaces is quite small for the assumption of shell theory. The alternative is to use solid elements. The influence can be analysed using a smaller model comparing shells and solids.

Ribs and cleats will be modelled with solid elements as they have a curved solid shape.

Flag 4 Is it necessary to use solid elements for the cleats? Check the possibility of modelling the cleats with shell elements. This would simplify the model.

The side frame will be modelled with shell elements. The connecting beams use beam elements. Rivets and bolts will be modelled with connector elements.

Flag 5 This model assumes a perfectly shaped geometry. How much does geometrical imperfection influence the solution? These imperfections result from the production process and are always present.

3.3 Dimensional reduction:

Using shell elements instead of solids simplifies the stiffener shape, especially at corners and edges. Hereby, the stiffeners are modelled using shell mid-surfaces.

Flag 6 Does the use of shell mid-surfaces lead to an error?

The shape of rivets and bolts is neglected, i.e. the bottom of the plates and the stiffeners are assumed plane. Consequently all joint holes are neglected as well.

3.4 Revision of essential and natural boundary conditions:

Nothing changes, as no simplification due to symmetry is applied and the idealisation of the geometry does not affect the boundary conditions.

4. Analysis type:

Nonlinear quasi-static collapse analysis.

5. Material idealisation:

Steel and different 7000-series alloys of aluminium are used. As the aluminium locally extends yield stress, the elastic-plastic material model will be utilised. Values of the stress-strain curves were provided by Airbus UK.

Flag 7 How much scattering is in the parameters E and σ_y ?

Output:

1. Overall idealisation of geometry and material properties.
2. Type of analysis: nonlinear quasi-static.
3. Structural behaviour:
   - Shells for plates, buttstrap, stiffeners and side frame,
   - Solid elements for ribs and cleats,
   - Beam elements for the side frame connecting beams.
4. Errors flagged out, otherwise not significant.

STEP 3: Breakdown of the structure or feature

Input:

1. Idealised geometry, boundary conditions and loading action for the structure or feature.
2. Load paths within the structure or feature.
3. Structural behaviour within the structure or feature.

Process:

1. Breakdown of the structure into lower level features:

Plates and buttstrap are very firmly connected and can be seen as one unit, as shown in Figure 4.3 and 4.4. The middle stiffener differs from the other stiffeners and is regarded as a different feature. The side frame assembly forms another unit, see Figure 4.7.

Feature 1: Plates and the connecting buttstrap

Feature 2: Middle stiffener

Feature 3: Stiffeners, except the middle one

Feature 4: Ribs

Feature 5: Cleats

Feature 6: Side frame

Output:

1. The structure is divided into six features.

STEP 4: Definition of boundary conditions and loading action for features

Input:

1. Features from Step 3
2. Outputs from Steps 1 and 2

Process:

1. Boundary conditions for features:

Feature 1: Plates and buttstrap

The connection between plates and buttstrap is assumed to be adequately stiff in order not to subdivide this feature.

The stiffeners, except the middle one, are riveted onto the plates. An appropriate model for surface contact and joints has to be found.

Flag 8 Study the influence of different possibilities to model rivets and bolts. The following joint models should be considered:

- Rigid and less rigid joints; e.g. ABAQUS Beam and Link Connector elements
- Spring elements
- Connector elements including elasticity and plasticity

The middle stiffener is bolted to the buttstrap and plates, see Flag 8. Ribs are also bolted to the plates, see Flag 8.

Boundary conditions for the interconnection of the panel with the test rig were considered at the global level.

The plates are elastically clamped into the side frame to prevent out-of-plane deformation. Side effects can influence the behaviour of the model assembly.

Flag 9 Investigate the connection between plates and the side frame. How is the frame best modelled? How does friction influence the simulation?

Feature 2: Middle stiffener

The middle stiffener is bolted to the buttstrap and the plates, see Feature 1. Both ends are rigidly clamped; this was considered at the global level.

The connection to the ribs is achieved via cleats, which are bolted to stiffeners and ribs, see Figures 4.3 and 4.5.

At their bottom, ribs are also bolted to the stiffeners. This connection also includes buttstrap and plates. The bolts are longer and could be less stable.

Flag 10 How is the rib-stiffener-buttstrap-plate connection best modelled? The contact now comprises four layers. This flag is similar to Flag 8. Differences are: longer bolts used and higher level of stress/strain.

Feature 3: Stiffeners, except the middle one

The stiffeners are riveted on the plates, see Flag 8. Both ends are rigidly clamped; this was considered at the global level.

The upper connection to the ribs is achieved via cleats. At the lower level, ribs are also bolted to the stiffeners bottom.

Feature 4: Ribs

Ribs are bolted onto the plates, the buttstrap and all stiffeners, see Features 1-3. Ribs are also connected to the stiffeners via cleats, see Features 2 and 3.

Feature 5: Cleats

Cleats connect ribs with stiffeners. They are bolted to stiffeners and ribs, shifted by 90 degrees, see Figure 4.3 and 4.5. This connection is investigated in Features 2-4.

Feature 6: Side frame

The side frame is assumed to be adequately stiff in order not to be subdivided. Heavy yielding is not likely, because it is made of steel. The contact with the plates is of interest, see Feature 1.

2. Loading actions for features: Feature 1-6

Loading actions specified earlier remain unchanged.

Output:

1. Idealised boundary condition.
2. Idealised loading known.
3. Errors: flagged out, otherwise not significant.

STEP 5: Definition and error treatment of load paths and idealisation of geometry for features

Input:

1. Idealised boundary conditions for the feature
2. Idealised loading for the feature
3. Real geometry of the feature
4. Qualification criteria

Process:

1. Behaviour of the feature	As before
2. Load paths	As before
3. Geometry idealisation	As before

3.1 Domain reduction	As before
3.2 Mathematical model	As before
3.3 Dimensional reduction	As before
3.4 Revision of essential and natural boundary conditions	As before
4. Analysis type	As before
5. Material idealisation	As before

Output:

1. Idealised geometry and material: as before.
2. Type of analysis: as before.
3. Structural behaviour: as before.
4. Errors: as before.

STEP 6: Assessment

Input:

1. Real world problem
2. Idealised structure
3. Error estimates

Process:

1. Assessment at the global level:

Flag 1-7	Error sources at the global level are: 1) Sensitivity to boundary conditions at top and bottom 2) Check if load path change when NL-behaviour start 3) Stiffener with shell or solid elements 4) Cleats with solid or shell elements 5) Geometrical imperfection 6) Influence of stiffener mid-surfaces 7) Scattering in material parameters

2. Assessment at feature level:

Flag 8-10	The error flags at the feature level are concerned with correctly modelling the interfaces between the features: 8) Joint modelling

9) Plate and side frame connection
10) Rib-stiffener-buttstrap-plate connection

Output:

1. A geometry scan is necessary (Flag 5) to obtain reliable values of the geometrical imperfection.

   Coupon tests will be required (Flag 7) in order to analyse material parameter variances.

2. Second iteration required.

STEP 7: Test program

Input:

1. Real world problem
2. Idealised structure
3. Error estimates

Process:

1. Measurements for geometrical imperfection.

2. Material tests to obtain stress-strain curves.

3. Joint tests to obtain stress-strain data and failure loads.

Output:

1. Values of geometrical imperfection.
2. Stress-strain curves from the tested materials and joints.

The outcome from this first stage of the error control procedure is an idealised description of the panel together with a list of error flags, where idealisations have been made which could lead to errors that are unknown at this stage.

4.3 Supporting Test Data

The panel test and additional investigations were performed before this study, and no additional data could be collected. All test data were provided by Airbus UK and is described in this section. This represents a far higher quality set of data than was available for the Cranfield test.

4.3.1 Displacement transducer

Available test data were used to verify the correctness of the reference model. It was noticed that the test equipment introduces some inaccuracy. Ideally, the test rig would compress the panel in a way that upper and lower part of the test machine stay parallel.

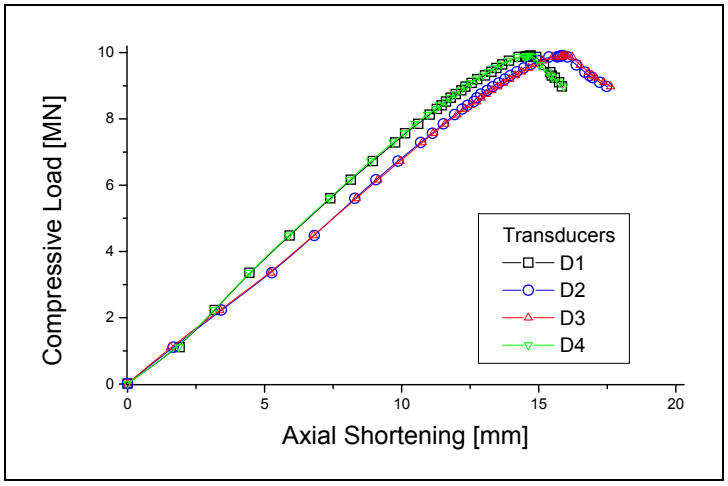

Figure 4.9: Load-shortening curve of the test panel

Figure 4.9 shows the experimental load-shortening curve for the panel. D1-D4 denote the displacement transducers located at each corner of the test structure, see Figure 4.10a. The difference between D1, D4 and D2, D3 is due to a small rotation about the lateral axis of the panel. It occurred early in the test at about 20% of ultimate load. This makes a correct interpretation of the failure location in the load-shortening curve difficult, as the difference is 1.28mm at failure. The fact is important for modelling boundary conditions and will be discussed at a later stage.

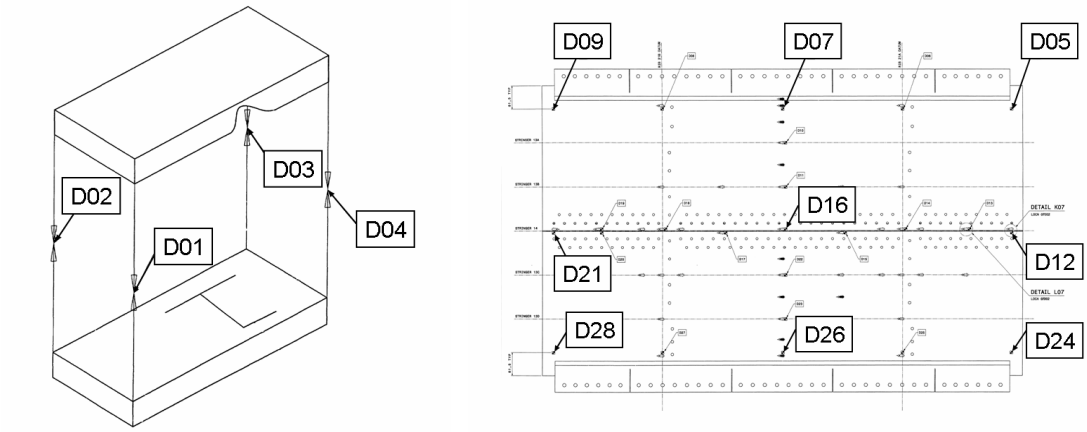

Figure 4.10a, b: Location of displacement transducers in the test

Figure 4.10a and 4.10b show the location of displacement transducers. D1 to D4 measure the load-shortening curves at each corner of the end platen. Another important transducer location is D16 for extracting the mid point out-of-plane displacement. D09, D21, D28 and D05, D12, D24 compare the out-of-plane movement at opposite ends of the panel. D07 and D26 provide information for the study of panel and frame interaction.

4.3.2 Material properties

Material coupon tests for the used aluminium alloys were performed at Airbus UK. The test output of the most important parts (plates and middle stiffener) can be found in Appendix A.3. The resulting stress-strain curves were transformed into the elastic-plastic ABAQUS input format. The provided material data could directly be incorporated to the FEM model.

4.3.3 Joint properties

For the panel assembly different joints were used: rivets, prot-head and countersunk bolts with varying lengths. Table 4.1 summarises their location and linear stiffness. Selected nonlinear properties can be found in the ABAQUS input, see Appendix B.2.

Type	Connection	Stiffness [N/mm]		
		x	y	Z
Rivet	Stiffener (except middle one) - plate	131338	131338	37300
Countersunk bolt 5b10	Buttstrap-plates, middle stiffener-buttstrap, rib-middle stiffener-buttstrap-panel	95000	95000	340000
Countersunk bolt 6b16	Rib-plate, rib-stringer-skin	139000	139000	494000
Prot-head bolt 4b9	Rib-cleat, stringer-cleat	33820	33820	257181

Table 4.1: Location and elastic properties of used joints

Z-stiffness is the axial stiffness of the joints, which is most significant. Important joints are the bolts between the stiffener-buttstrap-plate contact, see Figures 4.3 and 4.4.

4.3.4 Geometrical imperfection

The real panel geometry deviates from the ideal of plane surfaces. For the study of geometrical imperfection real thickness measurements were available.

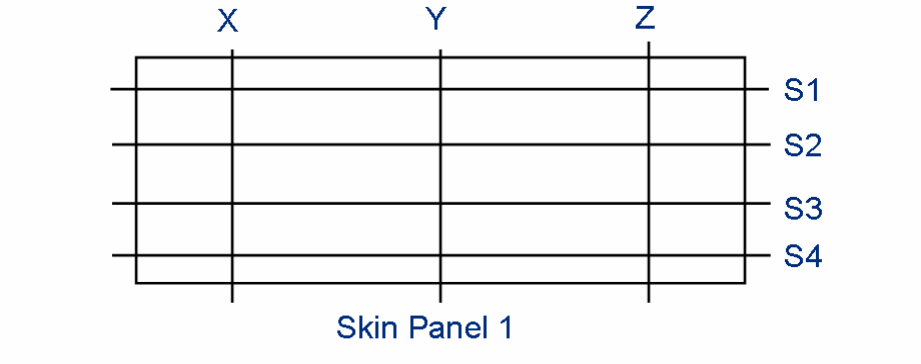

Figure 4.11: Measured thickness of the skin panel

Figure 4.11 and Table 4.2 illustrate the test data. The location where the skin panel thickness was measured is explained in Figure 4.11. Data were available for the skin plates, the buttstrap and the middle stiffener, see Appendix A.3.

Position	CAD [mm]	X [mm]	Y [mm]	Z [mm]	Peak diff. [mm]	Average diff. [mm]
S1	8.8	8.842	8.820	8.846	0.046	0.036
S2	8.8	8.846	8.831	8.855	0.055	0.044
S3	8.8	8.866	8.838	8.872	0.072	0.059
S4	15.9	15.992	15.964	15.984	0.092	0.080

Table 4.2: CAD specification and measured thickness of skin panel-1

“CAD” denotes the dimension from the CAD model, which was used to build up the model geometry. The measured values were usually bigger, as can be seen in the table. Values of the “peak difference” imply that the panel had an imperfection of the order 0.5 - 0.8% from the panel thickness.

4.4 Reference Model Building

After completing the idealisation analysis a FEM model was built, starting with the CAD geometry of the panel. The panel is attached on both ends to end platen and elastically placed in the test machine. While the test machine compresses the panel, rigid contact between the rig and the panel is assumed, see Figure 4.12. The unloaded edges of the structure are supported by a steel side frame to provide appropriate boundary conditions. In order to axially apply

a uniform displacement, the top side “C” is modelled clamped and the bottom side “A” is rigid. The side frame is entirely modelled. As there is no physical connection of the frame to the test rig, no additional boundary conditions apply for the sides.

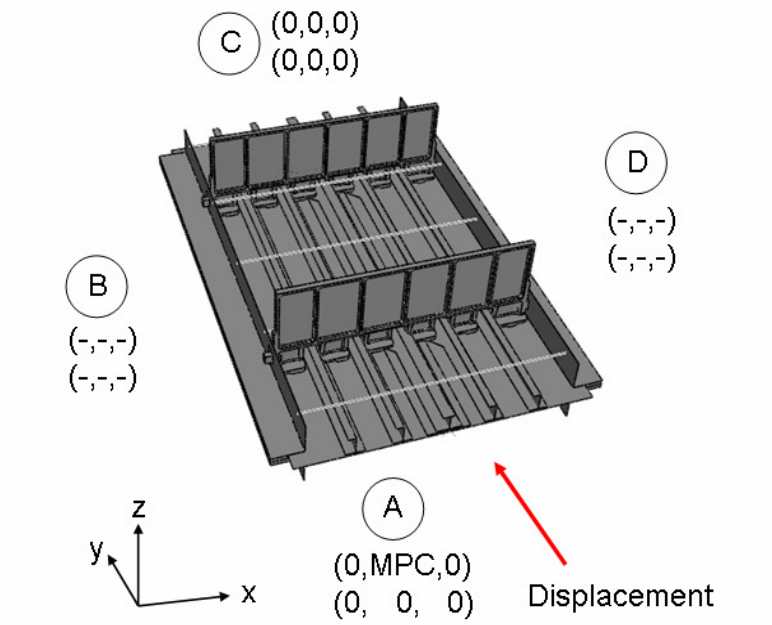

Figure 4.12: Model geometry with boundary conditions

All metals are modelled with the elastic-plastic material model, using supplied stress-strain data. Contacting surfaces apply the surface-to-surface and small sliding contact formulation. Rivets and joints are modelled using mesh independent connector elements (via *Fastener), neglecting their geometrical shape. The provided joint properties caused severe convergence problems. Therefore, only elastic joint properties were incorporated into the reference model.

The main motivation for the model design was to create an analysis-friendly pattern. Therefore, the model size was kept small. Plates, buttstrap, stiffeners and side frame are modelled with shell elements. Ribs and cleats consist of solid elements. As no major load path goes through these parts simple tetrahedral elements were used. The following analysis investigated the impact of these model simplifications.

4.4.1 P-mesh sensitivity study

The model was designed with the idea to reduce the number of unknowns without over-simplifying the structure. This section outlines the effect of using the simple C3D4 tetrahedral element for ribs and cleats instead of the reliable

but more expensive ten node C3D10M element. C3D10M instead of C3D10 is recommended for cases where contact is involved [1]. The reason for using the four node version is that ribs and cleats are not located in critical regions.

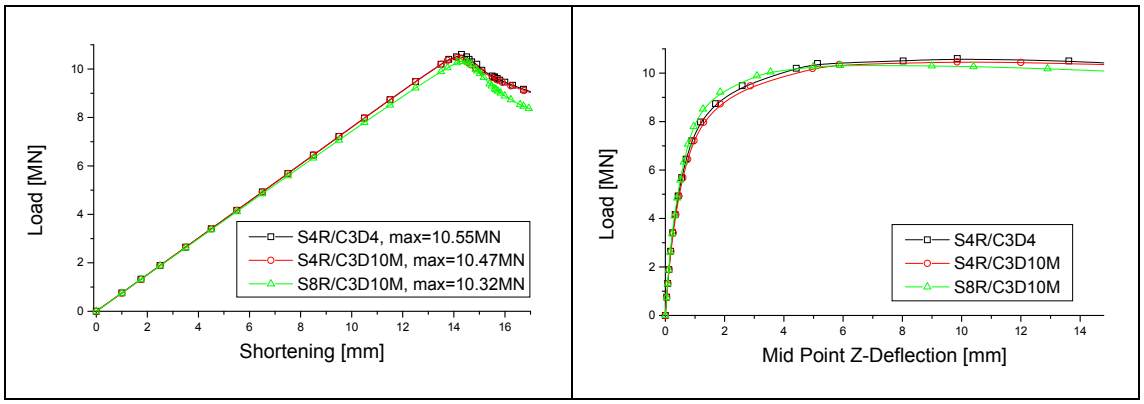

Figure 4.13a, b: Small difference in using C3D4 and C3D10M elements

“S4R/C3D4” and “S4R/C3D10M” in Figure 4.13a compare models using C3D4 and C3D10M solids. The difference in failure load is less than 1%, which is within the acceptable limit. Interestingly the failure load with C3D4 is lower, although the risk associated with the use of this element is that the structure behaves too stiff. “S8R/C3D10M” uses the eight node shell element S8R together with C3D10M solids. The small drop in failure load can be explained with the different shell properties, see section 2.4.4. In Figure 4.13b the mid point out-of-plane displacement is compared, which is measured in the test with transducer D16. This displacement was selected as the second validation criteria of the model. The curves of all FE models show a similar behaviour. It can be concluded that using C3D4 elements instead of C3D10M is acceptable.

4.4.2 H-mesh sensitivity and shell element selection

For the purpose of finding an appropriate shell element type and mesh size, the model was simplified to restrict the analysis only to shells. Ribs, cleats and the side frame were removed from the model. All contact formulation and connector elements were replaced with rigid TIE-contact between surfaces, which connect the nodes of involved surfaces and makes it a one piece for simulation. In order to model similar panel failure behaviour, the nodes at the former stringer-rib interface were restricted to move sideways, which is shown in Figure 4.14. Like the complete model, the simplified panel fails through global bending.

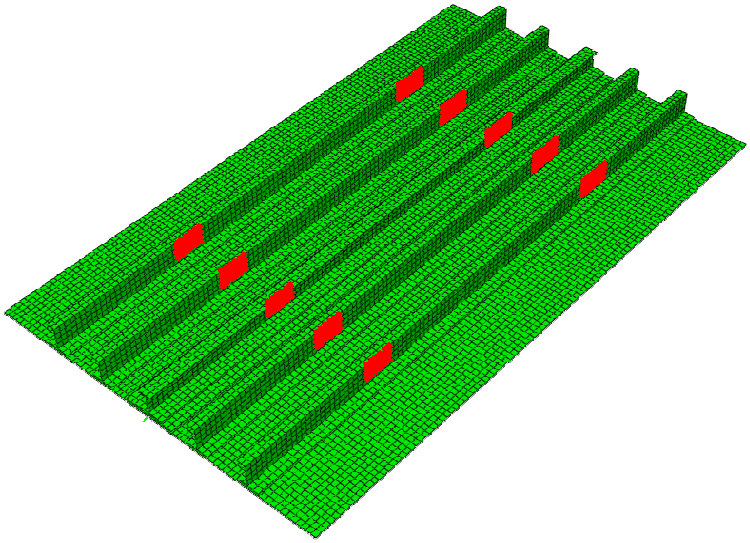

Figure 4.14: Simplified model with stringer-rib contact areas

Figure 4.15 shows load-shortening curves of models with different ABAQUS shell elements. The curves look very similar.

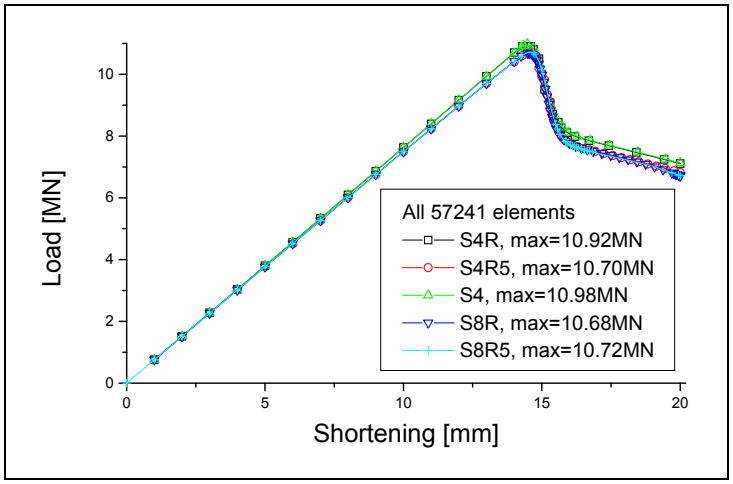

Figure 4.15: Shell element comparison using the middle mesh size

Table 4.3 compares the impact of different mesh sizes: coarse, middle and fine. Hereby, each next finer model has about four times more elements than the previous one. With the finest mesh and eight node elements (S8R5 and S8R) computing limits at Cranfield University were reached. The degrees of freedom “Dof’s” were extracted from the ABAQUS *.dat file and indicate the real model size. “Anal. [%]” displays the completed percentage of the analysis. 100 percent completion means that the maximum displacement of 20mm was successfully applied. This goes far beyond panel failure and analyses the post-buckling behaviour. The number of solution “Increments” indicates the computing work.

Model	El. Type	No. El.	Dof's	Anal. [%]	Incr.	Ult. load [MN]
	S4R5	14410	92574	100	43	10.76
	S4R	..	..	100	31	11.01
Coarse	S4	..	..	100	32	11.02
	S8R5	..	358212	78.3	40	10.60
	S8R	..	271752	100	42	10.69
	S4R5	57241	355860	100	53	10.70
	S4R	..	..	100	33	10.92
Middle	S4	..	..	100	30	10.98
	S8R5	..	1398540	84.8	100	10.72
	S8R	..	1055106	100	55	10.68
	S4R5	228959	1398324	100	67	10.66
	S4R	..	..	100	34	10.88
Fine	S4	..	..	100	33	10.88
	S8R5	..	5544060	34.2	26	-
	S8R	..	4170324	75.9	22	10.85

Table 4.3: Summary of the mesh sensitivity study

S4R and S4 performed almost identically. The panel failure load decreased when number of elements was increased to a value of 10.88 MN. For the thick shell element S8R, the opposite trend was observed; the failure load increased when the number of elements was increased to 10.85 MN. The thin shell formulations S4R5 and S8R5 are not suitable for the relatively thick panel plates. With S8R5 elements severe convergence problems occurred. From the results it is concluded that the middle mesh size with S4R elements is sufficient for the modelling purpose. All in all, the reference model consists of 65000 shell, 37000 solid, 500 connector and 400 beam elements.

4.5 Analysis of all Flagged Error Sources

With the reference model built, the idealisation error sources can now be addressed. The order in which the error sources will be analysed depends on the preference of the analyst. Joint modelling was of prime interest as it was already part of the reference model building.

4.5.1 Joint modelling

All joints were modelled using mesh independent connector elements on the basis of elastic and plastic properties supplied by Airbus UK [3]. The most important joints are the bolts involved in the stiffener-buttstrap-plate contact. As the panel bends globally, the greatest stress levels occur at the panel centre.

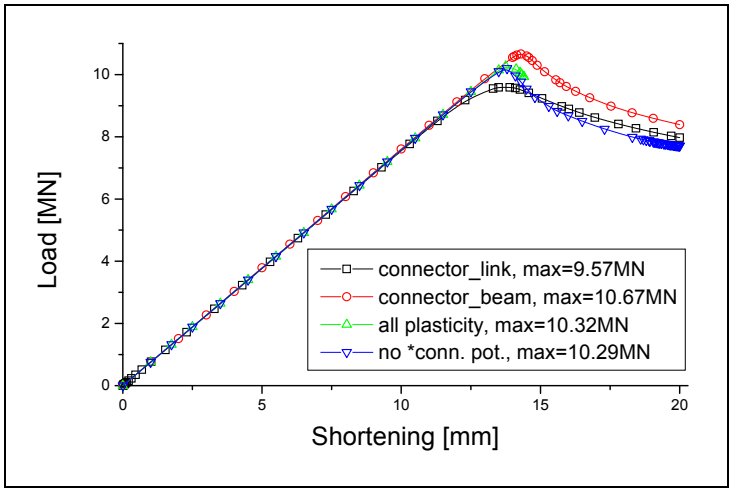

Figure 4.16: Joint models

Figure 4.16 shows the results from the joint analysis. The first step was to obtain an error bound by modelling all joints with connections that were too rigid and too loose. “connector_beam” constrains the displacement and rotation at the first node to the displacement and rotation at the second node. “connector_link” keeps the distance between two nodes constant, but allows rotations. The results show that the global failure is very sensitive to a correct joint modelling.

“all plasticity” uses the provided nonlinear connector properties, where the solution cannot progress beyond the point of maximum load due to convergence problems in the solution. The reason for this behaviour is the use of the ABAQUS command “*Connector potential” which leads to convergence problems. When replacing this potential function with independent hardening values, the problem disappeared. This can be seen in “no *conn. pot.”.

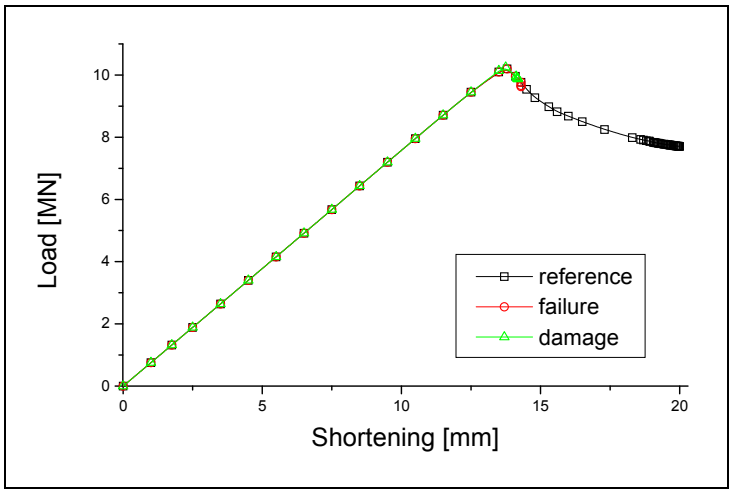

Figure 4.17: Joint failure and damage

Another important question is whether joint failure determines the global panel failure. “*Connector failure” is the simple ABAQUS failure command, which only removes the connector element when a limit was exceeded. “*Connector damage” is the more complex command, allowing smoother removal of the connector element. This removal can be defined as a linear, exponential or tabular function, which gradually reduces the element stiffness. The critical value chosen for both failure options was a joint elongation of 10% [17]. As can be seen in Figure 4.17, including joint failure did not change the load-shortening curve and is not necessary to determine the critical load.

Joint modelling has a big influence on the failure behaviour, because the joints connect important load bearing parts of the panel assembly. Model properties depend on accurate test data, which were not entirely accessible for this analysis. Therefore, a modelling error of up to 1% is assumed. The final model will incorporate elastic-plastic joint properties with pre-loading, omitting the “*Connector potential” formulation.

4.5.2 Stiffener and rib contact

This error source is closely related to the previous one and addresses the use of ABAQUS *Fastener elements. Possible idealisations are controlled by the capabilities of the specific FE code used. The ribs are connected to the panel and stiffeners with bolts using three or four layers of material.

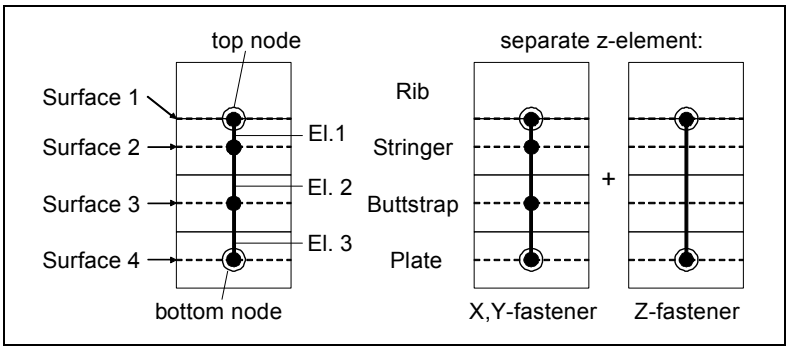

Figure 4.18: Bolt connection through four layers

Figure 4.18 displays the bolt connection at the rib and middle stiffener interface. When defining the connector element with help of *Fastener, the top node location at the rib surface and the three other involved surfaces needed to be specified. The bottom node and connector elements 1, 2 and 3 were generated internally with a length of 3.25, 6.5 and 7.65mm respectively. The problem with this approach is that the elements have a different length and therefore different axial properties, but use identical properties because they are part of one fastener definition. Element 1 is shorter because the top node is located at the rib surface. Ribs were modelled with solid elements and the surface nodes lie at the outer structural geometry, not at the shell mid-surface.

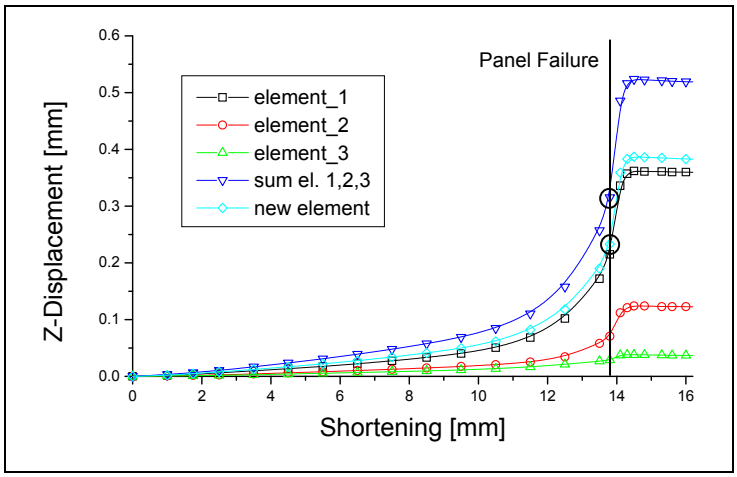

Figure 4.19: Z-displacements of three separate and one single connector

Figure 4.19 shows that element_1 gets stretched more even though it is shorter than element 2 and 3. This can be explained by the used hardening model. Due to its shortness the plastic deformation of this element starts earlier, because the element stress is calculated analogously as for springs: force = connector stiffness x displacement. The idea to model these joints in a more realistic way is to move the z-component definition into a separate element, as explained in Figure 4.18. Now, this connector will deform uniformly, leading to a more realistic model.

The impact of this approach is also shown in Figure 4.19. The new connector element deforms less than the sum of the three separate elements. The element deformation at panel failure decreases from 0.32 to 0.23mm, as indicated. This error source did not show much influence on the global failure behaviour because these bolts are located far from the panel centre. For analyses where mesh independent fasteners using several material layers are located in more critical regions it can become important. Nevertheless, the updated model will include this improvement.

4.5.3 Sensitivity to boundary conditions

This error source is due to the fact that the panel is not rigidly connected to the test machine. Top and bottom are attached to the end platen, as shown in Figure 4.20. The platens add additional support to both ends and prevent translation and rotation of the panel during the test. However, it is not a truly rigid connection and a small rotation around the end axes can occur.

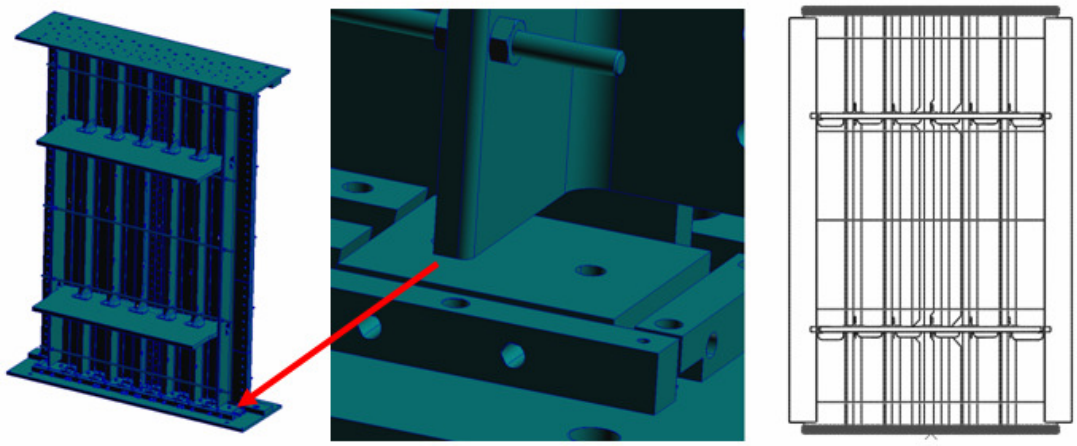

Figure 4.20: CAD model with end platen cast and FEM geometry with constraint band

The right side of Figure 4.20 shows the model with a constraint band. Marked nodes at both panel ends are only allowed to deform axially.

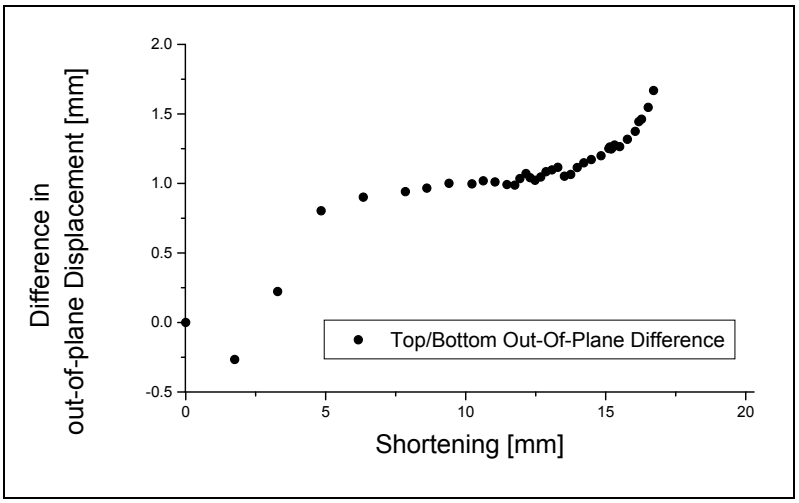

Figure 4.21: Load-shortening difference measured at panel top

As explained in section 4.3.1, top and bottom of the test machine are not compressed in parallel. The actual top/bottom difference is shown in Figure 4.21. These values were used to model the machine flexibility. But how big is the introduced error? Table 4.4 summarises the results of a sensitivity study. The reference model uses cast ends. “Constraint band” restrains the involved nodes to axial deformation only. “Constraint band + free rotation around ends” keeps the constraint band and allows the panel to rotate at the ends, which means in modelling language constraint (0,0,0,0,0,0) versus (0,0,0,-,0,0), see Figure 4.12. This case exaggerates the rotational influence, and shows a drop in failure load by 2%. “Machine flexibility” models the actual rotation observed in the test.

Model	**Collapse load [MN]**
Reference, ends cast	10.37
Constraint band	10.38
Constraint band + free rotation around ends	10.17
Machine flexibility	10.38

Table 4.4: Influence of different boundary conditions

The impact of the machine flexibility and of including the constraint band is very small, see Table 4.4. Allowing the panel to rotate around the axes of the ends is an exaggeration of the actual end flexibility. The conclusion of the analysis is that modelling the boundary condition as rigid has a small error influence, but adding the constraint band makes the model more realistic. As the end platen flexibility is not adequately modelled an idealisation error of up to 1% is estimated.

4.5.4 Check if load paths change when NL-behaviour starts

This investigation addresses geometrical nonlinearity. Thin walled stiffened panels start buckling locally in the skin between stiffeners when compressed axially. The main load is then sustained by the stiffeners. But the panel in this study is a thick one, and no local buckling of the skin plate occurs.

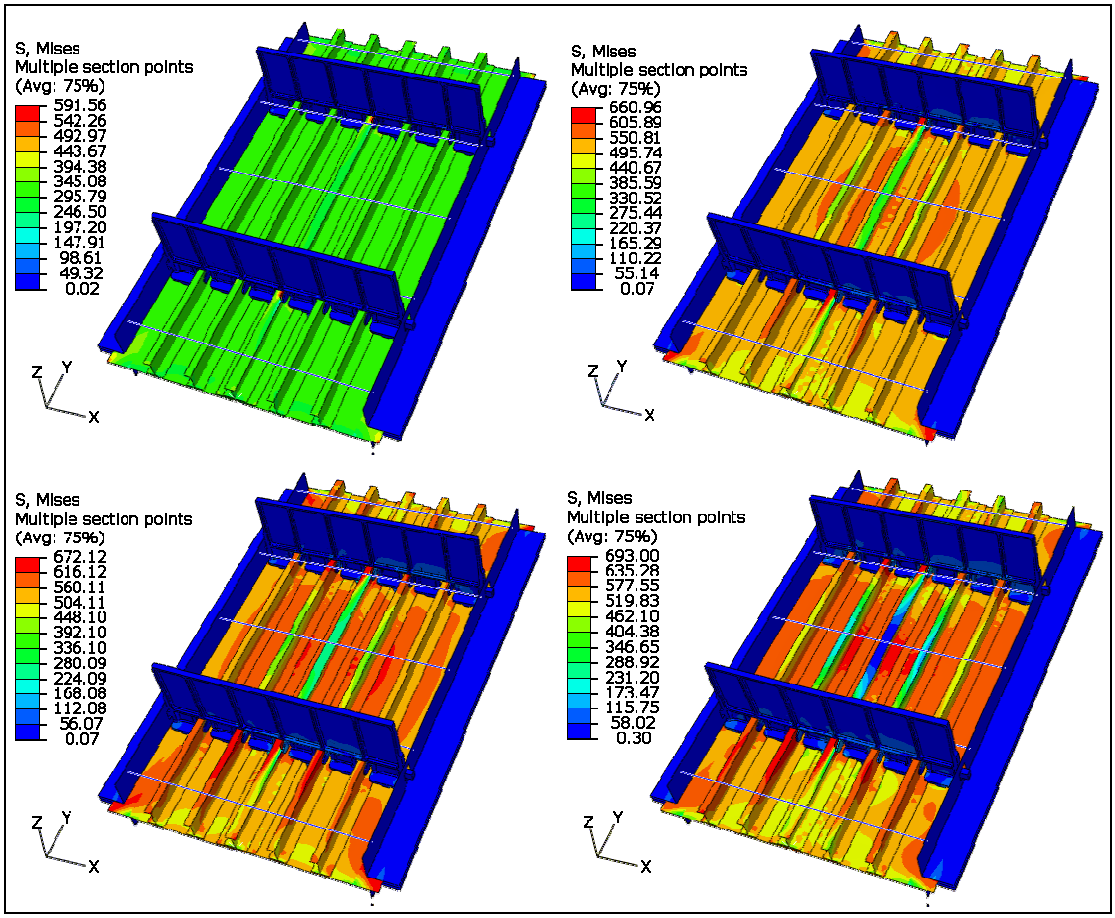

Figure 4.22a-d: Mises stress at 8, 12.8, 13.6 and 14.2mm displacement

Figure 4.22 shows stress plots of the panel during the loading process. They were taken at 8, 12.8, 13.6 and 14.2mm of applied displacement; failure occurred at 14mm. Figure 4.22a shows that the stress level is initially uniform across the panel. This changes in Figure 4.22b, where a round area in the panel centre show higher stress values. Figures 4.22c and 4.22d display the panel before and after failure. One can see that the stiffeners receive lower stress values than the skin plates, because they are already bent sidewise. During compression, the panel bends globally and the largest out-of-plane displacement occurs right in the panel's centre. Stiffeners buckle in the regions between ribs and loose stability. It can therefore be concluded that the model correctly reflects the loading process, including a change of the load path.

4.5.5 Stiffener modelling with shell or solid elements

The next three error sources were analysed using sub-models. The important question when extracting a part from the global model is if the part will show the same behaviour when analysed alone. For the study of the stiffeners the section between ribs was selected. Boundary conditions were chosen according to the full model: one side is clamped and on the other side a displacement is applied.

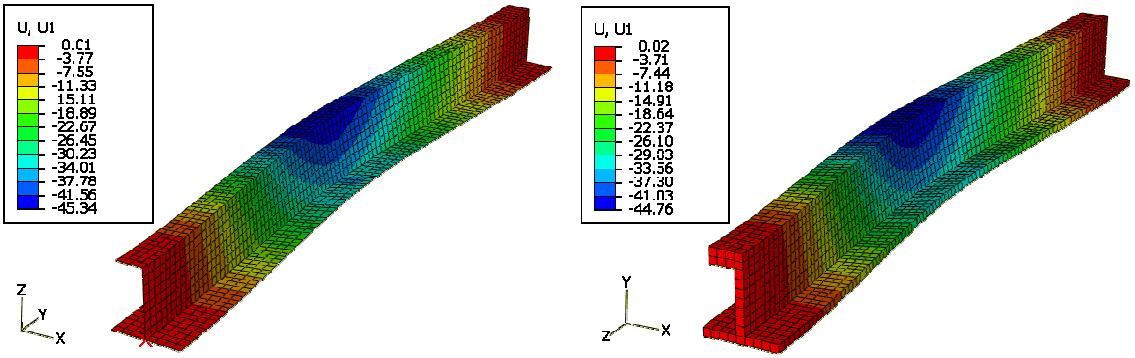

Figure 4.23: Deformation of shell and solid sub-models at failure

Shell and solid models show the same failure mode, bending sideways, which can be seen in Figure 4.23. Both models show almost the same x-displacement magnitude.

Model	S4R [kN]	S4 [kN]	No. el.	C3D8I [kN]	C3D20 [kN]	No. el.
Coarse	774.63	786.18	1960	782.73	791.18	2352
Middle	775.72	781.23	7840	784.87	786.12	18816
Fine	775.71	776.80	31360	783.66	783.25	150528

Table 4.5: Collapse load of stiffeners modelled with shell or solid elements

Table 4.5 summarises the outcome of this analysis. Three mesh sizes were used, each time halving the length of each element side. The stiffener failure load, which was measured as a drop in reaction force, is the interesting criterion. First order C3D8I and second order C3D20 solid elements were compared with S4 and S4R shells. The shell models converged to a failure load of 776kN and the solid models to a value of 783kN.

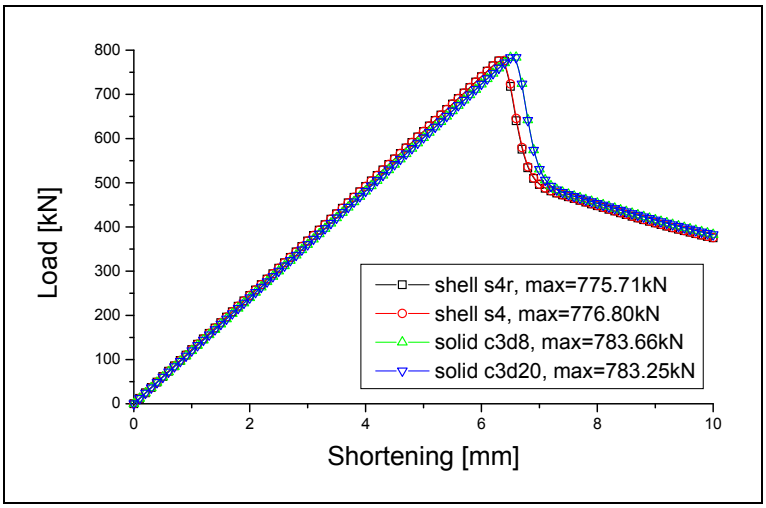

Figure 4.24: Stiffener modelled with shells and solids

Figure 4.24 shows the load shortening graph of the sub-models using the fine mesh. The solid models show a slightly stiffer behaviour, but the difference in failure load between S4R and C3D20 is less than 1%. The error introduced by using shell elements can be considered as minor. Shells have the great advantage of being more economic in computing.

4.5.6 Influence of stiffener mid-surfaces

As two dimensional shells model three dimensional structures some simplification are made in the mathematical model. One of these simplifications is that the shell nodes lie in one plane, which is usually the mid-surface of the shell. This simplification could introduce an idealisation error at the corners.

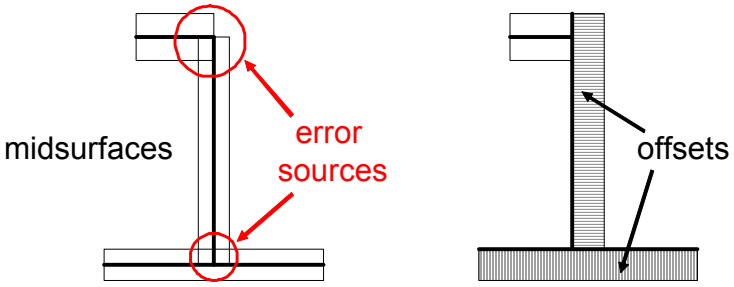

Figure 4.25: Midsurface and offset variants of the stiffener shell model

Figure 4.25 illustrates the potential error source when using mid-surfaces. At the bottom connection there is an area where the material is defined twice. At the upper connection the material is defined twice inside the bend and no material is located on the opposite side. The right model uses shell offsets for a uniform material definition within the stiffener. Using offsets requires a more complicated mesh design, as the geometry loses symmetry.

Model	Midsurfaces [kN]	No. El.	Offsets [kN]	No. El.
Coarse	774.63	1960	771.99	2100
Middle	775.72	7840	776.49	8400
Fine	775.71	31360	776.62	33600

Table 4.6: Collapse load of stiffeners using shell midsurfaces or offsets

Table 4.6 compares the results of these models. “Midsurfaces” are the same S4R shell models as in the previous section. It becomes clear that the difference in ultimate load is not important, and therefore no idealisation error is concluded.

4.5.7 Cleat modelling with solid or shell elements

Modelling the cleats with finite elements is a demanding task as they consist of two perpendicular planes with curved boundaries. Another challenge is to define a sub-model which can answer the posed question. A model consisting of two cleats and the stiffener from the two previous sections was chosen as appropriate. The cleats were attached to the stiffener using connector elements with a high stiffness and a contact definition between surfaces. Boundary conditions compress the assembly and were defined on the free cleat surfaces.

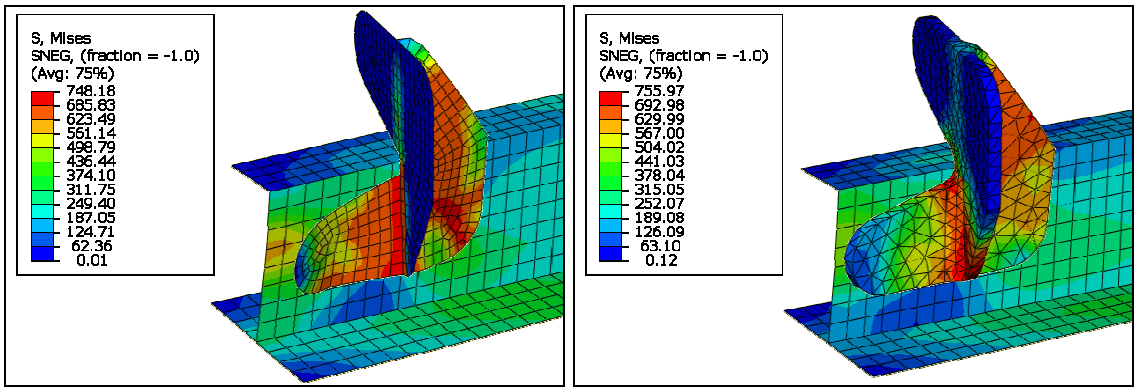

Figure 4.26a, b: Plots showing Mises stress for cleats using shell and solid elements at sub-model failure

Figure 4.26 shows stress plots from the sub-models at failure. Stress level and distribution for both models look similar.

Model	Shells (S4R) [kN]	No. el.	Solids (C3D4) [kN]	No. el.
Coarse	120.75	484	126.78	926
Fine	118.22	2775	117.79	11911

Table 4.7: Collapse load of cleats modelled with shell or solid elements

Table 4.7 summarise the analysis outcome. The critical value was again a drop in the load-shortening curve. From the results, it can be concluded that no modelling error is introduced by using shells or solids.

4.5.8 Plate and side frame contact

The side frame is attached to the panel in order to prevent out-of-plane deflection of the panel. This can be seen in Figures 4.2, 4.3 and 4.7. Although the frame is made of steel and quite stable, some deformation will occur. This means that energy is absorbed, and the panel assembly gains stiffness. Important frame dimensions are depicted in Figure 4.27.

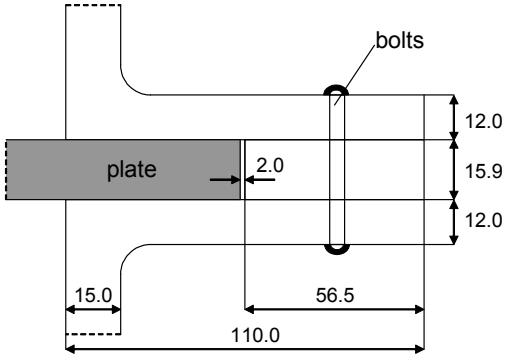

Figure 4.27: Side frame dimensions

The reference model uses three layers of plates to model the frame. The layers were rigidly merged using the surface *Tie command, i.e. the distance of the involved nodes is fixed. This idealisation is likely to be too stiff as in reality the layers are held together using bolts. Including bolts and defining contact between the material layers makes the plate-frame connection less stiff.

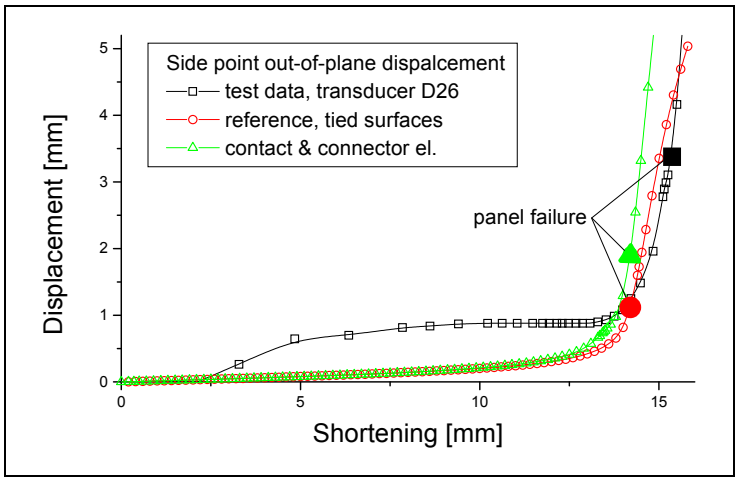

Figure 4.28: Impact of different frame idealisations

Figure 4.28 illustrates the model improvement. The graph compares FEM idealisations with the out-of-plane deflection at transducer D26, which is located close to the side frame, see Figure 4.10b. The test data are biased by the end platen rotations, as explained previously. The side point displacement at panel failure is indicated in the curves. It can be observed that “Contact & connector element” come closer to the test curve. The measured displacement should be about 1mm less than shown. Modelling bolts and defining contact has an impact on the global failure load of about 0.5%, as shown in Table 4.8.

Model	**Collapse load [MN]**
Contact & connector element	10.32
Reference, tied surfaces, friction=0.15	10.37
As reference, friction=0.0	10.36
As reference, friction=0.5	10.39
As reference, friction=1.0	10.45

Table 4.8: Effect of different friction values

The friction value for the plate and frame contact is the other uncertainty. The panel plate is made of a 7000 series aluminium alloy and the frame consists of steel. Literature suggests using a friction value of 0.61 for modelling aluminium-steel contact [6]. Other questions to consider are whether the surfaces are completely plane, whether a lubricant was used to reduce friction, how tight the frame was attached to the panel and whether the frame had an initial curvature. It can be concluded that including bolts improves the model reliability. The friction value of 0.15 was suggested by Airbus UK and is assumed to be correct.

4.5.9 Geometrical imperfection

The finite element model assumes perfectly even surfaces and all dimensions without local variations. The real geometry deviates from this perfect structure, as imperfections are always present. For the study of this error source measurements of plates, buttstrap and stiffeners that were provided could be used. The measured thickness was usually bigger than specified in the CAD model, but not evenly distributed. The peak difference had a magnitude of 0.5-0.8% of the panel thickness as described in section 4.3.4.

Model	Collapse load [MN]
Reference	10.37
Thickness updated	10.41
Local imperfection	10.38
1. eigenmode, 1% skin thickness	10.34

Table 4.9: Impact of geometrical imperfection

Table 4.9 lists results from the imperfections analysis. In “Thickness updated” the average thickness difference was added to the plates, which lead to a slight increase in failure load. This approach also uses perfect plane surfaces, which is not realistic. “Local imperfection” adds local imperfection to the FE mesh by changing node locations with the ABAQUS command *Imperfection. This did not significantly change the failure load. “1. eigenmode, 1% skin thickness” adds geometric imperfection with the shape of the first eigenmode and a magnitude of 1% skin thickness, which lead to a small decrease in failure load.

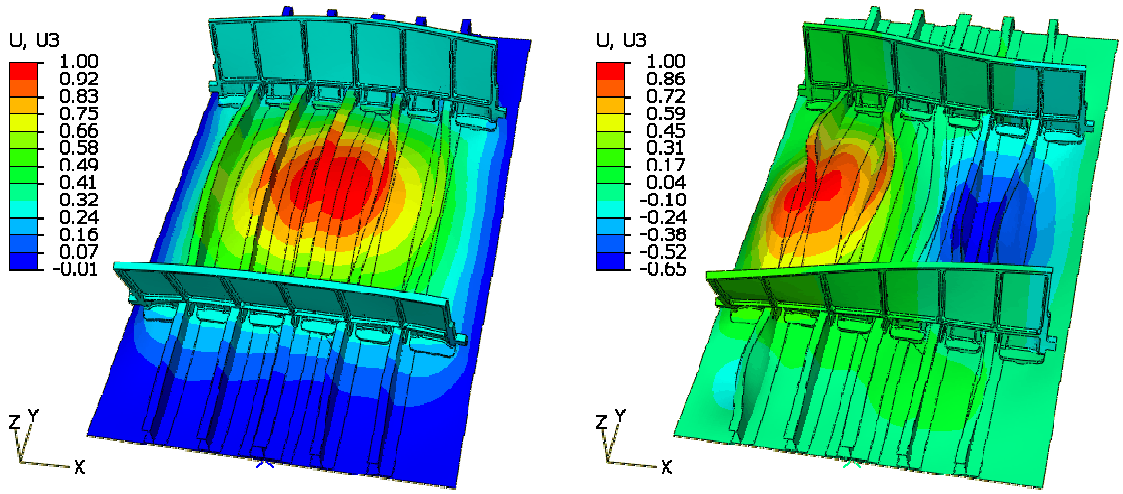

Figure 4.29a, b: First and second eigenmode of the panel without frame

Figure 4.29 shows contours of out-of-plane deformation of the first two eigenmodes. The side frame was replaced by an out-of-plane restriction of the nodes at the panel sides. Adding the shape of the first eigenvalue is the most severe imperfection as it represents the failure shape. But this imperfection pattern was not measured in the structure. The outcome of this analysis is that the panel is not sensitive to geometrical imperfection of the measured magnitude.

4.5.10 Scattering in material parameter

Scattering in material parameter is a natural phenomenon which will always be present. For this analysis no statistical significant test data could be analysed, but it is assumed that only high quality materials were used for this panel.

Material	Tensile yield strength			
	Mean [N/mm^2]	Mean [ksi]	Standard deviation	Sample size
7075-T6 (Bare sheet)	(496.44)	70.2	3.12	873
7075-T73 (Hand forging)	(417.15)	60.5	2.32	62

Table 4.10: Variation in static strength of aluminium 7055 [51]

Haugen [51] has published test data for various metals. Table 4.10 shows a small extract of the data. Published yield strengths were given in ksi units and were transformed in the table to $\mathrm{N/mm^2}$ using the factor 6.895 [82]. Data for aluminium 7075 were selected because it has similar characteristics to the used alloy 7055-T7751. The variation, which is high with a standard deviation of 3.12 and 2.32, was of interest for this issue.

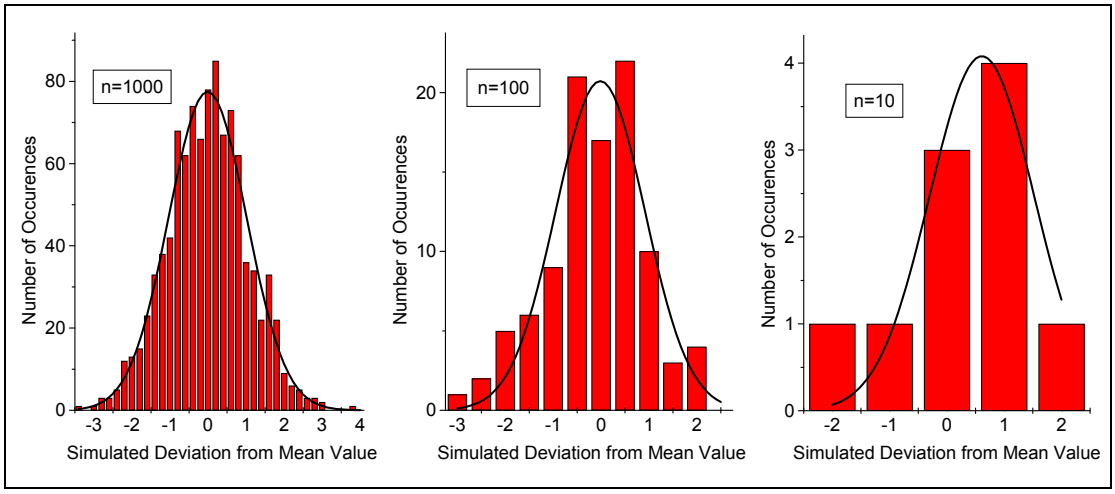

Figure 4.30: Randomly generated standard normal distributions

Simulated test data were generated using random normal distributions with a mean value of 0 and a standard deviation of 1.0. These distributions were transformed to the parameters of the elastic-plastic material model. This approach was aided by parameterising the ABAQUS input file with the *Parameter command. Some interesting analysis cases with n=10 repetitions are presented.

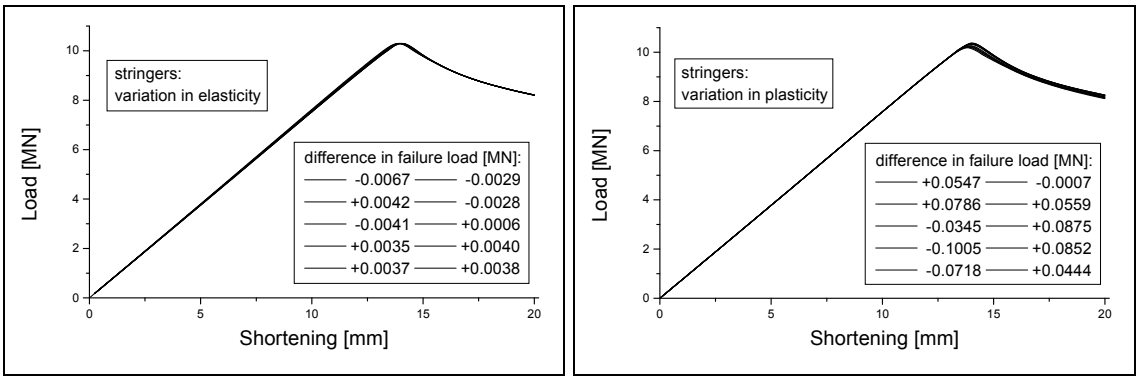

Figure 4.31a, b: Variation of elasticity and plasticity for stringers

Figures 4.31a and 4.31b show the results of elasticity and plasticity variation for stringers. It can be observed that the variational influence of plasticity is much larger than that of elasticity. The highest variation in Figure 16b leads to a change in ultimate load of 0.1005 MN, which is a difference of about 1%. This fact leads to the conclusion that the plasticity of stringers is a very important modelling parameter.

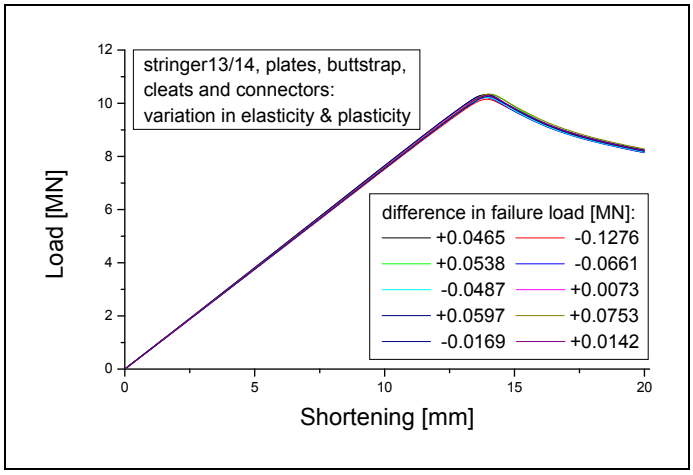

Figure 4.32: Variation of elasticity and plasticity for all model parts

Figure 4.32 shows the impact of varying elasticity and plasticity of many structural parts (stringers, bottom plates, buttstrap, cleats and joints) at the same time. Variances of different parts could equalise each other or re-enforce the global variance. The peak increase of failure load was 0.0597 MN, and peak decrease 0.1276 MN.

Only a selection of results from this analysis is shown here. A final error assessment is not possible because of the lack of real data. Plasticity values of major load bearing parts (stringers, plates and buttstrap) have a big influence on the variation of the panel failure load. An idealisation error of 1% is estimated.

4.5.11 Overall error assessment

Table 4.11 summarises the idealisation error analysis. “[%]“ lists the estimated error which will be left in the final model. The error from the side frame is corrected in the improved model and disappears.

Error source	Analysis outcome	[%]
Joint model	Influence on failure load, but no complete test data, final model with elastic-plastic joint model without the “*Connector potential” command	1.0
Stiffener-rib contact	Minor impact, model updated	-
Boundary condition	Small impact, constraint band included in final model	1.0
Load path	No error	-
Stiffeners: shells or solids	Minor impact	-
Stiffeners: midsurface or offsets	No error	-
Cleats: solids or shells	No error	-
Side frame model	Small influence, final model includes bolts and contact between frame layers	-
Geometrical imperfection	Minor impact	-
Scattering in material parameter	Influence on failure load, error analysis requires high-quality test data	1.0

Table 4.11: Overall error assessment

Joint model, boundary condition and material scattering contribute to the remaining idealisation error. In a worst case scenario, the error is cumulative and sums to 3%.

4.6 Final Model

In the final stage the idealised model is updated based on the conclusions from the study of each individual error source. The result is a model where the level of error introduced by the idealisation process is known and limited at a level acceptable to the analyst. Important parts of the ABAQUS input are provided in Appendix B.2.

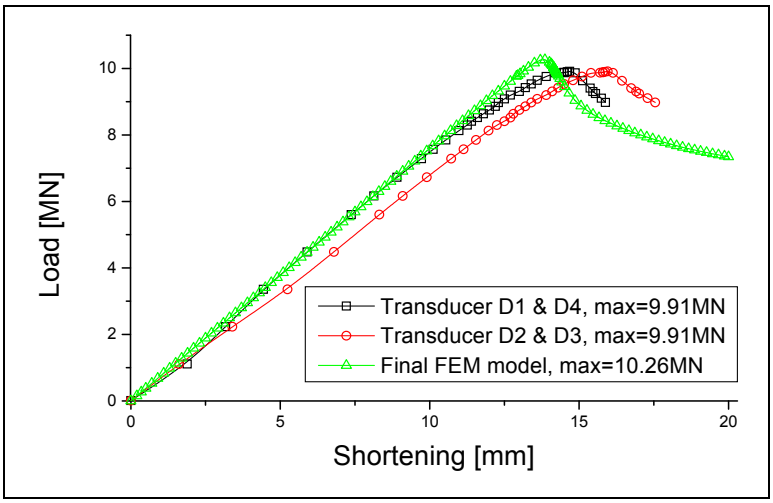

Figure 4.33: Load-shortening graph of the final model

Figure 4.33 shows the load-shortening curve of the final FE model together with the average of the test curves [3]. The FEM solution initially shows the same behaviour as transducer D1 and D4, but predicts the panel failure at less shortening. The deviation in failure load of the simulation and the test data is 0.35 MN, which corresponds to 3.5%.

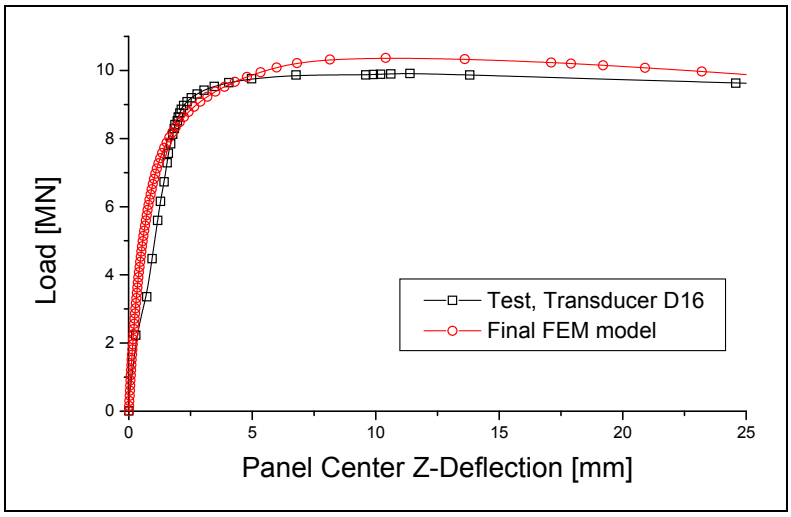

Figure 4.34: Mid-point out-of-plane displacement curve of the final model

The panel centre out-of-plane deflection curves are shown in Figure 4.34. A good agreement of simulation and test data can be observed.

Ten potential error sources were identified and analysed. The improved model includes an idealisation uncertainty of 3%, which is caused by the joint model, boundary conditions and material property variation. The difference in failure load between the final model and test data is 3.5%, which is quite a reliable prediction.

4.7 Discussion

This study showed that the SAFESA analysis requires considerable time and computational power but leads to more realistic simulations. The final model is an improvement on the reference one but is still not perfect. The important question is: Was the main behaviour simulated correctly?

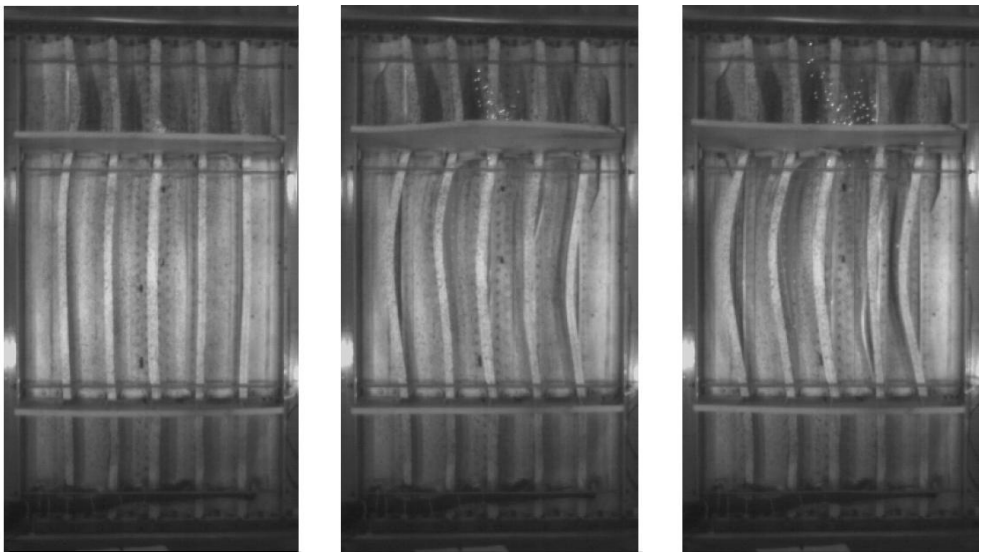

Figure 4.35: High-speed camera recording of the failure [91]

Figure 4.35 shows the panel failure sequence, which was recorded with high-speed cameras during the test. The time between the first and the last picture is about 10 ms. First the stiffeners start buckling. Then joints or material fail, and the structural assembly collapses. The upper rib and attached cleats detach in the final sequence.

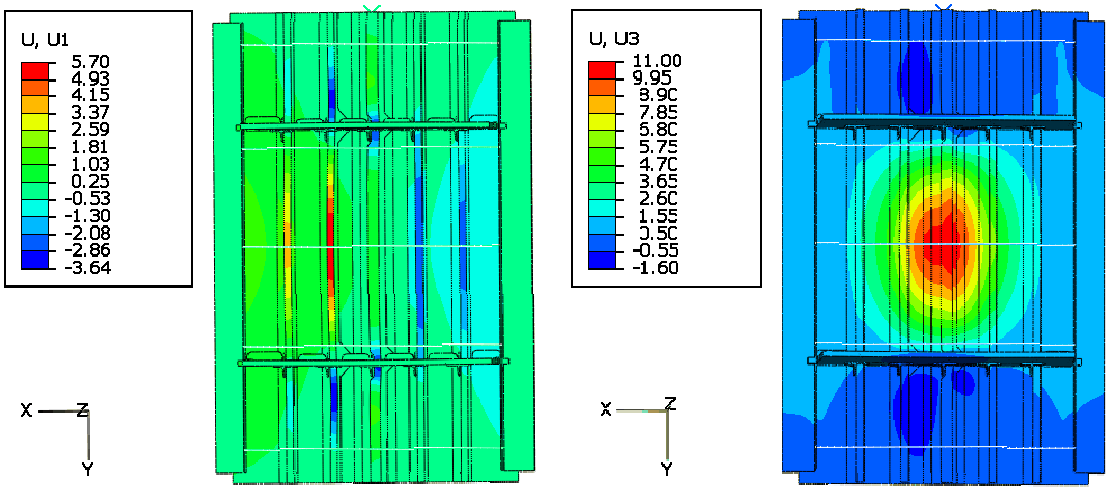

Figure 4.36a, b: Lateral and out-of-plane deformation at failure

Figure 4.36 shows the simulated lateral and out-of-plane deformation at panel failure. Initially, the stiffeners exhibit the same lateral deformation in the simulation like those in the test. The out-of-plane deformation in Figure 4.36b corresponds to the recorded values, see Figure 4.34. The panel behaviour during compression is mainly determined by out-of-plane bending of the bottom plates and attached stiffeners, starting in the panel centre. This behaviour is also the reason of global failure and was correctly modelled.

The panel failure criterion that was used is a drop in reaction force. Maybe another criterion is reasonable, e.g. a strain excess of 0.2%. The joint modelling analysis indicated that joints fail after global failure. Therefore, no joint failure was incorporated in the final model. Other improvement sources are the material model and the solver. The elastic-plastic material model does not account for material failure. Material cracking and even detaching of the upper stiffener part from their bottom can happen, as shown in Figure 4.35. The collapse process could not be covered in the quasi-static ABAQUS/Standard analysis. ABAQUS/Explicit and LS-Dyna are better tools to simulate dynamic failure.

FEM model size can be problematic. The provided Airbus model required five days calculation time on the Cranfield multi-processor machine and used more than 10 gigabyte disk space, which lead to simulation terminations. Therefore, the creation of an analysis-friendly pattern was the main focus during model building. This process was done iteratively and required much more debugging and error analysis than expected. The provided joint properties caused simulation terminations, without any error messages. The conclusion is that the used ABAQUS version has a bug in the command “*Connector potential”. The definition of contacts using several material layers and mesh-independent *Fastener elements was also demanding. The documentation is not very clear at this point.

Overall, the study provides a demonstration of idealisation error control on a large nonlinear analysis. The SAFESA methodology needed to be extended for the specific error sources. The updated method can be found in Appendix C. Several error sources related to internal structural contact were identified after a consequent progression of the error control method. Therefore, the idealisation expert system should guide the user through the step-by-step approach. The idealisation analysis could be further improved by performing joint and material coupon tests to study the parameter variance and failure behaviour.

5. EXPERT SYSTEM DEVELOPMENT

5.1 Introduction

Implementing an expert system for the SAFESA idealisation error control technology is one of the main objectives of this PhD project. The goal is to provide a tool which assists the FEM modelling phase and helps preventing idealisation errors.

Expert systems technology is based on research in the 1960s and is a special type of Artificial Intelligence (AI) that can successfully deal with complex problems in a narrow domain such as medical disease diagnosis. Expert Systems (ES) are also called Knowledge-Based Systems (KBS) or Knowledge-Based Expert Systems (KBES). They greatly increased in popularity since their commercial introduction in the 1980s. Today, expert systems are used in business, science, engineering, manufacturing and many other fields in which there is a well-defined problem domain [47]. Surprisingly, there is yet no widely accepted expert system for FEM modelling.

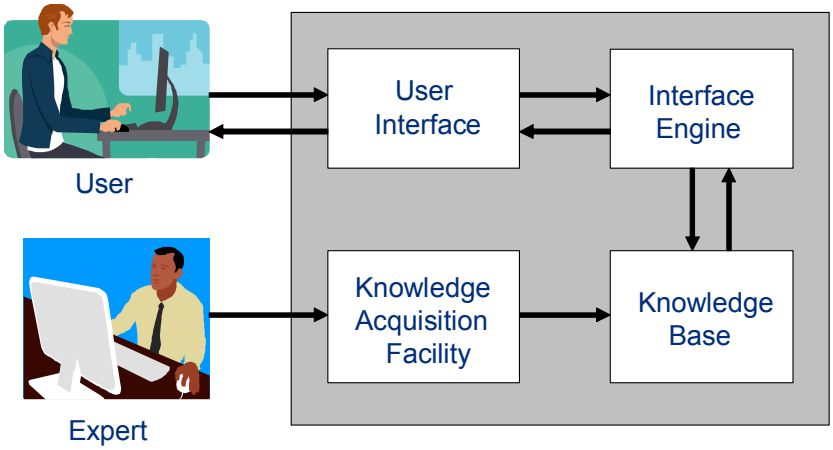

Figure 5.1: Basic functionality of an expert system

Expert systems are computer programs that use knowledge to solve problems which are difficult enough to require significant human expertise for their solution [47]. The expert is a person who has expertise in a certain area. That is, the expert has knowledge that is not known or available to most people. In this case the expert is a senior mechanical engineer with vast experience in FEM modelling. The user may be a junior engineer with none or limited experience. The expert system has one interface for the expert and one for the user, see Figure 5.1. Knowledge is saved in the knowledge base and accessed through the interface engine.

The expert system development process is described in this chapter. The development phases can be described with a modified waterfall model [126], because the project is relatively small and has a limited time frame.

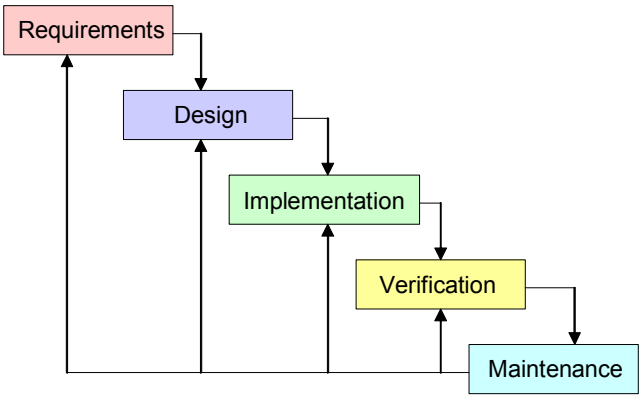

Figure 5.2: The software life cycle [126]

The modified waterfall model describes a process in which development is seen as a downward flow, see Figure 5.2. The phases are requirement analysis, design, implementation, verification (testing) and maintenance. One phase starts after the previous one has been completed. In practice, these stages overlap and feed information into each other. This chapter is structured similarly. First, literature and existing tools which lead to the requirements are summarised. Design and implementation phases are described afterwards. The program use is illustrated by the Airbus panel analysis. Finally, the program is verified and future improvements are discussed.

5.2 Related Literature

This section is an addition to the brief review in the first chapter. Today, a plethora of literature about FEM and expert systems is available. The selected publications are of interest either because of the program design or because of their area of application. Relevant for this project are the development environment, used programming languages, expert system shells, knowledge-based interfaces in CAE programs, CAD data import, FEM solver input generation and the modelling of aerospace structures. Tworzydlo and Oden [134] and Bechkoum [12] give an overview of this topic in their papers. They provide ideas and an historical review of implemented tools. The basic expert system reference Dym [37] is outdated. Current reference books are Jackson [62] and Giarratano and Riley [47]. Both explain comprehensively the theory and provide examples based on the CLIPS expert system shell.

This paragraph gives an overview of the early expert systems for aircraft structural analysis. Bennett et al [14] present SACON (Structural Analysis

CONsultant), which is an advising system for novice users of the FEM program Marc. It is based on the expert system shell EMYCIN and contains 170 rules and 140 consultant parameters. An example consultation of a Boeing 747 wing analysis is given. This kind of user interaction was applied in this work for the advisor facility that was finally implemented. Gregory and Shephard [48] describe FACS (Flexible Automatic Conversion System), a tool for performing FEM calculations for airframe structures. Starting from CAD drawings the program assists the structural analysis. The program is implemented in Pascal and PL/I. Taig [128] describes the development of FEASA (Finite Element Analysis Specification Aid) at the British Aerospace Laboratories. This program assists FEM modelling of airframe structures and provides an interface to Patran. Using the system shell SAVOIR (in Pascal implemented) this application contains a knowledge base of about 2000 rules. Cagan and Genberg [21] present PLASHTRAN (Plates And Shells sTRuctural ANalysis), which provides guidance for the creation of 2-dimensional structural calculations with NASTRAN. The program was implemented with the languages LISP.

The following publications are more recent. Li and Qiao [73] describe the expert system FEMHES for modelling aircraft fuselage frames. This program is developed in C++ and Visual Basic. The knowledge on which it is based is transformed into IF-THEN rules. CAD data can be imported via the dfx file format, and mesh generation is supported using AutoCAD. After complete model generation a NASTRAN input file can be generated. Rhodes [112] presents NextGRADE (Next Generation Revolutionary Analysis and Design Environment), which is a result of NASA research. The program was developed using the Open Inventor toolkit for the GUI. This tool supports the assembly of pre-meshed components and avoids complex meshing. Component geometries in IGES, STEP, VRML or Patran format can be imported. Yañez et al [140] outline DMAPS (Design, Manufacturing And Producibility Simulation). This expert system for rapid modelling is used at Boeing. It contains a geometry database and automates standard operations. Hierarchical modelling is supported by using an assembly tree. The component based software is implemented in Java, C++ and Patran. Unigraphics is used for geometry creation and Patran for meshing. Vandenbrande et al [136] explain modelling requirements for aircraft shape control. CAD interfaces and existing rule based environments, such as ICAD, Technosoft’s AML and Dassault KnowledgeWare are compared.

The following paragraph gives an overview over developments in the structural mechanics field. Chau and Albermani [26] describe the program LIQSTR for the design of liquid-retaining structures. The tool was developed in Visual Basic and applies ABAQUS as FEM solver. Knowledge is formulated via rules in the system shell VISUAL RULE STUDIO. Lin and Albermani [75] explain the program LADOME, which uses the Level5 object shell. This expert system for

architectural design of buildings takes into account wind speed and other design parameters. The program has its own nonlinear FEM solver and a CAD interface to AutoCAD. The program is implemented in C and Fortran. Kim [64] outlines an expert system for the design of composite materials. This program is developed in C++ and incorporates material databases and the expert shell CLIPS. Interactive FEM model generation is provided. Lockett [76] developed a knowledge based manufacturing advisor for CAD. Design and C++ implementation is explained in detail. Knowledge was extracted from the available literature and transformed into rules using the expert system shell CLIPS. This approach and its realisation were found to be appropriate for this project. Kim and Han [63] explain how a CAD system can be implemented in C++ with the public domain library Open CASCADE library. This technology was finally adapted in this project to provide CAD visualisation.

Expert systems with a direct linkage to FEM solver have a clear advantage. The MSC (MacNeal-Schwendler) corporation is one of the market leaders in FEM software for aircraft design. The pre- and postprocessor MSC.Patran and the solver MSC.Nastran are sophisticated programs which have been used for decades. Yeh and Vance [141] describe virtual reality techniques for NASTRAN. The application was a car chassis made of beams. The interactive stress analysis that was provided allowed the designer to change design variables and visualise the effects. This approach can help to generate ad-hoc designs and immediately identifies idealisation errors. Chiu et al [27] and Farley [44] developed expert systems which support engineers performing stress analyses for the airplane certification process. In [27] the tool CADSA (Computer Aided Detail Stress Analysis) is presented, which guides through the certification stress analysis and formal output reports. It is implemented as a Patran extension. The program can automate simulations with a high number of load case variations and helps to interprete results. [44] uses MSC.Supermodel and Patran PCL scripts for the certification process of a Boeing 747SP variation. The plane was modified to host a 5 meter radius infrared telescope at the fuselage. Using this expert system, the design modification and NASTRAN stress calculations could be performed with the least amount of effort and a high reliability.

Other CAE programs with integrated KBS interfaces are described in the following paragraph. ICAD was the first commercially successful knowledge based system for mechanical engineering. It provided the declarative language IDL (ICAD Design Language) that supported a mechanism for relating parts via a hierarchical set of relationships. Boeing and Airbus used ICAD extensively to develop various components in the past decades [139]. Bates et al [8] explain the program use for modelling aircraft structures and Bermell-Garcia [15] for modelling wind tunnels. Both articles report time and therefore cost savings by reusing the provided experience. CATIA is the most widely applied CAD

program in the aerospace industry today. Ledermann et al [72] discuss ideas for CATIA parametric modelling of airplanes, and Lin and Hsu [74] describe automated design for drawing dies using the integrated Knowledge Advisor. In both cases weight optimisations and a reduced design time were achieved. I-DEAS is another common simulation software. Nabhani and Wake [95] explain the integrated Simulation Advisor, which helps checking model consistency. Mukhopadhyay et al [89] and Stephenson [123] describe AMRaven as a CAE environment for the aerospace sector. The tool uses the Adaptive Modelling Language (AML) and is specialised for rapid prototype design. Interfaces to PATRAN and NASTRAN are provided. The presented results are promising in view of an effective employment of this CAE toolkit as a development platform.

Expert system research for aircraft development has a tradition at Cranfield University. One focus was on tools for reliable FEM idealisation, which lead to the SAFESA project. Kuntjoro [70] implemented a program for structural wing optimisation. Morris [83] and Tomlinson and Maguire [133] specify the requirements for a SAFESA expert system implementation, which were taken into account in this project. Dullaway [36] follows these guidelines and explore programming tools and techniques for an implementation. The result is a prototype written in the MSC.Patran language PCL.

The reviewed publications describe different possible development environments and implementation strategies. Interesting stand-alone expert systems are ICAD, MSC.Supermodel and CLIPS. CAE programs with integrated KBE interfaces were described as powerful and flexible. Therefore, I-DEAS, CATIA, MSC.Patran and AMRaven should be tested further. The other development option is programming in C++, Java or another language.

5.3 FEM Expert System Overview

In order to find out which nonlinear solver and modelling expert system is used in the aircraft industry, a questionnaire was composed and sent to the MUSCA industry partners. The questionnaire is provided in Appendix D.1. Table 5.1 summarises the feedback. With the exception of ICAD, no expert system was used.

Company	Solver	Preprocessor	Expert system
Airbus UK/France	ABAQUS	Patran, Hypermesh, ABAQUS/CAE	ICAD for generating wing models
Saab-Aerostructures	ABAQUS	Patran	none
EADS France	ABAQUS	ABAQUS/CAE	none

Table 5.1: FEM software and expert systems used in the industry

Following the suggestions from literature and MUSCA partners, the above mentioned software needed testing to find out whether they provided a suitable development environment. This task was quite complex, as many of the cited programs are hidden in design laboratories of companies or are confidential military applications. Due to the small number of customers for this highly specialised software, commercial expert systems are expensive.

The following section describes the outcome of the software evaluation. Computer Aided Engineering (CAE) packages like CATIA, I-DEAS or AMRaven offer CAD drawing, FEM pre- and post-processing and their own solver. Integrated expert systems seamlessly assist the CAE process. Both CATIA and I-DEAS offer a KBS interface. The second group of tested programs are pre-processors like MSC.Patran, ABAQUS/CAE or Hypermesh. Application programming interfaces (API), material and structure component databases usually exist, or can be integrated by buying a program extension.

- **CATIA** [25] is the most popular CAD system in the aerospace sector. This is due to its functionality, as well as its usability and look and feel. Its visualisation can be regarded as state of the art. The knowledge based expert system interface is called “Knowledge Advisor”. Rules and object dependencies can be defined for the creation of new geometries. This facility is very user friendly but restricted to geometry creation, and does not allow FEM model design.
- **ICAD** was a very successful knowledge-based mechanical design program, based on the Lisp programming language [139]. Boeing and Airbus used this software extensively to develop various airplane components in the 1990s and early 21st century. ICAD was bought by Dassault in 2003 and its maintenance was discontinued in 2005. This promising tool could not be tested because it has been taken off the market.
- **I-DEAS** [61] is a powerful CAE environment mainly used in the car industry. It has been part of the Siemens PLM software since 2007. Geometry modelling is assisted by a menu-guided graphical user interface. Its knowledge based expert system “Simulation Advisor” can carry out model consistency checking [95]. Due to license restrictions this tool was not available at Cranfield.
- **AMRaven** is a specialised CAE environment for the aerospace sector by TechnoSoft. This program is described as specialised for high fidelity geometry modelling and analysis accuracy from the early conceptual development stage [89, 123]. A student license could not be obtained, despite the fact that it was promised by the UK sales representative.

- **MSC.Patran** [88] is the preferred pre-processor for the MUSCA project partners and was used for model building in this research. CAD data import works best of all reviewed pre-processors. Ideally, the program to develop should provide similar facilities. The programming interface PCL offers an expansion of Patran's functionality. The usage of Patran and PCL follows its own logic, which is sometimes not obvious. The major drawback is the restricted functionality and bad documentation of the application programming interface (API).
- **MSC.Supermodel** is an add-on for MSC.Patran [88] with the focus on reliable FEM modelling [44]. It was chosen as the most appropriate environment for this PhD project. Upon request, the responsible MSC vendor offered a one year license for £10.000. A verification of this tool could not be carried out as it was not affordable.
- **ABAQUS/CAE** [2] is the pre- and postprocessor for ABAQUS. It is a very powerful tool for FEM result visualisation. CAD data import did not work satisfactorily with the version that was used (6.7). A plug-in interface offers program customisation with the Python scripting language. Compared with competing products, this tool is relatively young and still has limited facilities. The author used this program mainly for post-processing.
- **Hypermesh** [60] is another popular pre-processor from Altair. A programming interface similar to Patran's PCL exists, but is not development-friendly. The same conclusion as for Patran applies.

The most promising expert systems ICAD and MSC.Supermodel could not be tested. The functionality of ICAD is likely to be integrated into CATIA in the future. With its PCL scripting, Patran offers the most suitable approach of all the reviewed tools but its programming interface is a major drawback.

5.4 Specification Phase

Software specification or requirement definition is the process of evaluating what services are required from the system and identifying the constraints on the system's operation. This is an important development stage because unrealistic planning at this stage will lead to problems in the implementation. The timeframe of this project phase was roughly ten months with one developer working on it. Time was also needed to search and experiment with available tools and code.

The planned expert system is intended for FEM idealisation for design engineers with little modelling experience. The field of application is the aeronautical industry, but this might change in the future. The starting point is a

CAD geometry, which is built by another division of the company or supplied externally. Material and joint property data are usually provided, but will be incomplete to some extend. Output is a reliable FE model with analysed idealisation errors and an audit trail. This enables analysis repetition and reverse engineering. Finally, the use of the tool is to improve the overall confidence in the qualification process.

Where possible errors are identified, prior relevant experience with similar problems can be used to generate a suitable answer. The experience forms a knowledge base that can be captured und used by other analysts within a company. This motivates the development of a decision making interface.

The idealisation error control process is clearly structured into steps. This structure is clear enough to allow a software implementation. The software requirements are the result of the two idealisation error analyses described in the previous chapters. Specifications were already formulated during the original SAFESA project [133] and [83]. Table 5.2 lists the desirable program functionality.

Functionality	**Priority**
Provide guidance on the use of the best practice for carrying out finite element analysis as developed with the SAFESA methodology.	High
Increase confidence that the structural qualification process has been undertaken reliably and accurately.	High
Audit trail of the decisions made during the idealisation phase.	High
Saving and loading of analysis sessions.	High
Import and visualisation of CAD data via STEP/IGES file formats.	High
CAD processing (e.g. geometry separation).	Low
Direct input generation for the FEM solver.	Low
Facility for a final overall completeness check.	High
A user friendly graphical user interface (GUI).	High
Hardware-independent and portable code.	Medium
Decision making advisor.	High
Facility to print a report file.	Medium
Linkage to existing (material) database.	Low
Maintainability, reliability, usability.	High

Table 5.2: Expert system requirements and their priority

The convenient guidance through the idealisation error control process is the major goal for the expert system. As the FEM idealisation usually starts with pre-created geometries, CAD geometry import and visualisation are crucial. A decision making advisor is also important. Therefore, a knowledge input interface must be provided. The basic process requires quite a bit of record keeping in addition to the time spent building the FE model. The software can help reducing this time by providing the audit trail functionality. The expert system also needs to make sure that all parts of the model have been considered. So it can check that the union of all the features make up the entire model. All functionalities with a “High” priority were considered to be the minimum requirement. Since they would require a huge development effort, CAD processing and FEM input generation are unrealistic goals.

5.5 Design Phase

A software design is a structural description of the software to be implemented, the data which are part of the system, the interfaces between system components and sometimes the algorithms used. Designers do not arrive at a finished solution immediately but develop the design iteratively through a number of versions. The process involves adding formality and detail as the design is developed to improve earlier versions [126].

The decision about the development platform is of major importance with long-ranging consequences [62]. The following solutions seem possible:

- **Expert System Shell** as a stand-alone application has the advantage that experiences from similar projects can be used. No interfaces to CAD/FEM programs exist. A GUI development is also necessary.
- **MSC.Patran’s PCL** language is embedded in a convenient CAE environment. CAD data import and visualisation, FEM input generation and databases are already implemented. But the development is restricted to PCL capabilities and not portable.
- **C++/Qt** offers fast execution code. A professional GUI can be developed with the graphical library Qt [108]. Interfaces to CAD/FEM tools and databases exist. But the development will start “from scratch”.
- **Java** provides a solution that is independent from the operating system. Programming interfaces to CAD/FEM tools and databases exist. However, compared to C++ the program execution speed is slow.

The intensive CAE/FEM software investigation deduced that the expert system should not be developed within one of the CAE environments. None of the tested tools provides sufficient flexibility, changeability and FEM solver independence to be the perfect development environment. A stand-alone expert

system has no existing FEM/CAD connection. It seems more convenient to incorporate an expert system shell into a new program.

A complete new design was necessary, because no other program could be extended upon. The planned software focuses on providing a convenient platform for knowledge acquisition. It is intended to realise an expert system which can be used in different application areas. The knowledge is provided in textual format by the expert. This is a more flexible approach than providing multiple-choices for each idealisation decision. Each analysis session, including a decision audit trail and paths to CAD data, can be loaded and saved.

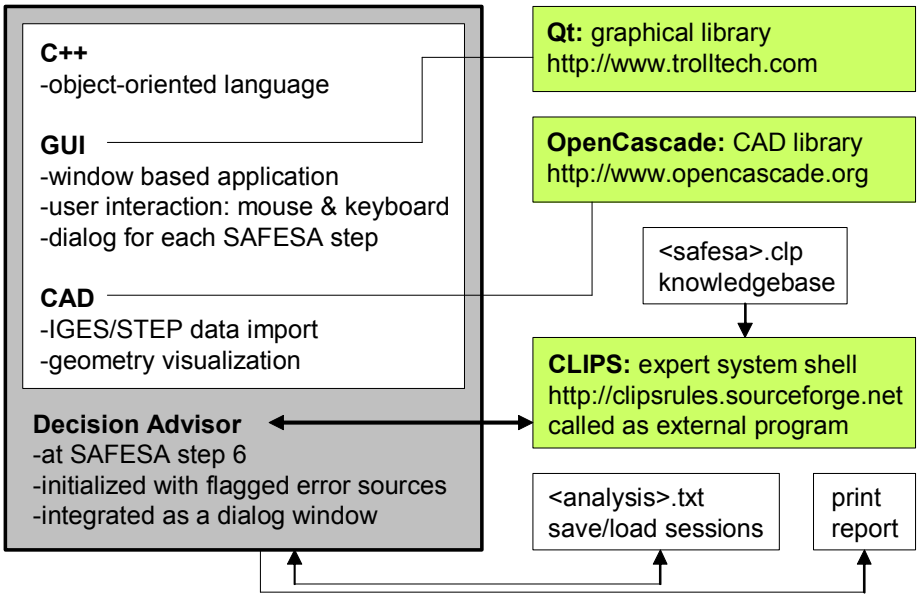

Figure 5.3: Expert system design

Figure 5.3 shows the design for the expert system implementation. The general idea is to use open source software and international standards where possible. This philosophy is driven by a desire to develop a flexible tool that can be easily modified to work in a variety of computing environments, but also by a practical need to minimise the cost of implementing the software. It was decided to program the new software in C++ with help of the libraries Qt and Open CASCADE. The decision advisor facility will be realised using the expert system shell CLIPS. This tool was selected because it is widely used as a research tool, and it is public domain software.

5.5.1 C++ and Qt

C++ is a general purpose programming language. It was developed by Bjarne Stroustrup in 1983 as an enhancement to C [125]. C++ is widely used for commercial and scientific projects because of the ability to develop very fast

code. The main new concepts are object-oriented programming with classes and inheritance, templates and exception handling. Several commercial and open-source compilers for all operating systems exist today.

Qt [108] is a cross-platform application development framework from Trolltech, a subsidiary of Nokia since 2008. It is widely used for the C++ development of GUI programs. Qt is developer friendly because it is well structured and comes with an excellent HTML documentation. The code readability is massively improved compared to the Microsoft Foundation Classes (MFC). Qt offers string handling and its own version of the standard template library with containers vector, list, map etc.

5.5.1.1 Qt class library

Qt consists of over 400 classes. Usually, only a part of this large set is required, but some classes are crucial for every Qt program. Figure 5.4 illustrates the inheritance hierarchy of selected classes. QObject is the base class of all Qt objects and is the heart of the Qt object model. The central feature in this model is a mechanism for object communication.

The QApplication class manages the GUI application's control flow and main settings. It contains the main event loop, where all events from the window system and other sources are processed and dispatched. It also handles the application's initialisation and finalisation, and provides session management. For any GUI application that uses Qt, there is precisely one QApplication object, no matter whether the application has more than one window.

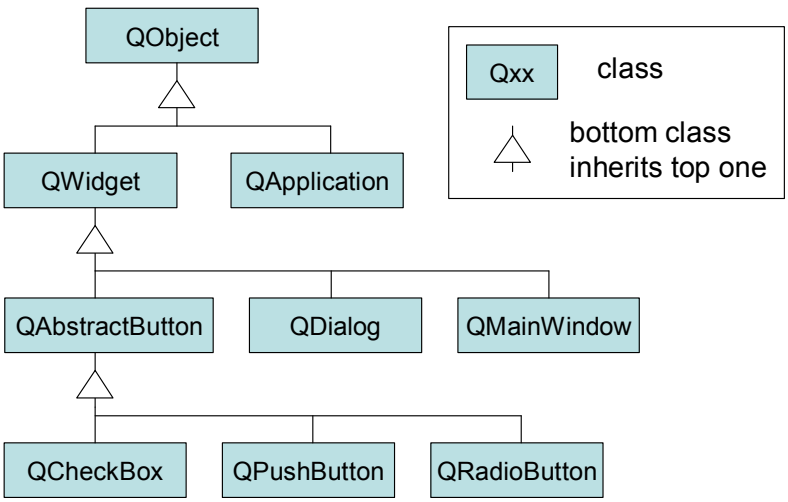

Figure 5.4: Inheritance hierarchy of selected Qt classes

QWidget is the base class of all user interface objects. It receives mouse, keyboard and other events from the window system, and paints a

representation of itself on the screen. Widgets are visual elements that are combined to create user interfaces. Buttons, menus, scroll bars, message boxes and application windows are all examples of widgets. Figure 5.4 also illustrates the inheritance structure for ordinary buttons. QAbstractButton inherits QWidget and is an abstract base class for all buttons. The real implementations are in QCheckBox, QPushButton and QRadioButton. Most applications use QDialog for dialog boxes to interact with the user. Qt provides standard dialogs for file selection and printing options. In most cases the programmer will derive its own dialog from QDialog. The QMainWindow class provides a framework for typical application main windows. A main window contains a menu bar, a toolbar and at the bottom a status bar. The central area contains a widget for displaying text, graphics or other content.

5.5.1.2 Qt object communication

GUI applications respond to user actions. For example, when a user clicks a menu item or a toolbar button, the application executes some code. Signals and slots make the communication between Qt objects available. Figure 5.5 shows how to connect objects.

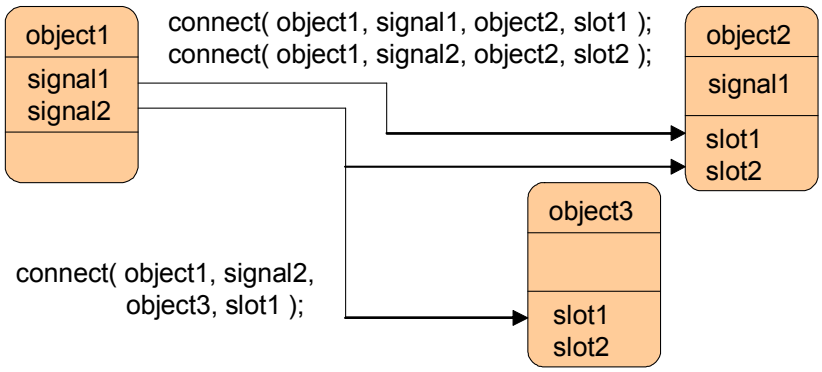

Figure 5.5: Signal and slot connections

Signals are emitted by an object when its internal state has changed. Only the class that defines a signal and its subclasses can emit the signal. A slot is called when a signal connected to it is emitted. Slots are C++ functions and can be called normally; their only special feature is that signals can be connected to them. The signals and slots mechanism cannot easily be realised in standard C++. Qt uses the C++ pre-processor and the moc (Meta Object Compiler), which is included in the toolkit. The moc reads the application's header files and generates the necessary code to support the signal and slots mechanism. Moc will be activated during the compilation process if the class header file contains the macro Q_OBJECT.

5.5.2 Open CASCADE

Open CASCADE (OCC) is a software development platform for three-dimensional CAD/CAE, and is supported by the Open CASCADE S.A.S. [99]. The public domain library was originally developed by Matra Datavision, which is now part of Dassault Systems, editor of CATIA. The library includes components for 3D surface and solid modeling, visualisation and CAD data exchange. Version 6.2 of the object-oriented C++ class library is structured in several modules, see Table 5.3.

Foundation classes	Modeling data	Modeling algorithms	Visualisation	Data exchange	Application framework
Kernel classes	2D geometry	Construction of primitives	2D visualisation	IGES STEP	Data storage
Math utilities	3D geometry	Boolean operation	3D visualisation	BREP	Data framework
		Geometric tools		…	
		…			

Table 5.3: Open CASCADE modules and their contents

Data exchange is a key factor when dealing with CAD data. The OCC library provides functions for im- and export of the formats STEP, IGES, STL, VRML and BREP. The basic types of geometrical entities are point, line, circle, plane and axis, which can be grouped into assemblies. When importing a CAD geometry it is translated into an OCC shape. The shapes are internally saved via OCC pointers, which allows fast access and rendering.

The 3D visualisation module provides presentation and object selection through the high-level AIS (Application Interactive Services) interface. Interactive objects are the entities which can be visualised. The interactive context manages the interactive objects. Created or imported OCC shapes are transformed into interactive objects by activating them in a context. The classes which regulate this process are AIS_Shape, AIS_InteractiveObject and AIS_InteractiveContext. The AIS_Drawer class controls the drawing to an output device, which can be defined as a Qt widget. This provides the seamless integration of OCC into Qt.

5.5.3 CLIPS expert system shell

The decision advisor facility will use the knowledge based system shell CLIPS [28]. CLIPS (C Language Integrated Production System) is an expert rule language that was originally developed by NASA's Johnson Space Center in the

1980s and is now maintained independently and distributed as public domain software. Although written in C, the procedural capabilities are similar to the programming languages Ada and Lisp. CLIPS is a tool for representing a wide range of knowledge using rule based, object oriented and procedural programming capabilities. The key point is the formulation of human knowledge in computer language. Figure 5.6 illustrates the process of setting up a knowledge base.

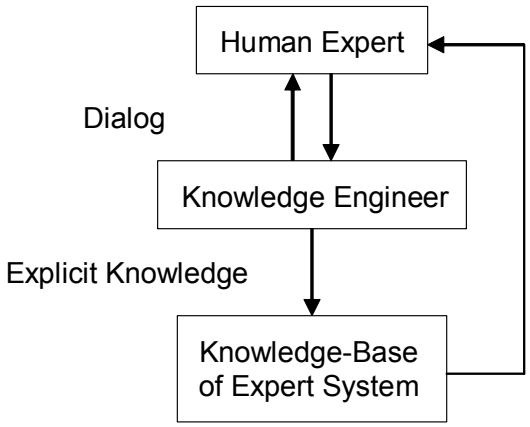

Figure 5.6: Expert system knowledge acquisition [47]

Knowledge acquisition is the transfer of knowledge usually accomplished by a series of interviews between a knowledge engineer, who is a computer specialist, and a domain expert who is able to articulate his expertise. It is estimated that this approach produces between two and five units of knowledge (for example, rules of thumb) per day. This rather low output has led researchers to call knowledge acquisition as the “bottleneck problem” of expert systems applications [62]. For this project, the expert and knowledge engineer is one person, the author of this text. The objective is to formulate the experience gained by the executed SAFESA analyses and to demonstrate a decision advisor.

CLIPS can be incorporated into the expert system in different ways because the C programming sources are freely available. It seems convenient to keep the CLIPS executable separated from the rest of the expert system. This way the knowledge acquisition can be used independently. CLIPS will be embedded in a dialog and called interactively. The decision advisor will be demonstrated for a crucial part of the expert system. It is the handling of the flagged errors at SAFESA step 6, by following the idealisation error control methodology. The advising functionality should also be provided for other program parts where idealisation decisions are made. This remains a task for the future.

5.6 Implementing Phase

During this stage, the software design is realised in several iteration loops. The first result was a GUI frame with the SAFESA steps as dialogs. The integration of the CAD visualisation and data exchange was the following complex task. Crucial programming knowledge was gained by consulting the Sourceforge project QtOpenCascade [109]. The last step was the integration of CLIPS.

5.6.1 C++, Qt and Open CASCADE development

Microsoft Visual C++ 2005 Express Edition [81], open source Qt version 4.3 [108] and Open CASCADE version 6.2 [99] were used. The operating system was Microsoft Windows XP Professional 2002, but this could be changed with very little effort as Qt and Open CASCADE are multi-platform libraries.

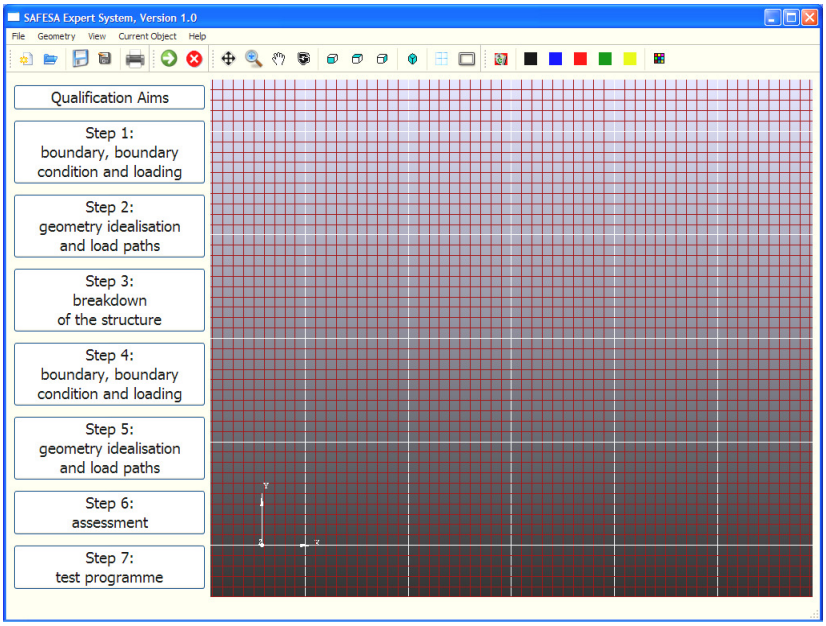

Figure 5.7: GUI of the expert system at program start

Figure 5.7 shows the expert system at program start. At the left side of the window, there are several buttons located, each starting a SAFESA step dialog. The major part of the GUI is occupied by the CAD visualisation widget.

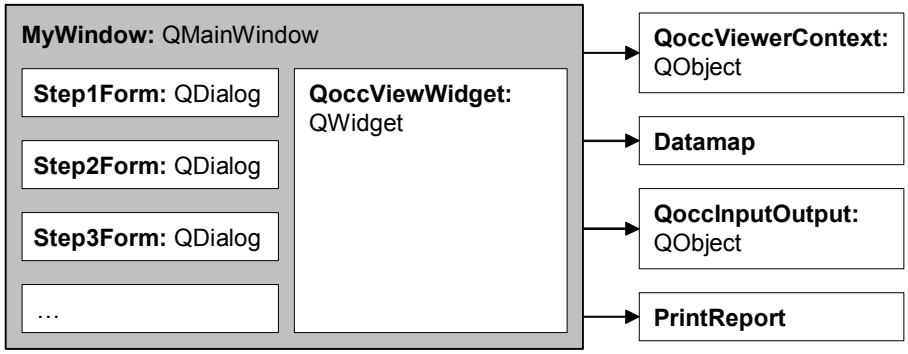

Figure 5.8: Main classes of the expert system

Figure 5.8 explains the main classes according to their position in Figure 5.7. MyWindow inherits QMainWindow and is the control center of the program. It has instances of the SAFESA dialogs, the visualisation widget QoccViewWidget and the other classes shown on the right hand side. Menu, tool and status bars make for a convenient use of the software. User interaction is handled with the Qt object communication, as explained in section 5.5.1.2. Step1Form to Step7Form are dialogs guiding the user through the error control procedure. PrintReport prints a summary of the performed analysis into a PDF file.

QoccInputOutput, QoccViewerContext and QoccViewWidget manage the CAD visualisation. QoccViewerContext organise geometry data and the Open CASCADE context. QoccViewWidget inherits paint and user interaction abilities of QWidget. This allows the implementation of displaying facilities like zooming, moving and rotation. QoccInputOutput provides the CAD data import for geometries saved in BREP, IGES or STEP format. Each imported part is transformed into a AIS_Shape and stored via a Handle(AIS_Shape) pointer.

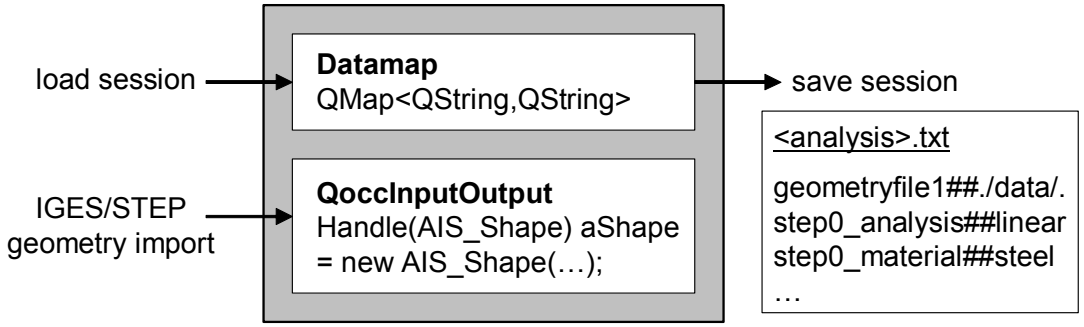

Figure 5.9: Classes for data import and export

Figures 5.9 shows the classes involved in the program data exchange. Datamap manages loading and saving of information from analysis sessions. Internally, all data are stored in a QMap with two QStrings. The data structure actually holds two text strings. The first entry is the key, and the second one is

the data. The information is permanently saved in an ASCII file. Each line contains the two strings, separated by “##”.

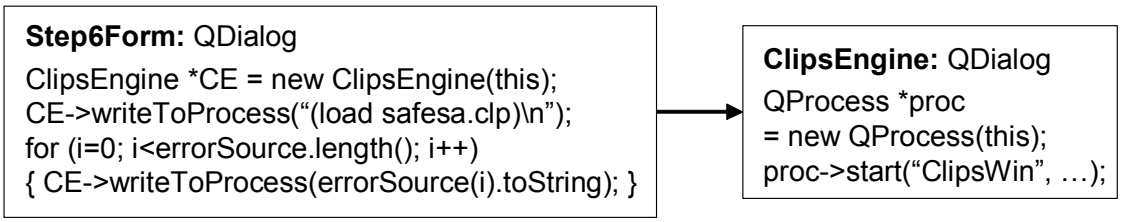

Figure 5.10: CLIPS is embedded in a dialog window

The CLIPS engine is started from Step6Form and embedded in a QDialog, see Figure 5.10. The engine needs the input file safesa.clp to set up its environment and load all facts and rules. It is then initialised from Step6Form with the list of flagged error sources. Each time the engine is accessed, ClipsEngine will start a new process. Standard in- and output from CLIPS is redirected to the in- and output of ClipsEngine. This way CLIPS remains separated from the other code but can be accessed from inside the program. Because CLIPS is used as an external program, the expert shell can easily be exchanged with a different one.

5.6.2 CLIPS programming

The current CLIPS version 6.24 [28] was used. Facts and rules are the basic elements of the CLIPS syntax. A fact is a piece of knowledge expressed in pairs like (material steel) or (element_type shell). Commands are enclosed by brackets. Facts can be created by using the command deffacts:

```
(deffacts initialisation
    (menu-status main-menu)
)
```

With this definition the “menu-status” receives the value “main-menu”. On their own, facts are of limited use. The application of rules is necessary to create program logic. In general, a rule is expressed in the form “IF something is true THEN do something”. To continue with the example a rule is defined which prints a message to the screen if the menu-status is print-message:

```
(defrule hello-message
    (menu-status print-message)
    =>
    (printout t "Hello World!" crlf crlf)
)
```

The rule definition consists of two parts, which are separated by the arrow sign “=>”. The upper part defines the condition (IF), and the bottom part the action (THEN do something). A pattern matching operation is used to determine whether the rule should execute. The CLIPS inference engine applies forward chaining, in which the system first identifies all the candidate rules, then uses a conflict resolution strategy to select the rule and finally executes the appropriate one.

Applying the SAFESA methodology, the rules were formulated and organised in eleven error categories. Each category contains rules for general and for specific knowledge. A general knowledge rule provides global guidelines. In a specific rule the user follows a decision tree by answering questions. The knowledge base currently consists of 42 rules. The corresponding CLIPS programming code is provided in Appendix D.2. It contains the code for the menu control and rules for the error source “[10] Analysis type”. Using this frame, it is convenient to extend the knowledge base. A new general rule “…” for the error category “analysis type” can be defined with:

```
(defrule analysis-general-knowledge
    (declare (salience 10))
    (menu-status selection 10)
    =>
    (assert (knowledge “…”))
)
```

A salience level is declared in the second line of code. This determines the order of execution when several rules meet the condition. The fact (main-menu-selection 10) becomes true if the user selects “10” in the program menu. In the THEN part of the rule the fact (knowledge “…”) is created, which will print the knowledge at the end of the error category. An example for a rule with specific knowledge and user interaction is provided in Appendix D.2.

5.7 Expert System Analysis Example

This section describes the expert system functionality and appearance. It is a walk trough the idealisation error control steps. The Airbus panel analysis has been selected as the demonstration example.

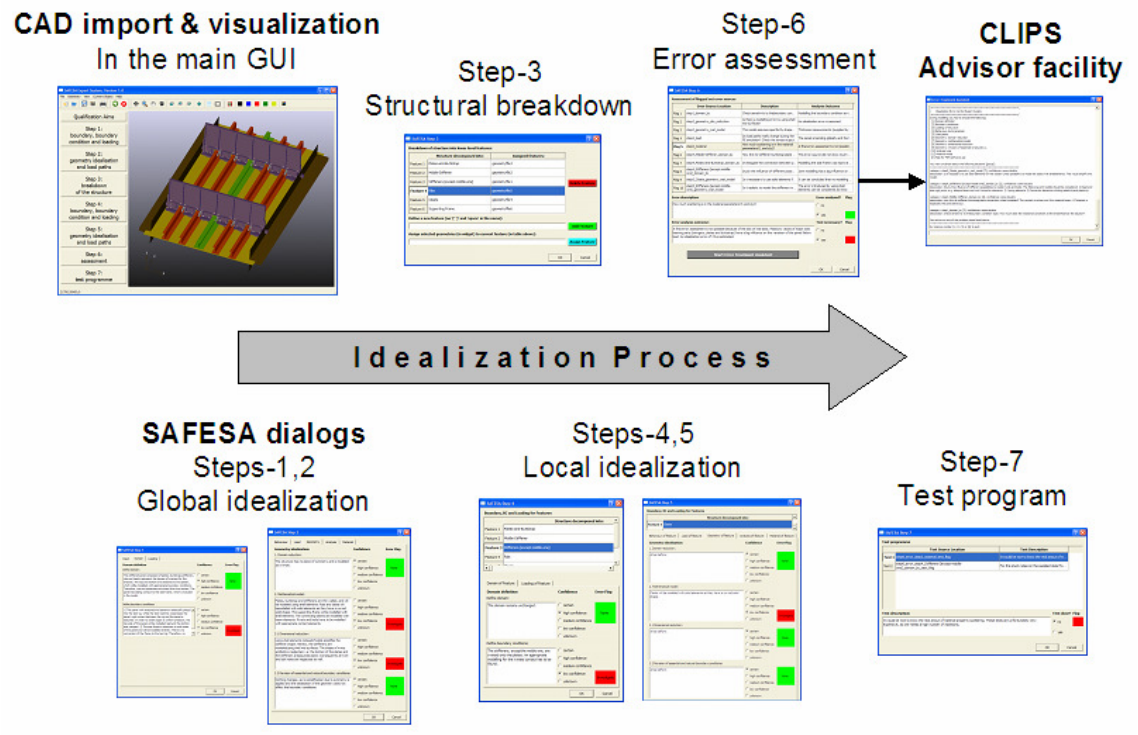

Figure 5.11: FEM idealisation using the SAFESA expert system

Figure 5.11 gives an overview over the steps of the idealisation process within the expert system. CAD import and visualisation are performed in the program's main window. The SAFESA steps one to seven use separate dialogs. In step-6 the advisor facility can be selected, which will be opened in a new window. The following text explains the dialogs in more detail.

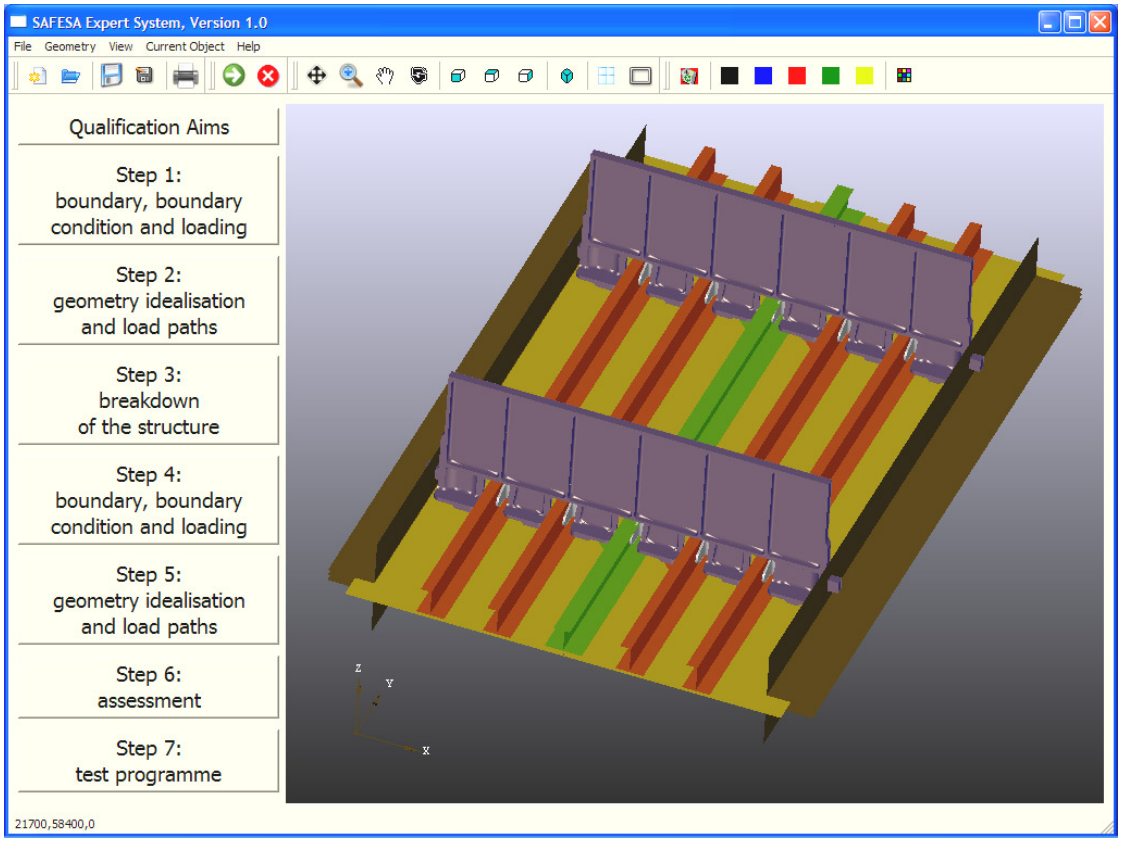

Figure 5.12: Expert system showing imported CAD data

The first step of the modelling process is to import the geometry, usually provided as CAD data. The expert system can import the formats BREP, IGES and STEP. Latter both are the most commonly used formats for CAD data exchange in the industry. IGES is the older and more common one, because the last standard was published in 1996. The STEP file format is still under development.

Figure 5.12 shows the Airbus panel geometry visualised in the GUI. The CAD assembly has to be split in advance, as the expert system does not offer CAD data modification. Each part can be assigned its own material and colour. The toolbar shows the visualisation options. The geometry can be fit into the window, zoomed, moved or rotated. A grid can be turned on or off. The complete program functionality is described in the user manual, which can be found in Appendix D.3.

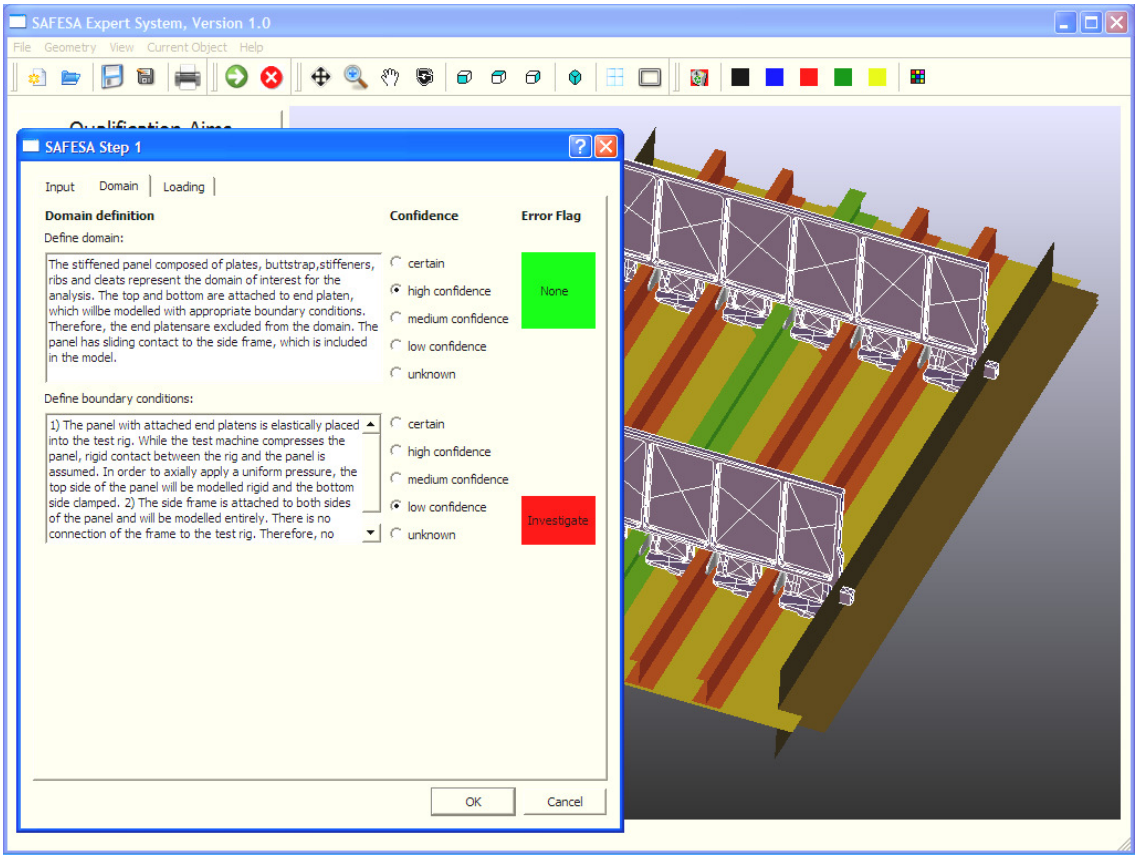

Figure 5.13: SAFESA step-1 dialog

Figure 5.13 shows the expert system with the dialog of SAFESA step-1. The dialog is separated in three tabulator views. The domain tabulator where the domain and boundary conditions are specified is shown here. These definitions are expressed in text. The confidence is specified by selecting a check-box from five categories: certain, high confidence, medium confidence, low confidence and unknown. Both “low confidence” and “unknown” will flag a potential error source, which is indicated with a red flag.

By pressing the OK button at the bottom of the dialog, all information is stored internally in the Datamap, as explained in section 5.6.1. To save an analysis file permanently the button with the floppy symbol in the main window (third from left in the toolbar) is pressed. Alternatively, this can be done via the menu: File -> Save.

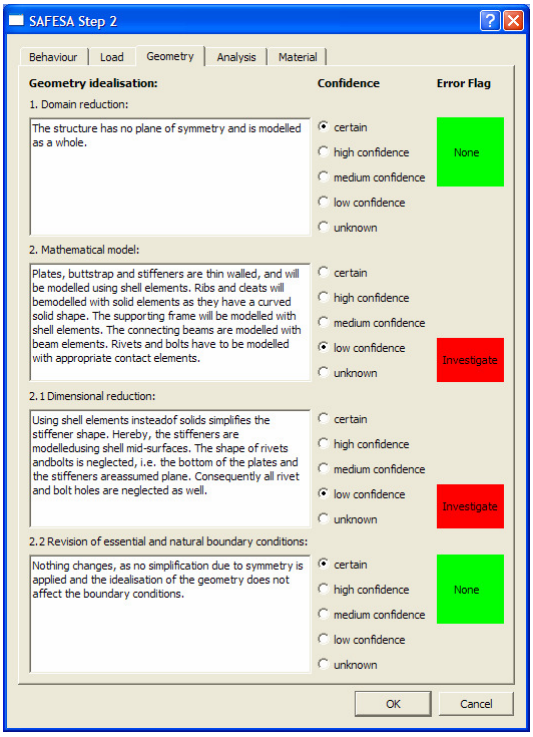

Figure 5.14: Step-2 dialog

The dialog for step-2 is similar to the previous one, see Figure 5.14. Five tabulator views are provided: behaviour, load, geometry, analysis and material. After completing this step, the global idealisation is finished.

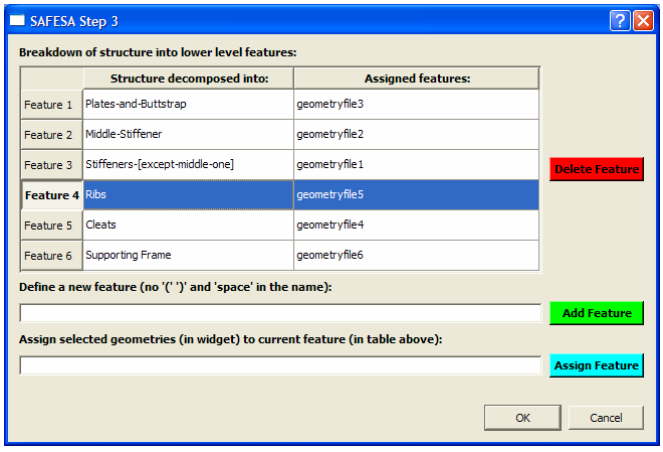

Figure 5.15: Feature definition at step-3

Figure 5.15 shows the dialog for step-3, where the structure is broken down into individual features. The six features of the Airbus panel assembly can be seen. A feature is defined by writing a name in the upper line-edit field and pressing the green button “Add Feature”. This generates a new row in the data matrix. After this, a geometry feature in the main window is selected by mouse-click. To connect the part with the name, the blue button “Assign Feature” is pressed.

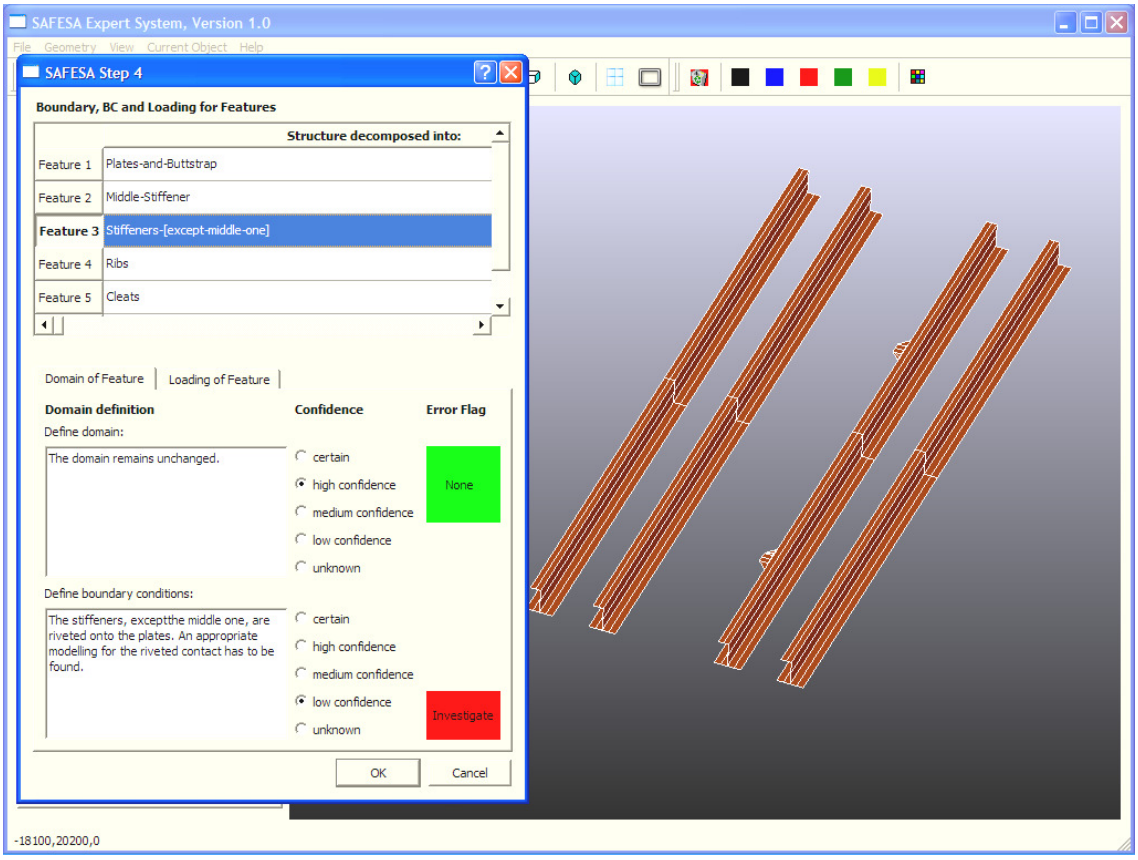

Figure 5.16: Feature idealisation at step-4

After step-3 the structure is divided into independent features. Further idealisations will be made on the feature level. Figure 5.16 shows the expert system together with the step-4 dialog. In the upper part, the dialog offers a list with all features. When highlighting one row, the relevant feature definitions are shown in the lower part of the dialog box. At the same time, the main window displays the selected feature and hides the others.

Step-4 is similar to step-1 as the same idealisation decisions have to be made, although this time on the feature level rather than at the global structure level. Step-5 resembles step-2.

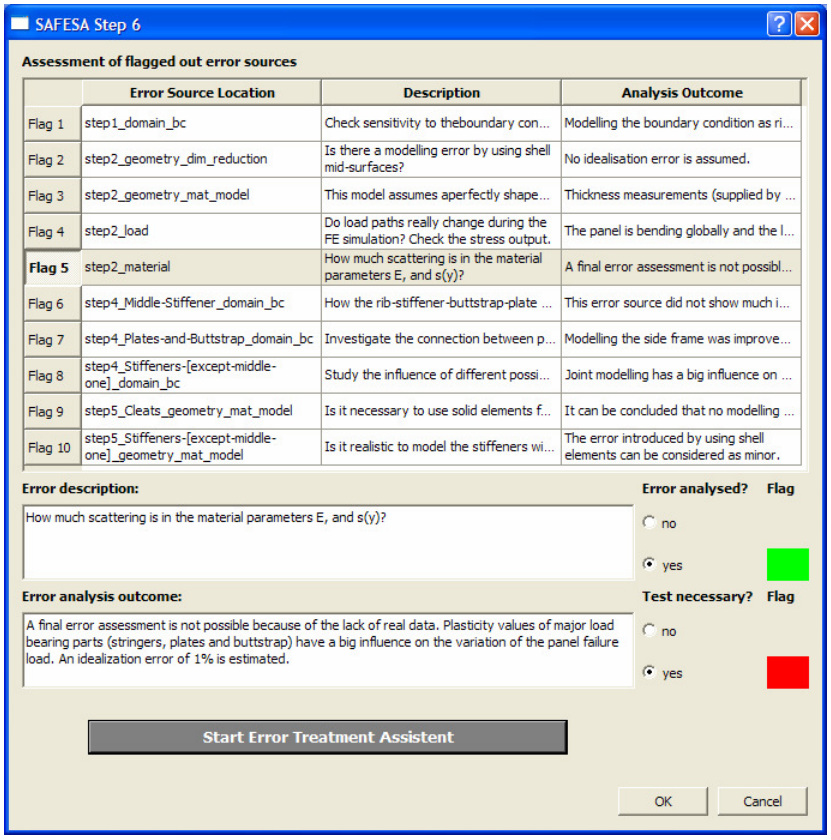

Figure 5.17: List of flagged error sources at step-6

In Figure 5.17 the dialog for step-6 can be seen. The upper part is a list of all previously flagged error sources. Ten error sources were flagged out for the Airbus panel during the analysis. At this stage the error description explaining the idealisation concern is added. Once the error source is analysed and the provided check-box clicked, the upper flag will turn from red to green. The lower text field provides space for a description of the error analysis outcome. The lower flag is red when additional testing has to be done. After the tests, the flag can be switched to green, which indicates the completion of the error treatment.

Step-6 is a very important stage in the idealisation error control process because the error sources have to be analysed and a remaining error value has to be estimated. Therefore, the decision advisor is applied at this stage. The CLIPS dialog is started by clicking on the dark grey button named “Start Error Treatment Assistant”. CLIPS will be initialised with all flagged error sources and the respective confidence level.

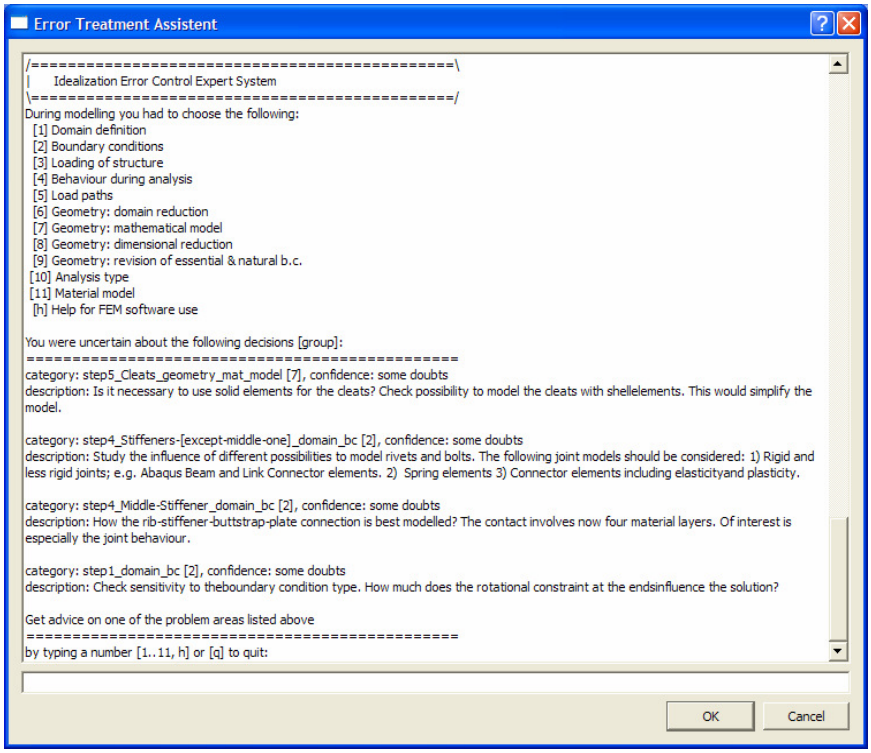

Figure 5.18: CLIPS engine showing menu and error list

Figure 5.18 shows the decision advisor. The user can read the output in the text field and respond to the system using the line-edit at the bottom. The consultation starts with a menu and lists all flagged errors and their description. The user can choose the error categories “1” to “11”, “h” for help or “q” for quit.

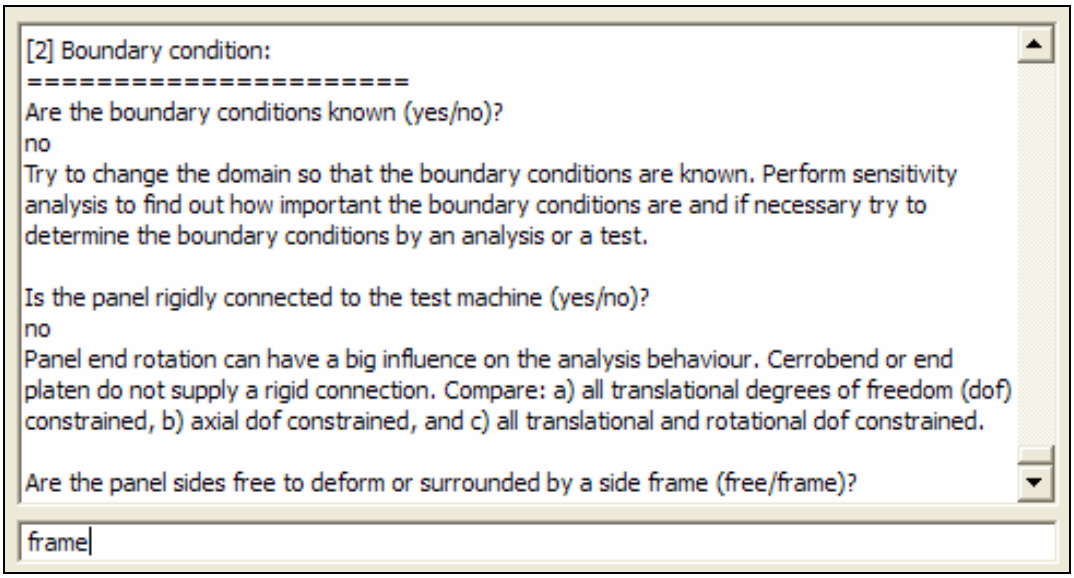

Figure 5.19: Expert consultation about boundary conditions

Figure 5.19 illustrates an expert consultation for the selection of appropriate boundary conditions. The system asks questions and leads the user through the

decision process. Advice is given depending on how the panel is connected to the test machine.

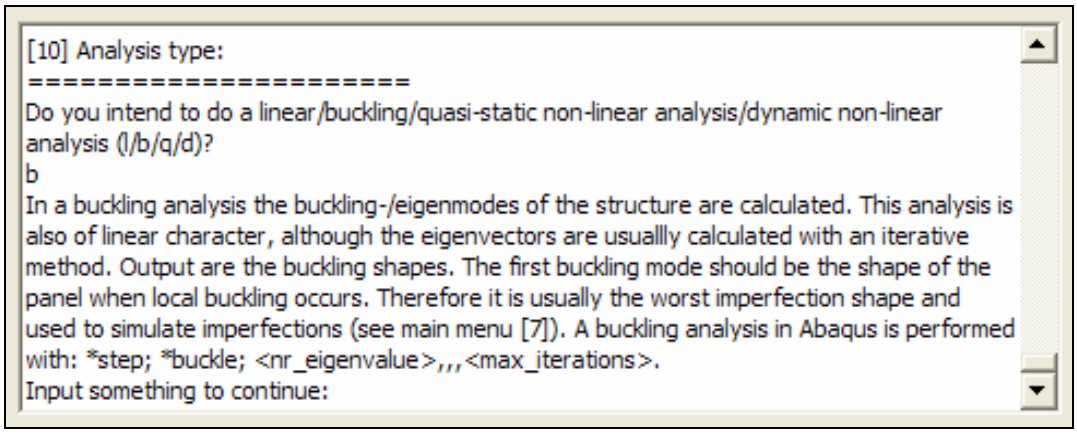

Figure 5.20: Expert consultation about the analysis type

The start of an expert consultation about the analysis type is presented in Figure 5.20. Users can select information about linear, buckling, nonlinear static and dynamic nonlinear analyses. CLIPS code of this rule can be found in Appendix D.2.

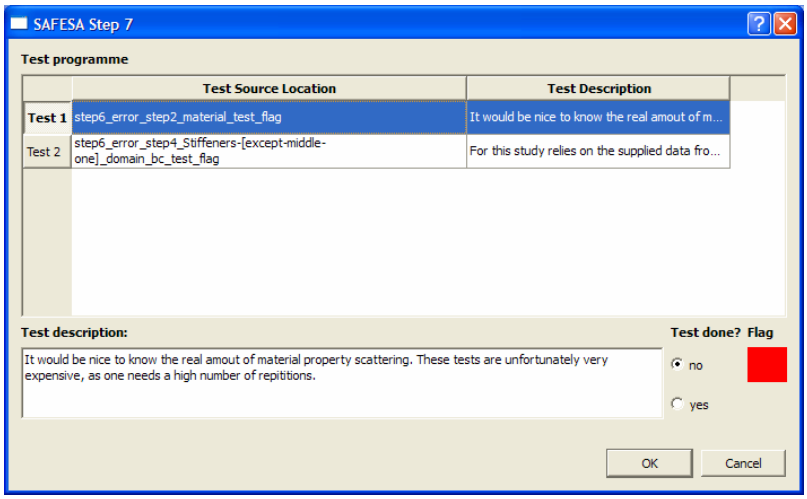

Figure 5.21: List of additional tests at step-7

Figure 5.21 shows the dialog for step-7. The upper part is a list of the tests which were marked at step-6. A description can be supplied in the text field at the bottom. After a test was performed, the “Test done?” check-box that switches the red flag to green can be selected. This was the last step in the SAFESA procedure. Successful idealisation error investigations are documented by saving (File -> Save As) and keeping the files. An analysis summary can be printed with: File -> Print Report. The output is a PDF file.

5.8 Verification Phase

Software verification is intended to show that a system conforms to its specification and meets the expectations of the users. It involves checking processes at each stage of the software process. Verification by the developer carries the great risk that logical errors are not detected because he is following his own logic. It is advisable to test the software with people of a different educational background.

The implemented expert system was used to perform and document the two FEM idealisation error analyses presented in chapters 3 and 4. These analyses are provided as tutorial examples in the delivered software. The immediate feedback influenced the final program structure.

The program was then tested by two engineers with knowledge of FEM modelling. The task was to repeat their last FEM modelling, this time with the focus on idealisation error control. The feedback was very promising because they liked the idea of the program and its visualisation facility. The study also revealed functionality errors which were corrected. Some other suggestions for improvement were expressed:

- An interactive help system in addition to the user guide.
- Better explanation of the advisor facility.
- More intuitive feature selection in the GUI.
- CAD geometry de-assembly facility.

On a technical level, the requirements expressed in section 5.4 were achieved. However, no formal usability studies were conducted, which leaves potential for improvement. Another point is that the SAFESA procedure was not intuitively understood during the tests, which is mainly due to its sequential structure. It might be helpful to give the steps more recognisable names, as “Global Analysis”, “Structural Decomposition”, “Local Analysis” etc. All in all, the involved engineers expressed an increased confidence in their FEM model, although a detailed analysis of the identified error sources could not be carried out.

5.9 Discussion

This chapter presented the development process of the idealisation error control expert system. The literature review and tool comparison showed that there is a need for this development. The chapter then described the specification, design, implementation and use of the implemented tool. Project goals were met, but there is still a list of things which have not yet been realised:

- Decision making facility for all idealisation decisions
- CAD geometry creation and changing facility
- Tree view of the CAD entities
- FEM input generation
- Linkage to existing databases
- Library optimisation to include only necessary code. Currently, additional DLL's are loaded at program start due to internal dependencies.

It turned out during the tool comparison that obtaining trial versions of special purpose software, such as MSC.Supermodel, AMRaven or ICAD, might be impossible. This also applies to other expert systems, which were recommended in the literature.

The software development has highlighted a number of practical difficulties. Especially the use of open source libraries requires a bigger effort in development work. Combining Qt 4.3 with the Microsoft C++ compiler was quite tricky and required special knowledge. The Open CASCADE library is freely available but not easy to integrate into a project. Without the discussions in the Sourceforge forum [109] the development might have required a software redesign. But the final program implementation is very satisfactory with respect to execution speed, appearance and maintainability.

Not all resources of CLIPS programming could be used in the current program version. The ClipsEngine is initialised with all flagged error sources, their descriptions and confidence levels. Only information about the error source is currently used. Also, more complex rules can be defined using CLIPS. The problem is that FEM idealisation knowledge cannot easily be formulated in general rules. Improved uncertainty treatment technologies, such as fuzzy logic or Monte-Carlo simulations, could not be applied with the available information. These aspects can be improved in the future using the provided expert system.

The program still can be improved and has yet to be tested by a larger number of users. However, the author believes that the created tool can be useful for the enhancement of any existing pre-processor. The implemented concept shows how a knowledge-based system can be used to aid the virtual testing process. The program code is compiler, CAD and FEM program independent. The design can be ported to any other system. The next step should be the program testing with a larger number of design engineers. This should be the starting point of a future project.

6. CONCLUSIONS

This thesis addresses the applicability of SAFESA to nonlinear analysis cases and contributes to the development of tools for more reliable FEM analyses. The method was applied to the failure analysis of stiffened metal panels loaded in compression. ABAQUS was the used nonlinear solver. The following paragraphs summarise the main conclusions and give recommendations for future work.

6.1 Research Contribution

The novelty in the research is the demonstration that SAFESA can be adapted to nonlinear analyses. Two stiffened panel compression tests were successfully modelled using the idealisation error control method, which provides reference cases. Using these results, a nonlinear update of the method was derived. The research also developed an expert system for FEM idealisation. The program is the first software implementation of the SAFESA methodology.

6.2 Stiffened Panel Failure Simulation

The analysed Cranfield panel is a relatively simple structure. Plate and stiffeners are connected by rivets and cast into Cerrobend at the ends. But the analysis behaviour is highly nonlinear due to the thin-walled properties of the structure. In the beginning of the compression test, the panel buckles locally between the stiffeners. This initial buckling interacts with the later failure mode as it determines where the panel will start collapsing. Failure is a combination of torsional and flexural buckling at the sides of the panel. The main idealisation errors were identified as boundary conditions, material modelling, contact between panel and stiffener and the stiffener shape. Material and contact modelling in particular needed to be analysed in the context of nonlinearity.

The Airbus panel is quite a complex structure composed of plates, stiffeners, buttstrap, ribs, cleats, side frame and lots of rivets and bolts. Until failure, the geometric behaviour of this structure is much less complicated because the major load bearing parts (plates, buttstrap and stiffeners) are thick walled. No local skin buckling takes place and the failure is determined by the out-of-plane bending of the panel centre. Idealisation errors were identified as joint modelling, boundary conditions and scattering in material parameters. Because high pressure values occur, the material behaviour has the biggest nonlinear impact.

The failure analyses demonstrated the applicability of the idealisation error control procedure to nonlinear analysis cases. In both cases, the method helped

to identify idealisation errors and building a reliable FEM model. This study provided practical experience of the error control process, which helped to design the expert system.

6.3 SAFESA Methodology Update

The SAFESA method is tailored to linear static tasks and, until now, has only been applied to linear deformation and eigenmode analyses. Small extensions to the original method had to be made in order to deal with the nonlinear error sources (material, boundary condition / contact and geometry change, as described in section 2.2.1). The general concept of the control procedure is to systematically review all idealisation decisions. This approach was found to be universally applicable and there was no need for a new methodology. The updated version of SAFESA is provided in Appendix C.

6.4 Expert System Development

The final objective of this research was to develop an expert system for idealisation error control. After reviewing the pertinent literature and software, the program was designed. Previously gained experience determined the look and functionality of the program. The key requirement was to provide guidance on carrying out reliable FEM analyses with the SAFESA methodology. A decision making advisor, CAD data import, geometry visualisation and audit trail functionality were additional important goals. The implemented program is the first documented software for the SAFESA methodology. The decision advisor was demonstrated on the idealisation error treatment of stiffened panels. This provides a prototype which can be extended or ported to other platforms. The software has been evaluated informally and proved to meet the program objectives.

6.5 Further Work

All project goals were met. The following points list potentially rewarding research topics which could not be performed due to budget, time or other constraints.

Cranfield panel analysis

- Use of better test equipment in order to record the complete load-shortening history.
- Testing different panel end boundary conditions.
- Performing coupon tests to refine material parameters and their variation.

- Measurement of the actual panel end rotations. More realistic boundary conditions can be modelled with the use of these data.
- For a new panel test design: providing more realistic panel side boundary conditions, e.g. by fastening the sides. The “natural” panel failure mode for panels used in aerospace structures is flexural buckling of skin-stiffener in the panel centre. The tested panels, however, failed at the sides.

Airbus panel analysis

- The model size was decreased to fit the computing facilities. Therefore, increasing the mesh size and using higher order tetrahedral elements.
- Assembly of high-quality joint test data. This could indicate that joint failure must be added to the model.
- Performing coupon tests to refine material parameters and their variation.
- Panel collapse analysis with explicit solvers LS-Dyna or ABAQUS/Explicit. One interesting aspect is the coupling of implicit and explicit solvers.
- Changing the test machine setup to prevent end platen rotation. The provided test data was biased.

Expert system development

- Usability study to quantify the functionality and usability of the program.
- Providing an advisor facility for all idealisation decisions.
- CAD creation and modification facility including a tree view.
- FEM input generation.
- Link to existing databases (materials, pre-meshed parts etc.).
- Library optimisation to load only necessary DLLs.

SAFESA

- Application to more complex cases like full-scale airplane loading.
- Research regarding applicability for dynamic FEM, impact and computational fluid dynamics (CFD) analyses.

REFERENCES

[1] Abaqus Inc., ABAQUS Version 6.7 Documentaion, 2007.

[2] ABAQUS Version 6.7, Software Package for Finite Element Analysis, Internet Resource: http://www.simulia.com/products/abaqus_fea.html (accessed March 2009).

[3] Airbus UK, Private Communication, 2006.

[4] P.S. Attwal, A SAFESA Based Free-Vibration Analysis of a Rocket Sled, MsC Thesis, Cranfield University, 1995.

[5] P.S. Attwal, Objective Error Measure Techniques for Error Analysis and Control within the Finite Element Analysis Process, EngD Thesis, Cranfield University, 2000.

[6] E.A. Avallone and Th. Baumeister, Mark's Standard Handbook for Mechanical Engineering, 10th ed., McGraw-Hill, 1996.

[7] I. Babuška and J.T. Oden, Verification and Validation in Computational Engineering and Science: Basic Concepts, Computer Methods in Applied Mechanics and Engineering, Vol. 193, pp. 4057-4066, 2004.

[8] J.P. Bates, A.J. Morris and P.N. Payne, Knowledge-Based Geometric Modeling of Aircraft Structures, Proc. of the Institution of Mechanical Engineers – Part G – Journal of Aerospace Engineering, Vol. 211, pp. 273-284, 1997.

[9] K.J. Bathe, On the Use of Hierarchical Models in Engineering Analysis, Computer Methods in Applied Mechanics and Engineering, Vol. 82, pp. 5-26, 1990.

[10] K.J. Bathe, Finite Element Procedures, Prentice Hall, 1996.

[11] K.J. Bathe, O. Guillermin, J. Walczak and H. Chen, Advances in Nonlinear Finite Element Analysis of Automobiles, Computers & Structures, Vol. 64, pp. 881-891, 1997.

[12] K. Bechkoum, Expert Systems for Engineering Applications, SAFESA Report 9034/TR/CIT/2001/1.0/7.7.93, 1993.

[13] T. Belytschko, W.K. Liu and B. Moran, Nonlinear Finite Elements for Continua and Structures, Wiley, 2000.

[14] J. Bennett, L. Creary, R. Englemore and R. Melosh, A Knowledge-Based Consultant for Structural Analysis, Technical Report, STAN-CS-78-699, Stanford University, 1978.

[15] P. Bermell-Garcia, A KBE System for the Design of Wind Tunnel Models Using Reusable Knowledge Components, Proc. of the 6th International Congress on Project Engineering, Barcelona, Spain, 2002.

[16] G. Bezine, On a Method of Comparison for Plate Elements in Finite Element Engineering Software Programs, Mechanics Research Communications, Vol. 29, pp. 35-43, 2002.

[17] J.H. Bickford and S. Nassar, Handbook of Bolts and Bolted Joints, Marcel Dekker, 1998.

[18] F. Bleich, Buckling Strength of Metal Structures, McGraw-Hill, 1952.

[19] E.F. Bruhn, Analysis and Design of Flight Vehicle Structures, Jacobs Publisher, 1973.

[20] C.G. Burge, Structural Principles and Data, 4th ed., Pitman, 1952.

[21] J. Cagan and V. Genberg, PLASHTRAN: An Expert Consultant on Two-Dimensional Finite Element Modeling Techniques, Engineering with Computers, Vol. 2, pp. 199-208, 1987.

[22] J. Campbell, Structural Stability, Lecture Notes, School of Engineering, Cranfield University, 2005.

[23] F. Caputo, R. Esposito, P. Perogini and D. Santoro, Numerical-Experimental Investigation on Post-Buckled Stiffened Composite Panels, Composite Structures, Vol. 55, pp. 347-357, 2002.

[24] D. Carroll, C. Bates, M. Zampino and K. Jones, A Novel Technique For Modeling Solder Joint Failure During System Level Drop Simulations, Proc. 10th InterSociety Conference on Thermal and Thermomechanical Phenomena in Electronic Systems, San Diego, pp. 861-868, 2006.

[25] CATIA V5, Multiplatform CAD/CAD/CAE Software, Internet Resource: http://www.3ds.com/products/catia/ (accessed March 2009).

[26] K.W. Chau and F. Albermani, A Coupled Knowledge-Based Expert System for Design of Liquid-Retaining Structures, Automation in Construction, Vol. 12, pp. 589-602, 2003.

[27] M. Chiu, T.-S. Wu, C.-H. Lee and N.-H. Lee, Integrating MSC Software and CADSA Program for the Aircraft Detail Stress Analysis, Proc. MSC 1999 Aerospace User's Conference, 1999.

[28] CLIPS Version 6.24, Public Domain Tool for Building Expert Systems, Internet Resource: http://clipsrules.sourceforge.net/ (accessed March 2009).

[29] R.D. Cook, D.S. Malkus, M.E. Plesha and R.J. Witt, Concepts and Applications of Finite Element Analysis, 4th ed., John Wiley, 2002.

[30] Cranfield University, Stressing Data Sheets, AVT-AVD 9632, Cranfield College of Aeronautics, 1999.

[31] M.A. Crisfield, Non-Linear Finite Element Analysis of Solids and Structures, Volume 1, John Wiley, 1991.

[32] M.A. Crisfield, Non-Linear Finite Element Analysis of Solids and Structures, Volume 2, John Wiley, 1997.

[33] R. Degenhardt, K. Rohwer, W. Wagner and J.P. Delsemme, Postbuckling and Collapse Analysis of CFRP Stringer Stiffened Panels – a Grateur Activity, Proc. of the 4th International Conference on Thin-Walled Structures, Loughborough, England, 2004.

[34] R. Degenhardt, A. Kling, K. Rohwer, A.C. Orifici and R.S. Thomson, Design and Analysis of Stiffened Composite Panels Including Post-Buckling and Collapse, Computers & Structures, Vol. 86, pp. 919-929, 2008.

[35] G.E. Dieter, Mechanical Metallurgy, 3rd ed., McGraw-Hill, 1986.

[36] N. Dullaway, The Design of an Intelligent Structural Qualification Environment, EngD Thesis, Cranfield University, 2000.

[37] C.L. Dym, Knowledge-Based Systems in Engineering, McGraw-Hill, 1991.

[38] Esdu 02.01.08, Buckling in Compression of Sheets Between Rivets, ESDU International Ltd, 1962.

[39] Esdu 71014, Local Buckling of Compression Panels with Flanged Stringers, ESDU International Ltd, 1971.

[40] Esdu 76016, Generalisation of Smooth Continuous Stress-Strain Curves for Metallic Materials, ESDU International Ltd, 1976.

[41] Esdu 77023, Shear Centre and Primary Warping Constant for Lipped and Unlipped Channel and Z-Sections, ESDU International Ltd, 1977.

[42] Esdu 01.01.01, The Strength of Struts, ESDU International Ltd, 1983.

[43] Esdu, Metallic Material Data Handbook, DEF STAN 00-932, ESDU International Ltd, 1990.

[44] M. Farley, Establishing New Methodologies with MSC Software Products to Develop a 747SP Finite Element Model for FAA Certification of Airframe Design Modification, Proc. MSC 1999 Aerospace User's Conference, 1999.

[45] C.A. Felippa, Introduction to Finite Element Methods, Lecture Notes, Department of Aerospace Engineering Sciences, University of Colorado, Internet Resource: http://www.colorado.edu/engineering/CAS/courses.d/IFEM.d/ (accessed March 2009).

[46] Flightglobal, Internet Resource: http://www.flightglobal.com/articles/2006/02/16/204716/airbus-a380-test-wing-breaks-just-below-ultimateload.html (accessed March 2009).

[47] J.C. Giarratano and G.D. Riley, Expert Systems: Principles and Programming, 4th ed., Course Technology, 2005.

[48] B.L. Gregory and M.S. Shephard, The Generation of Airframe Finite Element Models Using an Expert System, Engineering with Computers, Vol. 2, pp. 65-77, 1987.

[49] F. Gunbring, Prediction and Modelling of Fastener Flexibility Using FE, Technical Report, LIU-IEI-TEK-A-08/00368-SE, Linköping University, 2008.

[50] A.K. Hadi, Finite Element Error Control, MsC Thesis, Cranfield University, 1992.

[51] E.B. Haugen, Probabilistic Mechanical Design, John Wiley, 1980.

[52] M. Heitmann, P. Horst, M. Haupt and D. Fitzsimmons, Numerische Simulation von Teilschalenversuchen an Versteiften Metallischen Strukturen unter Kombinierter Druck- und Schubbeanspruchung, Deutscher Luft- und Raumfahrtkongress, DGLR-JT2001-110, 2001.

[53] M. Heitmann, P. Horst and D. Fitzsimmons, Effective Stiffness of Postbuckled Stiffened Metallic Panels Under Combined Compression and Shear Stress, J. Strain Analysis, Vol. 38, pp. 539-555, 2003.

[54] M. Heitmann, Untersuchung des Nachbeulverhaltens Rechteckig Versteifter Metallischer Strukturen Unter Kombinierter Druck- und Schubbespannung, (PhD Thesis), Berichte aus der Luft- und Raumfahrttechnik, Shaker, 2005.

[55] L. Herbeck and H. Wilmers, Design Rules for a CFRP Outer Wing, ICAS 2002, 23rd ICAS Congress of Aeronautical Sciences, Toronto, 2002.

[56] S.Z. Hu and L. Jiang, A Finite Element Simulation of the Test Procedure of Stiffened Panels, Marine Structures, Vol. 11, pp. 75-99, 1998.

[57] O.F. Hughes, B. Ghosh and Y. Chen, Improved Prediction of Simultaneous Local and Overall Buckling of Stiffened Panels, Thin-Walled Structures, Vol. 42, pp. 827-856, 2004.

[58] T.J.R. Hughes, The Finite Element Method: Linear Static and Dynamic Finite Element Analysis, Prentice-Hall, 1987.

[59] C. Hühne, R. Zimmermann, R. Rolfes and B. Geier, Sensitivities to Geometrical Loading Imperfections on Buckling of Composite Cylindrical Shells, Proc. of the European Conference on Spacecraft Structures, Materials and Mechanical Testing, Toulouse 2002.

[60] Hypermesh, Pre- and Post-Processing Software, Internet Resource: http://www.altair.com (accessed March 2009).

[61] I-DEAS, Computer-Aided Design Software, Internet Resource: http://www.plm.automation.siemens.com/en_us/ (accessed March 2009).

[62] P. Jackson, Introduction to Expert Systems, 3rd ed., Addison-Wesley, 1999.

[63] J. Kim and S. Han, Encapsulation of Geometric Functions for Ship Structural CAD Using a STEP Database as Native Storage, Computer-Aided Design, Vol. 35, pp. 1161-1170, 2003.

[64] J.-S. Kim, Development of a User-Friendly Expert System for Composite Laminate Design, Composite Structures, Vol. 79, pp. 76-83, 2007.

[65] A. Kling and R. Degenhardt, Nachbeulverhalten von Flugzeugrumpfschalen, Proc. of the 13th German ABAQUS User Conference, Freiburg, Germany, 2001.

[66] N.F. Knight Jr. and T.J. Stone, Rapid Modeling and Analysis Tools: Evolution, Status, Needs and Directions, Technical Report, NASA/CR-2002-211751, 2002.

[67] N.F. Knight Jr., M.P. Nemeth and M.W. Hilburger, Assessment of Technologies for the Space Shuttle External Tank Thermal Protection System and Recommendations for Technology Improvement: Part 2: Structural Analysis Technologies and Modeling Practices, Technical Report, NASA/TM-2004-213256, 2004.

[68] P. Kurowski and B. Szabó, How to Find Errors in the Finite Element Models, Machine Design, 25 September, 1997.

[69] P. Kurowski, Easily Made Errors Mar FEA Results, Machine Design, 13 September, 2001.

[70] W. Kuntjoro, Expert System for Structural Optimization Exploiting Past Experience and A-priori Knowledge, Volume 1: Main Thesis, PhD Thesis, Cranfield University, 1994.

[71] B. Langrand, E. Deletombe, E. Markiewicz and P. Drazetic, Riveted Joint Modelling for Numerical Analysis of Airframe Crashworthiness, Finite Elements in Analysis and Design, Vol. 38, pp. 21-44, 2001.

[72] C. Ledermann, C. Hanske, J. Wenzel, P. Ermanni and R. Kelm, Associative Parametric CAE Methods in the Aircraft Pre-Design, Aerospace Science and Technology, Vol. 9, pp. 641-651, 2005.

[73] S. Li and M. Qiao, A Hybrid Expert System for Finite Element Modeling of Fuselage Frames, Expert Systems with Applications, Vol. 24, pp. 87-93, 2003.

[74] B.T. Lin and S.H. Hsu, Automated Design System for Drawing Dies, Expert Systems with Applications, Vol. 34, pp. 1586-1598, 2008.

[75] S.P. Lin and F. Albermani, Lattice-Dome Design Using a Knowledge-Based System Approach, Computer-Aided Civil and Infrastructure Engineering, Vol. 16, pp. 268-286, 2001.

[76] H. Lockett, A Knowledge Based Manufacturing Advisor for CAD, PhD Thesis, Cranfield University, 2005.

[77] C.J. Lynch, A Finite Element Study of the Postbuckling Behaviour of a Typical Aircraft Fuselage Panel, PhD Thesis, The Queen's University of Belfast, 2000.

[78] C. Lynch, A. Murphy, M. Price and A. Gibson, The Computational Post Buckling Analysis of Fuselage Stiffened Panels Loaded in Compression, Thin-Walled Structures, Vol. 42, pp. 1445-1446, 2004.

[79] A. Mateus and J.A. Witz, A Parametric Study of the Post-Buckling Behaviour of Steel Plates, Engineering Structures, Vol. 23, pp. 172-185, 2001.

[80] T.H.G. Megson, Aircraft Structures for Engineering Students, 3rd ed., Butterworth-Heinemann, 1999.

[81] Microsoft Visual C++ 2005 Edition, Public Domain Compiler, Internet Resource: http://www.microsoft.com/express/vc/ (accessed March 2009).

[82] Military Handbook, Metallic Materials and Elements for Aerospace Vehicle Structures, MIL-HDBK-5, Department of Defence, Washington DC, 2001.

[83] A.J. Morris, Cranfield's Statement of Requirements for the Advisor Software, SAFESA Report 9034/TN/CIT/2021/0.0/28.9.93, 1993.

[84] A.J. Morris, The Qualification of Safety Critical Structures by Finite Element Analytical Methods, Proc. of the Institution of Mechanical Engineers - Part G – Journal of Aerospace Engineering, Vol. 210, pp. 203-208, 1996.

[85] A.J. Morris and R. Vignjevic, Consistent Finite Element Structural Analysis and Error Control, Computer Methods in Applied Mechanics and Engineering, Vol. 140, pp.87-108, 1997.

[86] A.J. Morris, A Practical Guide to Reliable Finite Element Modelling, John Wiley & Sons, 2008.

[87] MSC Software Corp., MSC.Nastran 2004 Reference Manual, 2003.

[88] MSC Software, The MacNeal Schwendler Corporation, Internet Resource: http://www.mscsoftware.com/products/ (accessed March 2009).

[89] V. Mukhopadhyay, S-Y. Hsu, B.H. Mason, D.W. Sleight, W.T. Jones, J. Chu, M.D. Hicks, J.L. Spangler, H. Kamhawi and J.L. Dahl, Adaptive Modeling, Engineering Analysis and Design of Advanced Aerospace Vehicles, Proc. of the 47th AIAA/ASME/ASCE/AHS/ASC Structures, Structural Dynamics, and Materials Conference, Newport, Rhode Island, AIAA 2006-2182, 2006.

[90] Musca Project Partners, Annex I – Description of Work MUSCA Project Contract, 2005.

[91] Musca Project, Private Communication, 2006.

[92] A. Murphy, Accurate and Efficient Buckling and Post Buckling Analysis of Fuselage Panels Loaded in Shear and Compression, PhD Thesis, The Queen's University of Belfast, 2002.

[93] A. Murphy, M. Price, A. Gibson and C.G. Armstrong, Efficient Non-Linear Idealisations of Aircraft Fuselage Panels in Compression, Finite Elements in Analysis and Design, Vol. 40, pp. 1977-1993, 2004.

[94] A. Murphy, M. Price, C. Lynch and A. Gibson, The Computational Post-Buckling Analysis of Fuselage Stiffened Panels Loaded in Shear, Thin-Walled Structures, Vol. 43, pp. 1455-1474, 2005.

[95] F. Nabhani and M. Wake, Computer Modeling and Stress Analysis of the Lumbar Spine, Journal of Materials Processing Technology, Vol. 127, pp. 40-47, 2002.

[96] M.C.-Y. Niu, Airframe Structural Design: Practical Design Information and Data on Aircraft Structures, Conmilit Press, 1988.

[97] M.C.-Y. Niu, Airframe Stress Analysis and Sizing, Conmilit Press, 1997.

[98] W.L. Oberkampf, T.T. Trucano and C. Hirsch, Verification, Validation, and Predictive Capability in Computational Engineering and Physics, Applied Mechanics Review, Vol. 57, pp. 345-384, 2004.

[99] Open CASCADE 6.2, Software Development Platform, Internet Resource: http://www.opencascade.org/ (accessed March 2009).

[100] A.C. Orifici, R.S. Thomsom, R. Degenhardt, A. Kling, K. Rohwer and J. Bayandor, Degradation Investigation in a Postbuckling Composite Stiffened Fuselage Panel, Proc. of the 13th International Conference on Composite Structures (ICCS-13), Melbourne, Australia, 2005.

[101] A.C. Orifici, R.S. Thomsom, A.J. Gunnion, R. Degenhardt, H. Abramovich and J. Bayandor, Benchmark Finite Element Simulations of Postbuckling Composite Stiffened Panels, Proc. of the 11th Australian Int. Aerospace Congress (AIAC-11), Melbourne, Australia, 2005.

[102] J.K. Paik, A.K. Thayamballi, B.J. Kim, G. Wang, Y.S. Shin and D. Liu, On Advanced Ultimate Limit State Design of Ship Stiffened Panels and Grillages, Proc. of the SNAME (Society of Naval Architects and Marine Engineers) Annual Meeting, Orlando, Florida, 2001.

[103] J.K. Paik and J.K. Seo, Nonlinear Finite Element Method Models for Ultimate Strength Analysis of Steel Stiffened-Plate Structures under Combined Biaxial Compression and Lateral Pressure Actions – Part I: Plate Elements, Thin-Walled Structures, to appear, 2009.

[104] J.K. Paik and J.K. Seo, Nonlinear Finite Element Method Models for Ultimate Strength Analysis of Steel Stiffened-Plate Structures under Combined Biaxial Compression and Lateral Pressure Actions – Part II: Stiffened Panels, Thin-Walled Structures, to appear, 2009.

[105] J.M. Palacios, Nonlinear Buckling Analysis of Stiffened Structural Parts Using MSC.Nastran SOL 600, Proc. of the MSC.Software's 2004 Virtual Product Development Conference, Munich, Germany, 2004.

[106] J.E. Pepin, B.H. Thacker and D.S. Riha, A Study of the Collapse of Spherical Shells, Part I: Uncertainty Quantification, EURODYN 2005, C. Soize & G.I. Schuëller (editors), Millpress, 2005.

[107] H.J. Pradlwarter, M.F. Pellissetti, C.A. Schenk, G.I. Schuëller, A. Kreis, S. Fransen, A. Calvi and M. Klein, Realistic and Efficient Reliability Estimation for Aerospace Structures, Computer Methods in Applied Mechanics and Engineering. Vol. 194, pp. 1597-1617, 2005.

[108] QT 4.3, Cross Platform Application Development Platform, Internet Resource: http://www.qtsoftware.com/ (accessed March 2009).

[109] QTOpenCascade, Framework for Integrating the Open CASCADE library with the Qt4 Toolkit, Internet Resource: http://sourceforge.net/projects/qtocc/ (accessed March 2009).

[110] W. Ramberg and W.R. Osgood, Description of Stress-Strain Curves by Three Parameters, NACA Technical Note 902, 1943.

[111] Renishaw, Scanning and Digitizing Systems – Cyclone Series 2 Scanning Machine, Internet Resource: http://www.rlstephenstool.com/cyclone.htm (accessed March 2009).

[112] G.S. Rhodes, The Nextgrade Prototype GUI for Intelligent Synthesis Environments, Proc. of the 40th AIAA/ASME/ASCE/AHS/ASC Structures, Structural Dynamics, and Material Conference, St. Louis, Missouri, AIAA-99-1362, 1999.

[113] P. Roache, Verification and Validation in Computational Science and Engineering, Hermosa Publishers, 1998.

[114] R. Rolfes, C. Hühne, A. Kling, H. Temmen, B. Geier, H. Klein, J. Teßmer and R. Zimmermann, Advances in Computational Stability Analysis of Thin-Walled Aerospace Structures Regarding Postbuckling, Robust Design and Dynamic Loading, In J. Loughlan (editor): Thin-Walled Structures, Advances in Research, Design and Manufacturing Technology, Proc. of the 4th International Conference on Thin-Walled Structures, Loughborough, 2004.

[115] A. Rutman and J. Bales-Kogan, Multi-Spring Representation of Fasteners for MSC/Nastran Modelling, Proc. of the MSC 1997 Aerospace Users' Conference, 1997.

[116] SAFESA Consortium, SAFESA Technical Manual to Structural Qualification Supported by Finite Element Analysis, NAFEMS R0041, 1995.

[117] C.A. Schenk and G.I. Schuëller, Buckling Analysis of Cylindrical Shells with Random Geometric Imperfections, International Journal of Non-Linear Mechanics, Vol. 38, pp. 1119-1132, 2003.

[118] M.H. Schneider Jr., R.J. Feldes, J.R. Halcomb and C.C. Hoff, Stability Analysis of Perfect and Imperfect Cylinders Using MSC/NASTRAN Linear and Nonlinear Buckling, Proc. of the MSC 1995 World User's Conference, 1995.

[119] H.J. Schwarz, Numerische Mathematik, Teubner, 1997.

[120] M.S. Shephard, E.V. Korngold, R.R. Collar and P.L. Baehmann, A Modeling Framework for Controlling Structural Idealization in Engineering Design, Computers & Structures, Vol. 37, pp. 181-191, 1990.

[121] J. Singer, J. Arbocz and T. Weller, Buckling Experiments, Volume 1: Basic Concepts, Columns, Beams and Plates, John Wiley, 1998.

[122] J. Singer, J. Arbocz and T. Weller, Buckling Experiments, Volume 2: Shells, Built-Up Structures, Composites, and Additional Topics, John Wiley, 2002.

[123] W.J. Stephenson, C.H. Zeune and M. Blair, Computational Design of an Advanced Mobility Concept, Proc. of the 11th AIAA/ISSMO Multidisciplinary Analysis and Optimization Conference, Portsmouth, Virginia, AIAA 2006-7123, 2006.

[124] A.E. Stockwell, A Verification Procedure for MSC/NASTRAN Finite Element Models, Technical Report, NASA-95-cr4675, 1995.

[125] B. Stroustrup, The C++ Programming Language, 3rd ed., Addison-Wesley, 1997.

[126] I. Sommerville, Software Engineering, 8th ed., Addison-Wesley, 2006.

[127] B. Szabó and I. Babuška, Finite Element Analysis, Wiley-Interscience, 1991.

[128] I.C. Taig, Expert Aids to Reliable Use of Finite Element Analysis, In: K.-J. Bathe and D.R.J. Owen (editors), Reliability of Methods for Engineering Analysis, pp. 457-474, Pineridge Press, 1986.

[129] B.H. Thacker, D.S. Riha and J.E. Pepin, Application of Probabilistic Methods to Weapon Reliability Assessment, Proc. of the 42nd AIAA/ASME/ASCE/AHS/ASC Structures, Structural Dynamics, and Materials Conference, Seattle, AIAA 2001-1458, 2001.

[130] B.H. Thacker, The Role of Nondeterminism in Verification and Validation of Computational Solid Mechanics Models, Proc. of the 2003 SAE World Congress, Detroit, 2003.

[131] B.H. Thacker, P.C. McKeighan and J.E. Pepin, A Study of the Collapse of Spherical Shells, Part II: Model Validation, EURODYN 2005, C. Soize & G.I. Schuëller (editors), Millpress, 2005.

[132] S.P. Timoshenko and J.M. Gere, Theory of Elastic Stability, 2nd ed., McGraw-Hill, 1961.

[133] C. Tomlinson and J.R. Maguire, Task F – Advisor Software Outline Specification, SAFESA Report 9034/TN/LRS/5081/0.0/5.11.93, 1993.

[134] W.W. Tworzydlo and J.T. Oden, Towards an Automated Environment in Computational Mechanics, Computer Methods in Applied Mechanics and Engineering, Vol. 104, pp. 87-143, 1993.

[135] UGS Corp., NX Nastran: Advanced Nonlinear Theory and Modeling Guide, 2005.

[136] J.H. Vandenbrande, T.A. Grandine and T. Hogan, The Search for the Perfect Body: Shape Control for Multidisciplinary Design Optimization, Proc. of the 44th AIAA Aerospace Sciences Meeting and Exhibit, Reno, Nevada, AIAA 2006-928, 2006.

[137] R. Vignjevic, A.J. Morris and A.D. Belagundu, Towards High Fidelity Finite Element Analysis, Advances in Engineering Software, Vol. 29, pp. 655-665, 1998.

[138] R. Vignjevic, A Finite Element Modelling Example, Lecture Notes, School of Engineering, Cranfield University, 2005.

[139] Wikipedia, Article about ICAD, Internet Resource: http://en.wikipedia.org/wiki/ICAD, (accessed March 2009).

[140] D.P. Yañez, R.M. Hauch and S.W. Prey, A Rapid Method for Creating High Fidelity Finite Element Models, Proc. of the 40th AIAA/ASME/ASCE/AHS/ASC Structures, Structural Dynamics, and Materials Conference, St. Louis, Missouri, AIAA-99-1361, 1999.

[141] T.-P. Yeh and J.M. Vance, Combining MSC/NASTRAN, Sensitivity Methods, and Virtual Reality to Facilitate Interactive Design, Finite Elements in Analysis and Design, Vol. 26, pp. 161-169, 1997.

[142] R.D. Young and C.C. Rankin, Modeling and Nonlinear Structural Analysis of a Large-Scale Lauch Vehicle, Journal of Spacecraft and Rockets, Vol. 36, pp. 804-811, 1999.

[143] R.D. Young, C.A. Rose and H. Starnes Jr., Skin, Stringer, and Fastener Loads in Buckled Fuselage Panels, Proc. of the 42nd AIAA/ASME/ASCE/ AHS/ASC Structures, Structural Dynamics, and Materials Conference, Seattle, Washington, AA2001-1326, 2001.

[144] O.C. Zienkiewicz and R.L. Taylor, The Finite Element Method: Volume 1 - The Basis, 5th ed., Elsevier, 2000.

[145] R. Zimmermann, H. Klein and A. Kling, Buckling and Postbuckling of Stringer Stiffened Fibre Composite Curved Panels – Tests and Computations, Composite Structures, Vol. 73, pp. 150-161, 2006.

APPENDIX A – PANEL DOCUMENTS

A.1 Cranfield Panel Design Sheet

The following panel is to be manufactured and tested

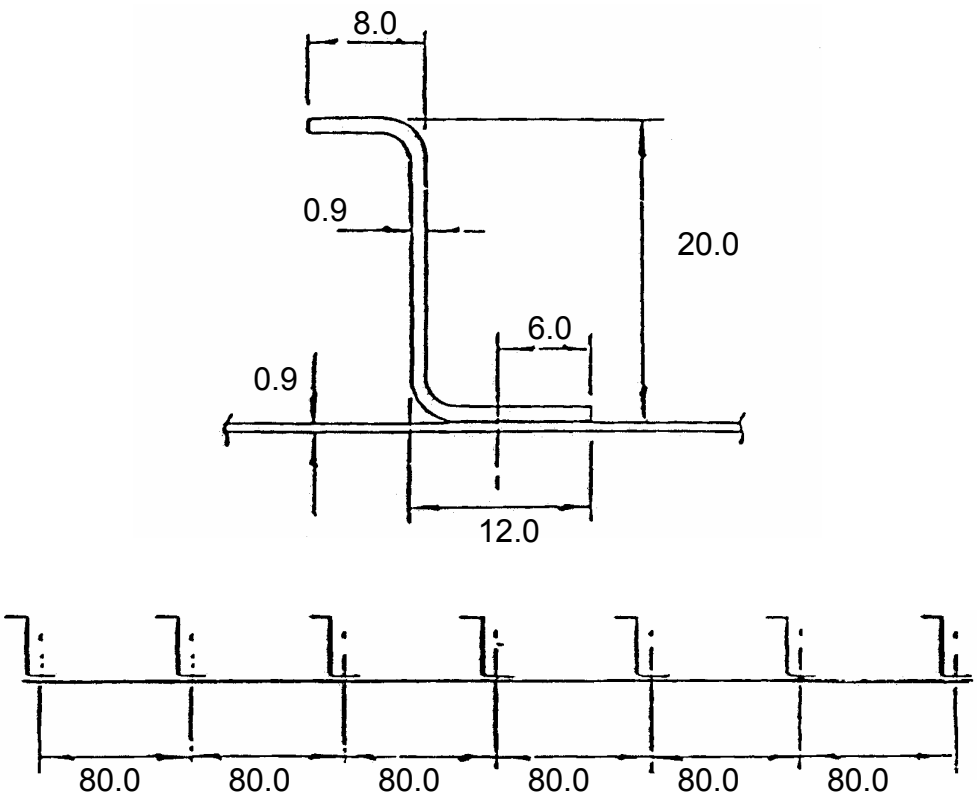

- All dimensions millimetres
- Ends cast in Cerrobend, actual panel length: 467 (Overall length 500)
- All bend radii: 1.5
- Skin and stringer material L165

  $f_n = 296 \text{N/mm}^2 \quad , \quad \frac{1}{\varepsilon_n} = 224 \quad , \quad m = 17$

- Rivets: 3/32” snap head, material L69, rivet pitch 14

A.2 Cranfield Panel Material Test

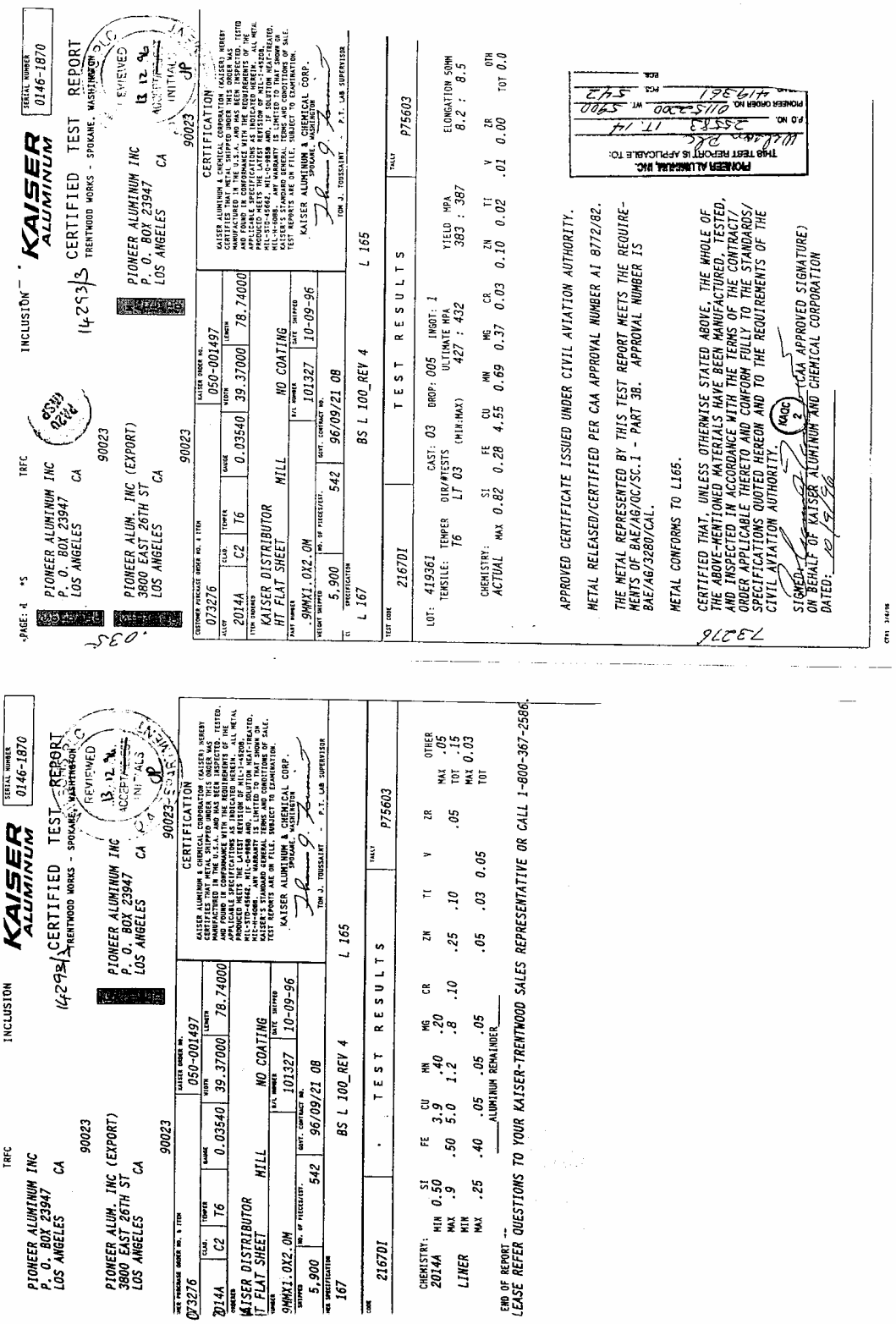

Figure A.1: Test certificate from Kaiser Aluminium

A.3 Airbus Panel Material Tests

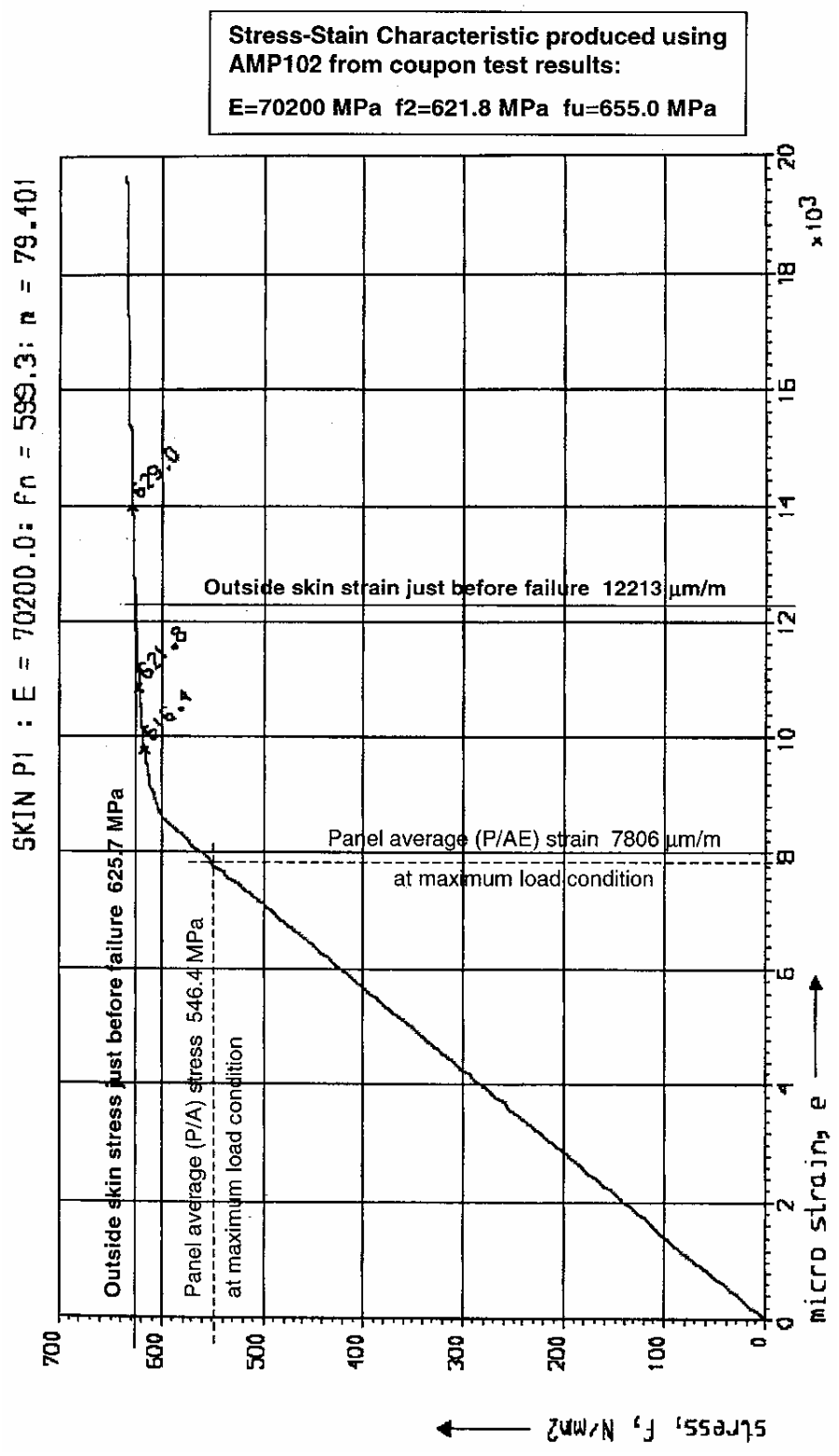

Figure A.2: Skin panel 1 – material stress-strain characteristic [3]

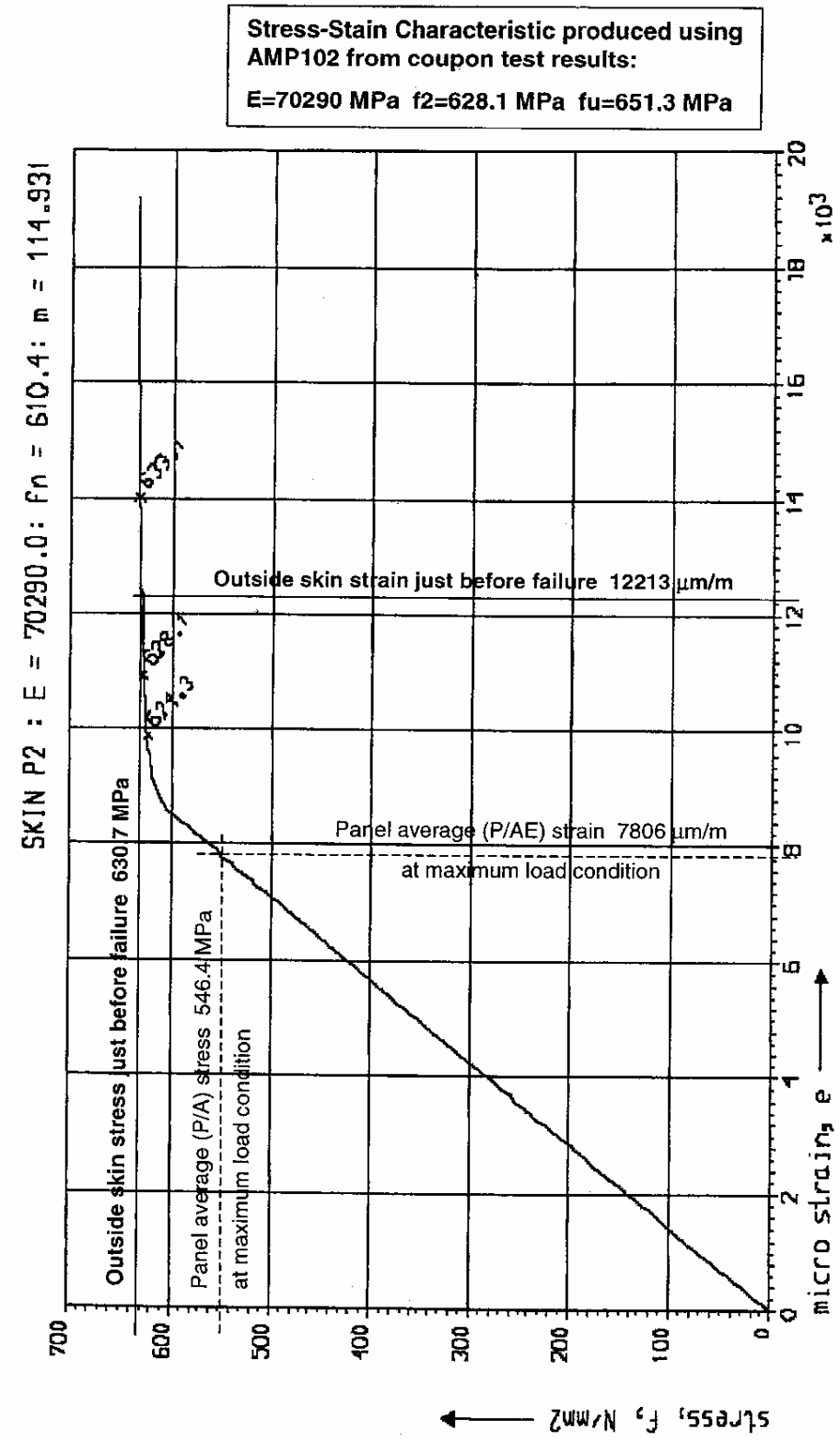

Figure A.3: Skin panel 2 – material stress-strain characteristic [3]

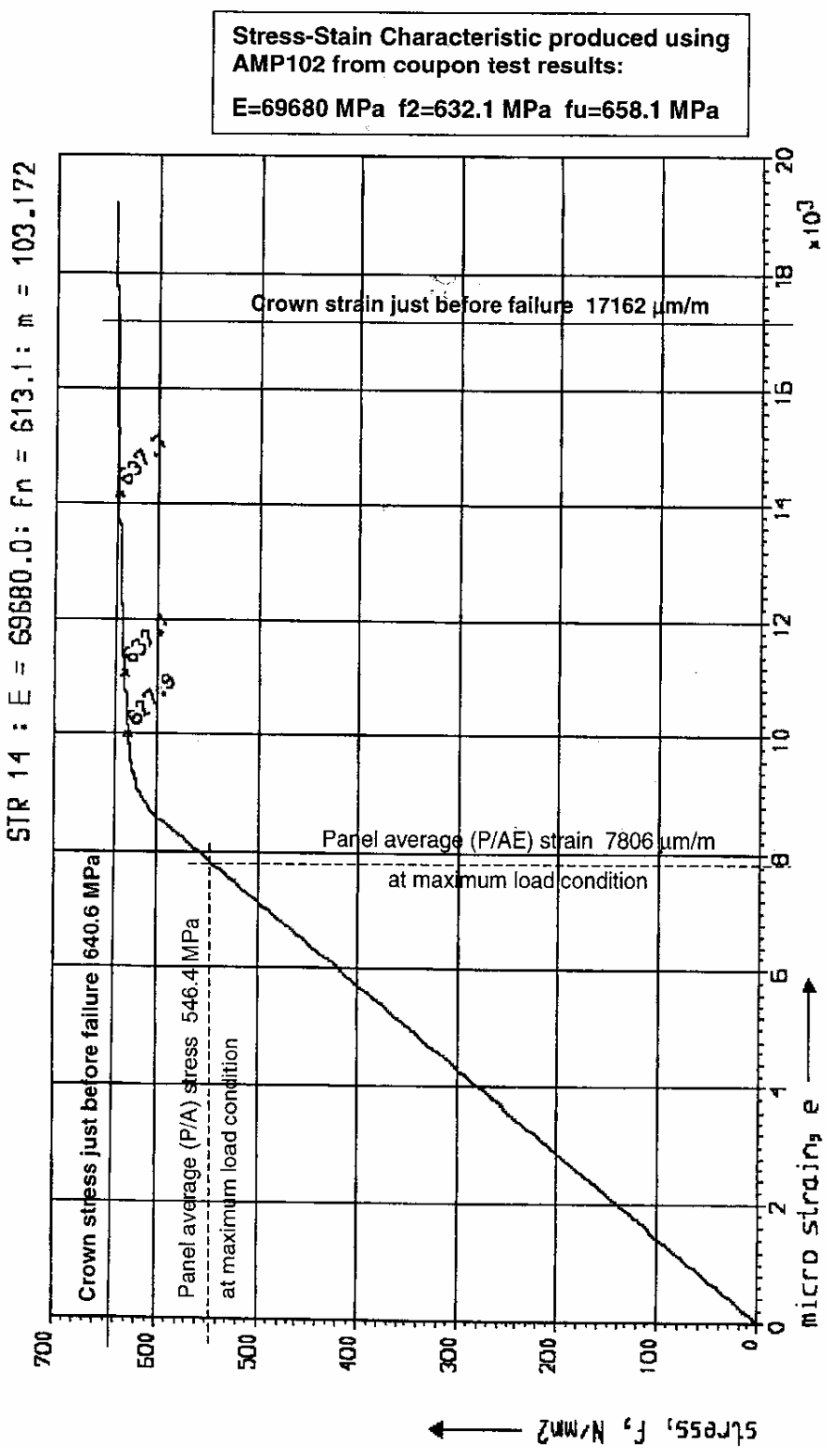

Figure A.4: Middle stiffener – material stress-strain characteristic [3]

A.4 Airbus Panel Geometrical Measurements

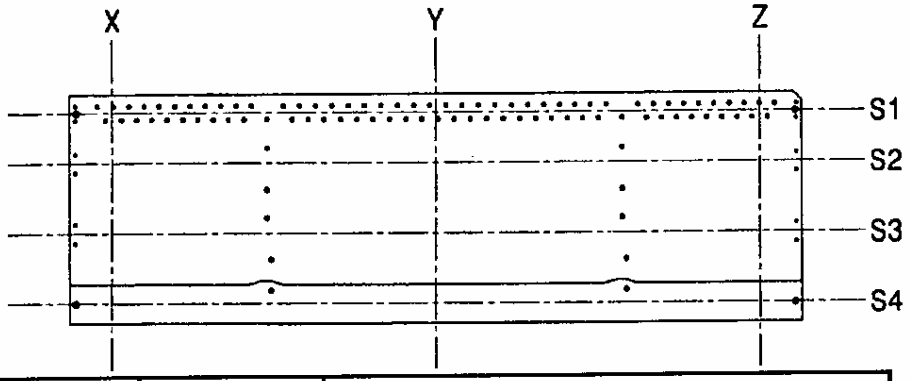

Position	Drawing Requirement mm	Skin Panel 1		
		X mm	Y mm	Z mm
S1	8.72/8.93	8.842	8.820	8.846
S2	8.72/8.93	8.846	8.831	8.855
S3	8.72/8.93	8.866	8.838	8.872
S4	15.9/16.0	15.992	15.964	15.984

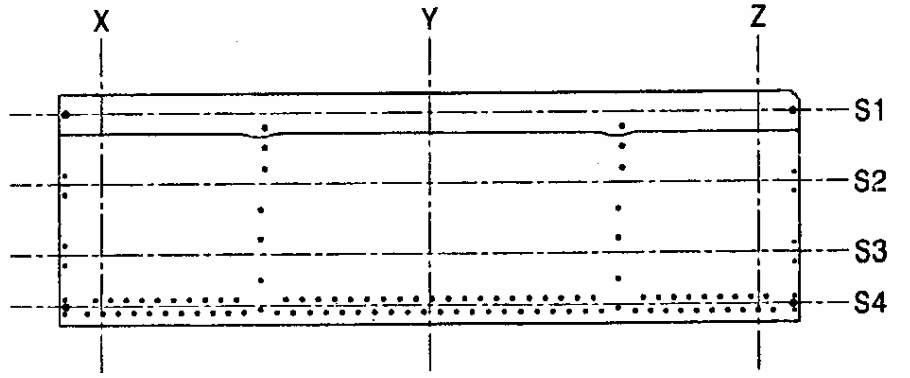

Position	Drawing Requirement mm	Skin Panel 2		
		X mm	Y mm	Z mm
S1	15.9/16.0	15.994	15.957	15.985
S2	8.72/8.93	8.860	8.818	8.861
S3	8.72/8.93	8.851	8.828	8.851
S4	8.72/8.93	8.852	8.824	8.855

Figure A.5: Skin panel 1,2 – measured thicknesses [3]

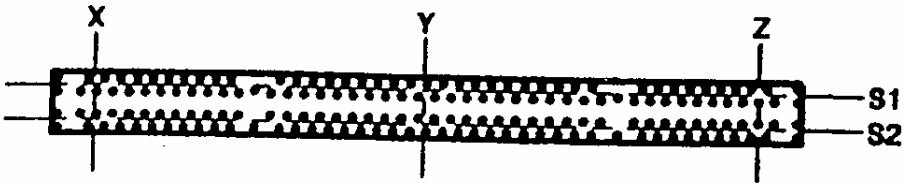

DIMENSIONAL CHECK FOR BUTTSTRAP			
POSITION	X	Y	Z
S1	6·578	6·562	6·587
S2	6·582	6·559	6·594

Figure A.6: Buttstrap – measured thicknesses [3]

Position	Drawing Requirement mm	Stringer		
		X mm	Y mm	Z mm
S1	6.34/6.67	6.57	6.57	6.66
S2	6.34/6.67	6.62	6.64	6.65
S3	9.10	9.13	9.19	9.12
S4	18.20	18.40	18.27	18.27
S5	39.00	39.12	39.13	39.08
S6	88.00	88.08	88.08	88.08
S7	68.50	68.56	68.53	68.55

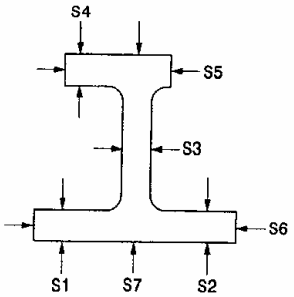

Figure A.7: Middle stiffener – measured thicknesses [3]

APPENDIX B - ABAQUS INPUT (IMPORTANT PARTS)

B.1 Cranfield Panel

```
*Node
      1,       -250.,         9.1,         500.
      2,       -250.,         9.1,           0.
…
*ELEMENT, TYPE=S4R, ELSET=PANEL
    1,     1,   113, 11745,   848
    2,   113,   114, 11746, 11745
…
*SHELL SECTION, ELSET=PANEL, MATERIAL=ALUMINUM
        0.9,       5
**
**********************************************************************************
**elastic-plastic material model for L165 according ESDU-76016
**
*MATERIAL, NAME=ALUMINUM
**
*ELASTIC, TYPE=ISO
68000.,0.33
**
*PLASTIC
330,0.
340,0.0066
350,0.0077
360,0.0093
370,0.0145
380,0.0248
390,0.0494
400,0.0762
410,0.0958
420,0.1294
430,0.1700
**
**********************************************************************************
*Elset, elset=_SurfTop1_SPOS, generate
 91501,  92750,      1
*Surface, type=ELEMENT, name=SURFTOP_1
_SurfTop1_SPOS, SPOS
**
*Elset, elset=_SurfBot1_SNEG, generate
  251,  1500,     1
*Surface, type=ELEMENT, name=SURFBOT_1
_SurfBot1_SNEG, SNEG
**
*CONTACT PAIR, INTERACTION=FRIC_1, TYPE=SURFACE TO SURFACE
SURFTOP_1, SURFBOT_1
*SURFACE INTERACTION, NAME=FRIC_1
**
**********************************************************************************
** mesh-independent fasteners
**
*NSET, NSET=FASTENER_NODES_1, GENERATE
100001, 100036, 1
```

```
*NSET, NSET=FASTENER_NODES_2, GENERATE
100101, 100136, 1
*NSET, NSET=FASTENER_NODES_3, GENERATE
100201, 100236, 1
*NSET, NSET=FASTENER_NODES_4, GENERATE
100301, 100336, 1
*NSET, NSET=FASTENER_NODES_5, GENERATE
100401, 100436, 1
*NSET, NSET=FASTENER_NODES_6, GENERATE
100501, 100536, 1
*NSET, NSET=FASTENER_NODES_7, GENERATE
100601, 100636, 1
**
************************************************************************
*FASTENER,INTERACTION
NAME=FASTENERS,PROPERTY=FAST_PROP,ELSET=FASTENER_1,REFERENCE NODE
SET=FASTENER_NODES_1

SURFTOP_1, SURFBOT_1
**
*FASTENER PROPERTY,NAME=FAST_PROP
2.0
**
*CONNECTOR SECTION,ELSET=FASTENER_1,BEHAVIOR=RIVET_SNAP_HEAD_P80
CARTESIAN
**
************************************************************************
*CONNECTOR BEHAVIOR,NAME=RIVET_SNAP_HEAD_P80
*CONNECTOR ELASTICITY, COMPONENT=1
3e+4
*CONNECTOR ELASTICITY, COMPONENT=3
3e+4
*CONNECTOR ELASTICITY, COMPONENT=2
2e+4
*******************
**** Plasticity
*******************
*Connector Plasticity, component=1
*Connector Hardening, definition=Tabular
875.,  0.0,    0.
1589., 0.0262, 0.
1944., 0.0902, 0.
2100., 0.6662, 0.
*Connector Plasticity, component=3
*Connector Hardening, definition=Tabular
875.,  0.0,    0.
1589., 0.0262, 0.
1944., 0.0902, 0.
2100., 0.6662, 0.
*Connector Plasticity, component=2
*Connector Hardening, definition=Tabular
215.,  0.0,    0.
445.,  0.158,  0.
667.,  0.343,  0.
870.,  0.553,  0.
1012., 1.072,  0.
1082., 1.6,    0.
**
```

```
**********************************************************************************
*Nset, nset=Clamped
 1,  16,  17,  18,  19,  20,  21,  22,  23,  24,  25,  26,  27,  28,  29,  30, ...
*Nset, nset=Rigid
 2,   3,   4,   5,   6,   7,   9,  10,  11,  12,  13,  14,  15,  31,  32,  34, ...
*Nset, nset=Global
 8,
*Nset, nset=Bound
 113, 114, 115, 116, 117, 118, 119, 120, 354, 355, 356, 357, 358, 359, 360, …
**
**********************************************************************************
*STEP, NLGEOM, INC=1200
** nlgeom == geom. nonlinear analysis, inc == max. # of increments in a step
**
*STATIC, STABILIZE
0.01,1,,0.01
** init. time incr., time period of step, min. time incr., max. time incr.
**
**********************************************************************************
*BOUNDARY, OP=NEW
CLAMPED, 1,6, 0.
**
*BOUNDARY, OP=NEW
GLOBAL, 1,2, 0.
GLOBAL, 4,6, 0.
GLOBAL, 3,,  2.
**
*BOUNDARY, OP=NEW
BOUND, 1,2,  0.
BOUND, 4,6,  0.
**
**********************************************************************************
*RIGID BODY, REF NODE=GLOBAL, TIE NSET=RIGID
**
**********************************************************************************
** ODB -> Field Outpt: contour/deformed shape plots
**
*OUTPUT, FIELD, FREQ=1
*NODE OUTPUT
U
*ELEMENT OUTPUT
S
**
** History Output: history XY-plots
**
*OUTPUT, HISTORY, FREQ=1
*NODE OUTPUT, NSET=GLOBAL
RF
**
*END STEP
```

B.2 Airbus Panel

```
**
*NODE
      1,          0.,        1721.,          4.4
      2,          0.,      1713.21,          4.4
…
*ELEMENT, TYPE=S4R, ELSET=ALL_SHELLS_VOID
      1,      1,      2,    224,    223
      2,      2,      3,    225,    224
…
*ELEMENT, TYPE=S3R, ELSET=ALL_SHELLS_VOID
  60016,   67267,   67305,   67272
  60017,   67301,   67272,   67305
…
*ELEMENT, TYPE=CONN3D2, ELSET=CONN_CARTESIAN_SKIN_STR13
 100000,   63279,   13090
 100001,   63284,   13085
…
*ELEMENT, TYPE=C3D4, ELSET=RIBS
 200000,   72808,   72049,   72038,   72040
 200001,   72808,   72049,   73709,   72038
…
*ELEMENT, TYPE=B31 , ELSET=FRAME_BEAMS
 500000,   86946,   95235
 500001,   95235,   95236
…
*ELSET, ELSET=CONT_M_SKIN_RIB, GENERATE
    56,     63,      1
   166,    173,      1
…
**********************************************************************************
** (LH) element sets for stringers, buttstrap & plates contact
*ELSET, ELSET=CONT_M_STR13A, GENERATE
  30720,   32487,      1
…
**
*ELSET, ELSET=CONT_S_STR13A, GENERATE
   5305,    7072,      1
…
**
*ELSET, ELSET=CONT_M_STR13B, GENERATE
  35140,   36907,      1
**
*ELSET, ELSET=CONT_S_STR13B, GENERATE
   7073,    8840,      1
**
**********************************************************************************
** (LH) contact definitions
**
*SURFACE, NAME=SURF_CONT_M_STR13A
CONT_M_STR13A, SPOS
**
*SURFACE, NAME=SURF_CONT_S_STR13A
CONT_S_STR13A, SPOS
**
```

```
*CONTACT PAIR, INTERACTION=FRIC_1, TYPE=SURFACE TO SURFACE, SMALL SLIDING
SURF_CONT_S_STR13A, SURF_CONT_M_STR13A
** (LH) first Slave, than Master
**
*SURFACE INTERACTION, NAME=FRIC_1
*SURFACE BEHAVIOR, PENALTY
**
************************************************************************
*SURFACE, NAME=SURF_CONT_M_STR13B
CONT_M_STR13B, SPOS
**
*SURFACE, NAME=SURF_CONT_S_STR13B
CONT_S_STR13B, SPOS
**
*CONTACT PAIR, INTERACTION=FRIC_2, TYPE=SURFACE TO SURFACE, SMALL SLIDING
SURF_CONT_S_STR13B, SURF_CONT_M_STR13B
*SURFACE INTERACTION, NAME=FRIC_2
*SURFACE BEHAVIOR, PENALTY
**
************************************************************************
*SURFACE, NAME=SURF_CONT_M_ANGLE_SKIN_LEFT_UPPER
CONT_M_ANGLE_SKIN_LEFT_UPPER, SPOS
**
*SURFACE, NAME=SURF_CONT_S_ANGLE_SKIN_LEFT_UPPER
CONT_S_ANGLE_SKIN_LEFT_UPPER, SPOS
**
*CONTACT PAIR, INTERACTION=FRIC_3, TYPE=SURFACE TO SURFACE, SMALL SLIDING
SURF_CONT_S_ANGLE_SKIN_LEFT_UPPER,
SURF_CONT_M_ANGLE_SKIN_LEFT_UPPER
*SURFACE INTERACTION, NAME=FRIC_3
*SURFACE BEHAVIOR, PENALTY
*FRICTION, SLIP TOLERANCE=0.02
0.15,
**
************************************************************************
** (LH) mesh-independent fasteners
**
*NSET, NSET=FASTENER_RIB_SKIN
  79988,  79989,  79991,  79997,  79999,  80000,  80011,  80012,
  80013,  80002,  80008,  80010, ...
**
*NSET, NSET=FASTENER_RIB_STR13_SKIN
80001,  80003,  80004,  80007,  80009,
79990,  79992,  79995,  79996,  79998
**
************************************************************************
*FASTENER,INTERACTION
NAME=RIB_SKIN_6B17,PROPERTY=FAST_PROP_6B17,ELSET=FASTENER1,REFERENCE
NODE SET=FASTENER_RIB_SKIN

SURF_CONT_S_SKIN_RIB, SURF_CONT_M_SKIN_RIB
**
*FASTENER PROPERTY,NAME=FAST_PROP_6B17
6.0
**
*CONNECTOR SECTION,ELSET=FASTENER1,BEHAVIOR=BOLT_CSK_6B16
CARTESIAN
**
```

```
**************************************************************************
*FASTENER,INTERACTION
NAME=RIB_STR13_SKIN_6B16,PROPERTY=FAST_PROP_6B16,ELSET=FASTENER2,
REFERENCE NODE SET=FASTENER_RIB_STR13_SKIN
**
SURF_CONT_M_SKIN_RIB
****
**************************************************************************
*FASTENER,INTERACTION
NAME=RIB_STR13_SKIN_6B16_XY,PROPERTY=FAST_PROP_6B16,ELSET=FASTENER2_
XY, REFERENCE NODE SET=FASTENER_RIB_STR13_SKIN

SURF_CONT_S_STRINGER_RIB, SURF_CONT_FAST_STR13ALL,
SURF_CONT_M_SKIN_RIB
**
*FASTENER PROPERTY,NAME=FAST_PROP_6B16
6.0
**
*CONNECTOR SECTION,ELSET=FASTENER2_XY,BEHAVIOR=BOLT_CSK_6B16_XY
CARTESIAN
**
**************************************************************************
** Rivet model:
**
*CONNECTOR BEHAVIOR,NAME=RIVET
*CONNECTOR ELASTICITY, COMPONENT=1
131338,
*CONNECTOR ELASTICITY, COMPONENT=2
131338,
*CONNECTOR ELASTICITY, COMPONENT=3
37300,
*******************
**** Plasticity
*******************
*Connector Plasticity, component=1
*Connector Hardening, definition=Tabular
3145.,  0.0,  0.
4089.,  0.0262,  0.
4844.,  0.0902,  0.
5300.,  0.6662,  0.
*Connector Plasticity, component=2
*Connector Hardening, definition=Tabular
3145.,  0.0,  0.
4089.,  0.0262,  0.
4844.,  0.0902,  0.
5300.,  0.6662,  0.
*Connector Plasticity, component=3
*Connector Hardening, definition=Tabular
2155., 0.0,  0.
4450., 0.158,  0.
6670., 0.343,  0.
8900., 0.553,  0.
11120., 1.072,  0.
11822., 1.6,  0.
**
```

```
**********************************************************************
** Bolts, Preload=11723N
**
*CONNECTOR BEHAVIOR,NAME=BOLT_5B10
*CONNECTOR ELASTICITY, COMPONENT=1
95000,
*CONNECTOR ELASTICITY, COMPONENT=2
95000,
*CONNECTOR ELASTICITY, COMPONENT=3
340000,
*Connector Plasticity, component=1
*Connector Hardening, definition=Tabular
11314.,  0.0,  0.
18385.,  0.3,  0.
22627.,  0.83,  0.
25951.,  1.7,  0.
*Connector Plasticity, component=2
*Connector Hardening, definition=Tabular
11314.,  0.0,  0.
18385.,  0.3,  0.
22627.,  0.83,  0.
25951.,  1.7,  0.
*Connector Plasticity, component=3
*Connector Hardening, definition=Tabular
730.4,0
1976.3,0.009819
3222.2,0.0204476
4468.4,0.0331278
5714.4,0.0497282
6960.7,0.0720426
8207,0.103622
9453.7,0.150252
10700.4,0.22359
11012.2,0.246914
11479.8,0.286264
11819.4,0.32517
11967.3,0.341866
12272.4,0.380354
12397.2,0.395011
12584.7,0.425413
12816.1,0.460653
12949.7,0.483234
13093.2,0.520133
13142.7,0.536298
**
**********************************************************************
*MATERIAL, NAME=SKINMAT
**
*ELASTIC, TYPE=ISO
     70290.,         0.3
*PLASTIC
629.1284925, 0.0
640.953995,  0.003480727
657.5761684, 0.016434406
670.2608238, 0.030065129
690.526804,  0.054297427
720.4719221, 0.09154463
741.8611614, 0.118192026
```

```
*MATERIAL, NAME=SKINMAT_7449
**
*ELASTIC, TYPE=ISO
     70200.,         0.3
*PLASTIC
616.9410764, 0.0
627.493958,  0.001227996
634.3857555, 0.00307426
645.635168,  0.008591204
668.0326656, 0.027967872
715.5010746, 0.082195505
742.0776684, 0.114003105
**
**
*MATERIAL, NAME=BAR_MAT
**
*ELASTIC, TYPE=ISO
    210000.,         0.3
**
**
*MATERIAL, NAME=ANGLE_MAT
**
*ELASTIC, TYPE=ISO
    210000.,         0.3
**
********************************************************************************
*SHELL SECTION, ELSET=PROP_SKIN_8_8_7449_0, MATERIAL=SKINMAT_7449
8.8,       5
*SHELL SECTION, ELSET=PROP_SKIN_15_9_7449_0, MATERIAL=SKINMAT_7449
15.9,       5
**
*SOLID SECTION, ELSET=RIBS, MATERIAL=RIB_MAT
1.,
*SOLID SECTION, ELSET=CLEATS, MATERIAL=CLEAT_MAT
1.,
**
********************************************************************************
** boundary conditions sets
**
*NSET, NSET=CLAMPED
 1,    223,    445,    667,    889,    1111,    1333,    1555, ...
*NSET, NSET=GLOBAL
 53724
*NSET, NSET=RIGID
 222,    444,    666,    888,    1110,   67266, …
*NSET, NSET=CONSTRAINT_BAND
 2,  3,  4,  219,  220,  221,  224,  225,  226,  441,  442,  443,  446,  47,  448,  663 …

**
********************************************************************************
*NSET, NSET=TOP_MIDDLE_STIFFENER
20758
*NSET, NSET=BOTTOM_PLATE_D16
47619
*NSET, NSET=MIDDLE_SIDE_TRANSDUCERS
2331, 3441
**
```

```
**********************************************************************
** step 1: joint pre-stress
**
*STEP, INC=1200, NLGEOM, CONVERT SDI=YES
*STATIC, STABILIZE
0.1,1,,
**
**********************************************************************
*CONNECTOR LOAD, OP=NEW
**
** rivets
CONN_CARTESIAN_SKIN_STR13,3,750
**
** (str14)-butt-skin
CONN_CARTESIAN_SKIN_BUTT,3,11723
CONN_CARTESIAN_SKIN_BUTT_STR14,3,11723
**
** rib-whatsoever
FASTENER1,3,15500
FASTENER2_Z,3,15500
FASTENER3_Z,3,15500
**
** Str-Cleat
FASTENER5_PART1,3,5000
FASTENER5_PART2,3,5000
FASTENER5_PART3,3,5000
FASTENER5_PART4,3,5000
FASTENER5_PART5,3,5000
**
**********************************************************************
*BOUNDARY, OP=NEW
CLAMPED, 1,6,         0.
**
*BOUNDARY, OP=NEW
GLOBAL, 1,6,          0.
**
**********************************************************************
** History Output: history XY-plots
**
*OUTPUT, HISTORY, FREQ=1
*NODE OUTPUT, NSET=GLOBAL
RF2
*NODE OUTPUT, NSET=BOTTOM_PLATE_D16
U3
**
*END STEP
**
**********************************************************************
** step 2: panel compression
**
*STEP, INC=1200, NLGEOM, CONVERT SDI=YES
** nlgeom == geom. nonlinear analysis, inc == max. # of increments in a step
**
*STATIC, STABILIZE
0.01,1,,0.01
**
```

```
**********************************************************************************
*BOUNDARY, OP=NEW
CLAMPED, 1,6,         0.
**
*BOUNDARY, OP=NEW
GLOBAL, 1,,           0.
GLOBAL, 2,,          20.
GLOBAL, 3,6,          0.
**
*BOUNDARY, OP=NEW
CONSTRAINT_BAND, 1,,  0.
CONSTRAINT_BAND, 3,6, 0.
**
**********************************************************************************
*RIGID BODY, REF NODE=GLOBAL, TIE NSET=RIGID
**
**********************************************************************************
** History Output: history XY-plots
**
*OUTPUT, HISTORY, FREQ=1
*NODE OUTPUT, NSET=GLOBAL
RF2
*NODE OUTPUT, NSET=BOTTOM_PLATE_D16
U3
**
**********************************************************************************
*END STEP
```

APPENDIX C - REVISED NONLINEAR SAFESA METHOD

The process of controlling and treating errors in the idealisation process requires that a step-wise procedure is followed. Each step within this process may itself be considered as a process with input data, an action (an assumption making performed with this data) and output data [138]. The qualification criteria can be expressed as requirements on parameter of interest, e.g. the failure load or a displacement value. The criteria is chosen before the analysis and used to draw final conclusions. The original SAFESA method [116] was extended to include nonlinear effects. New parts appear underlined in this version.

STEP 1: DEFINITION OF BOUNDARY, BOUNDARY CONDITIONS AND LOADING ACTIONS

Input:

1. Real World Problem
2. Qualification Criteria

Process:

1. Domain definition and error treatment

1.1 Define domain, i.e. domain boundary (of the 'Whole Structure') (the domain should be compatible with the qualification criteria or other customer requirements)

1.2 Boundary conditions: definition and error treatment

i) If the boundary conditions are known then:

- assess the extent of errors likely to be introduced at this stage (experience based, simple hand calculations, comparison with test results)
- assume the most likely boundary conditions
- <u>study if boundary conditions are applied uniformly or if local variations are present, e.g. weaker areas in a support</u>
- <u>check if boundary conditions change during the analysis, e.g. caused by geometric deformation</u>

second and further iterations

- do sensitivity analysis and if necessary hierarchical modelling

ii) If the boundary conditions are unknown then:

- try to change the domain so that the boundary conditions are known, or

- make the best possible guess and flag out need for sensitivity analysis in the next iteration.

error treatment at second and further iterations

- perform sensitivity analysis to find out how important the boundary conditions are and if necessary try to determine the boundary conditions by an analysis or a test,
- quantify the error due to boundary condition idealisation

2. Loading: assessment and error treatment
Assess loading actions, at a coarse level appropriate to the high level view being taken of the structure at this stage. More detail may be considered in later steps.

- assess the extent of errors likely to be introduced at this stage (experience based, simple hand calculations, comparison with test results)
- check if loading is applied uniformly
- check if the loading application will change due to a geometric change of the structure

error treatment at second and further iterations

- do sensitivity analysis and if necessary hierarchical modelling

Output:

1. Boundary of the structure and idealised boundary conditions
2. Idealised loading actions (at a coarse level)
3. Statement of level of errors at this stage, for consideration at Step 6

STEP 2: DEFINITION AND ERROR TREATMENT OF LOAD PATHS AND IDEALISATION OF GEOMETRY

Input:

1. Coarse idealisation of boundary conditions
2. Coarse idealisation of loading
3. Real structure geometry
4. Qualification criteria

Process:

1. Assess the overall structural behaviour of the structure in terms of responses to applied loads or mass and stiffness distribution in a nonlinear analysis. If this cannot be done build a course FE model and analyse the behaviour.

2. Define the major and minor load paths.

3. Idealise the geometry at overall level (detail not necessary yet)

3.1 Domain reduction: if any kind of symmetry is present, reduce the domain of analysis to the minimum needed. If the domain is simplified to achieve symmetry then:

- assess the errors due to simplifications (experience based)
- flag out need for hierarchical modelling

error treatment at second and further iterations

- perform hierarchical modelling and if necessary analyse whole structure and quantify the error

3.2 Choose mathematical models, flag out dimensional reduction performed

- assess the errors due to assumptions made (experience based)
- flag out need for hierarchical modelling

error treatment at second and further iterations

- apply hierarchical modelling to quantify the errors at the global level

3.3 Define simplified geometry (geometrical details ignored)

- assess the errors due to simplifications (experience based, simple calculations)
- flag out need hierarchical modelling

error treatment at second and further iterations

- perform hierarchical modelling and quantify the errors

3.4 Revise essential and natural boundary conditions, i.e. geometrical boundary conditions and loading (make them compatible with the adopted mathematical model and idealised geometry). Check if the simplifications made can introduce nonlinearity in boundary conditions and loading.

4. Define type of analysis (if overall definition is possible)

Experience, comparison with known physical limits and verification of the mathematical model basic assumptions are relatively simple ways to check validity of the analysis used. For instance, in a linear stress analysis stresses should be below the material elastic limit.

5. Material idealisation and error treatment

Select an appropriate material model depending on used material and expected stresses. If necessary, include material nonlinearity, fracture or failure. The error inherent to material parameters used should be taken into account. If the error can not be quantified (experience based) flag out need for sensitivity analysis.

error treatment at second and further iterations

- apply sensitivity analysis to find out if a test or additional analysis should be done to quantify the error

Output:

1. Overall idealisation of geometry and material
2. Type of analysis
3. Structural behaviour (in overall terms)
4. Statement of likely level of errors, for assessment in Step 6

STEP 3: BREAKDOWN OF STRUCTURE OR FEATURE

This step will first be carried out following Step 2, to break down the whole structure, but may then be carried out again for individual features, following Step 6 for those features.

Input:

1. Idealised geometry, boundary conditions and loading action for the structure
2. Load paths within the structure
3. Structural behaviour within the structure

Process:

Breakdown of structure into lower level features. Any division of a structure into sub-features is acceptable as long as it allows for an efficient treatment of errors in the process of idealisation. It would be useful if:

- boundary conditions for sub-features are easy to define
- primitives have unique behavioural properties and as a consequence are meshing units to which “off the peg” mesh can be applied
- the main error sources on primitives are easy to locate and analyse/test

Output:

1. Structure or feature divided into lower level features

STEP 4: DEFINITION OF BOUNDARY CONDITIONS AND LOADING ACTION FOR FEATURES

Input:

1. Feature
2. Outputs from Step 1 and 2

Process:

1. Define and treat boundary condition errors for the feature. These may follow directly from the boundary conditions defined at a higher level, or may require more detailed description here.

    1.1 Define boundary conditions that have not been considered at the higher level. These are usually the feature interfaces, which were part of the global structure. If the boundary conditions are known then:

- assess the extent of errors likely to be introduced at this stage (experience based, simple hand calculations, comparison with test results)
- check if any change of the boundary conditions due to the nonlinear behaviour of the analysis can occur

error treatment at second and further iterations
- sensitivity analysis and if necessary hierarchical modelling

If the boundary conditions are unknown then:
- try to change the domain, i.e. feature boundary so that the boundary conditions for the feature can be defined
- make the best possible guess and flag out need for sensitivity analysis in the next iteration.

error treatment at second and further iterations
- perform sensitivity analysis to find out how important the boundary conditions are and if necessary try to determine the boundary conditions by an analysis or a test
- quantify the error due to boundary condition idealisation at the local and global level

2. Define loading action for the feature. Again this may follow directly from the loading action defined at the higher level.
- assess the extent of errors likely to be introduced at this stage (experience based, simple hand calculations, comparison with test results)
- check if loading nonlinearity can occur during the analysis

error treatment at second and further iterations
- sensitivity analysis and if necessary hierarchical modelling

Output:
1. Idealised boundary conditions for the feature
2. Idealised loading for the feature
3. Statement of likely error levels, for consideration in Step 6

STEP 5: DEFINITION AND ERROR TREATMENT OF LOAD PATHS AND IDEALISATION OF GEOMETRY FOR FEATURES

Input:
1. Idealised boundary conditions for the feature
2. Idealised loading for the feature
3. Real geometry of the feature
4. Qualification criteria

Process:

1. Assess the structural behaviour of the feature in terms of responses to applied loads, if this has not already been adequately defined at a higher level.

2. Define the major and minor load paths. Check if the load paths can change due to nonlinear analysis behaviour.

3. Behaviour and geometry idealisation

3.1 Choose the mathematical model/models, flag out dimensional reduction performed

- assess the errors due to assumptions made (experience based)
- flag out need for hierarchical modelling

error treatment at second and further iterations

- apply hierarchical modelling to quantify the errors at the feature/sub-feature level

3.2 Define simplified geometry (geometrical details ignored)

- assess the errors due to simplifications (experience based, simple calculations)
- flag out need hierarchical modelling

error treatment at second and further iterations

- perform hierarchical modelling
- quantify the errors at the feature/sub-feature level

3.3 Revise essential and natural boundary conditions, i.e. geometrical boundary conditions, loading and influence of nonlinearity.

4. Define type of analysis, if different from overall type defined in Step 2.
Again, use the available experience as in Section 4 of Step 2.

5. Idealise material, if more detail required than at Step 2.
The error inherent to material parameters used should be taken into account. If the error can not be quantified (experience based) flag out need for sensitivity analysis.

error treatment at second and further iterations

- apply sensitivity analysis to find out if a test or additional analysis should be done to quantify the error

Output:

1. Idealised geometry and material for the feature
2. Type of analysis
3. Structural behaviour of feature
4. Statement of likely level of errors, for consideration in Step 6

STEP 6: ASSESSMENT

Input:

1. Real world problem
2. Idealised features
3. Errors from previous steps

Process:

1. Assessment at feature level

Assess the idealised feature as an adequate representation of the appropriate part of the real world problem, with reference to the quantified errors. If the confidence level is too low go for another idealisation iteration. If feature/sub-feature idealisation cannot be improved due to lack of reliable data, then define tests either at the detailed or at the global level.

2. Assessment at the global level

Assess the idealised structure as an adequate representation of the real world problem, with reference to the quantified errors. If the confidence level is too low go for another idealisation iteration. If global the idealisation cannot be improved due to lack of reliable data, then define tests either at the detailed or at the global level.

Output:

1. Corroborative tests

STEP 7: TEST PROGRAMME

This step is only carried out if the need for tests has been indicated at Step 6.

Input:

1. Real world problem
2. Idealised feature or primitive
3. Definition of corroborative test

Process:

Perform corroborative tests and compare the outputs against the assumed structural actions and responses. If these are inappropriate define changes to response or action assumptions.

Output:

1. If tests confirm assumptions, proceed at the current feature (looping back to Step 3 if further subdivision is required).
2. If tests indicate modifications then define changes to assumptions.

APPENDIX D – EXPERT SYSTEM IMPLEMENTATION

D.1 FEM Best Practice Questionnaire

Which FEM tools are you using for linear/nonlinear static analysis?

Which CAD tool is used? How is the CAD data transferred into the FE software? If directly importing, do you use the STEP or IGES format? Are there assistance tools for this step?

When using NASTRAN, ABAQUS or ANSYS, which pre-processor is used?

If using PATRAN, are you using the PCL (PATRAN Command Language) interface to facilitate user interaction?

Are any expert systems for the idealisation / modelling step in use (e.g. MSC/Supermodel, MSC/Acumen, …)?

Do databases exist with FE models, parts (like stiffened panels), material properties, …?

Are tools for dealing with input uncertainties (e.g. variation of material yield stress) in use (e.g. NESSUS)?

D.2 CLIPS Source Code (important parts)

```
;;;======================================================
;;; The Safesa expert system. To execute: start Clips -> load, reset and run.
;;;======================================================

;;***************
;;
;;* DEFFUNCTIONS *
;;***************
;;

(deffunction ask-question (?question $?allowed-values)
  (printout t ?question)
  (bind ?answer (read))
  (if (lexemep ?answer)
    then (bind ?answer (lowcase ?answer)))
  (while (not (member ?answer ?allowed-values)) do
    (printout t ?question)
    (bind ?answer (read))
    (if (lexemep ?answer)
      then (bind ?answer (lowcase ?answer))))
  ?answer)

(deffunction yes-or-no-q (?question)
   (bind ?response (ask-question ?question yes no y n))
   (if (or (eq ?response yes) (eq ?response y))
       then TRUE
       else FALSE))

;;***************
;;
;;* DEFFACTS *
;;***************
;;

(deffacts initialisation
  (menu-status main-menu)
)

;;;***************
;;;
;;;* RULES *
;;;***************
;;;

;;The main menu provides the program interaction. Several options can be selected.
(defrule main-menu1
  ?ms <- (menu-status main-menu)
=>
  (retract ?ms)
  (printout t crlf
  "/=============================================\\" crlf
  "|      Idealisation Error Control Expert System" crlf
  "\\=============================================/" crlf
  "During modelling you had to choose the following:" crlf
  "  [1] Domain definition" crlf
  "  [2] Boundary conditions" crlf
  "  [3] Loading of structure" crlf
  "  [4] Behaviour during analysis" crlf
  "  [5] Load paths" crlf
  "  [6] Geometry: domain reduction" crlf
  "  [7] Geometry: mathematical model" crlf
```

```
  "  [8] Geometry: dimensional reduction" crlf
  "  [9] Geometry: revision of essential & natural b.c." crlf
  " [10] Analysis type" crlf
  " [11] Material model" crlf
  "  [h] Help for FEM software use" crlf crlf)
;  (printout t "Input something to continue: ")(read)
  (printout t
  "You were uncertain about the following decisions [group]:" crlf
  "==============================================" crlf)
  (assert (menu-status main-menu2))
  (assert (menu-status main-menu3))
)

(defrule main-menu2;  User input is parsed and the selection printed to the screen.
  (menu-status main-menu2)
  (error ?x ?y ?z)
  =>
  (printout t "category: " ?x)
  (if (str-index _domain_domain ?x) then (printout t " [1]"))
  (if (str-index _domain_bc ?x) then (printout t " [2]"))
  (if (str-index _loading ?x) then (printout t " [3]"))
  (if (str-index _behaviour ?x) then (printout t " [4]"))
  (if (str-index "_load " ?x) then (printout t " [5]"))
  (if (str-index step2_load ?x) then (printout t " [5]"))
  (if (str-index _geometry_dom_reduction ?x) then (printout t " [6]"))
  (if (str-index _geometry_mat_model ?x) then (printout t " [7]"))
  (if (str-index _geometry_dim_reduction ?x) then (printout t " [8]"))
  (if (str-index _geometry_revision_bc ?x) then (printout t " [9]"))
  (if (str-index _analysis ?x) then (printout t " [10]"))
  (if (str-index _material ?x) then (printout t " [11]"))
  (if (eq ?y Button4) then
    (printout t ", confidence: some doubts" crlf)
  else
    (printout t ", confidence: not sure" crlf)
  )
  (printout t "description: " ?z crlf crlf)
)

(defrule main-menu3; Depending on the choice the main-menu-selection fact is initialized.
  (declare (salience -10))
  ?ms1 <- (menu-status main-menu2)
  ?ms2 <- (menu-status main-menu3)
  =>
  (retract ?ms1 ?ms2)
  (printout t
  "Get advice on one of the problem areas listed above" crlf
  "==============================================" crlf
  "by typing a number [1..11, h] or [q] to quit: ")
  (bind ?response (ask-question " " 1 2 3 4 5 6 7 8 9 10 11 h q))
  (assert (main-menu-selection ?response))
  (printout t crlf)
)

(defrule end-message; This rule processes the selection “q” to quit the program.
  ?mms <- (main-menu-selection q)
  =>
  (retract ?mms)
  (printout t "You have QUIT the program." crlf crlf)
```

```
  (assert (menu-status end-clearing))
)

(defrule clearing1; deletes all error facts
  ?ms <- (menu-status end-clearing)
  ?er <- (error ?x ?y ?z)
  =>
  (retract ?er)
)

(defrule clearing2; deletes menu-status end-clearing
  ?ms <- (menu-status end-clearing)
  (not (error ?x ?y ?z))
  =>
  (retract ?ms)
)

..................................................................... 10
;;;;;;;;;;;;;;;;;;;;;;;;;;;;;;;;;;;;;;;;;;;;;;;;;;;;;;;;;;;;;;;;;;;;;;;;
(defrule submenu-analysis
  (declare (salience 20))
  (main-menu-selection 10); The rule fires if “10” was selected in the main menu.
  =>
  (printout t "[10] Analysis type:" crlf)
  (printout t "======================" crlf)
)

(defrule analysis-general-knowledge1; Outputs general knowledge.
  (declare (salience 10))
  (main-menu-selection 10)
  =>
  (assert (knowledge "Experience is the main guide at this point in the process. For example,
          comparison with known physical limits and verification of the mathematical model
          basic assumptions are relatively simple ways to check validity of the analysis used."))
)

(defrule analysis-rule-advice1; Handles an advice rule, here depending on user input.
  (declare (salience 0))
  (main-menu-selection 10)
  =>
  (bind ?response (ask-question "Do you intend to do a linear/buckling/quasi-static nonlinear
                  analysis/dynamic nonlinear analysis (l/b/q/d)?" l b n))
  (if (eq ?response l)
    then
      (printout t "In a linear analysis the structure will deform elastically and reverse to it's original
       shape after releasing of the applied load/displacement. This analysis type is not suitable for
       a stiffened panel post-buckling analysis. Check the stress output if the yield stress was
       reached in any part; if it did you must do a nonlinear analysis. Linear analyses are run in
       Abaqus with e.g.: *step, amplitude=ramp, perturbation." crlf)
  )

  (if (eq ?response b)
    then
      (printout t "In a buckling analysis the buckling-modes of the structure are calculated. This
       analysis is also of linear character, although the eigenvectors are usually calculated with an
       iterative method. Output are the buckling shapes. The first buckling mode should be the
       shape of the panel when local buckling occurs. Therefore it is usually the worst imperfection
```

```
      shape and used to simulate imperfections (see main menu [7]). A buckling analysis in
      Abaqus is performed with: *step; *buckle; <nr_eigenvalue>,,,<max_iterations>." crlf)
  )
  (if (eq ?response q)
    then
      (printout t "Panel failure tests are usually executed in a way that the FEM analysis is quasi-
      static nonlinear. This means that the compression panel is slowly compressed in the test
      machine. The analysis has to deal with three sources of nonlinearity: material, geometry
      and boundary condition. This is best achieved by applying a modified Newton-Raphson
      solution algorithm. In Abaqus with: *step, nlgeom, inc=<nr_increments>; *static, stabilize;
      [...]" crlf)
  )
  (if (eq ?response d)
    then
      (printout t "A dynamic analysis is necessary when the panel test is performed with high a
      velocity similar to crash tests. Hereby, an explicit FEM solver as LS-Dyna Abaqus/Explicit
      must be used. For deatails read the e.g. the Abaqus/Explicit manual." crlf)
  )
)

(defrule analysis-report
  (declare (salience -5))
  (main-menu-selection 10)
  =>
  (printout t "Input something to continue: ")(read)
  (printout t crlf "Following knowledge and advice can be given:" crlf)
  (printout t "======================" crlf crlf)
)

(defrule analysis-report-knowledge
  (declare (salience -10))
  (main-menu-selection 10)
  ?kn <- (knowledge ?know)
  =>
  (retract ?kn)
  (printout t ?know crlf crlf)
)

(defrule analysis-report-advice
  (declare (salience -10))
  (main-menu-selection 10)
  ?ad <- (advice ?adv)
  =>
  (retract ?ad)
  (printout t ?adv crlf crlf)
)
```

D.3 Expert System User Guide

1) Introduction

This user guide presents the SAFESA (SAFE Structural Analysis) expert system. The purpose of the program is to assist the FEM idealisation in order to avoid modelling errors. Guidance will be given for important aspects, such as material modelling, boundary conditions and joint modelling. The expert system guides the user step by step through the idealisation process. Each decision is documented and a confidence level must be supplied. This way every modelling uncertainty is flagged out as potential error source. An interactive interface was created, which provides expert advice on how to treat the idealisation errors.

2) Interface Overview

2.1) Main Window

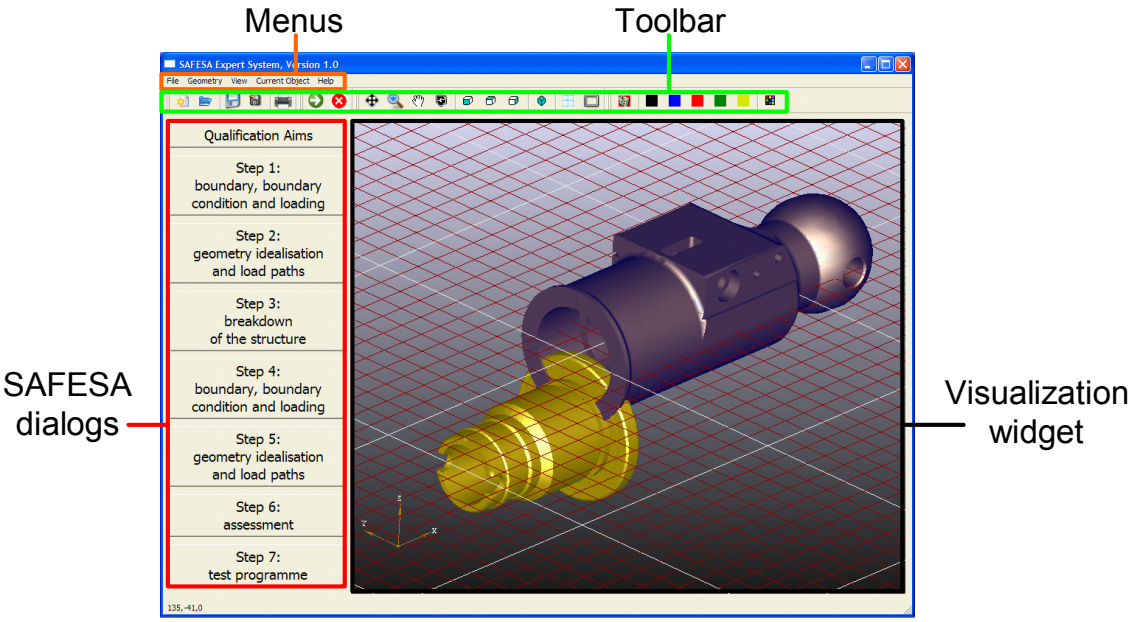

Figure D.1: Main window of the expert system

Figure D.1 shows the main window of the program. Menus and the toolbar ensure convenient user interaction. The SAFESA dialogs are located on the left hand side. The major part of the window is made up by the visualisation widget, which shows the loaded CAD geometries.

2.2) File Menu

New, Open, Save, Save As

These commands apply to the SAFESA analysis files. **New**, **Open**, **Save** and **Save As** are self-explanatory. The data are saved in ASCII files. CAD geometry is imported via Geometry -> Import Geometry, and paths are saved within analysis files.

Print Report

Prints out an analysis report in PDF format. The standard file name is report.pdf.

Exit

Exit the program. Make sure you save all data before exiting the program!

2.3) Geometry Menu

Import Geometry

This opens an open-file dialog. CAD geometries in IGES, STEP and BREP format can be imported. Different colours, materials and transparencies can be applied to imported geometries. The program is not aimed at manipulating CAD geometry. Therefore, the structure should be broken down into features beforehand. This can easily be done in a CAD environment like CATIA.

Delete All Geometry

All imported geometries and internal references to them will be deleted. To delete the analysis file paths as well, the analysis needs to be saved.

2.4) View Menu

Actions: Fit Window, Zoom, Move, Rotate

These commands help to navigate within the CAD visualisation widget. **Fit Window** will show a maximised view of all displayed geometries. **Zoom**, **Move** and **Rotate** are self-explanatory.

Perspective

These commands allow changing the point of view. The available options are **Front**, **Back**, **Top**, **Bottom**, **Right**, **Left** and **Axo View**.

Grid

With this command the grid appearance can be selected. **Grid On** / **Off** enables / disables the grid. **XY**, **XZ** and **YZ Grid** determine the orientation of the grid.

Display: Wireframe/Shading & Hidden On/Off

Each object can be displayed in **Wireframe** or **Shading** mode. Wireframe mode shows only the edges. **Hidden On/Off** determines whether logically hidden lines are shown or not.

2.5) Current Object Menu

The concept of the current object is a basic concept of the underlying library Open Cascade. Once an object is selected, its properties can be changed. Objects are selected by simply clicking on them, or with Ctrl + Left Mouse Button + Mouse Move, dragging a rubber-band about all objects. Selected objects are highlighted.

Hide/Show

With **Hide** single objects can be hidden. When **Show All Objects** is selected, any imported geometries, which have not been deleted are displayed.

Delete

Using **Delete**, individual objects are deleted. (Geometry Menu -> **Delete All Geometry** deletes all.)

Set Color/Material/Transparency

This set of commands helps to distinguish the individual parts of the structure. **Color**, **Material** and **Transparency** of objects can be set. With the current program version these settings cannot be saved permanently (via File –> Save).

2.6) Help Menu

This menu provides access to the help features. **About** and **About Qt** give brief information about the program. **Manual** will open this manual. The file **manual.pdf** needs to be stored in the same directory as SAFESA, or in subfolder ./debug or ./data/manual.

2.7) Toolbar

The toolbar is a movable panel that contains a set of control buttons, see Figure D.1. Each button shows an icon which represents a command. All functionality provided by the menus can be executed using the toolbar, which is permanently shown.

3) SAFESA Dialogs

This section describes the main functionality of the program. The provided dialogs guide the user through the FEM idealisation error analysis. In each step the analyst needs to consider potential error sources and to describe his decisions.

3.1) Qualification Aims

The first dialog documents general information of the analysis.

3.2) Step-1,2: Analysis at the Global Level

In the step-1 and step-2 dialogs the global FEM idealisation is documented. Domain, loading, global behaviour during the analysis, applied loads, geometry, boundary, boundary conditions and material are selected.

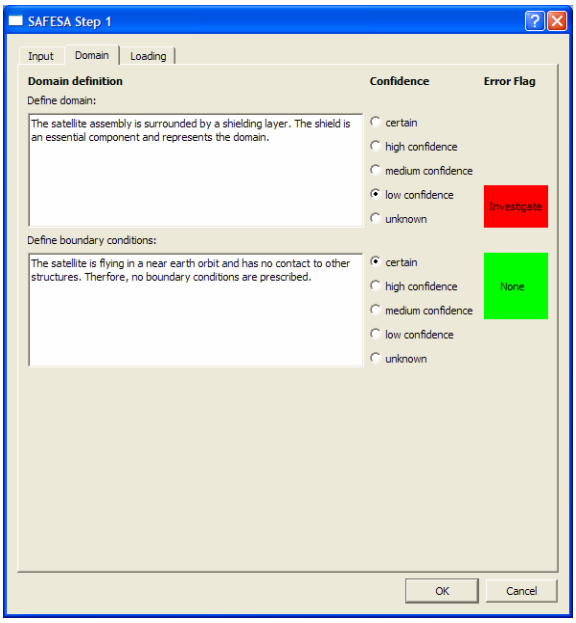

Figure D.2: SAFESA step-1 dialog

Figure D.2 shows the step-1 dialog. The dialog is separated in three tabulator views. The example shows the domain tabulator where the domain and boundary conditions are specified. A confidence level should be supplied for each design decision. A potential error source is detected if the user selects “low confidence” or “unknown”. By pressing the **OK** button, all information is stored in the program database.

3.3) Step-3: Disassembling the Structure

This dialog helps disassembling the structure into individual features with by following steps:

1.) Features are defined by entering a name into the field **Define a new feature** and pressing **Add Feature**. A new feature will appear in the table above.

2.) By selecting a part with the mouse, and then clicking the **Assign Feature** button, a structural part is assigned to the new defined feature. The assigned geometry-file will be displayed in the second column of the above table.

3.) Leaving the dialog with **OK** will write an entry in the program database. **Cancel** leaves the dialog without saving.

3.4) Step-4,5: Analysis at the Feature Level

Steps 4 and 5 repeat the idealisation analysis on the feature level. The dialogs have similar functionality as those for Step-1 and 2.

3.5) Step-6: Error Assessment

Step-6 dialog lists all flagged idealisation error sources. For each error source an analysis is requested. The outcome of the study is described in the provided text field **Error description**. When the error analysis is completed, the **Error analysed?** checkbox can be set. This will switch the flag from red to green. If the error could not be analysed sufficiently, the **Test necessary?** flag must be set to red. The necessary additional tests are then summarised in the step-7 dialog.

Step-6 is a very important stage in the error control process, because the remaining error values have to be determined. Therefore, the decision advisor is supplied here, and can be accessed by clicking the **Start Error Treatment Assistant** button.

3.6) Decision Advisor

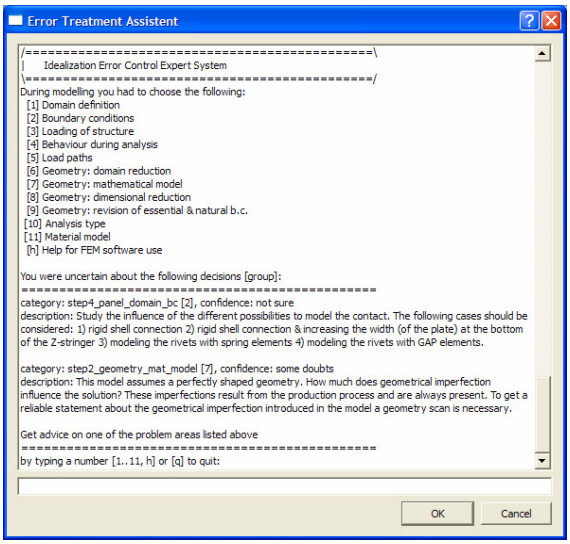

Figure D.3: Decision advisor showing menu and error list

Figure D.3 shows the decision advisor dialog. The user can read the output in the text field and respond to the system using the provided line edit at the bottom. The error categories “1” to “11”, “h” for help or “q” for quit can be selected to start an expert consultation about the flagged error sources.

3.7) Step-7: Test Program

Step-7 lists the necessary additional tests, which were marked at Step-6.

4) Properties of the GUI

4.1) Fast User Interaction with Mouse and Ctrl Button

Pressing Ctrl and using the mouse allows for quick interaction with the SAFESA program. The following shortcuts are available:

- Ctrl + Left Mouse Button + Mouse Move: **Select** several objects
- Ctrl + Middle Mouse Button + Mouse Move: **Move**
- Ctrl + Right Mouse Button + Mouse Move: **Rotate**

4.2) Selecting Geometry Objects

As already mentioned in sections 3.3 and 4.1, a single object is selected by clicking on it. Multiple objects are selected with: Ctrl + Left Mouse Button + Mouse Move; a rubber-band will appear and highlight the objects.

4.3) Modal/Non-modal Dialogs

The used graphic library allows the creation of modal and modeless dialogs. Opening a modal dialog moves the dialog to the top level window. Only after closing this dialog, can the user interact with the main GUI. All (except step-3) SAFESA dialogs are modal. A modeless dialog allows working with multiple windows at the same time. Step-3 dialog is modeless, which enables user interaction with the main program to select objects.

4.4) Toolbar and Shortcuts

For the most common actions a toolbar and in many cases a shortcut as well is provided. These can be found in the following table:

GUI Symbol	Shortcut	Action Name
	Ctrl+N	New
	Ctrl+O	Open
	Ctrl+S	Save
		Save As
		Print Report
	Ctrl+Q, Alt+F4	Exit
		Import Geometry
		Delete All Geometry
	Ctrl+F	Fit Window
	Ctrl+Z, Mouse-wheel	Zoom
	Ctrl+M, Ctrl+Middle Mouse Button	Move
	Ctrl+R, Ctrl+Right Mouse Button	Rotate
		Front, Top, Right View
		AxoView
	Ctrl+G	Grid On
	Ctrl+D	Grid Off
		Delete Selected Object
		Paint Selected Object: Black, Blue, Red, Green, Yellow
		Choose Color for Selected Object

Table D.1: GUI actions and their toolbar symbols and shortcuts